

Tevatron data

- Wealth of data from the Tevatron, both Run 1 and Run 2, that allows us to test/add to our pQCD formalism

- ◆ with analysis procedures/systematic errors that are very mature

- Consider for example W/Z production

- ◆ cross section increases with center-of-mass energy as expected

- We've already seen that the data is in reasonable agreement with the theoretical predictions

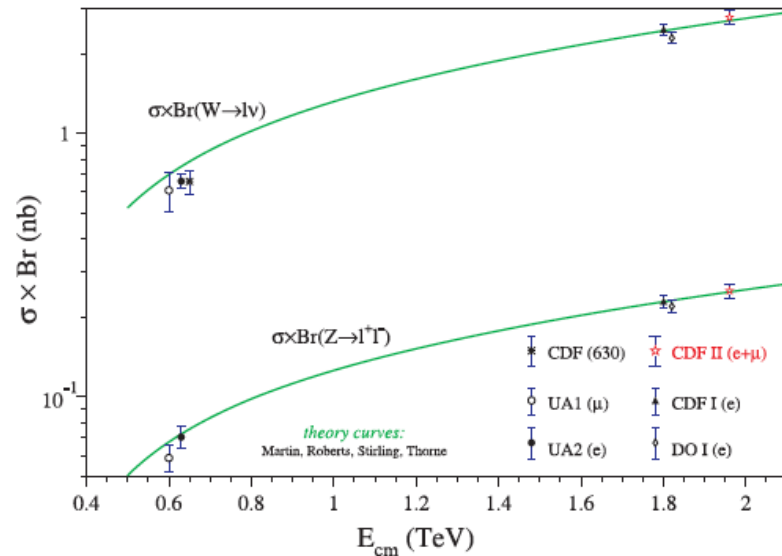


Figure 37. W and Z cross sections as a function of the centre-of-mass energy.

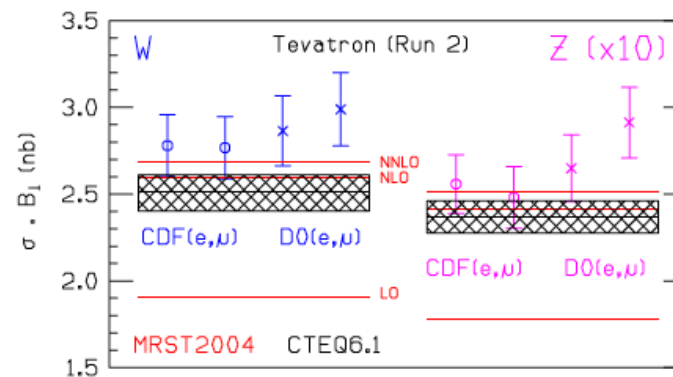


Figure 4. Predictions for the W and Z total cross sections at the Tevatron and LHC, using MRST2004 [10] and CTEQ6.1 pdfs [11], compared with recent data from CDF and D0. The MRST predictions are shown at LO, NLO and NNLO. The CTEQ6.1 NLO predictions and the accompanying pdf error bands are also shown.

Rapidity distributions

- Effect of NNLO is basically a small normalization shift from NLO
- Data is in good agreement
- Provides some further constraints in pdf fits

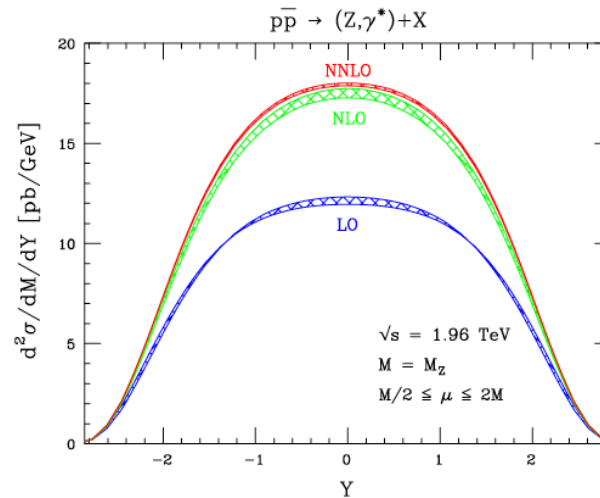


Figure 38. Predictions for the rapidity distribution of an on-shell Z boson in Run 2 at the Tevatron at LO, NLO and NNLO. The bands indicate the variation of the renormalization and factorization scales within the range $M_Z/2$ to $2M_Z$.

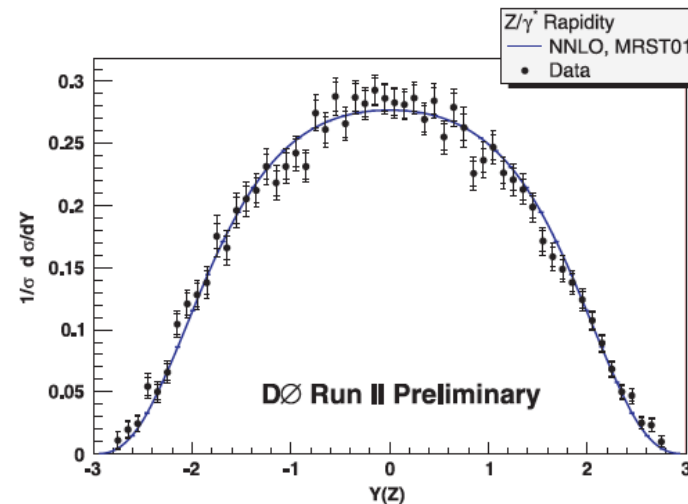


Figure 39. Z rapidity distribution from D0 in Run 2.

Transverse momentum distributions

- Soft (and hard) gluon effects cause W/Z bosons to be produced at non-zero transverse momentum, as we saw in a previous lecture
- Well-described by ResBos and parton shower Monte Carlos
 - ◆ although latter need to have non-perturbative k_T added in by hand
 - ◆ but resummation programs do not

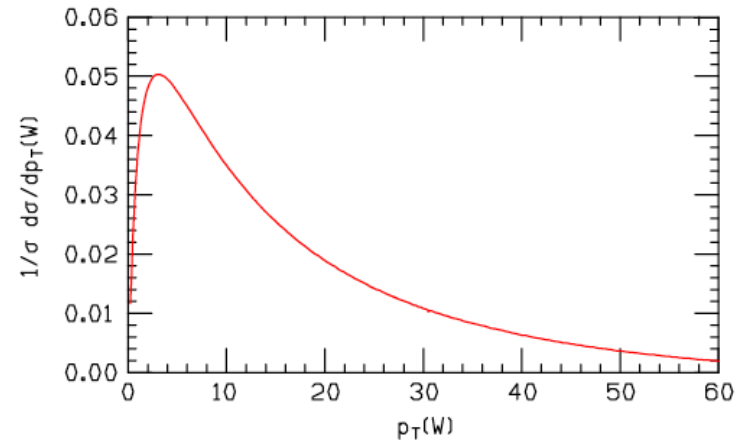


Figure 20. The resummed (leading log) W boson transverse momentum distribution.

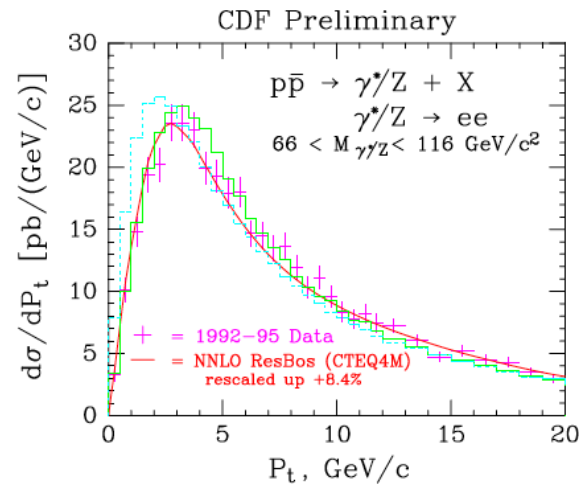


Figure 40. The transverse momentum distribution (low p_T) for $Z \rightarrow e^+e^-$ from CDF in Run 1, along with comparisons to predictions from PYTHIA and ResBos. The dashed blue curve is the default PYTHIA prediction. The PYTHIA solid-green curve has had an additional 2 GeV of k_T added to the parton shower.

p_T distributions

- If we look at average transverse momentum of Drell-Yan pairs as a function of mass, we see that there is an increase that is roughly logarithmic with the mass
 - ◆ as expected from the logs that we saw accompanying soft gluon emission
- If we look at the average transverse momentum of Drell-Yan pairs as a function of center-of-mass energy, there is an increase that is roughly logarithmic with the center of mass energy
 - ◆ as we expect from the logs resulting from the increase in phase space for gluon emission as the center of mass energy grows

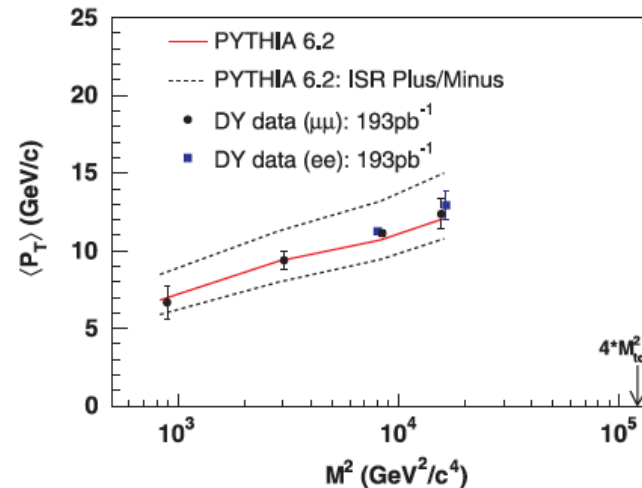
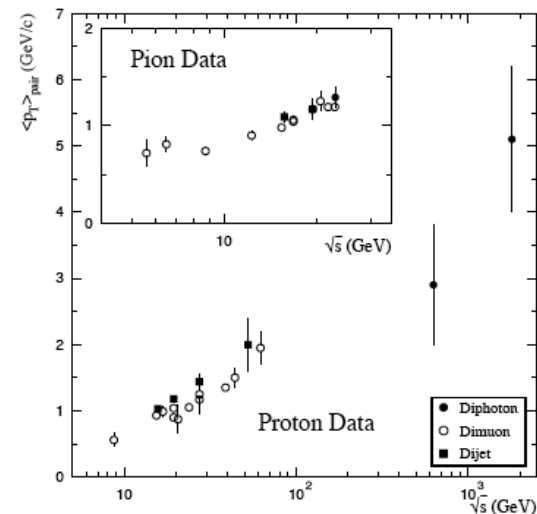


Figure 42. The average transverse momentum for Drell-Yan pairs from CDF in Run 2, along with comparisons to predictions from PYTHIA.



p_T distributions

- High p_T region is due to hard gluon(s) emission, the realm of fixed order predictions, but is also well-described by resummation predictions such as ResBos, which rely on such fixed order predictions for the high p_T range

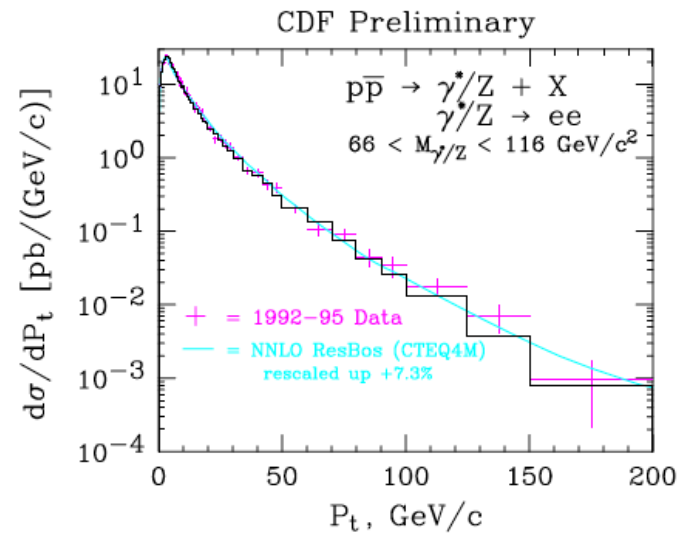


Figure 41. The transverse momentum distribution (full p_T range) for $Z \rightarrow e^+e^-$ from CDF in Run 1, along with comparisons to predictions from PYTHIA (solid histogram) and ResBos.

Look in more detail at W/Z p_T distribution

- One of tuning parameters in Monte Carlos is the amount of intrinsic k_T to add in
- From size of proton, expect truly *intrinsic* k_T to be on the order of 500 MeV/c
- For Z production at the Tevatron, you have in add in ~ 2 GeV/c to get a good description of the data
- ResBos describes it well out of the box
 - ◆ has non-perturbative Sudakov factors at low p_T
 - ◆ two main parameters g_1 and g_2 fit to fixed target/Tevatron data
- This extra bit has to be added to the Monte Carlos to account for the parton shower cutoff
- That amount depends on the center of mass energy and on the mass of the system, so in that sense it's a very undesirable tuning parameter

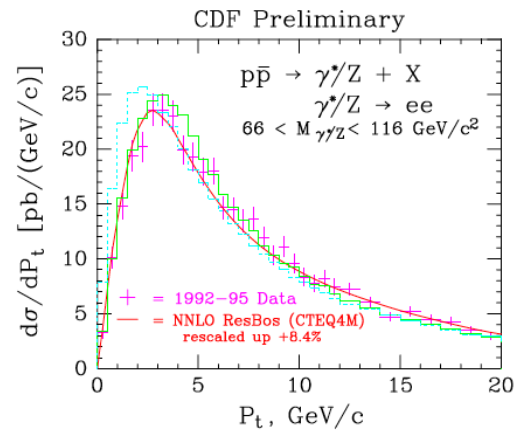
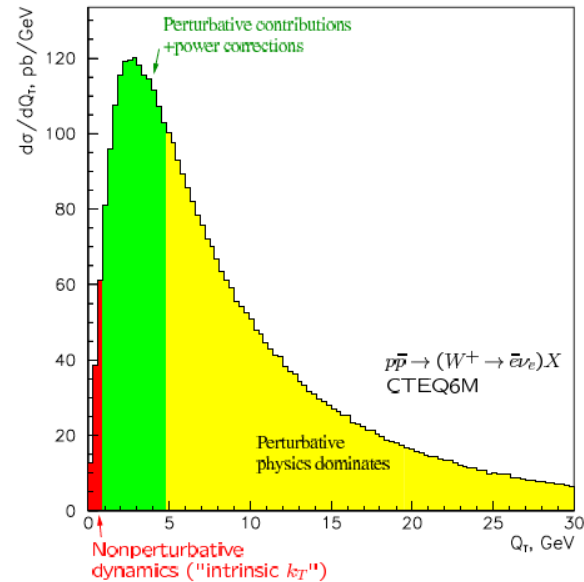


Figure 40. The transverse momentum distribution (low p_T) for $Z \rightarrow e^+e^-$ from CDF in Run 1, along with comparisons to predictions from PYTHIA and ResBos. The dashed blue curve is the default PYTHIA prediction. The PYTHIA solid-green curve has had an additional 2 GeV of k_T added to the parton shower.

This can be added to parton showers

- Let's consider the Sudakov formfactor for backward evolution from some scale \tilde{q}_{\max} down to \tilde{q} :

$$\Delta(\tilde{q}; p_{\perp_{\max}}, p_{\perp_0}) = \exp \left\{ - \int_{\tilde{q}^2}^{\tilde{q}_{\max}^2} \frac{d\tilde{q}'^2}{\tilde{q}'^2} \int_{z_0}^{z_1} dz \frac{\alpha_S(p_{\perp})}{2\pi} \frac{x' f_b(x', \tilde{q}'^2)}{x f_a(x, \tilde{q}'^2)} P_{ba}(z, \tilde{q}'^2) \right\} .$$

p_{\perp_0} is cut-off scale at which the coupling would diverge, if extrapolated outside the perturbative domain \implies no radiation below p_{\perp_0}

- We introduce additional non-perturbative emissions in terms of an additional Sudakov form factor Δ_{NP} , such that we have:

$$\Delta(\tilde{q}; p_{\perp_{\max}}, 0) = \Delta_{\text{pert}}(\tilde{q}; p_{\perp_{\max}}, p_{\perp_0}) \Delta_{\text{np}}(\tilde{q}; p_{\perp_0}, 0)$$

- For technical simplicity we can achieve this by modifying our implementation of $\alpha_S(p_{\perp})$

$$\alpha_S(p_{\perp}) = \alpha_S^{(\text{pert})}(p_{\perp}) + \alpha_S^{(\text{NP})}(p_{\perp}).$$
$$\alpha_S(p_{\perp}) = \begin{cases} \varphi(p_{\perp}), & p_{\perp} < p_{\perp_0} \\ \alpha_S^{(\text{pert})}(p_{\perp}), & p_{\perp} \geq p_{\perp_0} \end{cases} .$$

In this way, the kinematics and phase space of each non-perturbative emission are exactly as in the perturbative case.

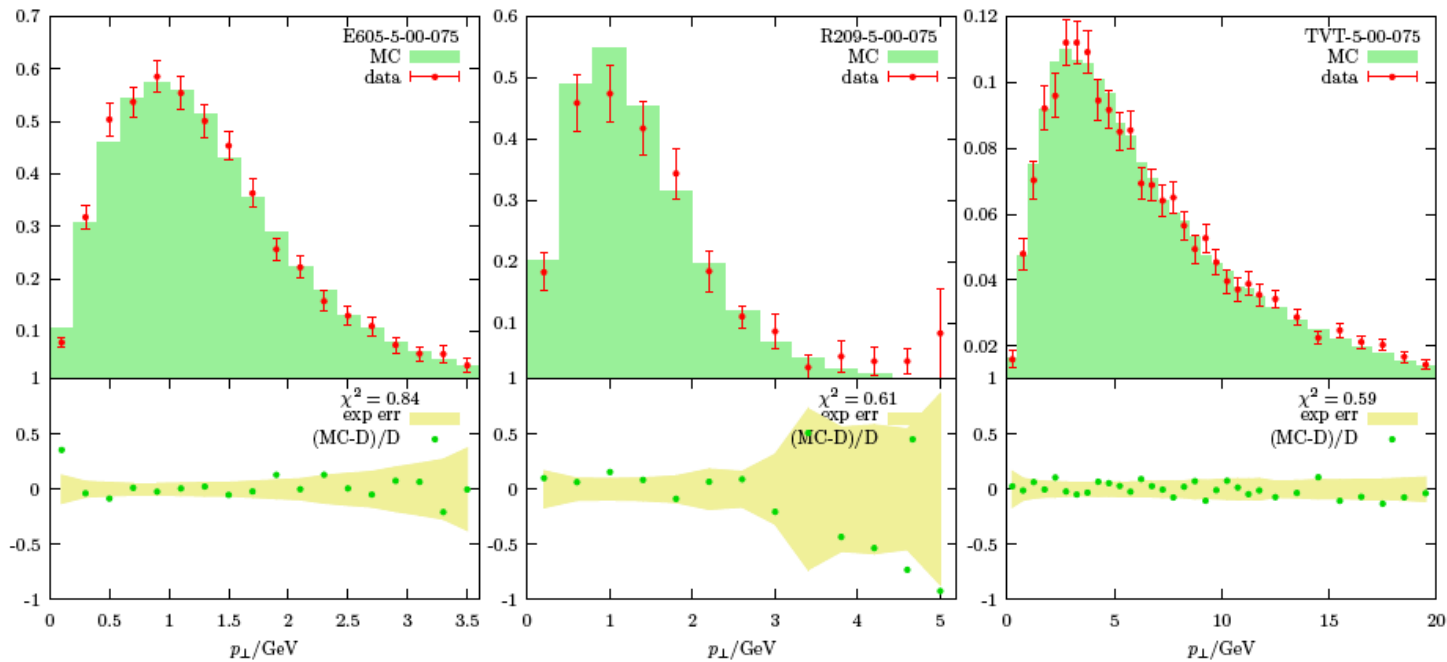
This has been implemented in Herwig++*

The optimal results for our parameter is $\varphi_0 = 0.0, p_{\perp 0} = 0.75$ GeV

Fermilab E605

CERN-R209

Tevatron-CDF



$$\chi^2 = 0.84$$

$$\chi^2 = 0.61$$

$$\chi^2 = 0.59$$

Inclusive jet production

- This cross section/ measurement spans a very wide kinematical range, including the highest transverse momenta (smallest distance scales) of any process
- Note in the cartoon to the right that in addition to the 2->2 hard scatter that we are interested in, we also have to deal with the collision of the remaining constituents of the proton and anti-proton (the “underlying event”)
- This has to be accounted for/ subtracted for any comparisons of data to pQCD predictions

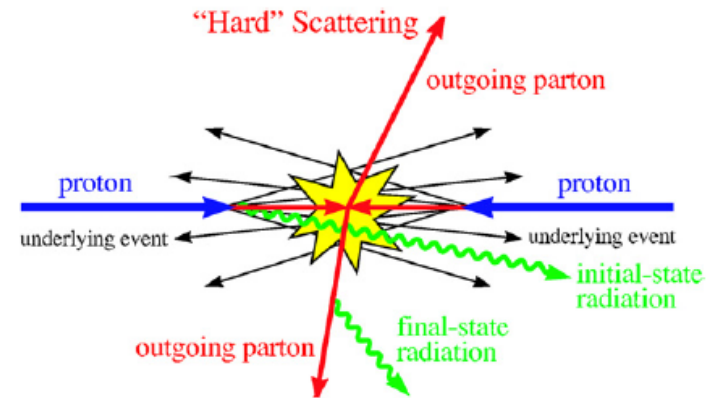


Figure 43. Schematic cartoon of a 2 → 2 hard-scattering event.

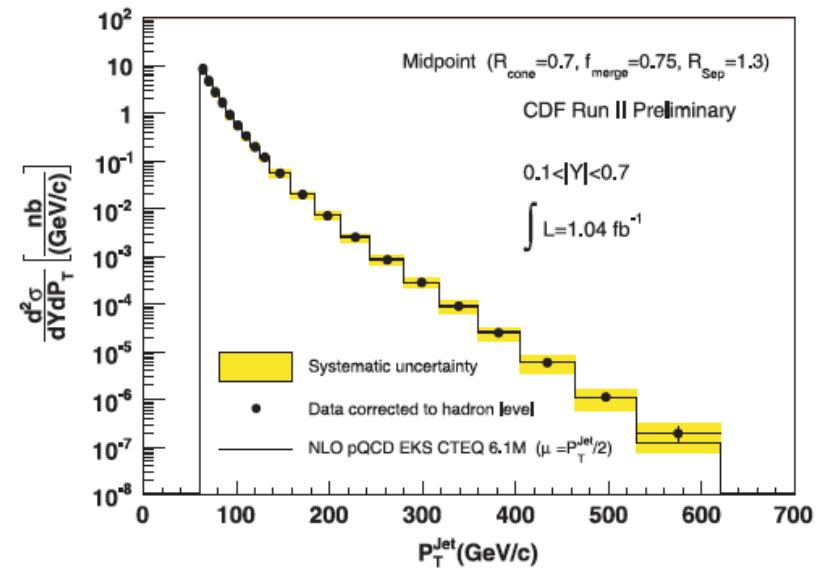


Figure 44. The inclusive jet cross section from CDF in Run 2.

Study of inclusive jet events

- Look at the charged particle transverse momenta in the regions transverse to the dijet direction
- Label the one with the larger amount of transverse momenta the max direction and the one with the smaller amount the min direction
- The momenta in the max direction increases with the p_T of the lead jet, while the momenta in the min cone is constant and is approximately equal to that in a minimum bias event
- “Tunes” to the underlying event model in parton shower Monte Carlos can correctly describe both the max and min regions and can be used for the correct subtraction of UE energy in jet measurements

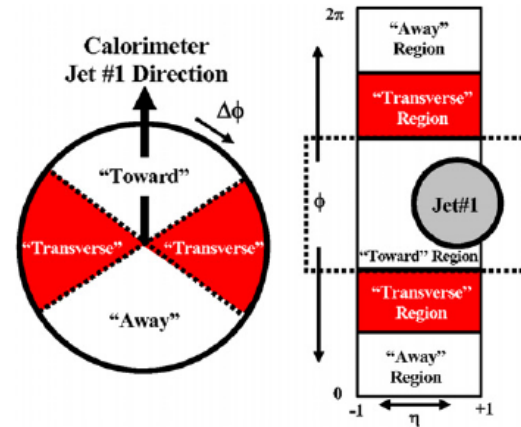


Figure 45. Definition of the ‘toward’, ‘away’ and ‘transverse’ regions.

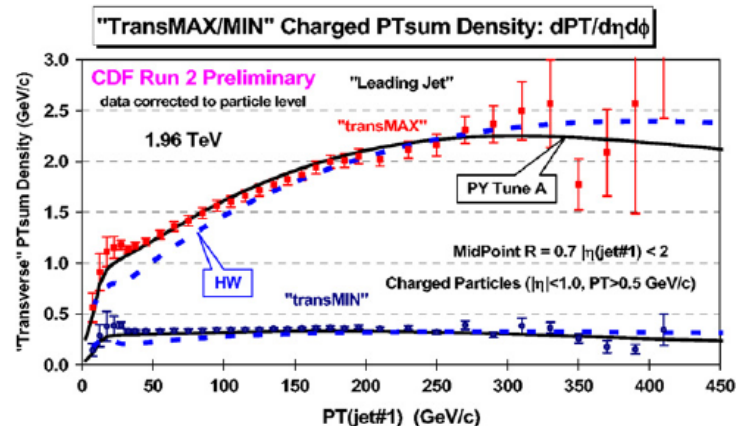


Figure 46. The sum of the transverse momenta of charged particles inside the TransMAX and TransMIN regions, as a function of the transverse momentum of the leading jet.

Hadronization

- Parton showers in the initial and final state produce a large multiplicity of gluons
- The parton shower evolution variable t decreases (for the final state) from a scale similar to the scale of the hard scatter to a scale at which pQCD is no longer applicable (near Λ_{QCD})
- At this point, we must construct models as to how the colored quarks and gluons recombine to form the (colorless) final state hadrons
- The two most popular models are the cluster and string models

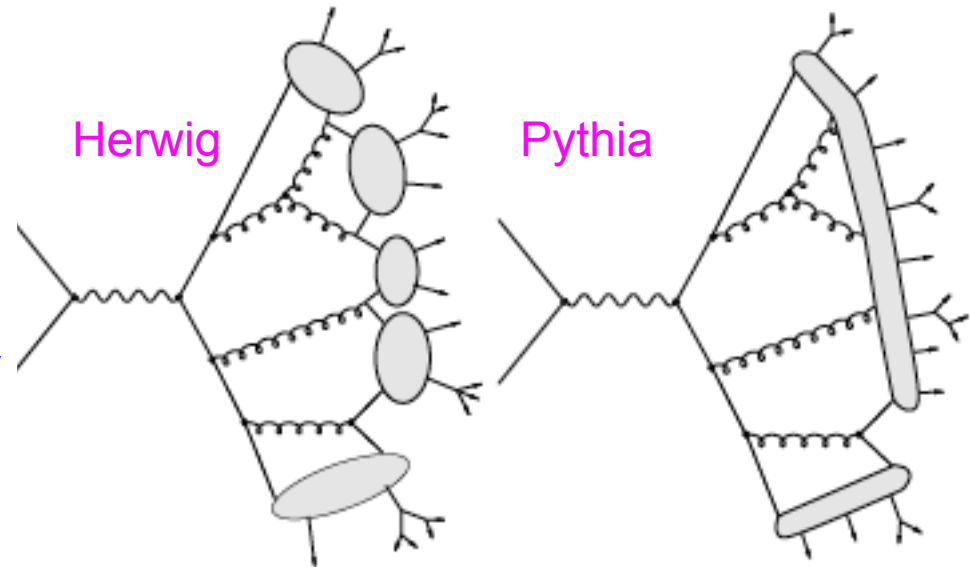


Figure 2: Cluster and string hadronization models.

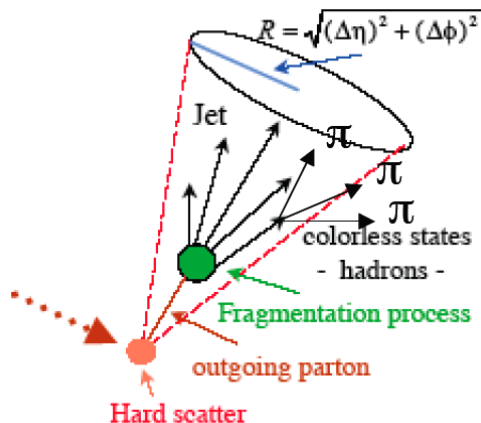
- In cluster model, there is a non-perturbative splitting of gluons into q-qbar pairs; color-singlet combinations of q-qbar pairs form clusters which isotropically decay into pairs of hadrons
- In string model, relativistic string represents color flux; string breaks up into hadrons via q-qbar production in its intense color field

Corrections

- Hadron to parton level corrections

- ◆ subtract energy from the jet cone due to the underlying event
- ◆ add energy back due to hadronization

- ▲ partons whose trajectories lie inside the jet cone produce hadrons landing outside



...partially cancel, but UE correction is larger for cone of 0.7
hadronization corrections for Pythia and Herwig basically identical

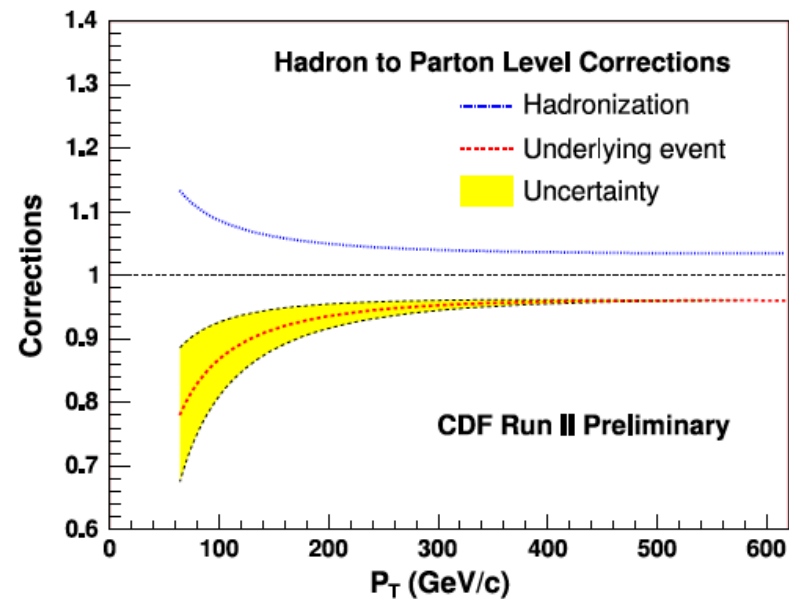


Figure 48. Fragmentation and underlying event corrections for the CDF inclusive jet result, for a cone size $R = 0.7$.

Hadronization corrections

- Can do a back-of-the-envelope calculation with a Field-Feynman-like model

Splash-out. Some of the partonic transverse energy can leak out of the jet cone. The order α_s^3 perturbation theory gets this effect partly right: in a three parton final state the third parton can escape the jet cone. However, using the picture embedded in Monte Carlo models, the late stages of partonic branching and the final hadronization of the partons can also result in transverse energy escaping the jet cone. Here is a simple model for this effect.

Consider the hadrons that represent the decay products of a high E_T parton. Let η be the rapidity of the hadrons relative to jet axis. Let \vec{k}_T be the transverse momentum of the particles relative to jet axis. Let the distribution of hadrons be

$$\frac{dN}{d\eta d\vec{k}_T} = \frac{A}{\pi \langle k_T^2 \rangle} \exp \left\{ -k_T^2 / \langle k_T^2 \rangle \right\}, \quad (10)$$

where A is the number of hadrons per unit rapidity and $\langle k_T^2 \rangle$ is average k_T^2 of the hadrons. Then the E_T lost is approximately

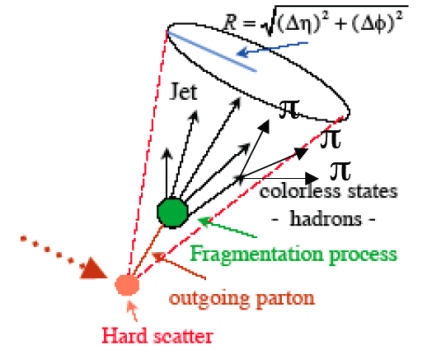
$$E_T^{\text{out}} = \int_0^{\eta_1} d\eta \int d\vec{k}_T \frac{1}{2} |\vec{k}_T| e^\eta \frac{dN}{d\eta d\vec{k}_T}, \quad (11)$$

where $\eta_1 = -\ln(\tan(R/2))$. Performing the integral gives

$$E_T^{\text{out}} = \frac{\sqrt{\pi}}{4} A \sqrt{\langle k_T^2 \rangle} (e^{\eta_1} - 1). \quad (12)$$

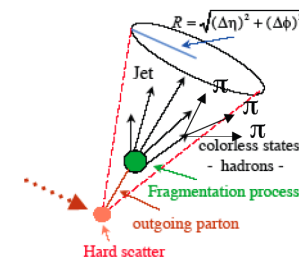
Taking $\sqrt{\langle k_T^2 \rangle} = 0.3 \text{ GeV}$ and¹⁰⁾ $A = 5$, I find

$$E_T^{\text{out}} \approx 1.1 \text{ GeV}. \quad (13)$$



Hadronization corrections

- Or can study a parton shower Monte Carlo with hadronization on/off
 - ◆ and again find on the order of 1 GeV/c (for a cone of radius 0.7 at the Tevatron)
 - ◆ NB: hadronization correction for NLO (at most 2 partons in a jet) = the correction for parton showers (many partons in a jet) to the extent that the jet shapes are the same at the NLO and parton shower level
- What is the dependence of the hadronization corrections (also called splashout) on jet transverse momentum?
 - ◆ not so much (as Borat might say)
- This may seem surprising (that the correction does not increase with the jet p_T)
- But jets get narrower as the p_T increases (see later), so the parton level energy in the outermost annulus of the jet (where the splashout originates) is fairly constant as a function of jet p_T



Corrections

- Hadron to parton level corrections
 - ◆ subtract energy from the jet cone due to the underlying event
 - ◆ add energy back due to hadronization
 - ▲ partons whose trajectories lie inside the jet cone produce hadrons landing outside
- Corrections determined by Monte Carlo, turning on/off each element
 - ◆ possible because the UE was tuned to describe global event characteristics at the Tevatron
- Result is in good agreement with NLO pQCD predictions using CTEQ6.1 pdf's
 - ◆ pdf uncertainty is similar to experimental systematic errors

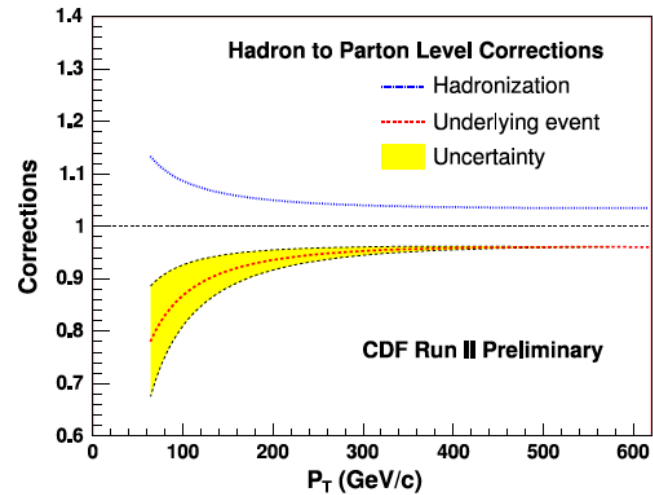


Figure 48. Fragmentation and underlying event corrections for the CDF inclusive jet result, for a cone size $R = 0.7$.

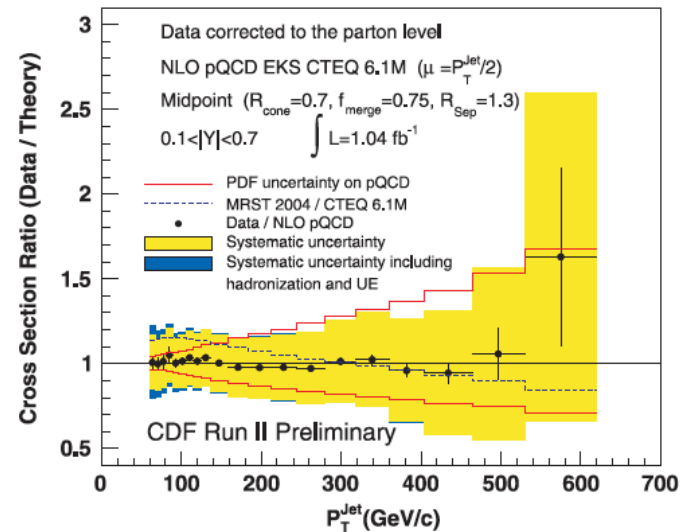


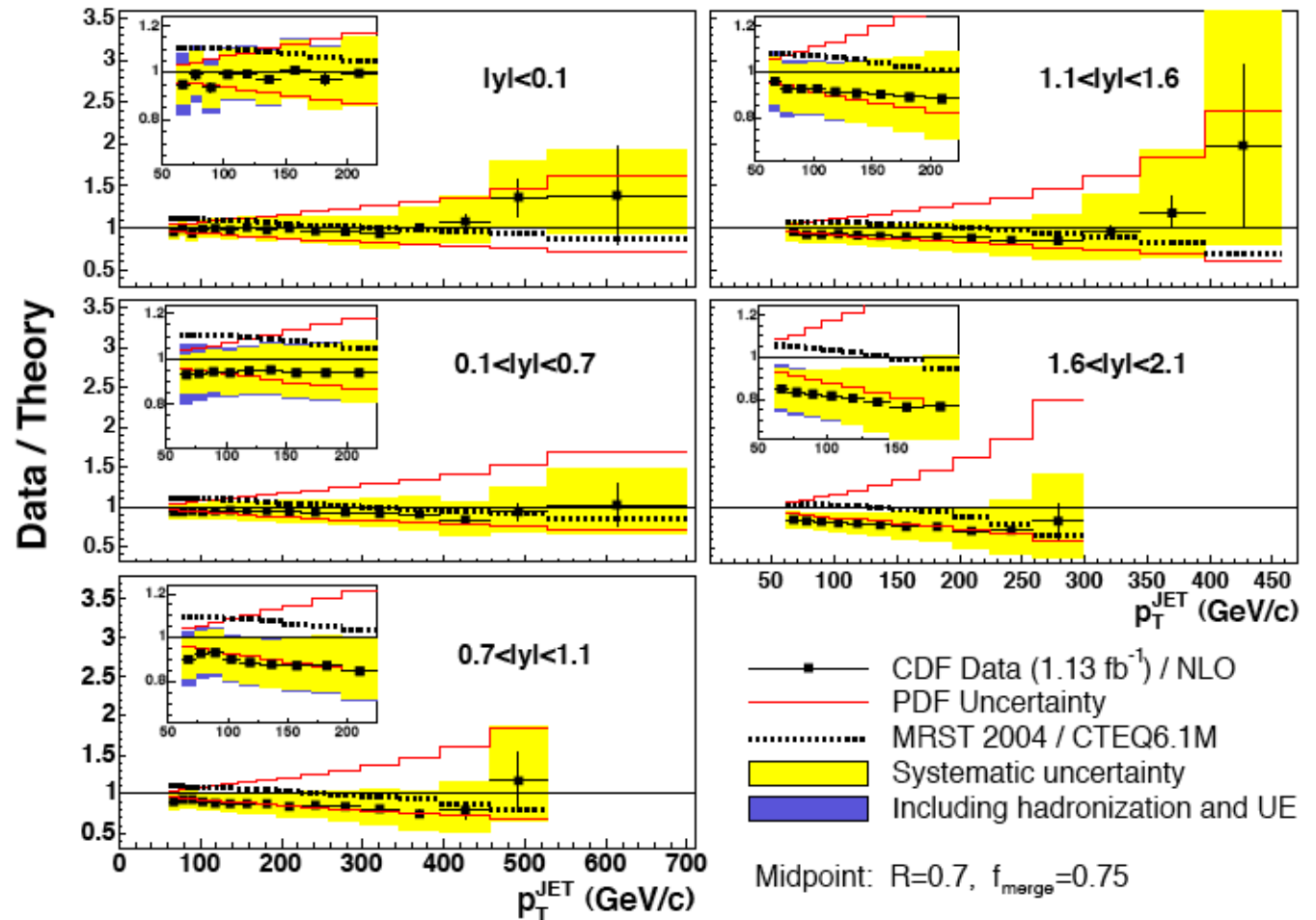
Figure 49. The inclusive jet cross section from CDF in Run 2 compared on a linear scale to NLO theoretical predictions using CTEQ6.1 and MRST2004 pdfs.

Inclusive jet cross section

new physics tends to be central

pdf explanations are universal

crucial to measure over a wide rapidity interval



Full disclosure for experimentalists

- Every cross section should be quoted at the hadron level with an explicit correction given between the hadron and parton levels

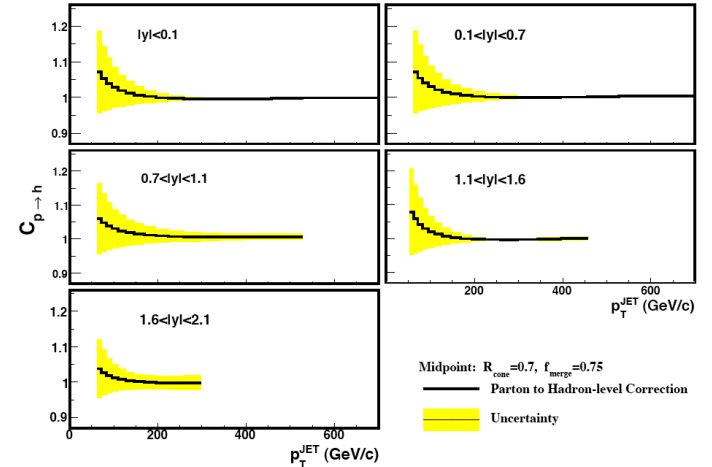


TABLE IX: Measured inclusive jet cross sections as a function of p_T for jets in the region $0.1 < |y| < 0.7$ together with the statistical (*stat.*) and systematic (*sys.*) uncertainties. The bin-by-bin parton-to-hadron-level ($C_{p \rightarrow h}$) corrections are also shown.

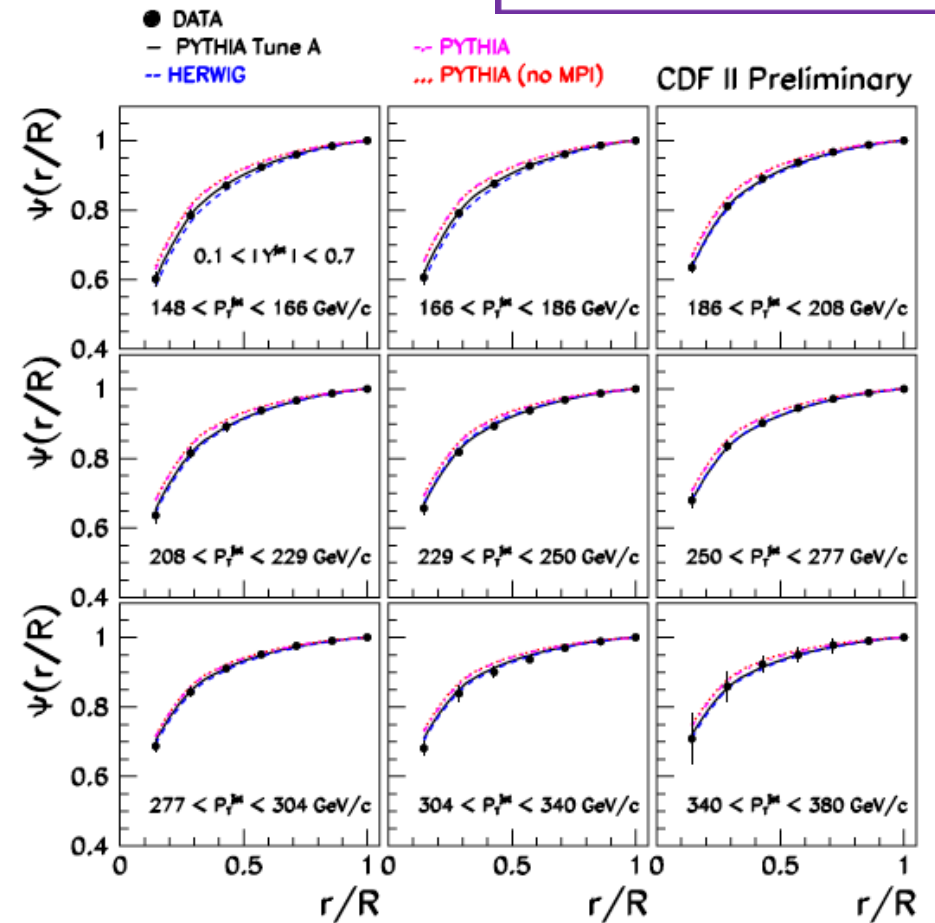
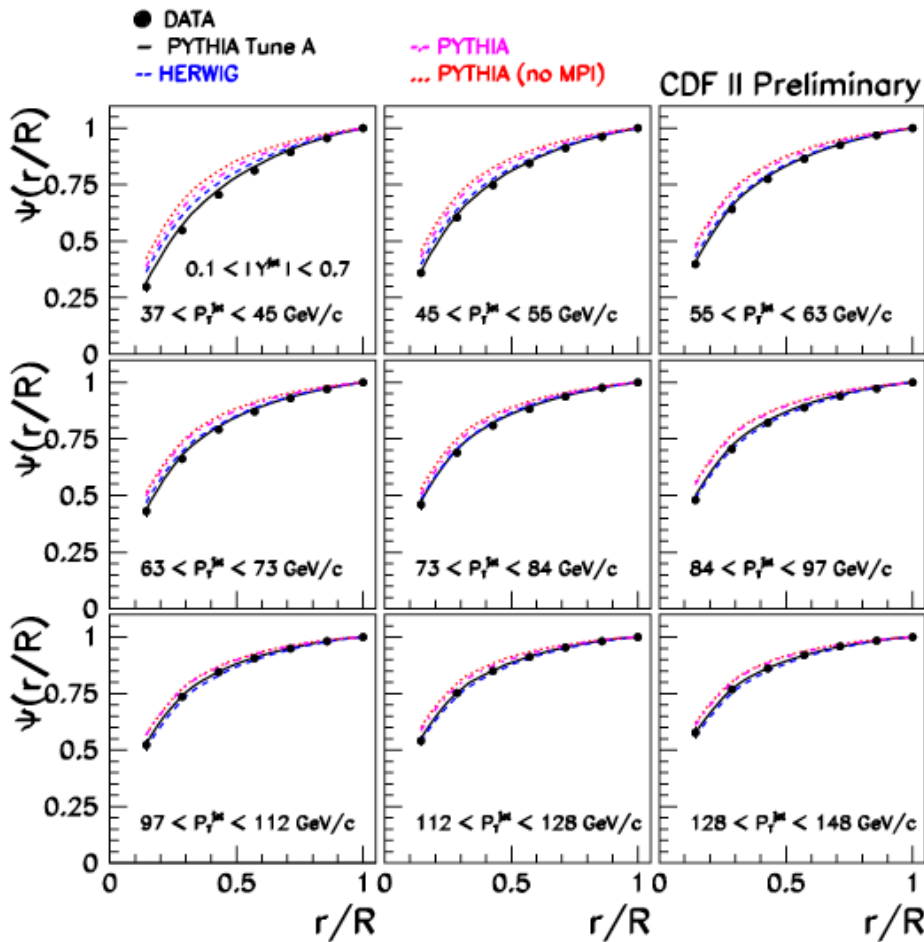
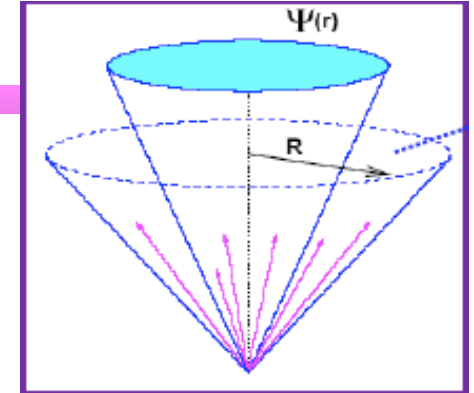
p_T (GeV/c)	$0.1 < y < 0.7$ $\sigma \pm (stat.) \pm (sys.)$ [nb/(GeV/c)]	$C_{p \rightarrow h}$
62 – 72	$(6.28 \pm 0.04^{+0.59}_{-0.56}) \times 10^0$	1.072 ± 0.108
72 – 83	$(2.70 \pm 0.02^{+0.26}_{-0.25}) \times 10^0$	1.055 ± 0.088
83 – 96	$(1.15 \pm 0.01^{+0.11}_{-0.11}) \times 10^0$	1.041 ± 0.071
96 – 110	$(4.88 \pm 0.03^{+0.51}_{-0.48}) \times 10^{-1}$	1.030 ± 0.057
110 – 127	$(2.07 \pm 0.01^{+0.22}_{-0.21}) \times 10^{-1}$	1.022 ± 0.045
127 – 146	$(8.50 \pm 0.04^{+0.98}_{-0.91}) \times 10^{-2}$	1.015 ± 0.035
146 – 169	$(3.30 \pm 0.01^{+0.41}_{-0.38}) \times 10^{-2}$	1.010 ± 0.027
169 – 195	$(1.24 \pm 0.01^{+0.17}_{-0.15}) \times 10^{-2}$	1.006 ± 0.020
195 – 224	$(4.55 \pm 0.05^{+0.67}_{-0.61}) \times 10^{-3}$	1.003 ± 0.014
224 – 259	$(1.56 \pm 0.01^{+0.25}_{-0.23}) \times 10^{-3}$	1.002 ± 0.010
259 – 298	$(4.94 \pm 0.06^{+0.91}_{-0.80}) \times 10^{-4}$	1.001 ± 0.006
298 – 344	$(1.42 \pm 0.02^{+0.30}_{-0.26}) \times 10^{-4}$	1.000 ± 0.003
344 – 396	$(3.53 \pm 0.08^{+0.85}_{-0.73}) \times 10^{-5}$	1.001 ± 0.001
396 – 457	$(6.87 \pm 0.35^{+1.93}_{-1.64}) \times 10^{-6}$	1.001 ± 0.000
457 – 527	$(1.22 \pm 0.13^{+0.40}_{-0.34}) \times 10^{-6}$	1.003 ± 0.001
527 – 700	$(7.08 \pm 1.97^{+3.09}_{-2.54}) \times 10^{-8}$	1.005 ± 0.001

regions. The correction is derived from PYTHIA (solid line) for the correction is conservatively taken as the systematic

note the correction rapidly approaches unity

Jet Shapes

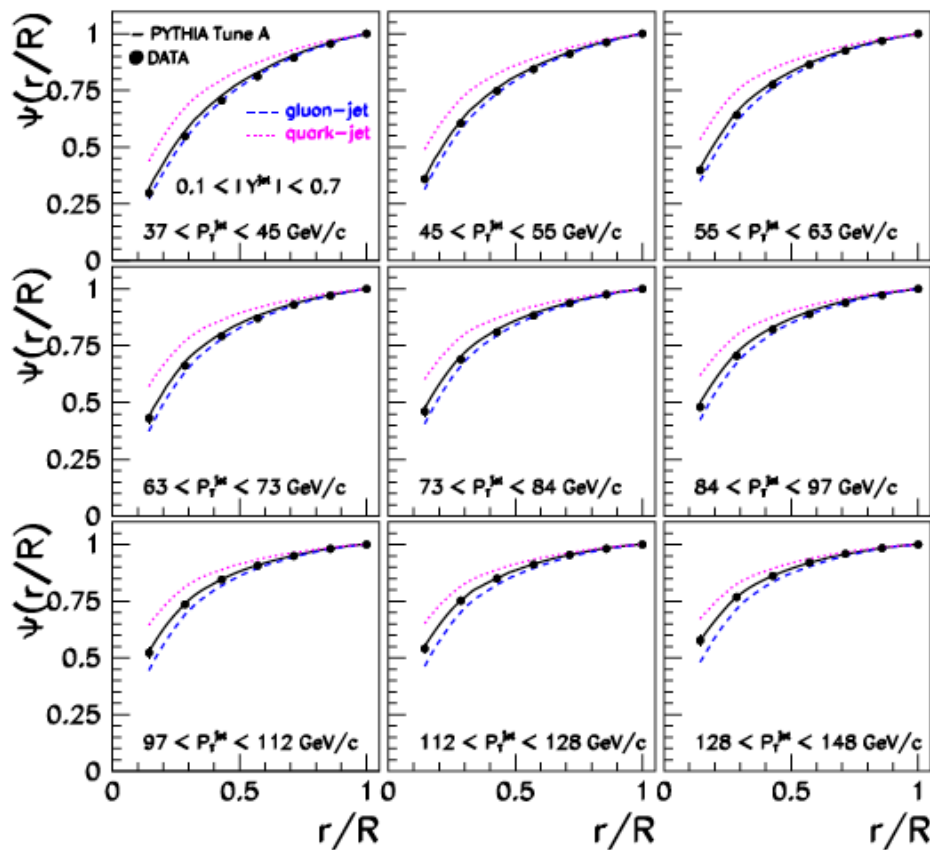
- Jets get narrower as the jet p_T increases
 - ◆ smaller rate of hard gluon emission as α_s decreases (can be used to try to determine α_s)
 - ◆ jets switch from being gluon-induced to quark-induced



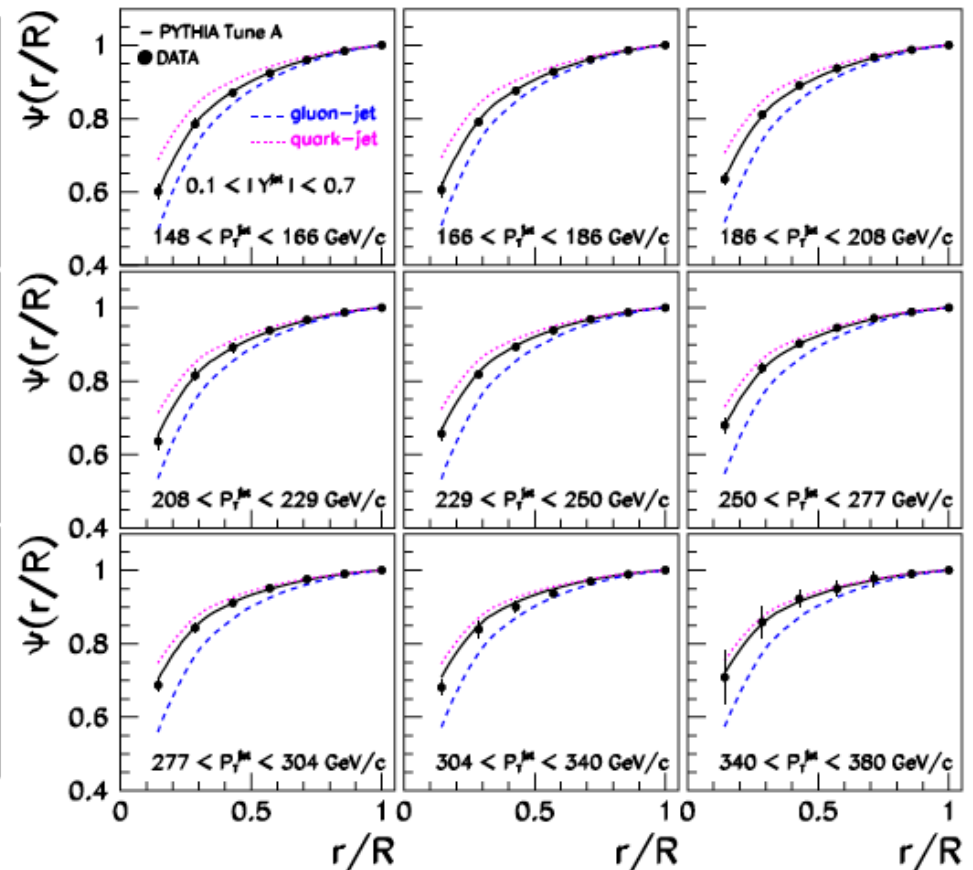
Jet Shapes: quark and gluon differences

- Pythia does a good job of describing jet shapes
 - ◆ parton showering + hadronization + multiple parton interactions
- If effects of the underlying event are subtracted out, NLO (where a jet is described by at most two partons) also describes the jet shapes well

CDF II Preliminary



CDF II Preliminary



Quark/gluon jet shape differences

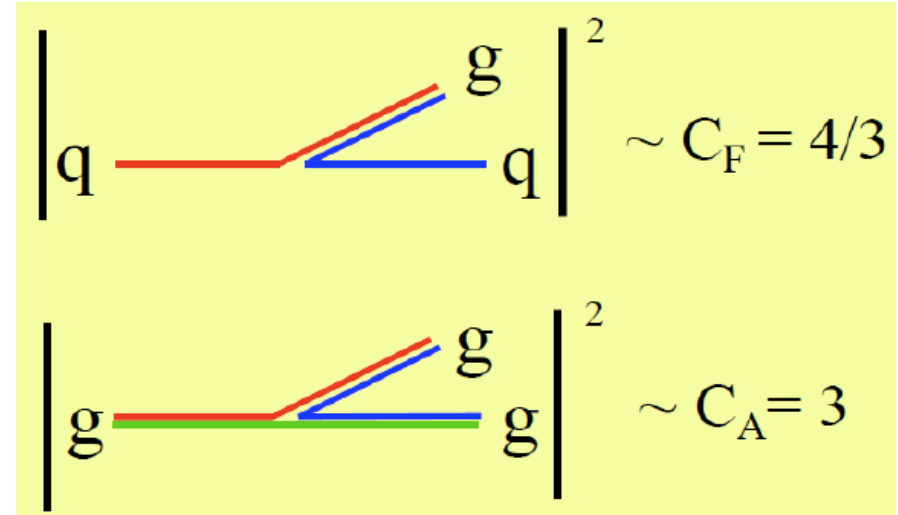
- Quarks and gluons radiate proportional to their color factors

$$r \equiv \frac{\langle n_g \rangle}{\langle n_q \rangle} \equiv \frac{\langle \text{gluon jet multiplicity} \rangle}{\langle \text{quark jet multiplicity} \rangle}$$

- At leading order

$$r = \frac{\langle C_A \rangle}{\langle C_F \rangle} = \frac{9}{4} = 2.25$$

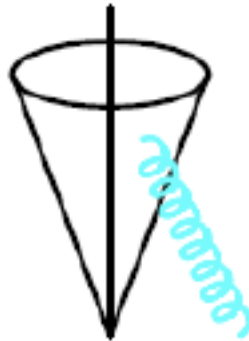
- With higher order corrections, $r \sim 1.5$



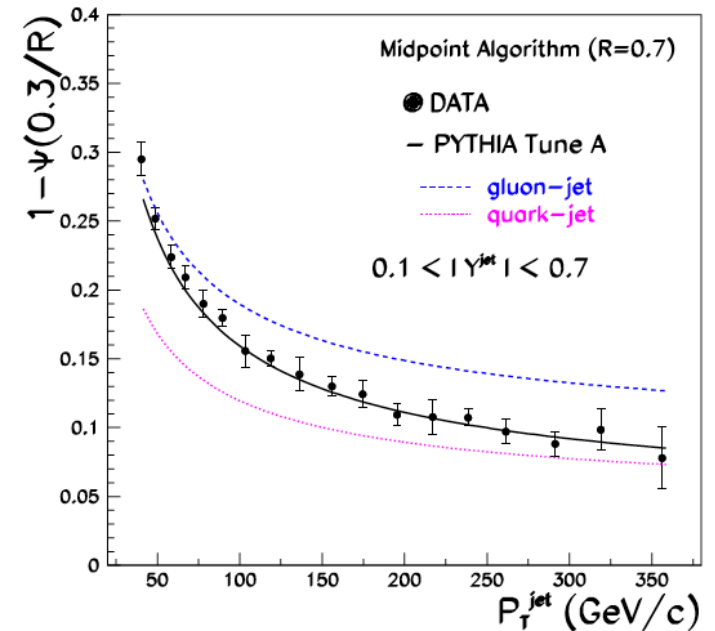
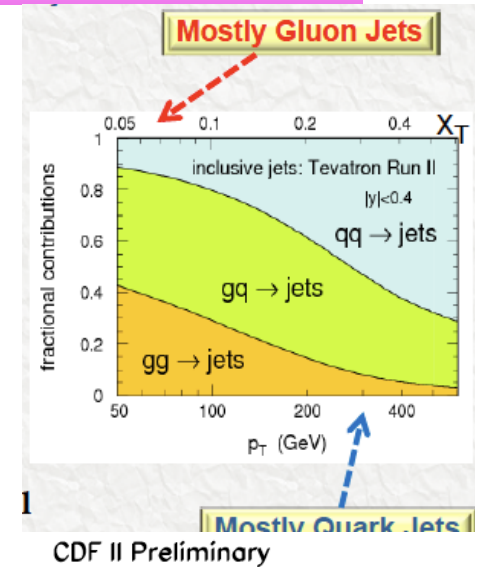
Jet shapes

- Look at the fraction of jet energy in cone of radius 0.7 that is outside the “core” (0.3)
- Gluon jets are always broader than quark jets, but both get narrower with increasing jet p_T
- How to correct for the jet energy outside the prescribed cone?

- ◆ a NLO calculation “knows” about the energy outside the cone, so no correction is needed/wanted
- ◆ for LO comparisons, can correct based on Monte Carlo simulations



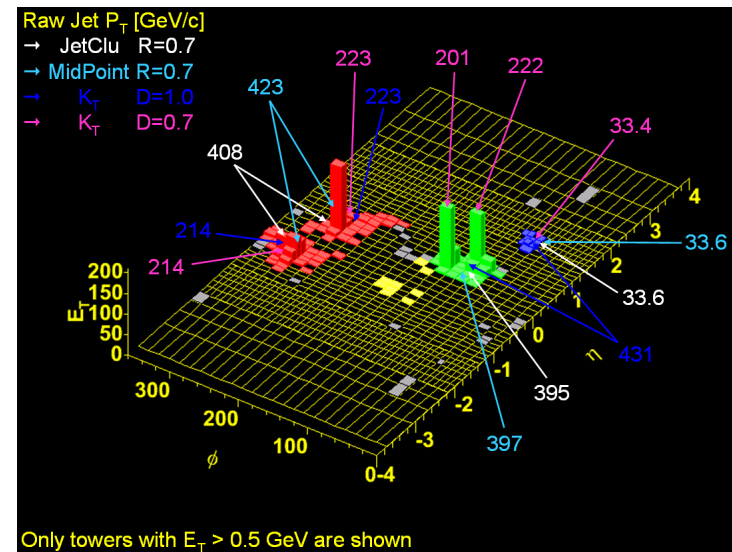
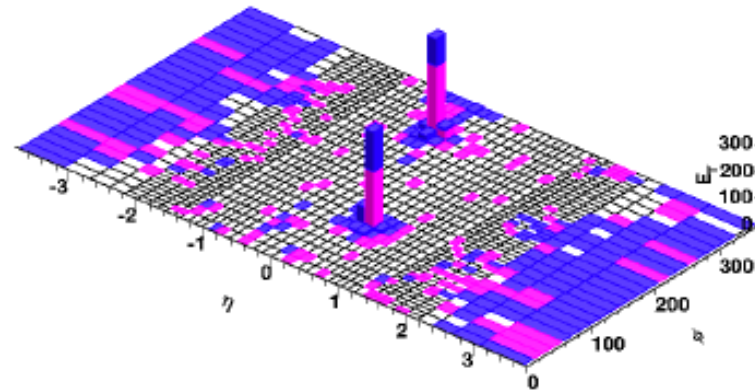
at small p_T , jet production dominated by gg and gq scattering due to large gluon distribution at low x



Back to jet algorithms

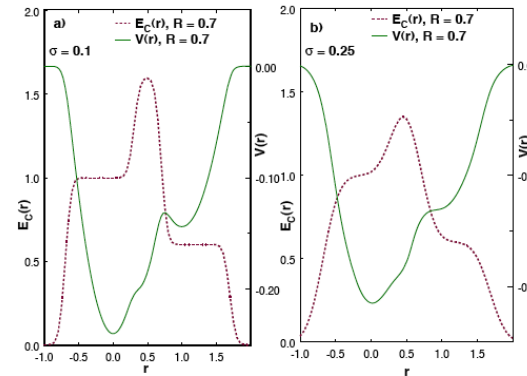
- For some events, the jet structure is very clear and there's little ambiguity about the assignment of towers to the jet
- But for other events, there is ambiguity and the jet algorithm must make decisions that impact precision measurements
- If comparison is to hadron-level Monte Carlo, then hope is that the Monte Carlo will reproduce all of the physics present in the data and influence of jet algorithms can be understood
 - ◆ more difficulty when comparing to parton level calculations

CDF Run II events



Jets in real life

- Jets don't consist of 1 fermi partons but have a spatial distribution
- Can approximate jet shape as a Gaussian smearing of the spatial distribution of the parton energy
 - ◆ the effective sigma ranges between around 0.1 and 0.3 depending on the parton type (quark or gluon) and on the parton p_T
- Note that because of the effects of smearing that
 - ◆ the midpoint solution is **(almost always) lost**
 - ▲ thus region II is effectively truncated to the area shown on the right
 - ◆ the solution corresponding to the lower energy parton can also be lost
 - ▲ resulting in dark towers



remember the Snowmass potentials

Figure 52. A schematic depiction of the effects of smearing on the midpoint cone jet clustering algorithm.

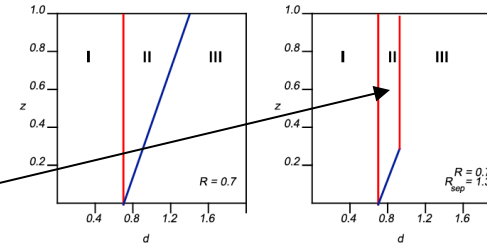


Figure 22. The parameter space (d, Z) for which two partons will be merged into a single jet.

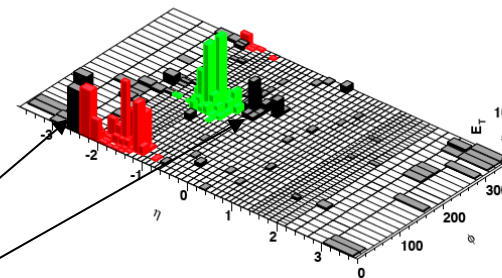


Figure 50. An example of a Monte Carlo inclusive jet event where the midpoint algorithm has left substantial energy unclustered.

Jets in real life

- In NLO theory, can mimic the impact of the truncation of Region II by including a parameter called R_{sep}
 - ◆ only merge two partons if they are within $R_{\text{sep}} * R_{\text{cone}}$ of each other
 - ▲ $R_{\text{sep}} \sim 1.3$
 - ◆ ~4-5% effect on the theory cross section; effect is smaller with the use of p_T rather than E_T
 - ◆ really upsets the theorists (but there are also disadvantages)
- Dark tower effect is also on order of few (<5)% effect on the (experimental) cross section
- Dark towers affect every cone algorithm

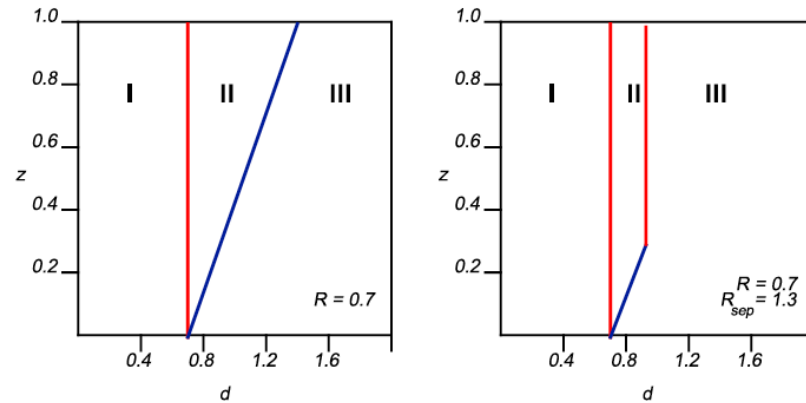


Figure 22. The parameter space (d, Z) for which two partons will be merged into a single jet.

Comparison of k_T and cone results

- Remember
 - at NLO the k_T algorithm corresponds to Region I (for $D=R$); thus at parton level, the cone algorithm is always larger than the k_T algorithm
- Let's check this out with CDF results after applying hadronization corrections
- Nice confirmation of the perturbative picture

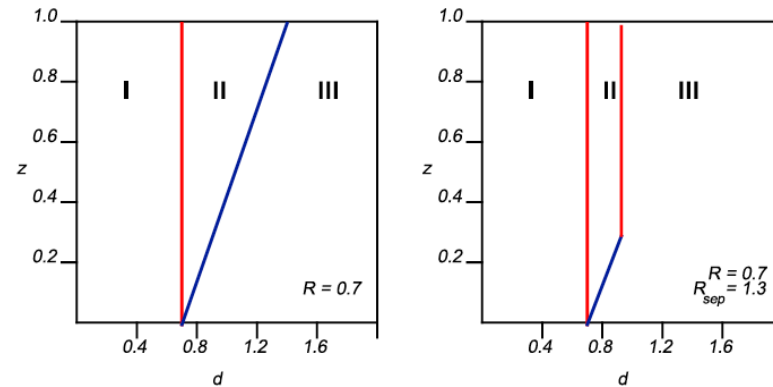
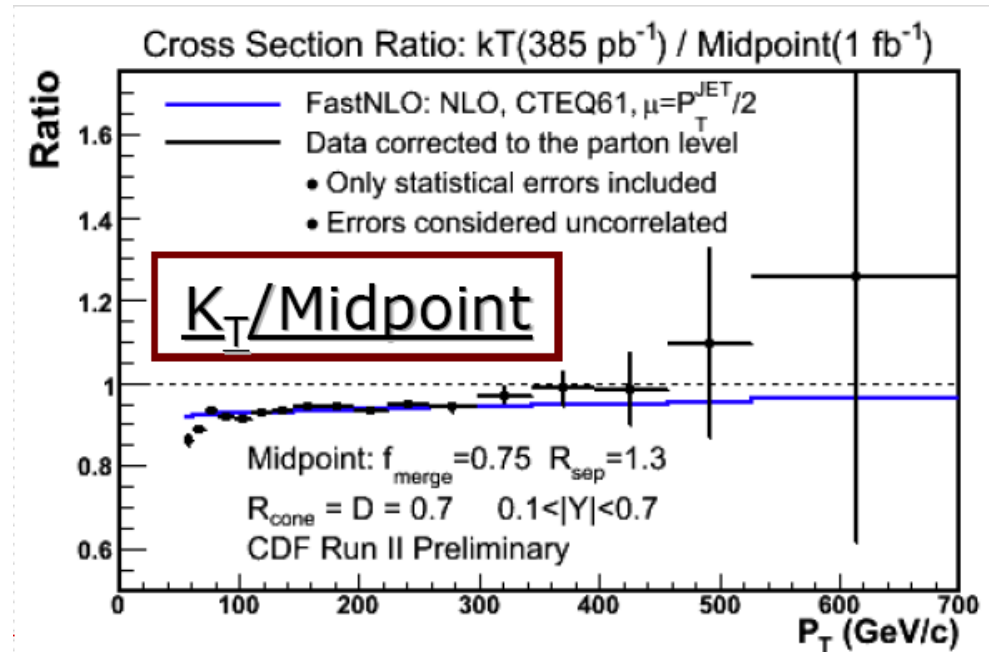


Figure 22. The parameter space (d, Z) for which two partons will be merged into a single jet.



k_T /midpoint ratios for all rapidities

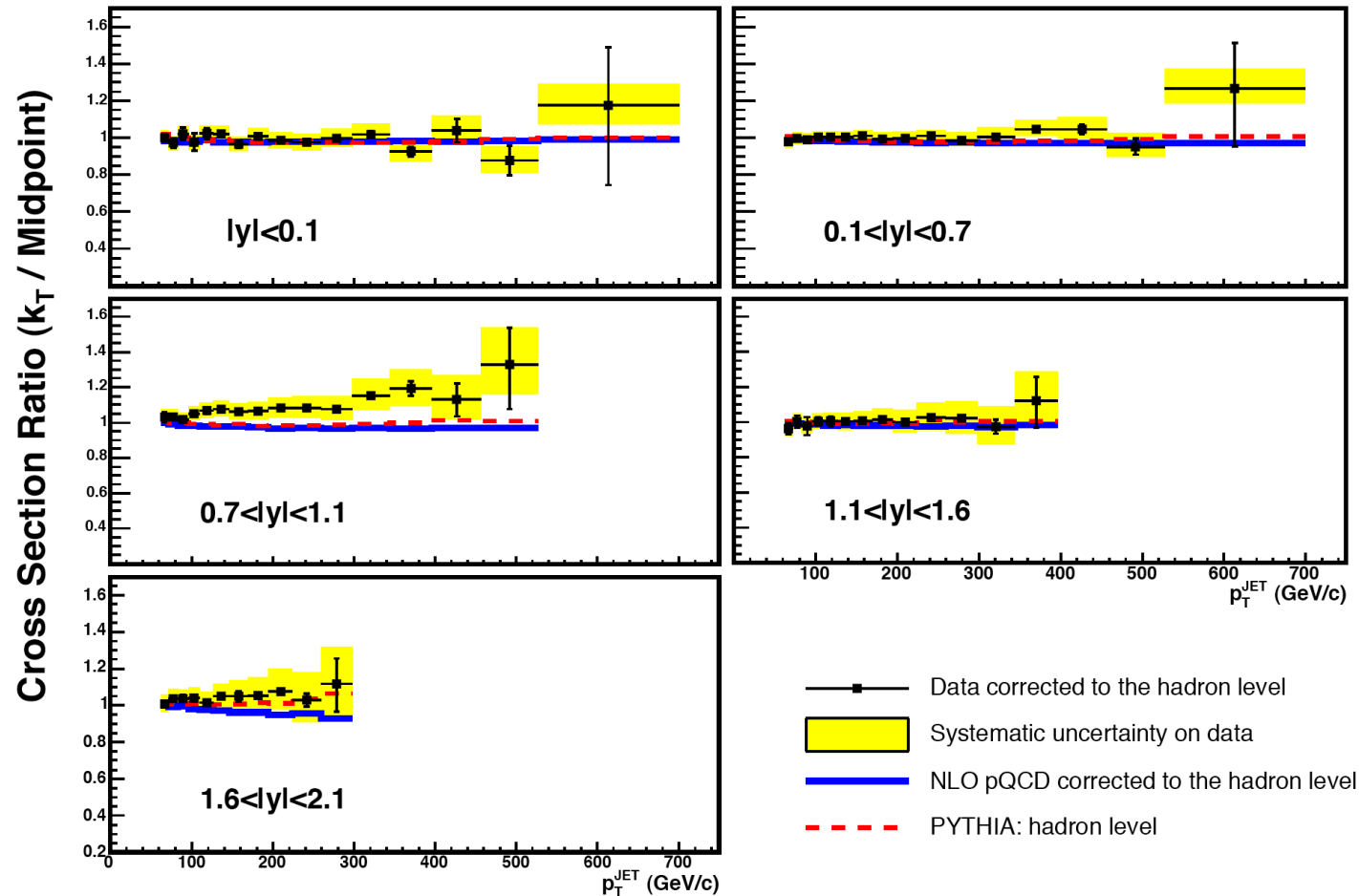
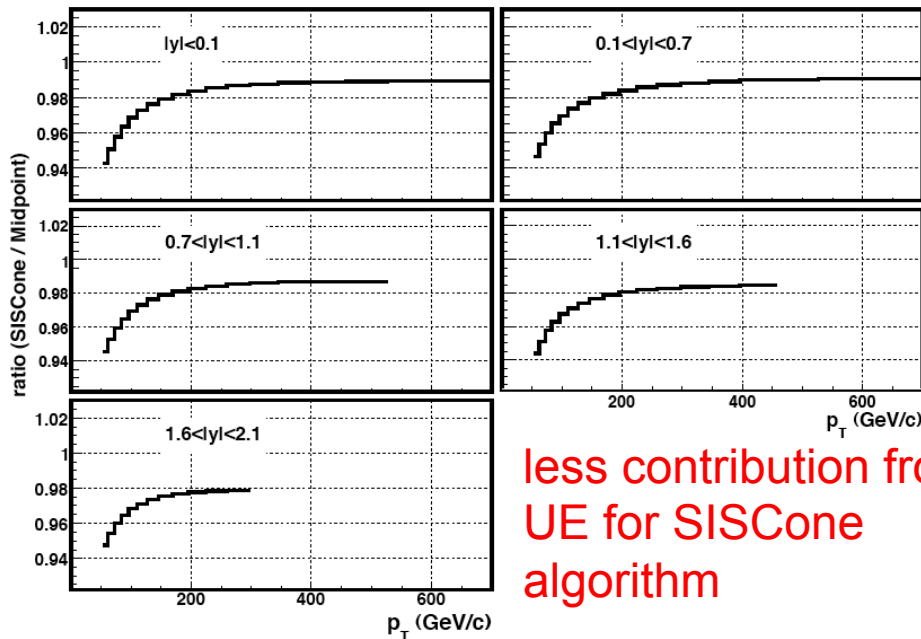


FIG. 17: The ratios of the inclusive jet cross sections measured using the k_T algorithm with $D = 0.7$ [9] to those measured using the Midpoint jet finding algorithm with $R_{\text{cone}} = 0.7$ in this paper (points). The systematic uncertainty on the ratio is given as the yellow band. The predictions from NLO pQCD (solid lines) and PYTHIA (dashed lines) for this ratio are also shown.

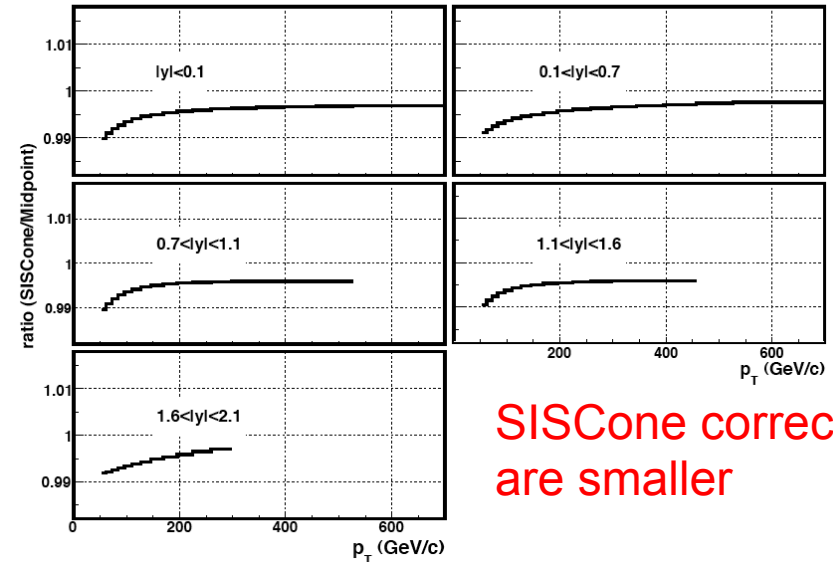
SISCone vs Midpoint

- The SISCone jet algorithm developed by Salam et al is preferred from a theoretical basis, as there is less IR sensitivity from not requiring any seeds as the starting point of a jet

Hadron Level: Midpoint versus SISCone



Parton Level (UE off): Midpoint versus SISCone



- So far, at the Tevatron, we have not explicitly measured a jet cross section using the SISCone algorithm, although studies are underway, but we have done some Monte Carlo comparisons for the inclusive cross sections
- Differences of the order of a few percent at the hadron level reduce to $< 1\%$ at the parton level

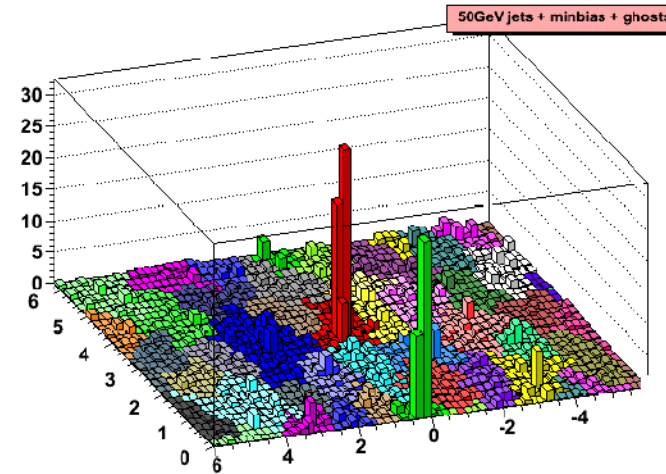
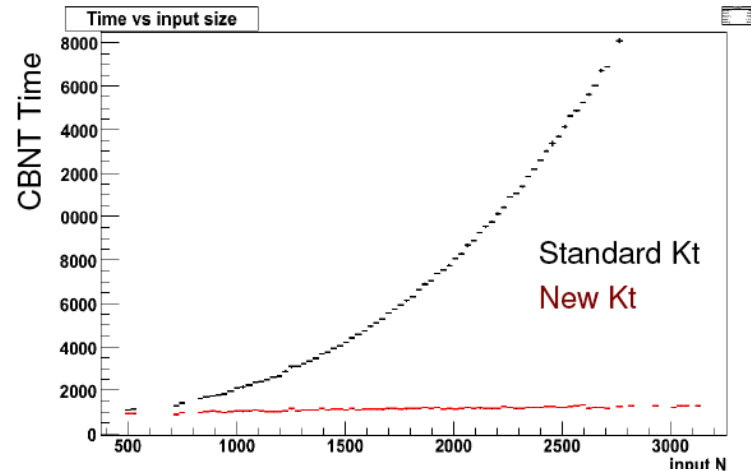
New k_T family algorithms

- k_T algorithms are typically slow because speed goes as $O(N^3)$, where N is the number of inputs (towers, particles,...)
- Cacciari and Salam (hep-ph/0512210) have shown that complexity can be reduced and speed increased to $O(N)$ by using information relating to geometric nearest neighbors
- Anti- k_T from Cacciari and Salam (reverse k_T : Pierre-Antoine Delsart) clusters soft particles with hard particles first
- Now the algorithm of choice for both ATLAS and CMS

$$d_{ij} = \min\left(p_{T,i}^{2p}, p_{T,j}^{2p}\right) \frac{\Delta R_{ij}^2}{D^2}$$

$$d_{ii} = p_{T,i}^{2p}$$

$p=0$; C-A
 $p=1$: k_T
 $p=-1$ anti- k_T

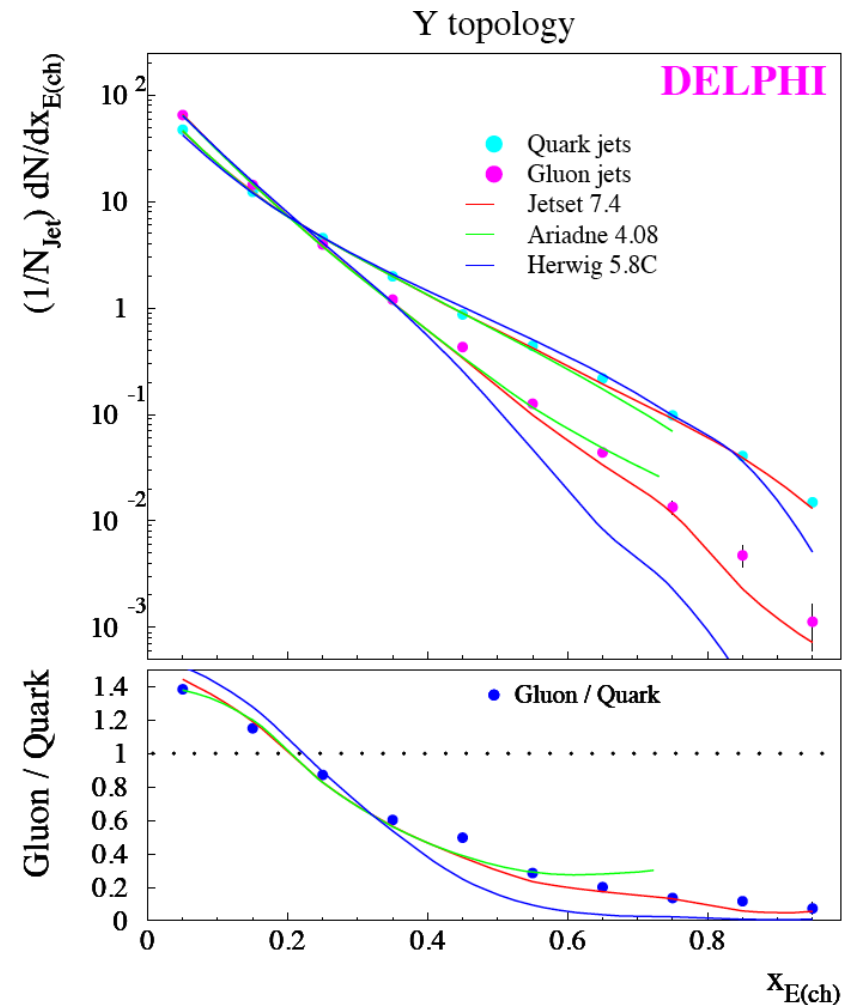


~ 10000 particles
 Clustering takes ~ 20 minutes with old methods.
 0.6s with FastJet.



Fragmentation functions

- On a more inclusive note, can define a fragmentation function $D(z, Q^2)$ that describes the probability to find a hadron of momentum fraction z (of the parent parton) at a scale Q
- The parton shower dynamically generates the fragmentation function, but the evolution of the fragmentation function with Q^2 can be calculated in pQCD (just as the evolution of the parton distribution functions can be calculated)
- But, like the PDFs, the value of $D(z, Q_0)$ is not known and must be determined by fits to data
- The data from LEP are the most useful for their determination



NB: the gluon fragmentation function is much softer; Herwig does not describe the high z gluon fragmentation function well

Some more details

- For outgoing quarks and gluons, have collinear singularities just as for the parton distribution functions
- Fragmentation functions acquire μ dependence just as PDFs did

$$\mu^2 \frac{\partial}{\partial \mu^2} D_i(x, \mu^2) = \sum_j \int_x^1 \frac{dz}{z} \frac{\alpha_s(\mu^2)}{2\pi} D_j\left(\frac{x}{z}, \mu^2\right) P_{ji}(z, \alpha_s(\mu^2))$$

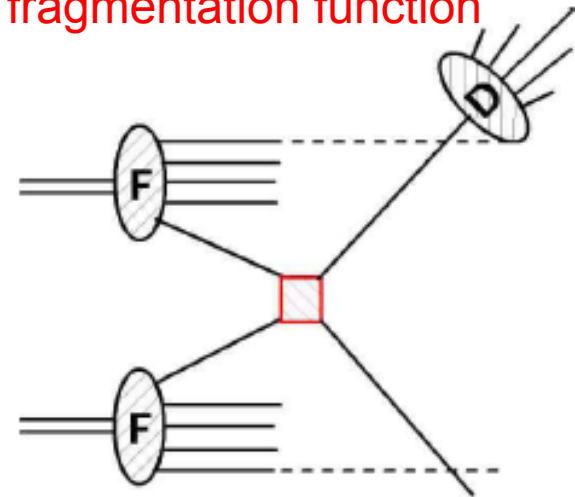
- ...just like DGLAP

$$\frac{d\sigma_{pp}^\pi}{d\eta dp_T^2} = \iiint f_{a/p}(x_a, \mu_F) \otimes f_{b/p}(x_b, \mu_F) \otimes \hat{\sigma}_{ab \rightarrow c}\left(p_T, \frac{s}{p_T^2}, x_1, x_2, z, \frac{p_T}{\mu_F}, \frac{p_T}{\mu}\right) \otimes D_{\pi/c}(z, \mu_F) \times \left\{1 + \mathcal{O}\left(\frac{m^2}{p_T^2}\right)\right\}$$

- Lowest order splitting functions are identical to those discussed for PDFs

$$P_{ji}(z, \alpha_s(\mu^2)) = P_{ji}^{(0)} + \frac{\alpha_s(\mu^2)}{2\pi} P_{ji}^{(1)}(z) + \dots$$

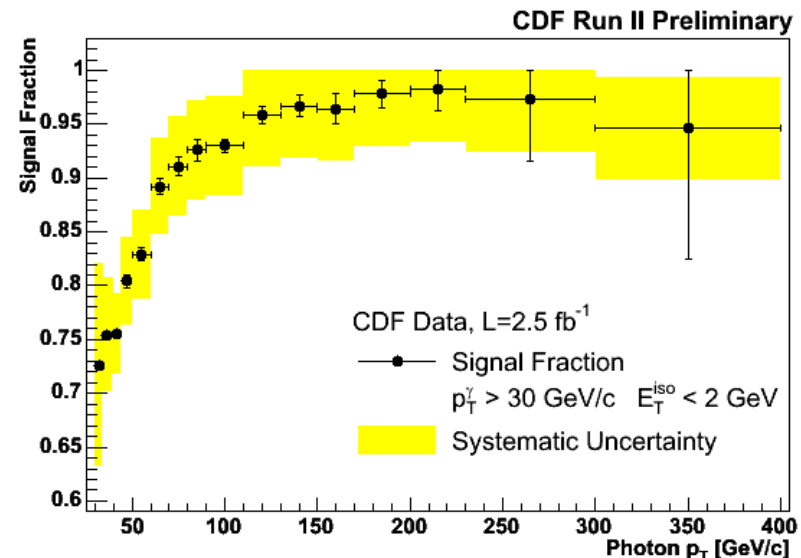
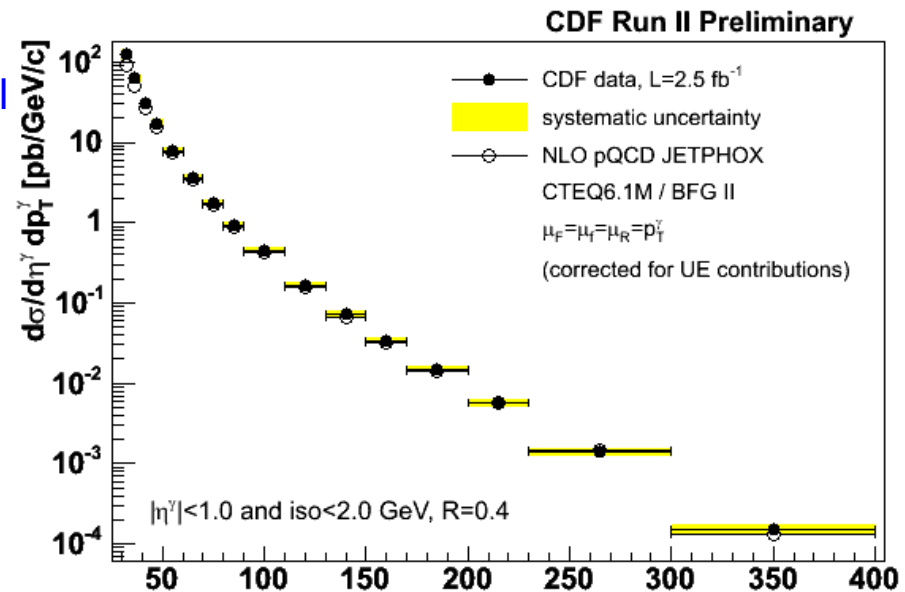
Calculate single particle cross section by convoluting over fragmentation function



Sum over all fragmentation functions, apply a jet algorithm and voila you have a jet cross section

Photon production

- Production doesn't go out to as high a transverse momentum as for jets since the cross section is proportional to $\alpha\alpha_s$
- Photons can either be direct or from fragmentation processes
 - ◆ $q \rightarrow q\gamma$
- There are backgrounds from jets which fragment into π^0 's which contain most of the momentum (i.e. high z) of the original parton (quarks, not gluons)
- By imposing an isolation cut around the photon direction, the signal fraction can be greatly increased
- The isolation cut can either be a fraction of the photon transverse momentum, or a fixed cut
- To the right, the energy in the isolation cone is required to be less than 2 GeV (corrected for pileup)
 - ◆ this energy is dominated by the UE



Comparison to NLO prediction

- Good agreement above 50 GeV/c
- Discrepancy below 50 GeV/c
- Also seen by D0 and by previous collider measurements of photon cross sections
- What gives?
- Remember the p_T of the W; here we had a two-scale problem (m_W and p_T^W); near $p_T \sim 0$, the log was large and the effects of soft gluon radiation had to be resummed

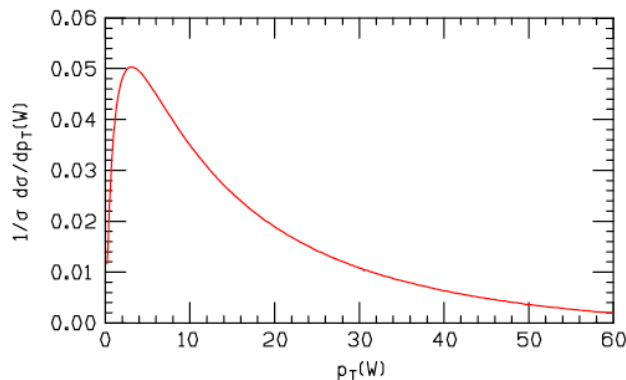
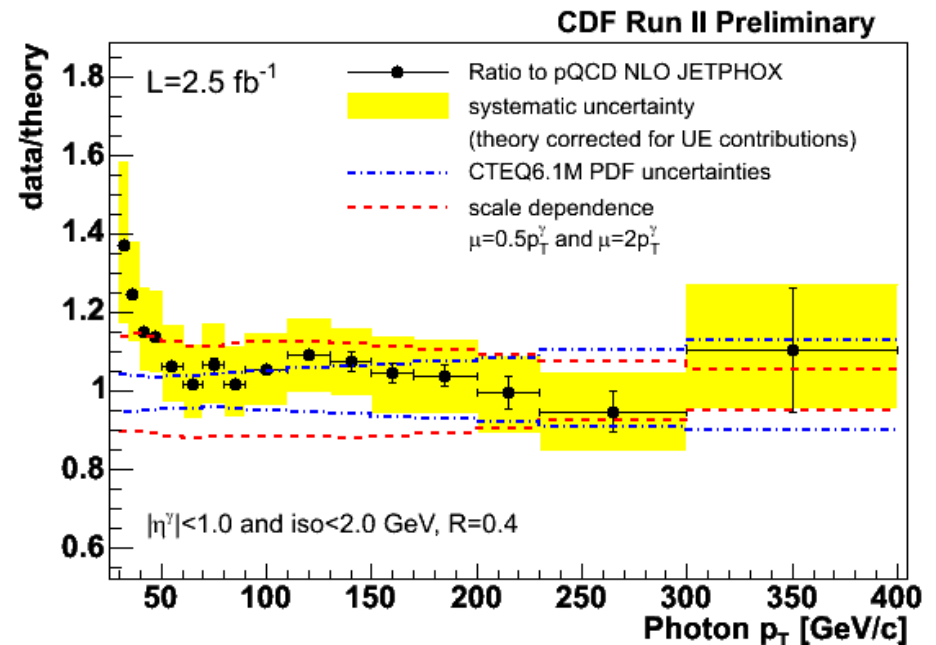
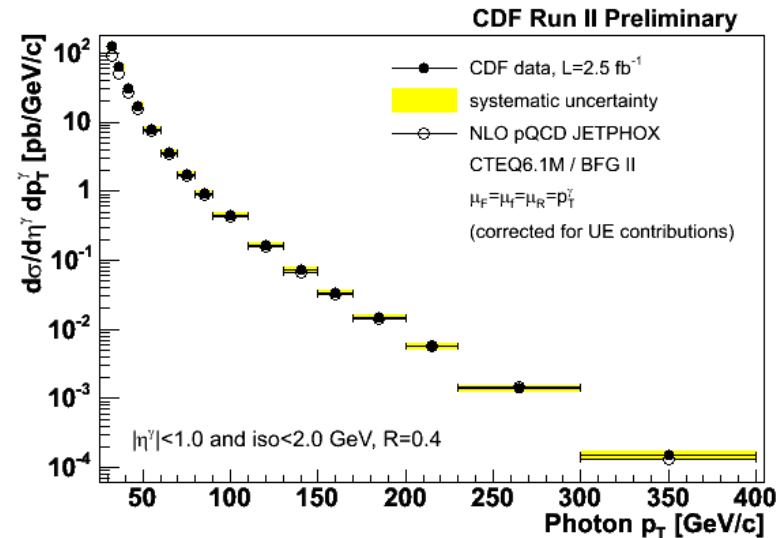
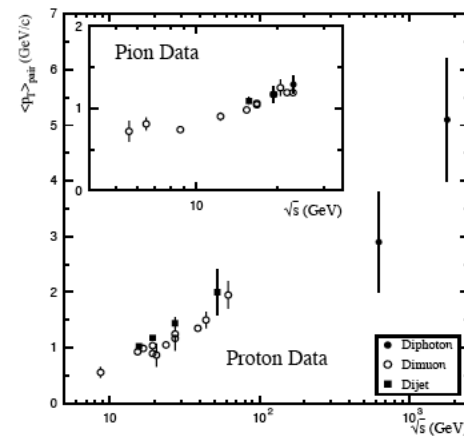
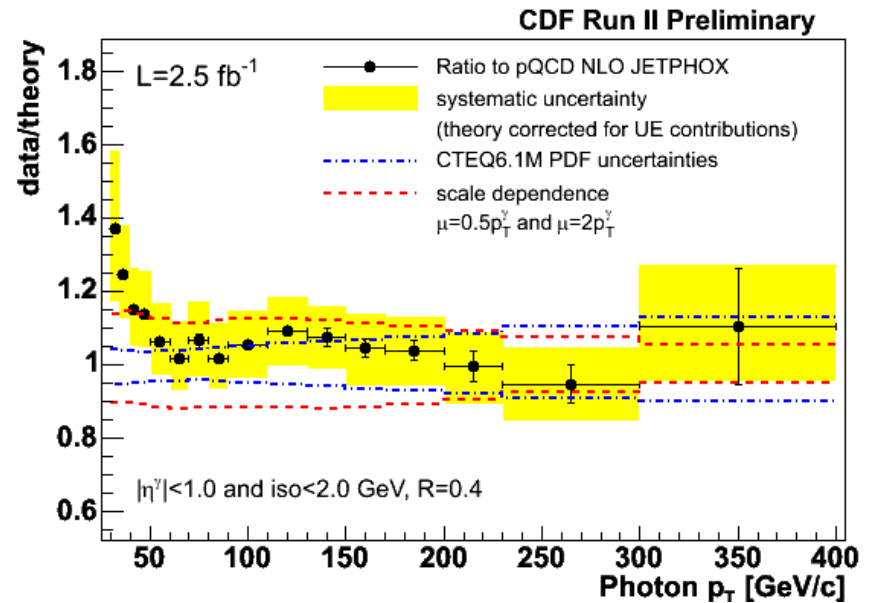


Figure 20. The resummed (leading log) W boson transverse momentum distribution.



k_T kick

- Here we only have 1 scale (p_T^γ) but fixed order pQCD does not seem to be doing well at low p_T
- Soft gluons are radiated by the incoming partons as they head towards the hard collision producing the photon
 - ◆ as we saw earlier that the PDF's have a Q^2 dependence because of this soft radiation
- They reduce the momentum fraction x carried by the parton but also give the parton a transverse momentum
- So that when the two partons collide, they have a relative transverse momentum
- This gives the photon a k_T kick, in a manner not described by fixed order pQCD



this kick gets larger as the center of mass increases (and as the mass of the final state increases)

FIG. 1. $\langle p_T \rangle$ of pairs of muons, photons, and jets produced in hadronic collisions versus \sqrt{s} .

k_T kick

- Since there aren't two scales can't use the normal q_T resummation formalism
- But can do a back-of-the-envelope calculation

For definiteness, let us consider direct-photon production. The full 2-dimensional convolution of the (parametrized) differential cross section Σ (for example, $\Sigma = d\sigma/dp_T$) with the Gaussian k_T -smearing functions can be written as:

$$\Sigma'(p_T) = \int d^2k_{T1} d^2k_{T2} d^2q_T \frac{1}{\pi \langle k_{T1}^2 \rangle} e^{-k_{T1}^2 / \langle k_{T1}^2 \rangle} \frac{1}{\pi \langle k_{T2}^2 \rangle} e^{-k_{T2}^2 / \langle k_{T2}^2 \rangle} \times \Sigma(q_T) \delta^{(2)}(\vec{p}_T - \vec{q}_T - \frac{1}{\gamma}(\vec{k}_{T1} + \vec{k}_{T2})), \quad (11)$$

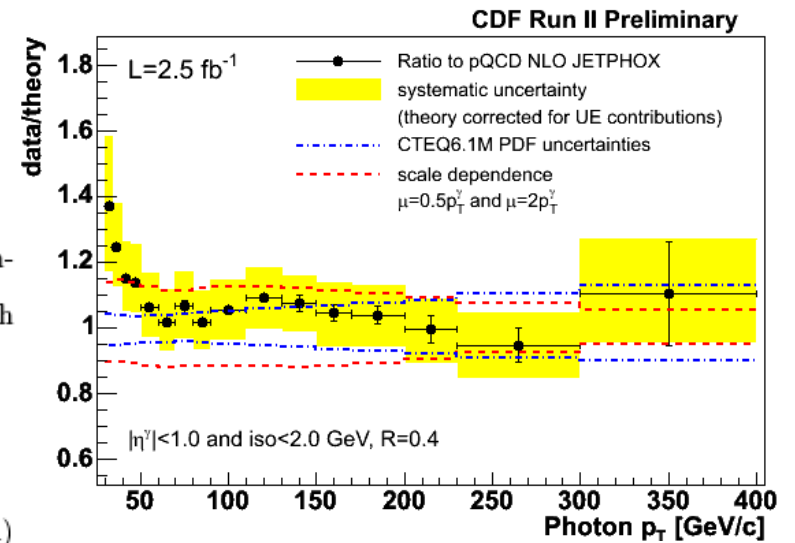
A different representation, useful, for example, for parametrizing CDF and DØ measurements, assumes $\Sigma \sim 1/p_T^n$. For this parametrization (or more general functional forms) one can expand $\Sigma(p_T - k_T)$ as a power series in k_T (for k_T small compared to p_T):

$$\Sigma(p_T - k_T) = \Sigma(p_T) + \frac{1}{2!} k_T^2 \Sigma''(p_T) + \frac{1}{4!} k_T^4 \Sigma^{(4)}(p_T) + \dots \quad (16)$$

(the odd powers of k_T integrate out to zero). One obtains:

$$K(p_T) = 1 + \frac{\langle k_T \rangle^2 n(n+1)}{2\pi p_T^2} + \frac{\langle k_T \rangle^4 n(n+1)(n+2)(n+3)}{8\pi^2 p_T^4} + \dots \quad (17)$$

For a constant (or a slowly changing) slope parameter n (and for $\langle k_T \rangle \ll p_T$), the effects of k_T smearing decrease as $1/p_T^2$, as might be expected for a power-suppressed process.

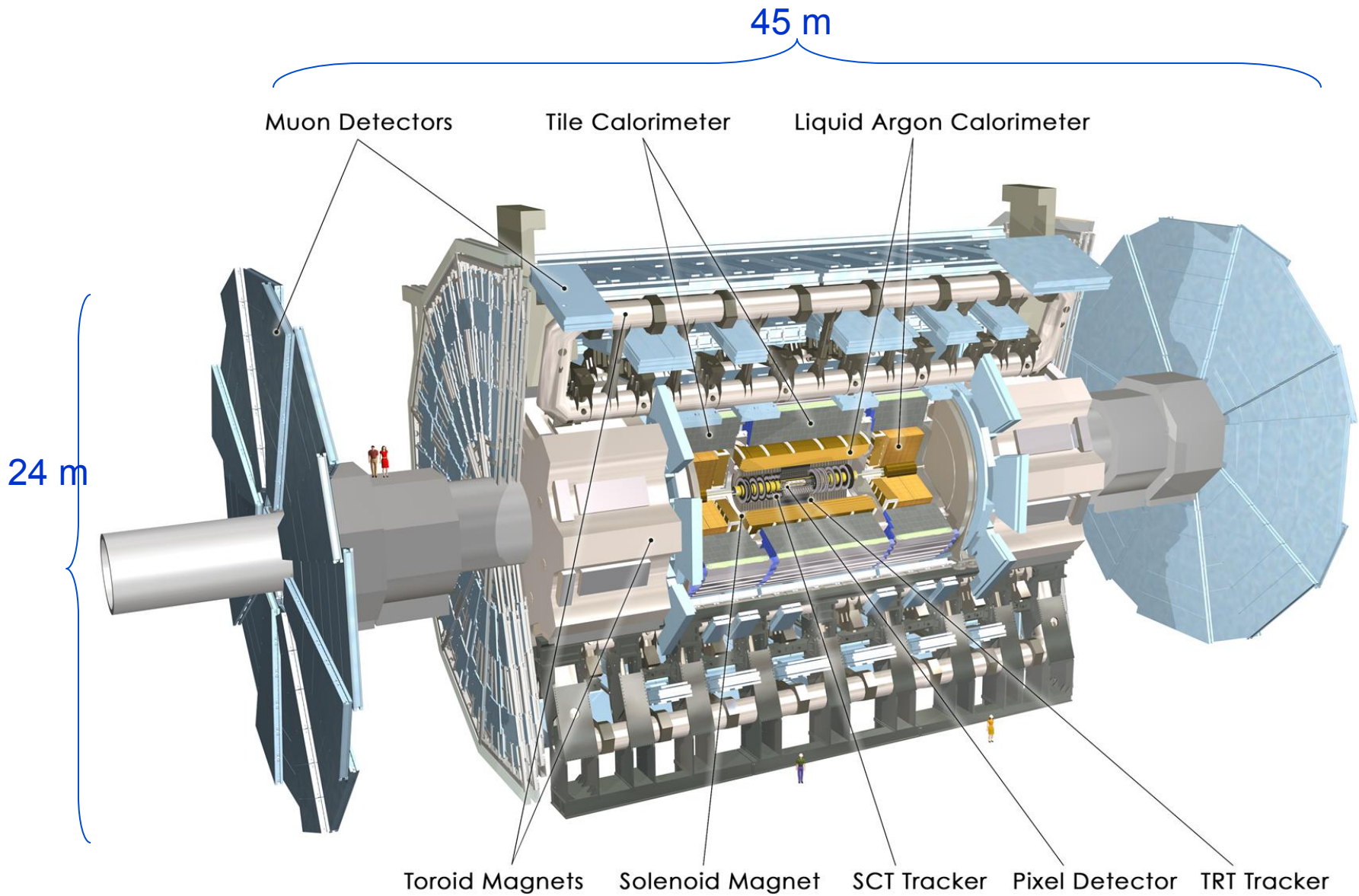


hep-ph/9808467

effect falls off by 50 GeV/c
should be similar at LHC

in hep-ph/0002078, George Sterman and collaborators developed a formalism to handle this situation

Onto the LHC



Underlying event at the LHC

- There's also a great deal of uncertainty regarding the level of underlying event at 14 TeV (or 7 TeV...), but it's clear that the UE is larger at the LHC than at the Tevatron
- Great deal of current effort on finding tunes for 7 TeV UE

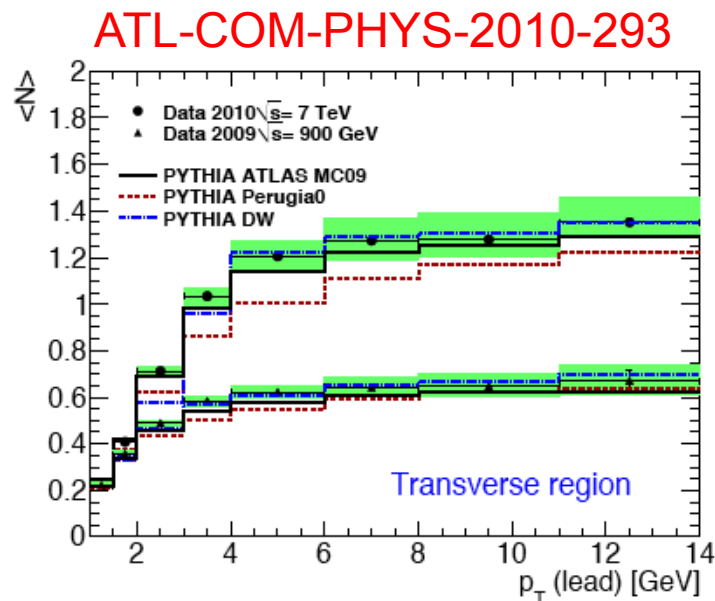
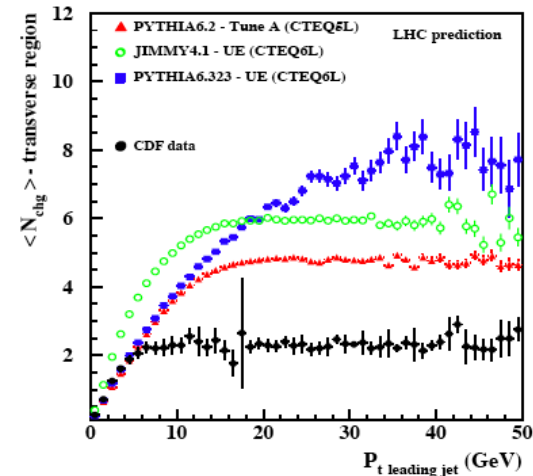
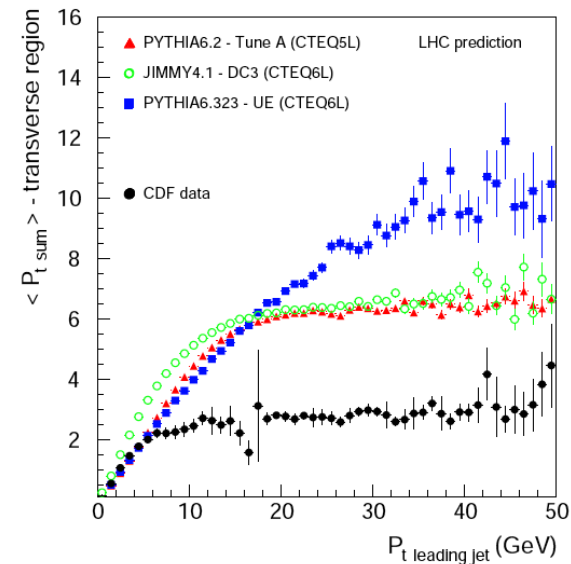


Figure 30: The average number of particles per event in one unit interval in η and ϕ as a function of the $p_T(\text{lead})$ for the transverse region indicated in Fig. 1 compared to 900 GeV data.

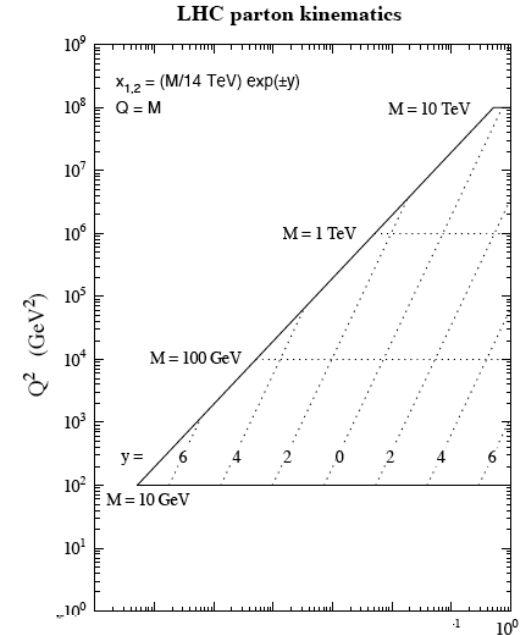


2 - Tune A, Jimmy4.1 - UE and Pythia6.323 - UE predictions for the average y in the underlying event for LHC pp collisions.



LHC parton kinematics

- To serve as a handy “look-up” table, it’s useful to define a parton-parton luminosity
 - ◆ this is from the CHS review paper
 - ◆ It’s for 14 TeV, but it still introduces some useful stuff
- Equation 3 can be used to estimate the production rate for a hard scattering at the LHC as the product of a differential parton luminosity and a scaled hard scatter matrix element



$$\frac{dL_{ij}}{d\hat{s} dy} = \frac{1}{s} \frac{1}{1 + \delta_{ij}} [f_i(x_1, \mu) f_j(x_2, \mu) + (1 \leftrightarrow 2)] . \quad (1)$$

The prefactor with the Kronecker delta avoids double-counting in case the partons are identical. The generic parton-model formula

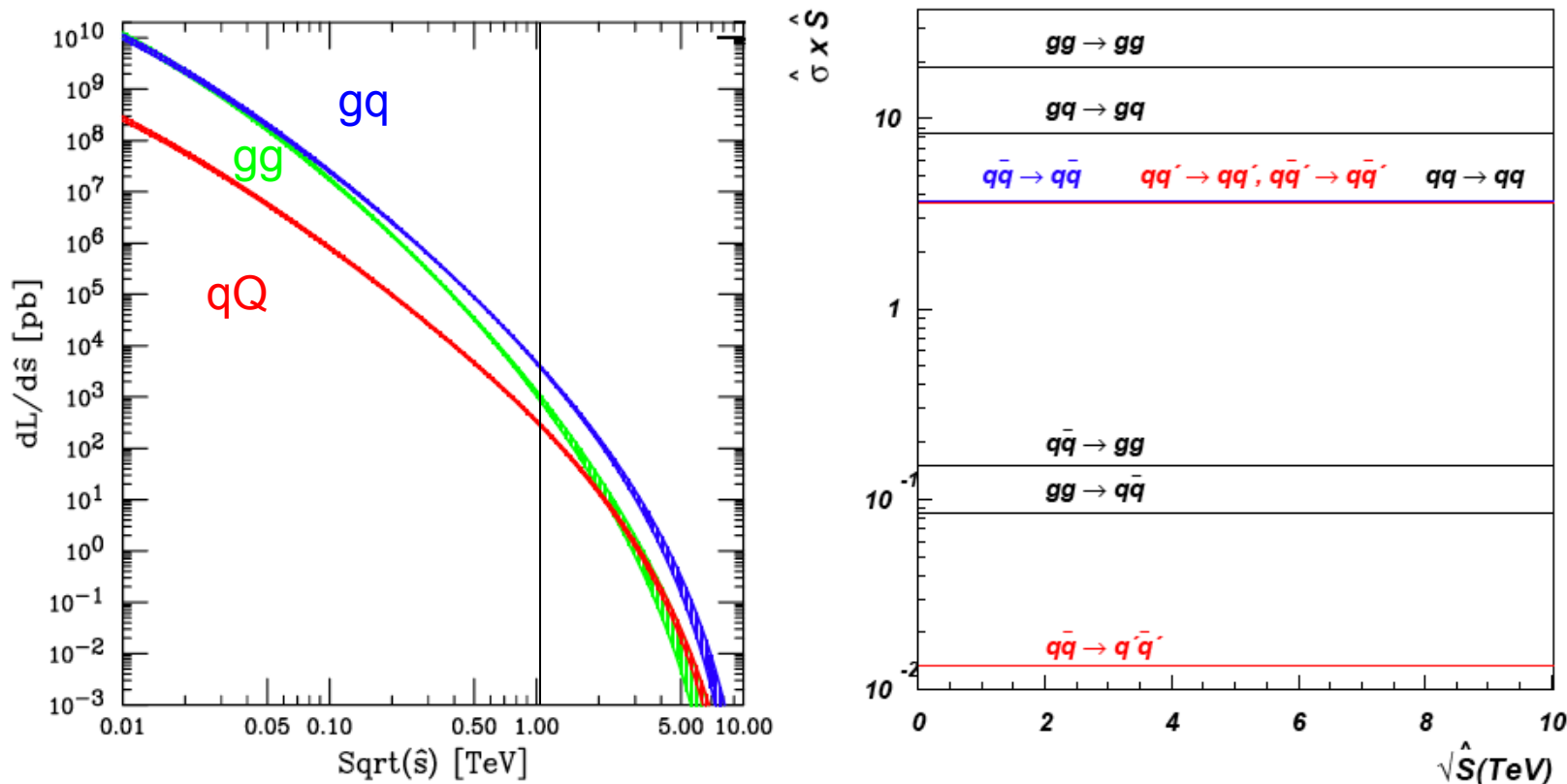
$$\sigma = \sum_{i,j} \int_0^1 dx_1 dx_2 f_i(x_1, \mu) f_j(x_2, \mu) \hat{\sigma}_{ij} \quad (2)$$

can then be written as

$$\sigma = \sum_{i,j} \int \left(\frac{d\hat{s}}{\hat{s}} dy \right) \left(\frac{dL_{ij}}{d\hat{s} dy} \right) (\hat{s} \hat{\sigma}_{ij}) . \quad (3)$$

Cross section estimates

$\sigma = \frac{\Delta \hat{s}}{\hat{s}} \left(\frac{dL_{ij}}{d\hat{s}} \right) (\hat{s} \hat{\sigma}_{ij})$
 for the gluon pair production rate for $\hat{s}=1$ TeV and $\Delta \hat{s} = 0.01 \hat{s}$,
 we have $\frac{dL_{gg}}{d\hat{s}} \simeq 10^3$ pb and $\hat{s} \hat{\sigma}_{gg} \simeq 20$ leading to $\sigma \simeq 200$ pb



for
 $p_T = 0.1 * \sqrt{\hat{s}}$

Fig. 2: Left: luminosity $\left[\frac{1}{\hat{s}} \frac{dL_{ij}}{d\tau} \right]$ in pb integrated over y . Green= gg , Blue= $g(d + u + s + c + b) + g(\bar{d} + \bar{u} + \bar{s} + \bar{c} + \bar{b}) + (d + u + s + c + b)g + (\bar{d} + \bar{u} + \bar{s} + \bar{c} + \bar{b})g$, Red= $d\bar{d} + u\bar{u} + s\bar{s} + c\bar{c} + b\bar{b} + \bar{d}d + \bar{u}u + \bar{s}s + \bar{c}c + \bar{b}b$. Right: parton level cross sections $[\hat{s} \hat{\sigma}_{ij}]$ for various processes

PDF luminosities as a function of y

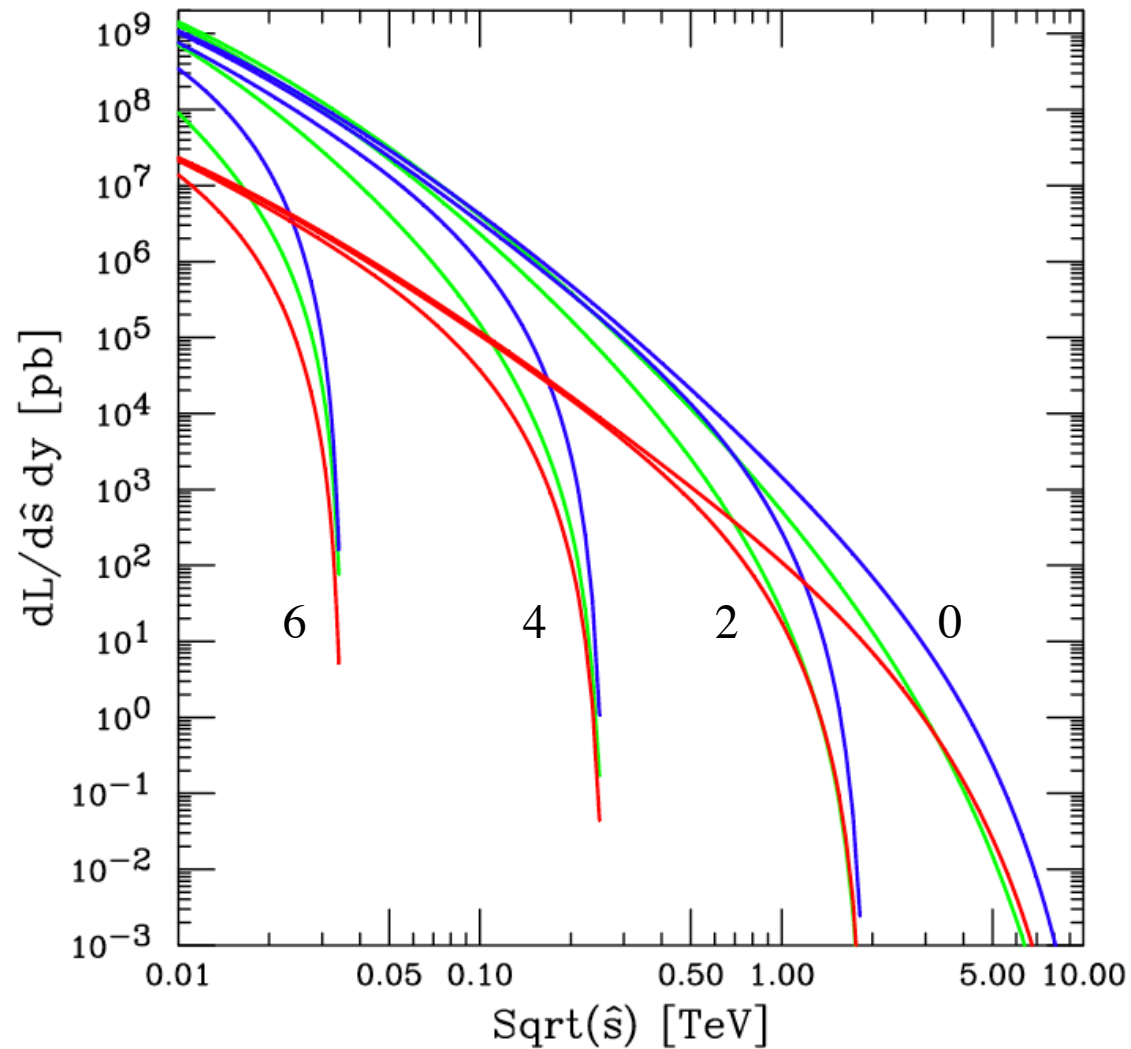


Fig. 3: $dLuminosity/dy$ at $y = 0, 2, 4, 6$. **Green**= gg , **Blue**= $g(d + u + s + c + b) + g(\bar{d} + \bar{u} + \bar{s} + \bar{c} + \bar{b}) + (d + u + s + c + b)g + (\bar{d} + \bar{u} + \bar{s} + \bar{c} + \bar{b})g$, **Red**= $d\bar{d} + u\bar{u} + s\bar{s} + c\bar{c} + b\bar{b} + \bar{d}d + \bar{u}u + \bar{s}s + \bar{c}c + \bar{b}b$.

PDF uncertainties at the LHC

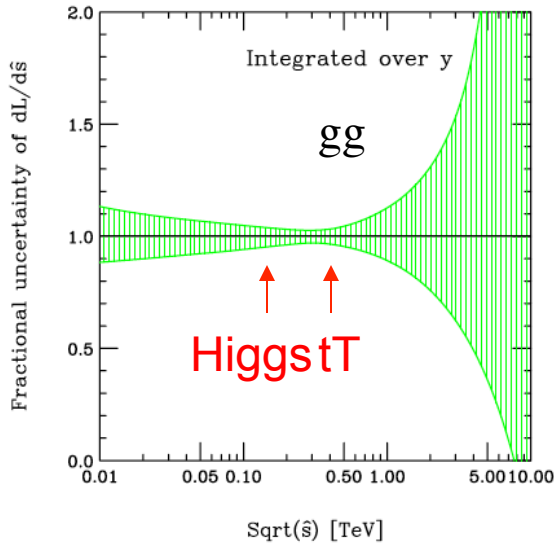


Fig. 4: Fractional uncertainty of gg luminosity integrated over y .

NBIII: tT uncertainty is of the same order as W/Z production

Note that for much of the SM/discovery range, the pdf luminosity uncertainty is small

Need similar level of precision in theory calculations

It will be a while, i.e. not in the first pb^{-1} , before the LHC data starts to constrain pdf's

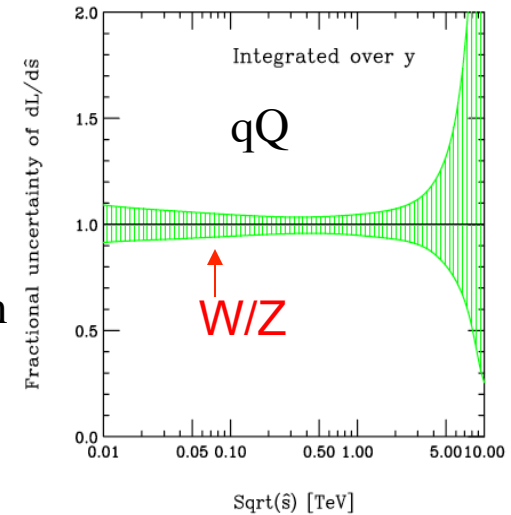


Fig. 7: Fractional uncertainty for Luminosity integrated over y for $d\bar{d} + u\bar{u} + s\bar{s} + c\bar{c} + b\bar{b} + \bar{d}d + \bar{u}u + \bar{s}s + \bar{c}c + \bar{b}b$.

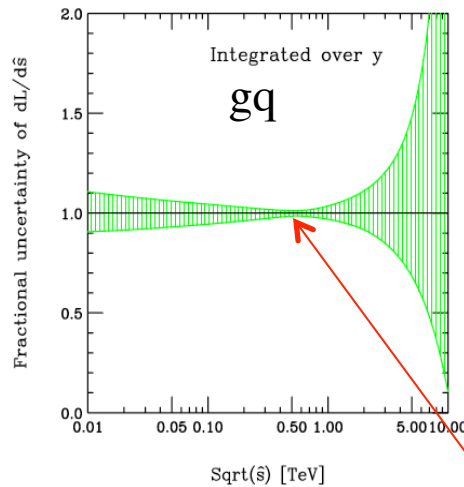


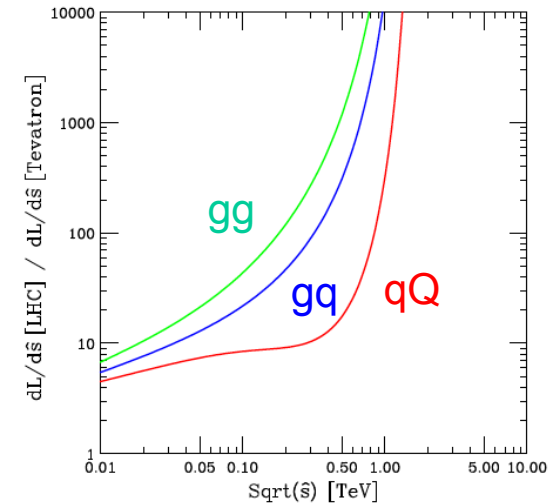
Fig. 6: Fractional uncertainty for Luminosity integrated over y for $g(d+u+s+c+b) + g(\bar{d}+\bar{u}+\bar{s}+\bar{c}+\bar{b}) + (d+u+s+c+b)g + (\bar{d}+\bar{u}+\bar{s}+\bar{c}+\bar{b})g$.

NB I: the errors are determined using the Hessian method for a $\Delta\chi^2$ of 100 using only experimental uncertainties, i.e. no theory uncertainties

NB II: the pdf uncertainties for W/Z cross sections are not the smallest

Ratios:LHC to Tevatron pdf luminosities

- Processes that depend on qQ initial states (e.g. chargino pair production) have small enhancements
- Most backgrounds have gg or gq initial states and thus large enhancement factors (500 for W + 4 jets for example, which is primarily gq) at the LHC (14 TeV)
- W+4 jets is a background to tT production both at the Tevatron and at the LHC
- tT production at the Tevatron is largely through a qQ initial states and so qQ->tT has an enhancement factor at the LHC of ~10
- Luckily tT has a gg initial state as well as qQ so total enhancement at the LHC is a factor of 100 (14 TeV)
 - but increased W + jets background means that a higher jet cut is necessary at the LHC
 - known known: jet cuts have to be higher at LHC than at Tevatron



14 TeV

Figure 11. The ratio of parton-parton luminosity $\left[\frac{1}{s} \frac{dL}{d\tau}\right]$ in pb integrated over y at the LHC and Tevatron. Green= gg (top), Blue= $g(d+u+s+c+b)+g(\bar{d}+\bar{u}+\bar{s}+\bar{c}+\bar{b})+(d+u+s+c+b)g+(\bar{d}+\bar{u}+\bar{s}+\bar{c}+\bar{b})g$ (middle), Red= $d\bar{d}+u\bar{u}+s\bar{s}+c\bar{c}+b\bar{b}+\bar{d}d+\bar{u}u+\bar{s}s+\bar{c}c+\bar{b}b$ (bottom).

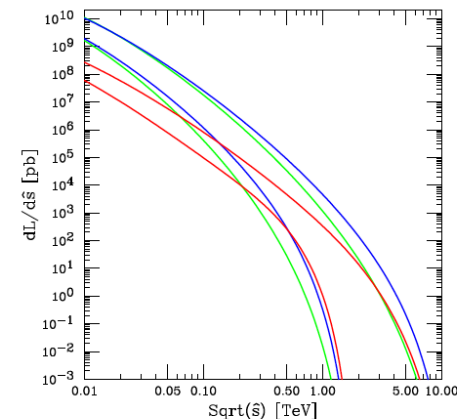


Figure 10. The parton-parton luminosity $\left[\frac{1}{s} \frac{dL}{d\tau}\right]$ in pb integrated over y . Green= gg , Blue= $g(d+u+s+c+b)+g(\bar{d}+\bar{u}+\bar{s}+\bar{c}+\bar{b})+(d+u+s+c+b)g+(\bar{d}+\bar{u}+\bar{s}+\bar{c}+\bar{b})g$, Red= $d\bar{d}+u\bar{u}+s\bar{s}+c\bar{c}+b\bar{b}+\bar{d}d+\bar{u}u+\bar{s}s+\bar{c}c+\bar{b}b$. The top family of curves are for the LHC and the bottom for the Tevatron.

The LHC ~~will be~~ ^{is} a very jetty place

- Total cross sections for $t\bar{t}$ and Higgs production saturated by $t\bar{t}$ (Higgs) + jet production for jet p_T values of order 10-20 GeV/c
- $\sigma_{W+3 \text{ jets}} > \sigma_{W+2 \text{ jets}}$

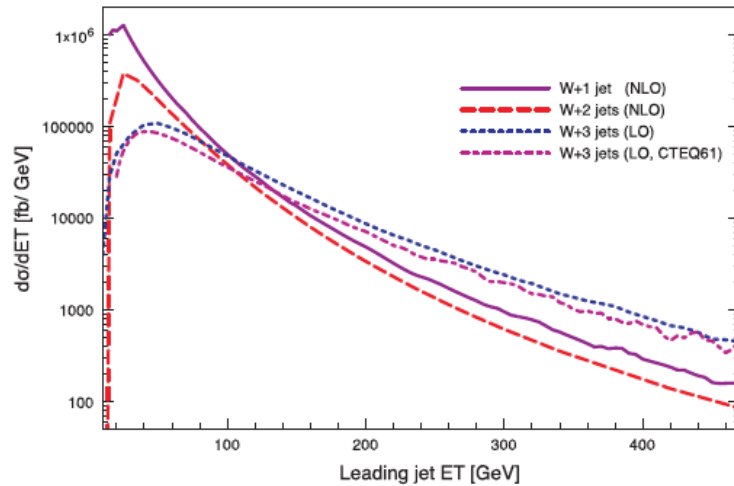


Figure 91. Predictions for the production of $W + \geq 1, 2, 3$ jets at the LHC shown as a function of the transverse energy of the lead jet. A cut of 20 GeV has been placed on the other jets in the prediction.

- indication that can expect interesting events at LHC to be very jetty (especially from gg initial states)
- also can be understood from point-of-view of Sudakov form factors

14 TeV

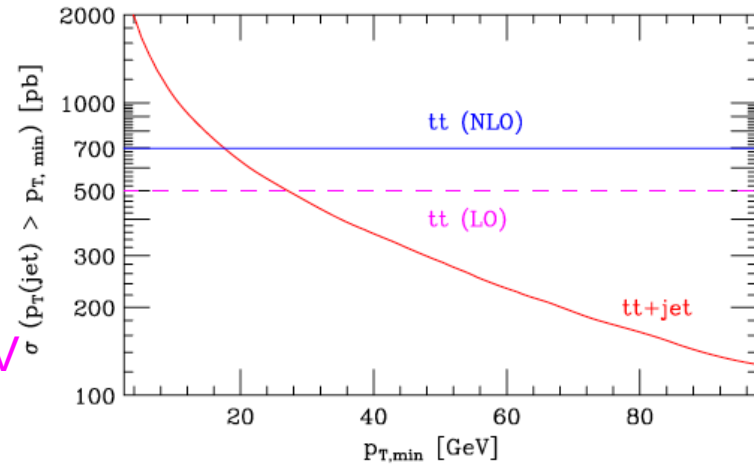


Figure 95. The dependence of the LO $t\bar{t}$ +jet cross section on the jet-defining parameter $p_{T,min}$, together with the top pair production cross sections at LO and NLO.

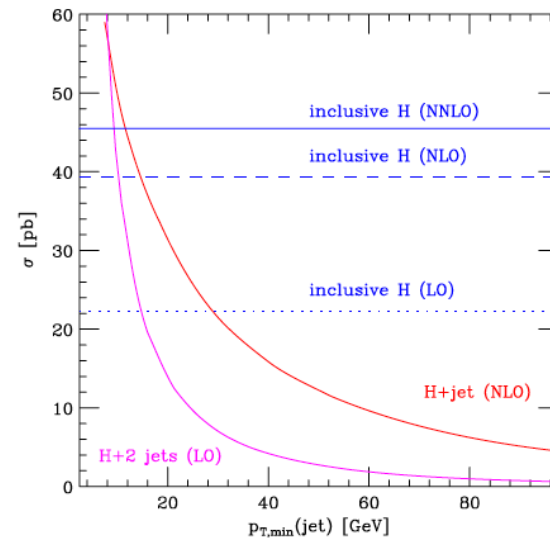


Figure 100. The dependence of the LO $t\bar{t}$ +jet cross section on the jet-defining parameter $p_{T,min}$, together with the top pair production cross sections at LO and NLO.

Sudakov form factors for tT

- tT production at the LHC dominated by gg at x values factor of 7 lower than Tevatron
- So dominant Sudakov form factor goes from
- to

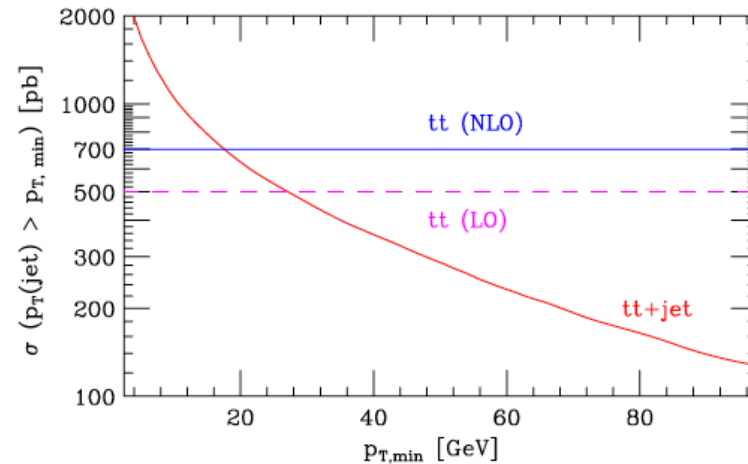


Figure 95. The dependence of the LO $t\bar{t}$ +jet cross section on the jet-defining parameter $p_{T,\min}$, together with the top pair production cross sections at LO and NLO.

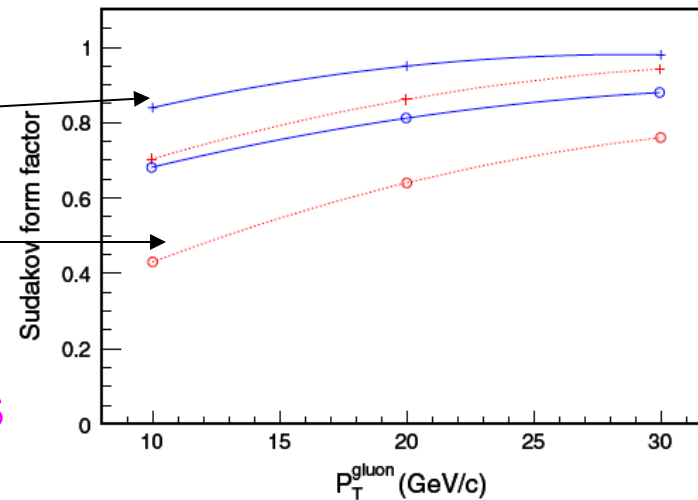


Figure 96. The Sudakov form factors for initial-state quarks and gluons at a hard scale of 200 GeV as a function of the transverse momentum of the emitted gluon. The form factors are for quarks (blue-solid) and gluons (red-dashed) at parton x values of 0.3 (crosses) and 0.03 (open circles).

even at 7 TeV, > 50% of tT events have a jet > 30 GeV/c

PDF4LHC report

- We carried out an exercise to which all PDF groups were invited to participate
- A comparison of NLO predictions for benchmark cross sections at the LHC (7 TeV) using MCFM with prescribed input files
- Benchmarks included
 - ◆ W/Z production/rapidity distributions
 - ◆ $t\bar{t}$ production
 - ◆ Higgs production through gg fusion
 - ▲ masses of 120, 180 and 240 GeV
- PDFs used include CTEQ6.6, MSTW08, NNPDF2.0, HERAPDF 1.0, ABKM09, GJR08
- In some of comparisons, updates to above PDFs may also be shown

The PDF4LHC Working Group Interim Report

Sergey Alekhin^{1,2}, Simone Alioti¹, Richard D. Ball³, Valerio Bertone⁴, Johannes Blümlein¹, Michiel Botje⁵, Jon Butterworth⁶, Francesco Cerutti⁷, Amanda Cooper-Sarkar⁸, Albert de Roeck⁹, Luigi Del Debbio⁹, Joel Feltesse¹⁰, Stefano Forte¹¹, Alexander Glazov¹², Alberto Guffanti⁴, Claire Gwenlan⁸, Joey Huston¹³, Pedro Jimenez-Delgado¹⁴, Hung-Liang Lai¹⁵, José I. Latorre⁷, Ronan McNulty¹⁶, Pavel Nadolsky¹⁷, Sven Olf Moch¹, Jon Pumplin¹³, Voica Radescu¹⁸, Juan Rojo¹¹, Torbjörn Sjöstrand¹⁹, W.J. Stirling²⁰, Daniel Stump¹³, Robert S. Thorne⁶, Maria Ubial²¹, Alessandro Vicini¹¹, Graeme Watt²², C.-P. Yuan¹³

¹ Deutsches Elektronen-Synchrotron, DESY, Platanenallee 6, D-15738 Zeuthen, Germany

² Institute for High Energy Physics, IHEP, Pobeda 1, 142281 Protvino, Russia

³ School of Physics and Astronomy, University of Edinburgh, JCMB, KB, Mayfield Rd, Edinburgh EH9 3JZ, Scotland

⁴ Physikalisches Institut, Albert-Ludwigs-Universität Freiburg, Hermann-Herder-Straße 3, D-79104 Freiburg i. B., Germany

⁵ NIKHEF, Science Park, Amsterdam, The Netherlands

⁶ Department of Physics and Astronomy, University College, London, WC1E 6BT, UK

⁷ Departament d'Estructura i Constituents de la Matèria, Universitat de Barcelona, Diagonal 647, E-08028 Barcelona, Spain

⁸ Department of Physics, Oxford University, Denys Wilkinson Bldg, Keble Rd, Oxford, OX1 3RH, UK
⁹ CERN, CH-1211 Genève 23, Switzerland; Antwerp University, B-2610 Wilrijk, Belgium; University of California Davis, CA, USA

¹⁰ CEA, DSM/IRFU, CE-Saclay, Gif-sur-Yvette, France

¹¹ Dipartimento di Fisica, Università di Milano and INFN, Sezione di Milano, Via Celoria 16, I-20133 Milano, Italy

¹² Deutsches Elektronensynchrotron DESY Notkestraße 85 D-22607 Hamburg, Germany

¹³ Physics and Astronomy Department, Michigan State University, East Lansing, MI 48824, USA

¹⁴ Institut für Theoretische Physik, Universität Zürich, CH-8057 Zürich, Switzerland

¹⁵ Taipei Municipal University of Education, Taipei, Taiwan

¹⁶ School of Physics, University College Dublin Science Centre North, UCD Belfield, Dublin 4, Ireland

¹⁷ Department of Physics, Southern Methodist University, Dallas, TX 75275-0175, USA

¹⁸ Physikalisches Institut, Universität Heidelberg Philosophenweg 12, D-69120 Heidelberg, Germany

¹⁹ Department of Astronomy and Theoretical Physics, Lund University, Sölvegatan 14A, S-223 62 Lund, Sweden

²⁰ Cavendish Laboratory, University of Cambridge, CB3 0HE, UK

²¹ Institut für Theoretische Teilchenphysik und Kosmologie, RWTH Aachen University, D-52056 Aachen, Germany

²² Theory Group, Physics Department, CERN, CH-1211 Geneva 23, Switzerland

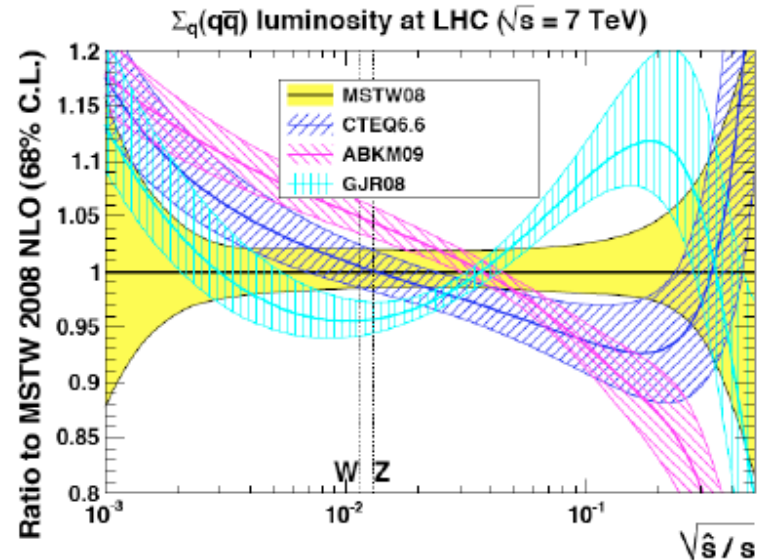
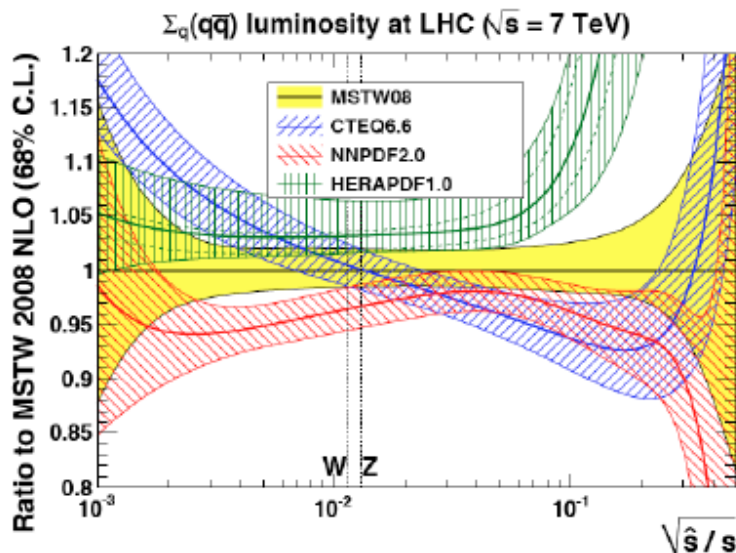
arXiv:1101.0536v1 [hep-ph] 3 Jan 2011

All of the benchmark processes were to be calculated with the following settings:

1. at NLO in the \overline{MS} scheme
2. all calculation done in a the 5-flavor quark ZM-VFNS scheme, though each group uses a different treatment of heavy quarks
3. at a center-of-mass energy of 7 TeV
4. for the central value predictions, and for $\pm 68\%$ and $\pm 90\%$ c.l. PDF uncertainties
5. with and without the α_s uncertainties, with the prescription for combining the PDF and α_s errors to be specified
6. repeating the calculation with a central value of $\alpha_s(m_Z)$ of 0.119.

PDF luminosities

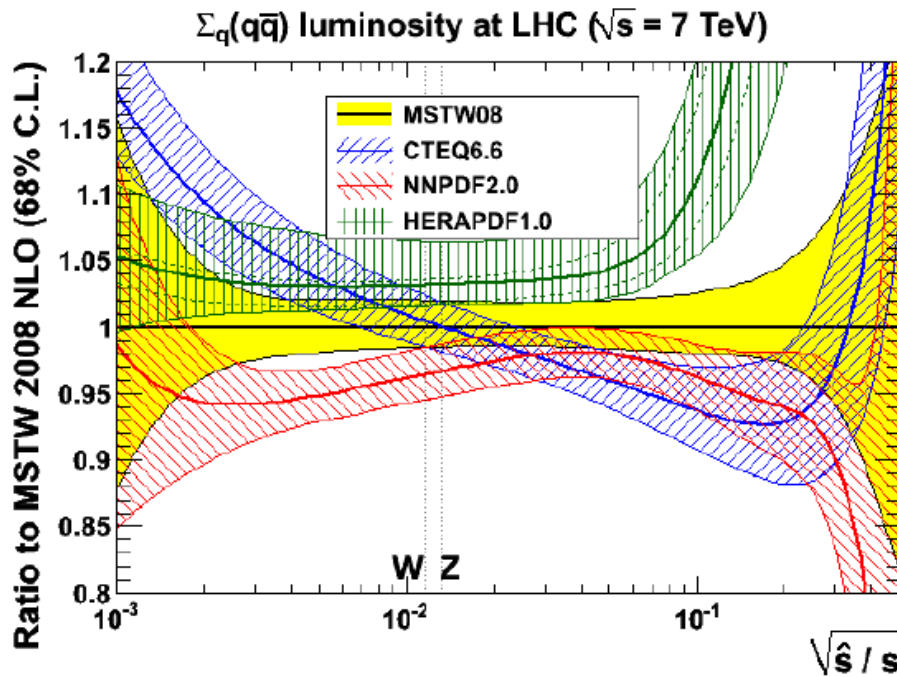
- The qQ luminosities for the groups tend to have different behaviors at low mass and at high mass
- The reasons can often be understood
 - ◆ NNPDF2.0 does not use a heavy quark flavor scheme; this suppresses the low x quark and anti-quark distributions (NNPDF2.1 does use such a scheme)
 - ◆ HERAPDF uses the HERA combined Run 1 dataset that prefers a higher normalization
- The agreement tends to be much better in the W/Z region



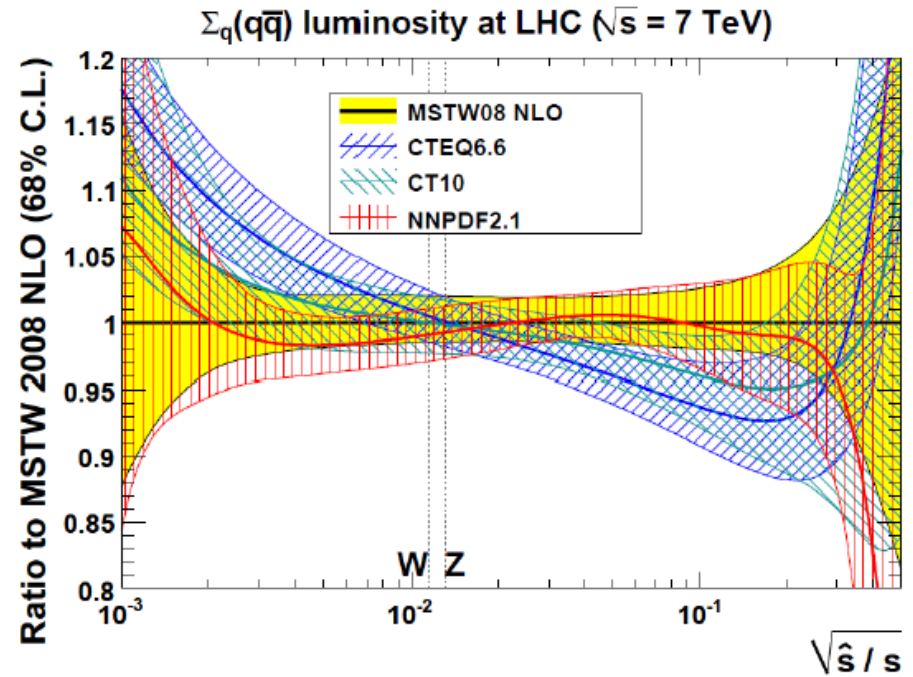
Plots by
G. Watt
arXiv:
1106.5788

PDFs are tending to get closer

plots from Graeme Watt



2010



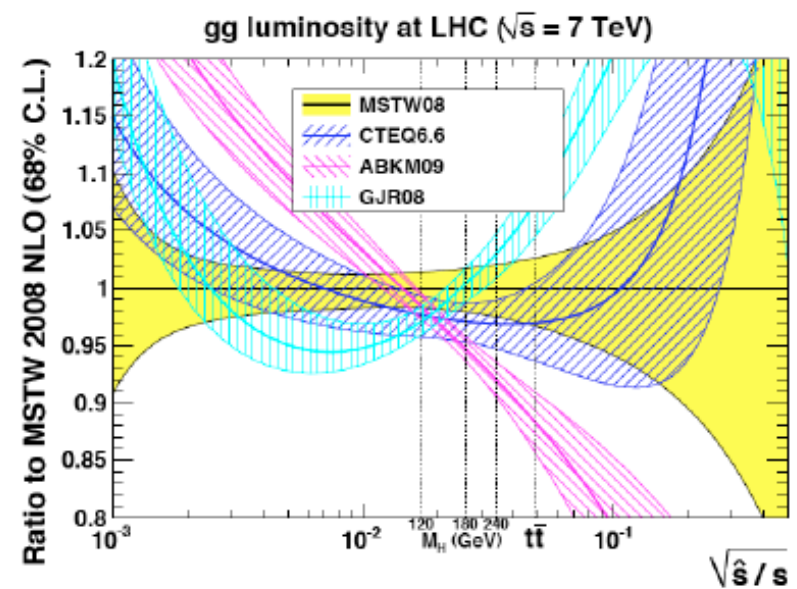
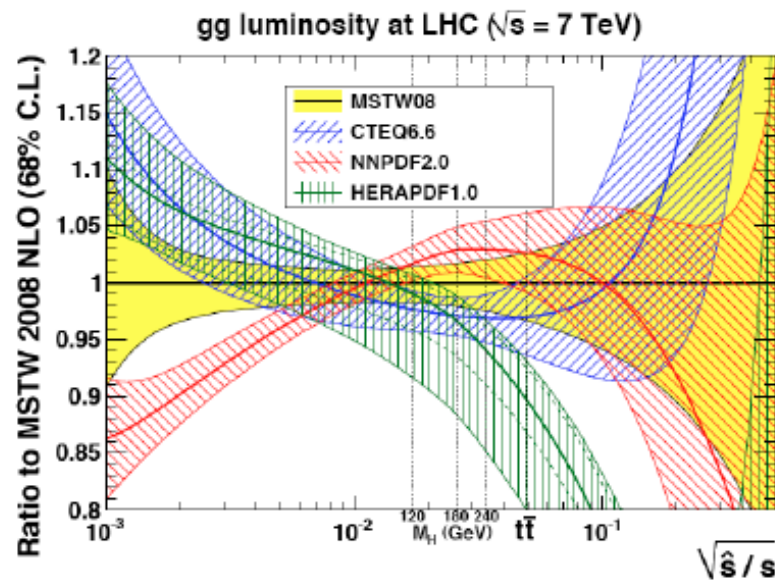
2011

... although still some differences with **ABKM, GJR, HERAPDF**

NNPDF2.1 has a GM-VFNS treatment (FONLL) -> increase in low x quarks
CT10 includes Tevatron Run II jet data

PDFs

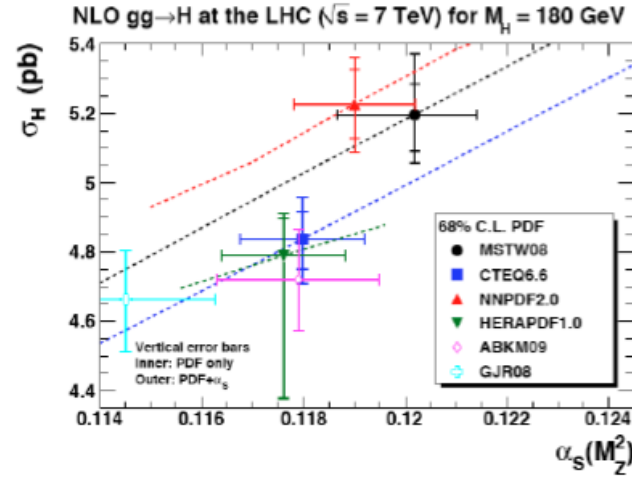
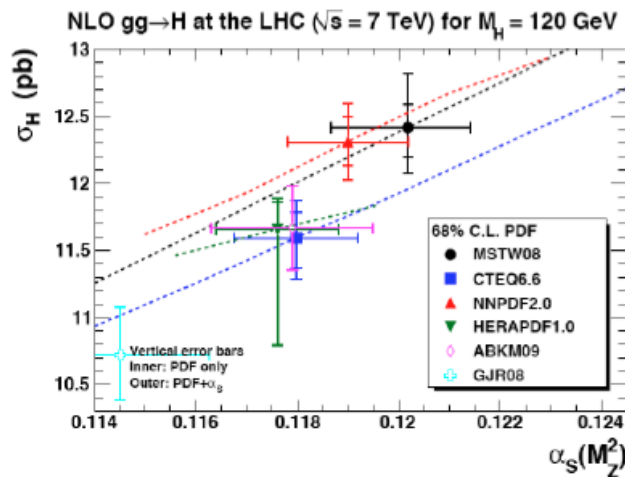
- Larger differences are observed for gg luminosities, especially at high mass
 - ◆ critically depends on whether Tevatron inclusive jet data have been used or not



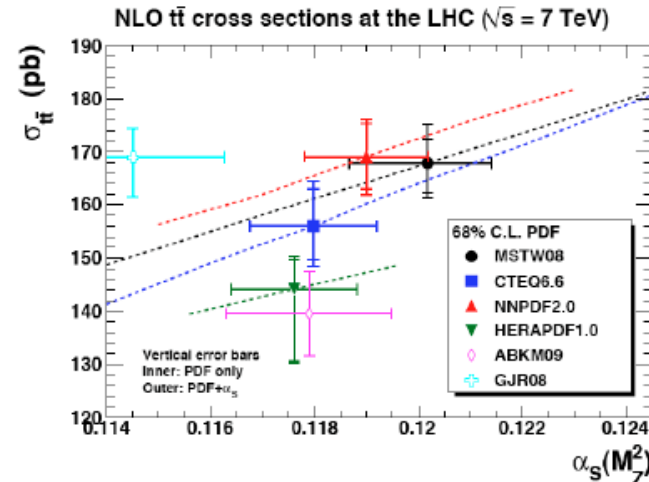
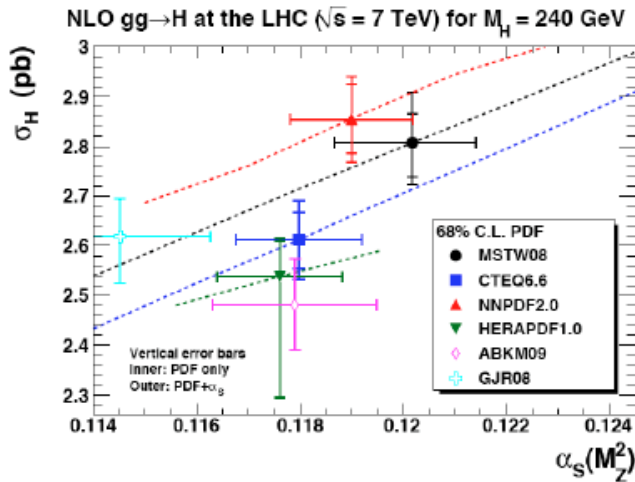
Plots by
G. Watt
arXiv:
1106.5788

Cross section comparisons

- Larger gg differences and greater dependence on α_s lead to larger differences in Higgs/tT cross section



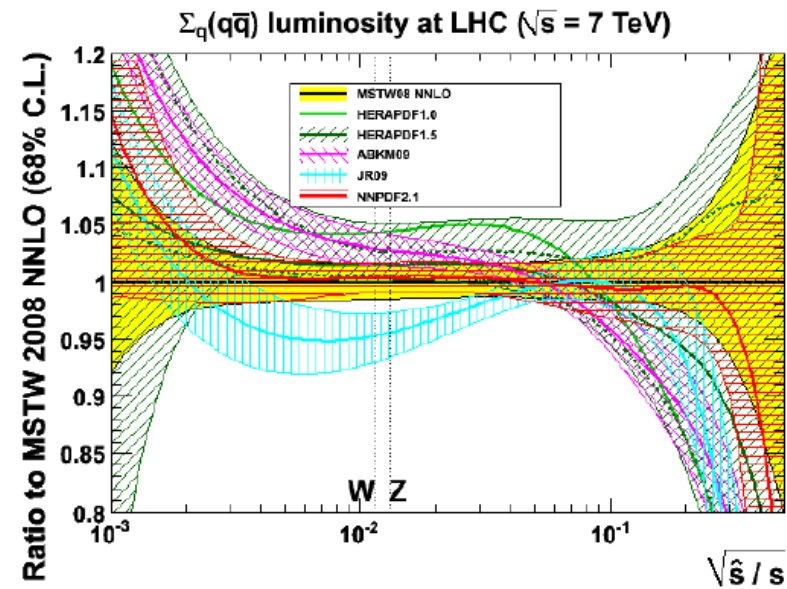
Note that there tends to be two groupings



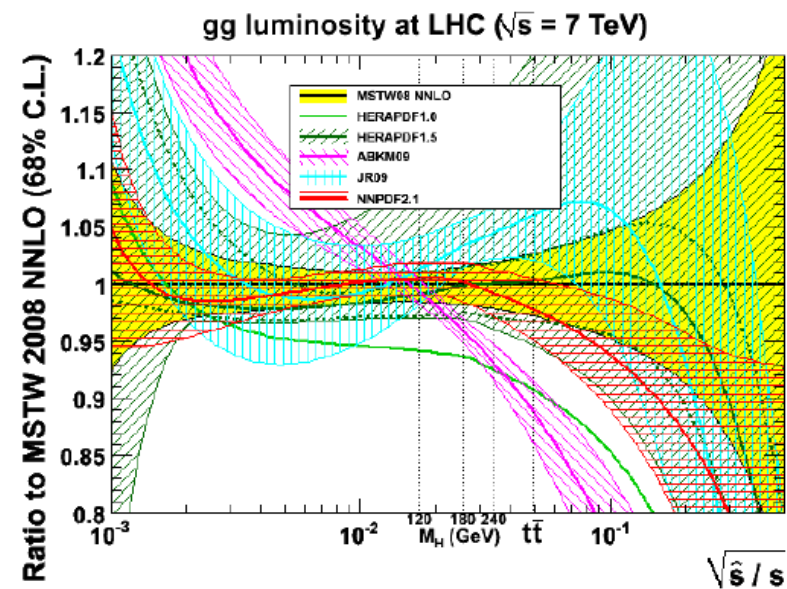
Plots by
G. Watt
arXiv:
1106.578

Comparison of NNLO PDF luminosity functions

- NNLO trends are similar to those observed at NLO

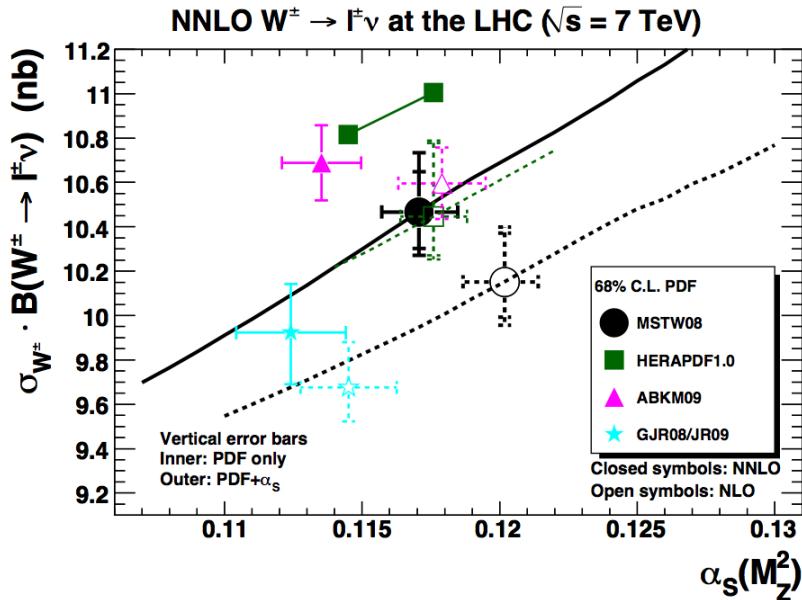


G. Watt (September 2011)

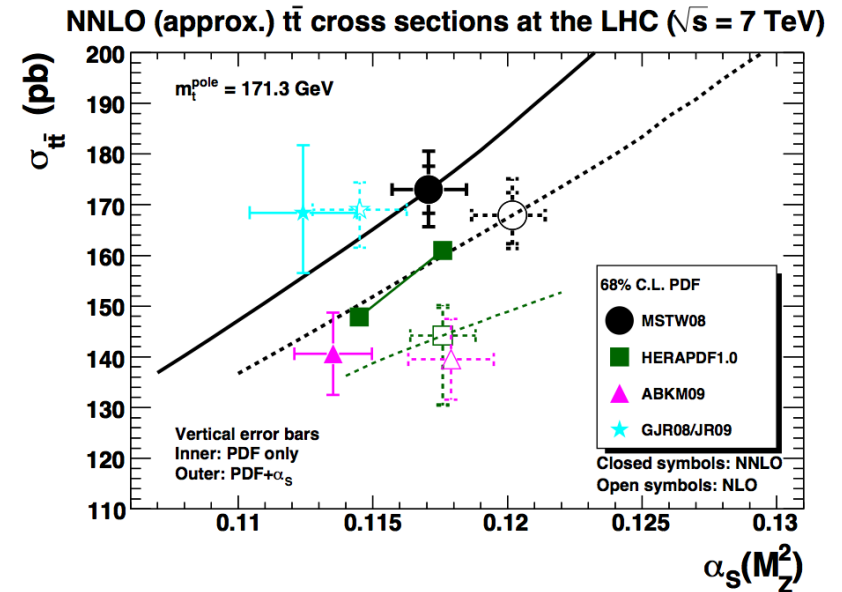


G. Watt (September 2011)

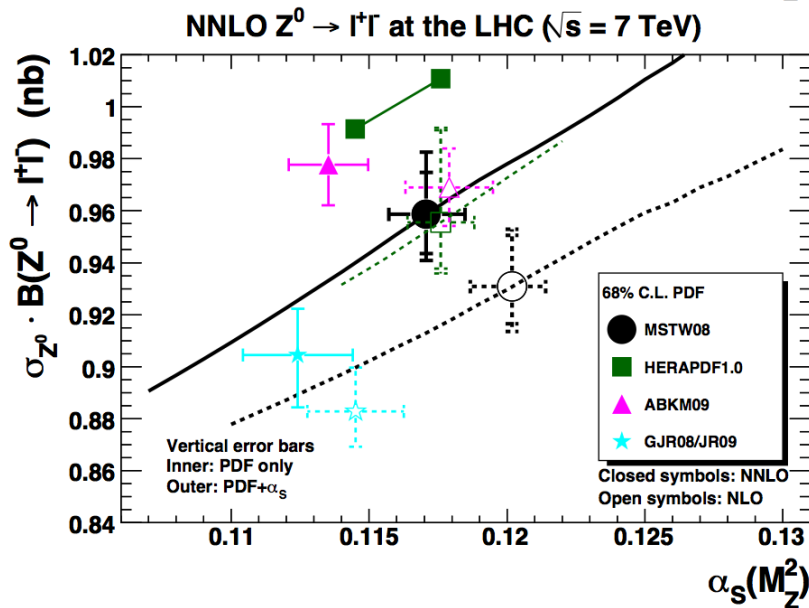
Comparison of NNLO predictions



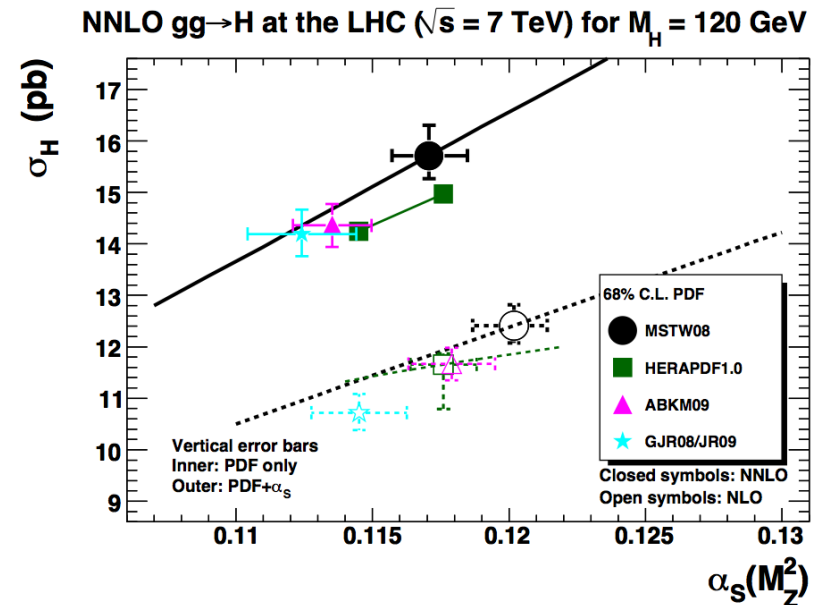
G. Watt (April 2011)



G. Watt (April 2011)



G. Watt (April 2011)



G. Watt (April 2011)

PDF4LHC recommendations

2. The PDF4LHC recommendation

Before the recommendation is presented, it is useful to highlight the differences between two use cases: (1) cross sections which have not yet been measured (such as, for example, Higgs production) and (2) comparisons to existing cross sections. For the latter, the most useful comparisons should be to the predictions using individual PDFs (and their uncertainty bands). Such cross sections have the potential, for example, to provide information useful for modification of those PDFs. For the former, in particular the cross section predictions in this report, we would like to provide a reliable estimate of the true uncertainty, taking into account possible differences between the central values of predictions using different PDFs ¹. From the results seen it is clear that this uncertainty will be larger than that from any single PDF set, but we feel it should not lose all connection to the individual PDF uncertainties (which would happen for many processes if the full spread of all PDFs were used), so some compromise is proposed.

PDF4LHC recommendations(arXiv:1101.0538)

So the prescription for NLO is as follows:

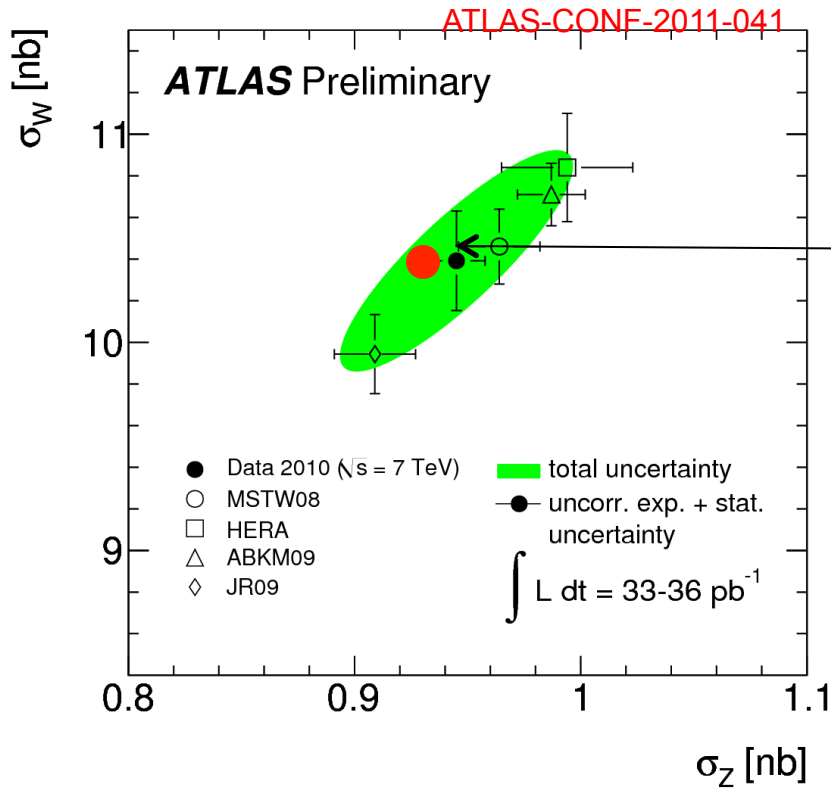
- For the calculation of uncertainties at the LHC, use the envelope provided by the central values and PDF+ α_s errors from the MSTW08, CTEQ6.6 and NNPDF2.0 PDFs, using each group's prescriptions for combining the two types of errors. We propose this definition of an envelope because the deviations between the predictions are as large as their uncertainties. As a central value, use the midpoint of this envelope. We recommend that a 68% c.l. uncertainty envelope be calculated and the α_s variation suggested is consistent with this. Note that the CTEQ6.6 set has uncertainties and α_s variations provided only at 90% c.l. and thus their uncertainties should be reduced by a factor of 1.645 for 68% c.l.. Within the quadratic approximation, this procedure is completely correct.

So the prescription at NNLO is:

- As a central value, use the MSTW08 prediction. As an uncertainty, take the same percentage uncertainty on this NNLO prediction as found using the NLO uncertainty prescription given above.

Of course, there is the freedom/encouragement to use any individual PDF desired for comparison to measured cross sections. This has been the norm for the 2010 LHC results.

LHC: W, Z cross sections

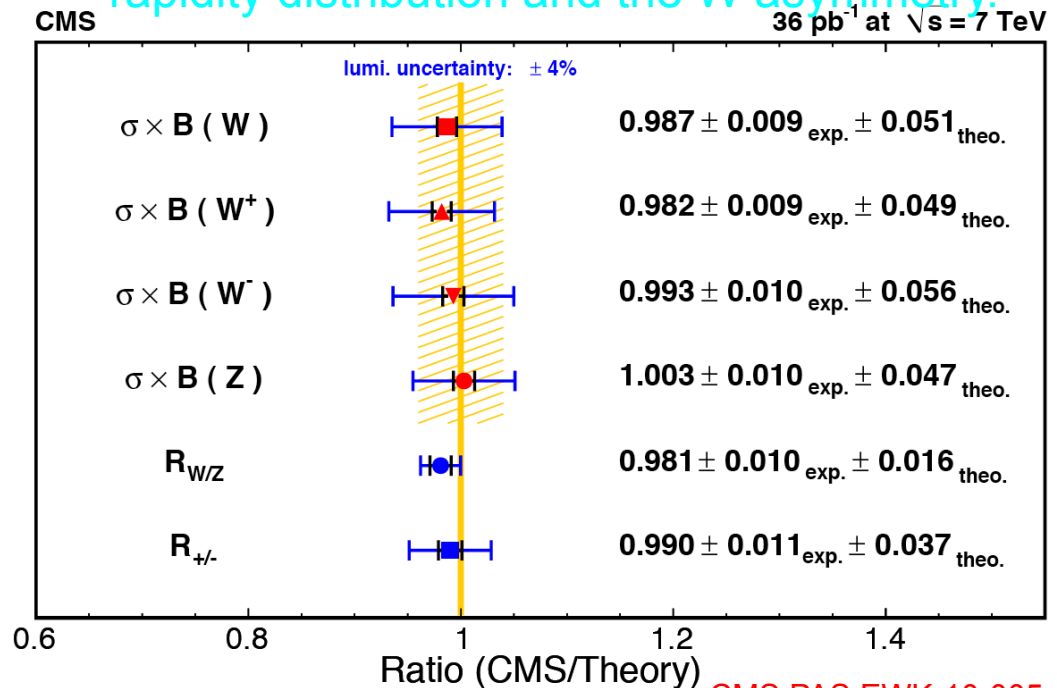


Many of the experimental/theory errors cancel with the ratio

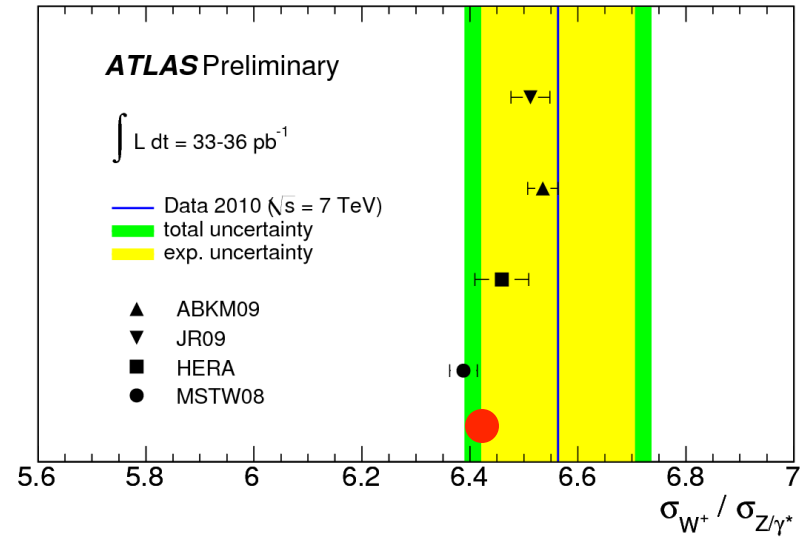
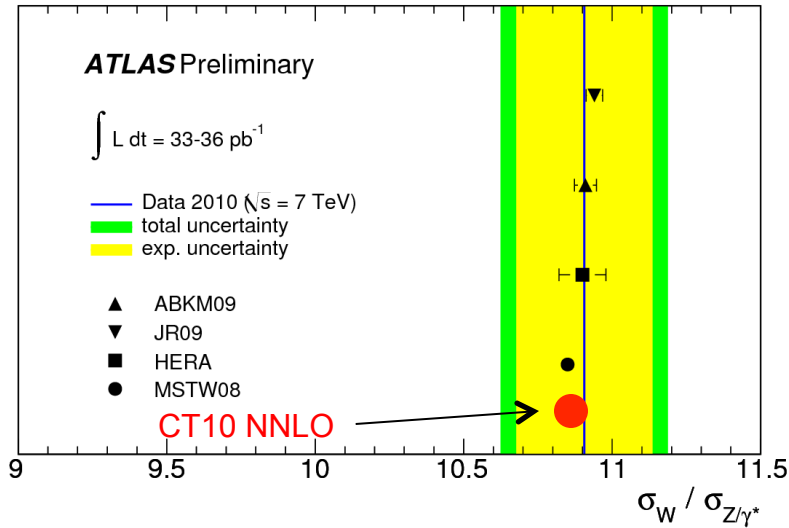
CT10 NNLO prediction

Of course, there is much additional information that will be used in PDF fits, such as the Z rapidity distribution and the W asymmetry.

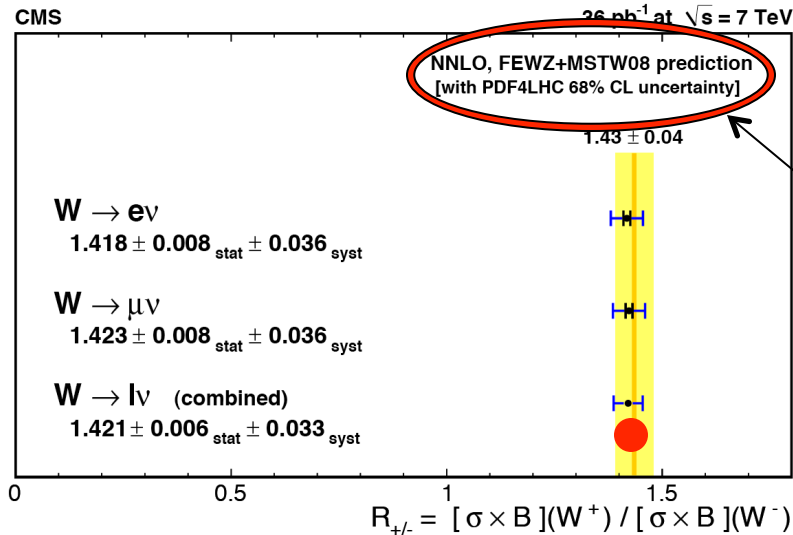
ATLAS W/Z cross section ratio in good agreement with NNLO predictions from the PDF groups shown



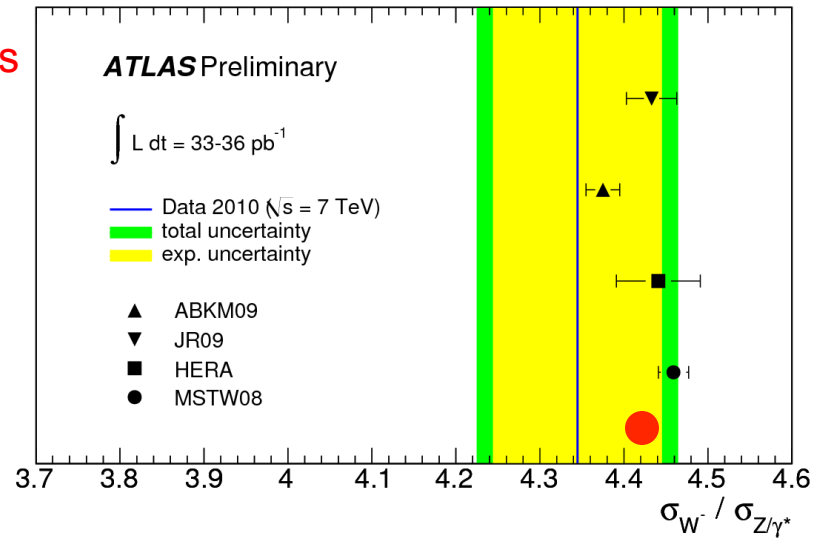
LHC: W/Z ratios



Total W/Z ratio from ATLAS in good agreement with theory, but separate W^+/Z and W^-/Z ratios show some differences (at 1 sigma level) for some of PDFs



CMS results for W,Z use PDF4LHC recipe for NNLO; good agreement with theory



Z p_T

- We said it should peak higher than Tevatron
 - ◆ it does
- Fit with ResBos without any adjustments

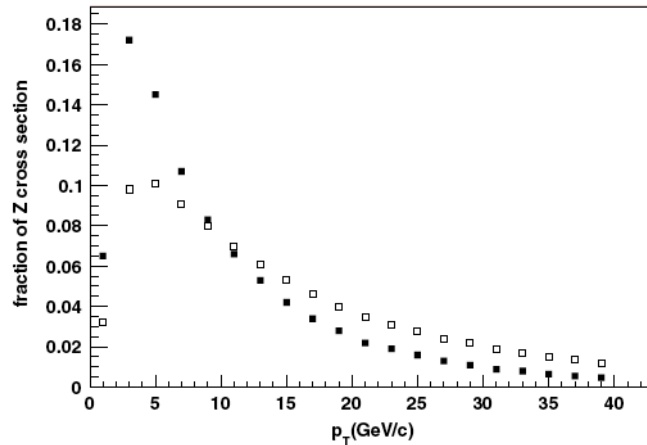


Figure 89. Predictions for the transverse momentum distributions for Z production at the Tevatron (solid squares) and LHC (open squares).

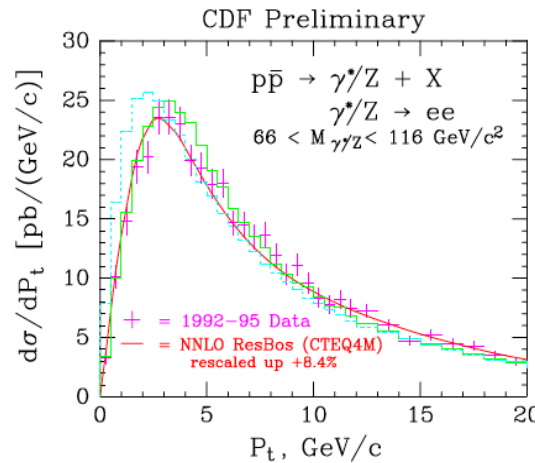
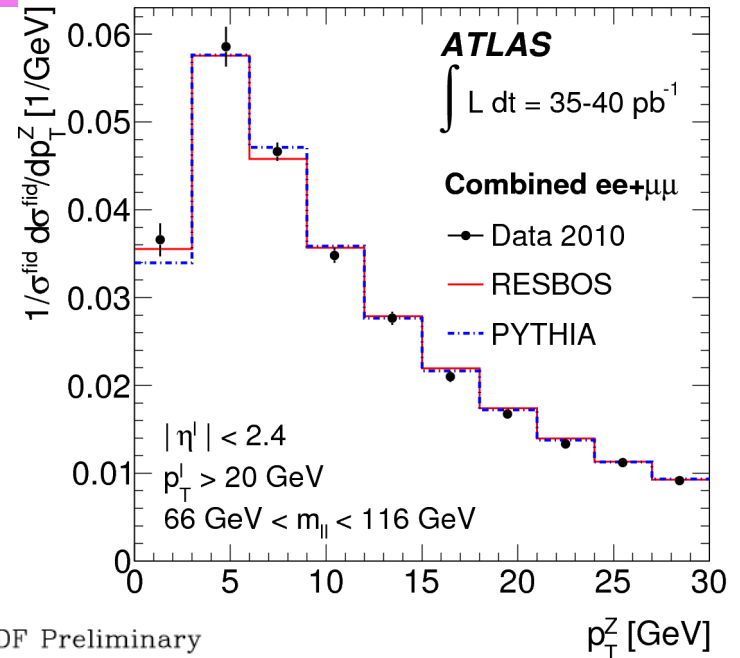
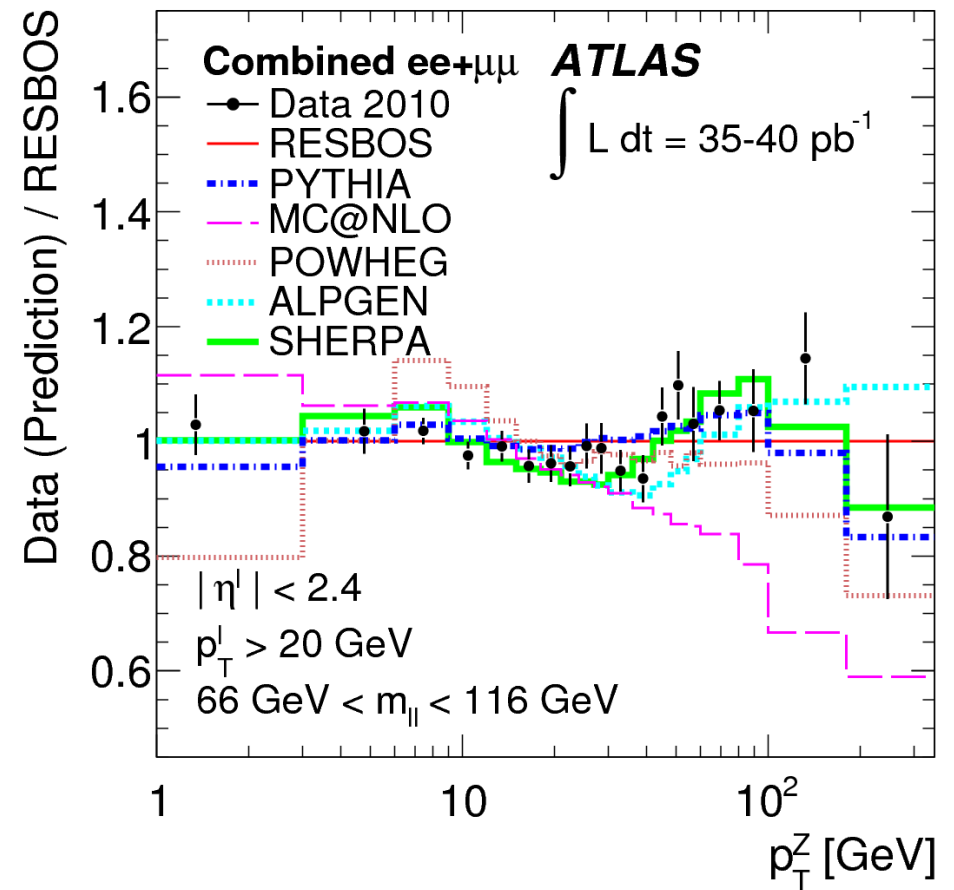
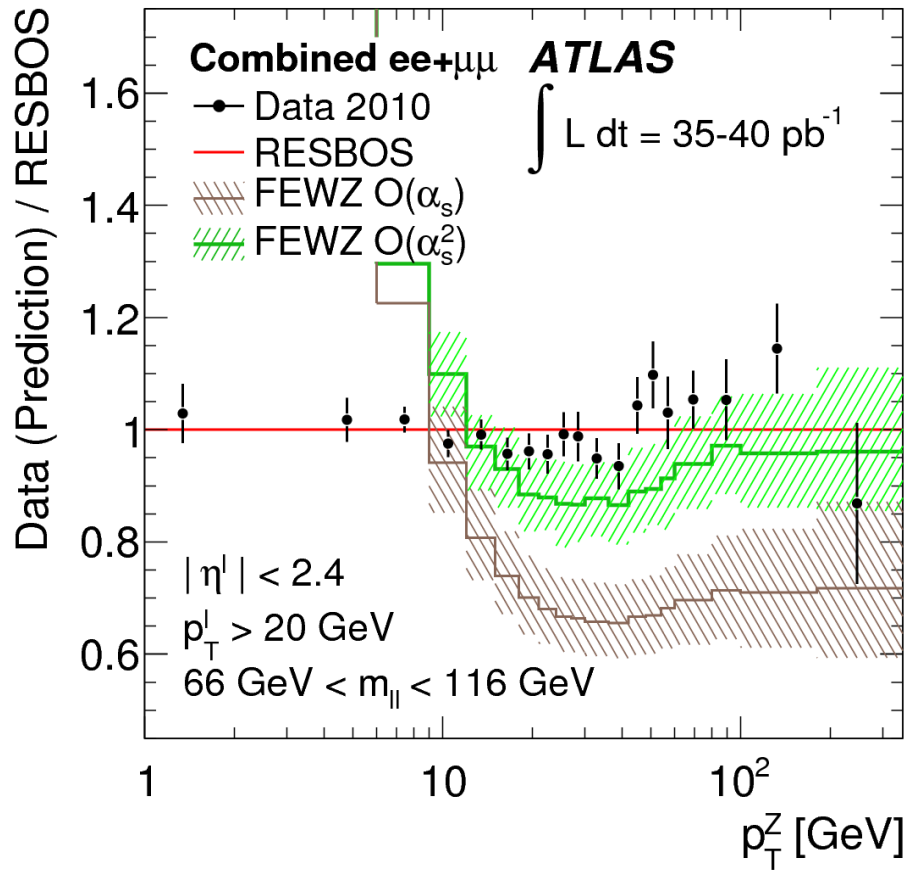
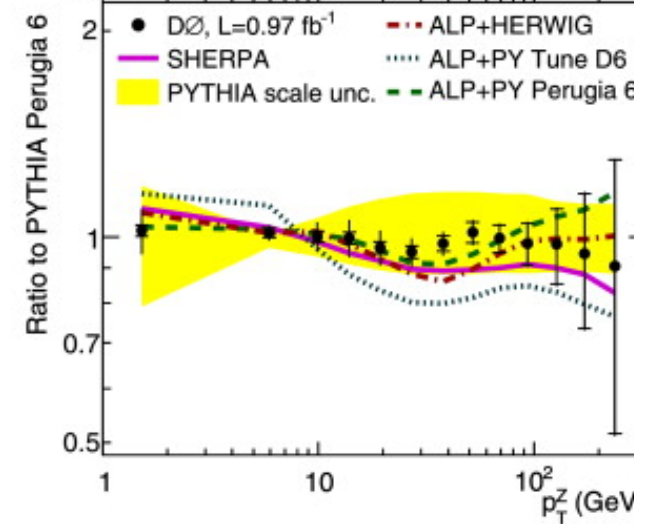
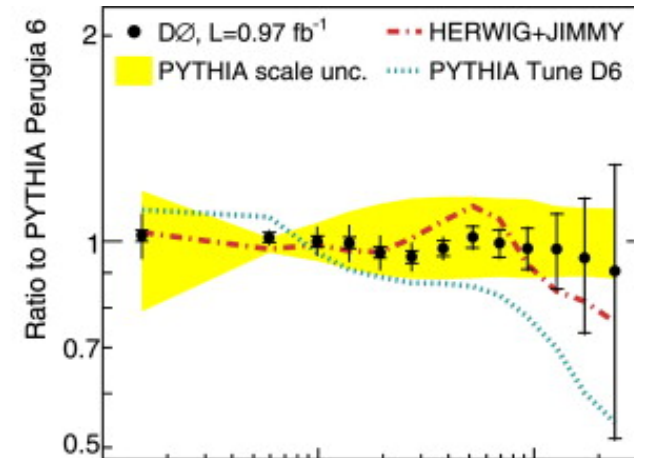
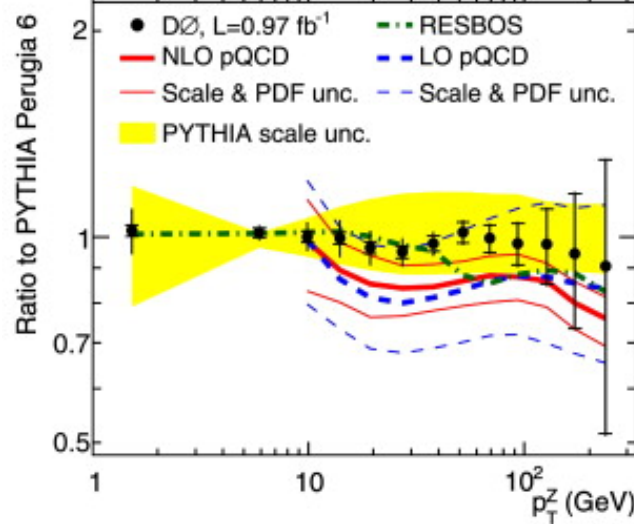
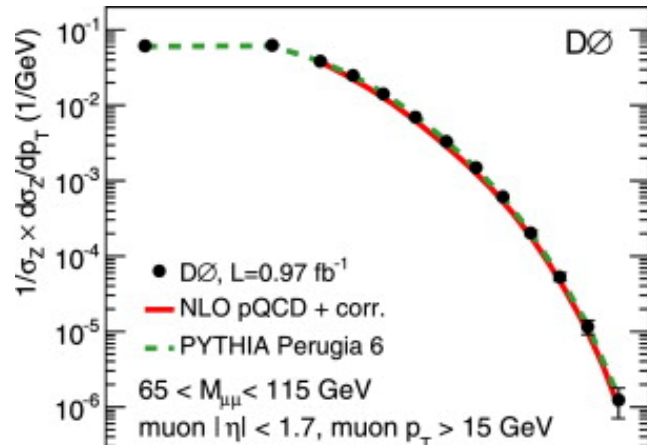
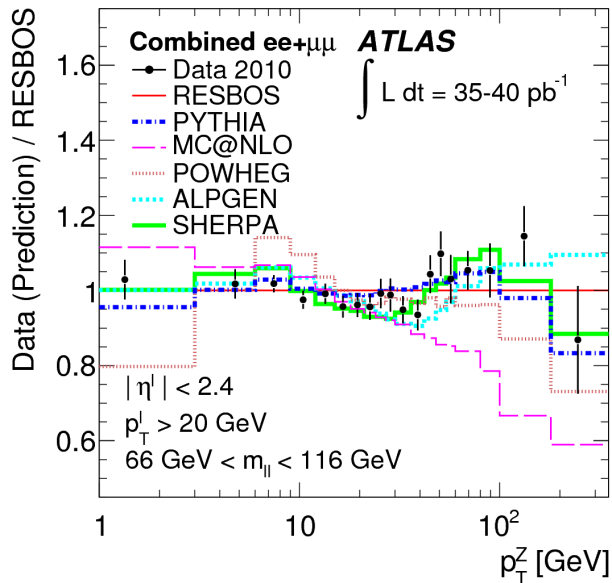
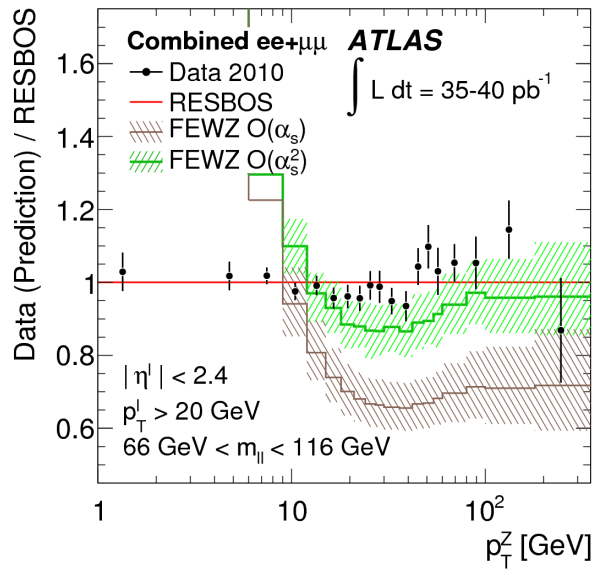


Figure 40. The transverse momentum distribution (low p_T) for $Z \rightarrow e^+e^-$ from CDF in Run 1, along with comparisons to predictions from PYTHIA and ResBos. The dashed blue curve is the default PYTHIA prediction. The PYTHIA solid-green curve has had an additional 2 GeV of k_T added to the parton shower.

More $Z p_T$



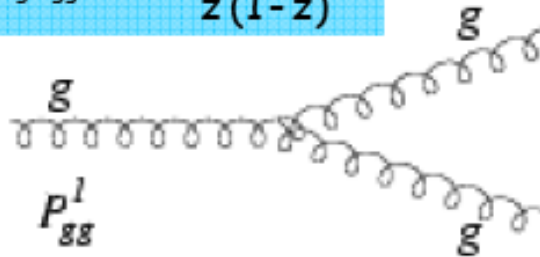
More Z p_T



Higgs p_T distribution

- The Higgs acquires a non-zero p_T through initial state gluon radiation
- Note the peak is much higher than the peak for W or Z production at the LHC, for two reasons
 - ◆ larger color charge for $g \rightarrow gg$ coupling, so more radiation
 - ◆ the $g \rightarrow gg$ splitting function has poles at both $z \rightarrow 0$ and $z \rightarrow 1$

$$P_{g \rightarrow gg} = 3 \frac{(1-z)(1-z)^2}{z(1-z)}$$



- ◆ whenever the initial gluon gives most of its momentum to the radiated gluon in a branching, there is also a large k_T kick
- ◆ I will call this the Sjostrand conjecture

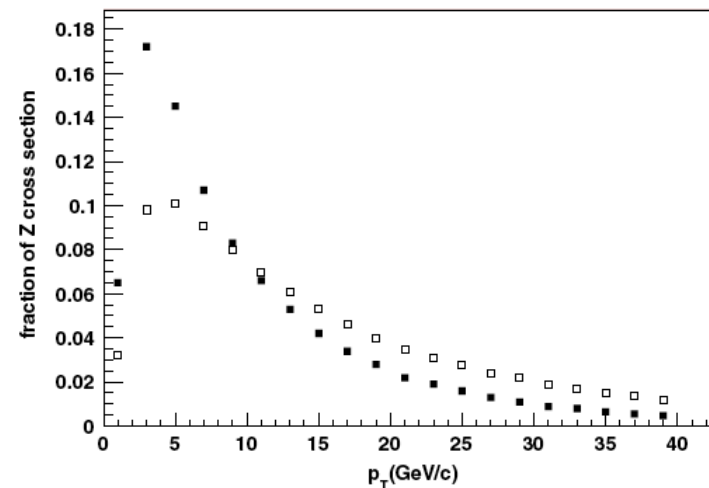
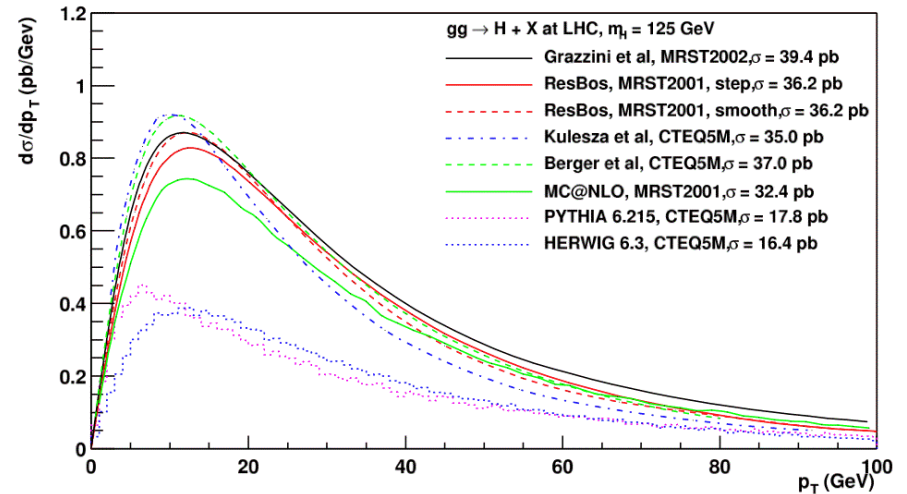
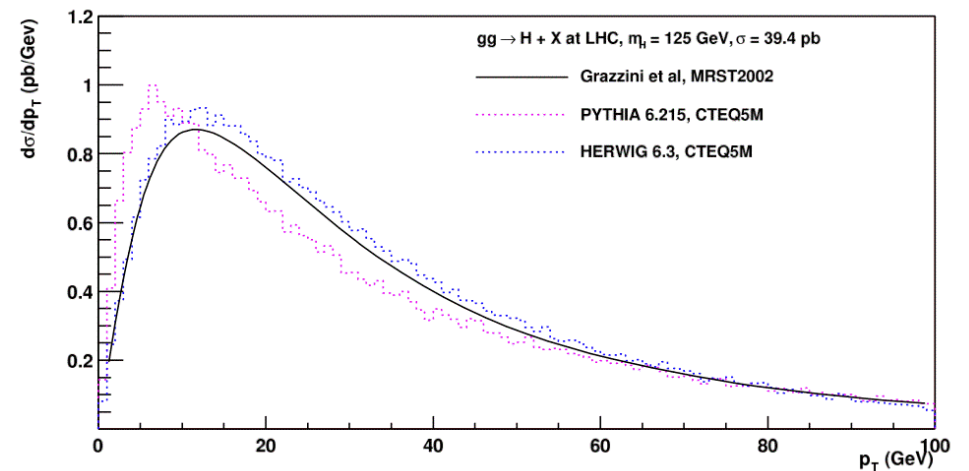
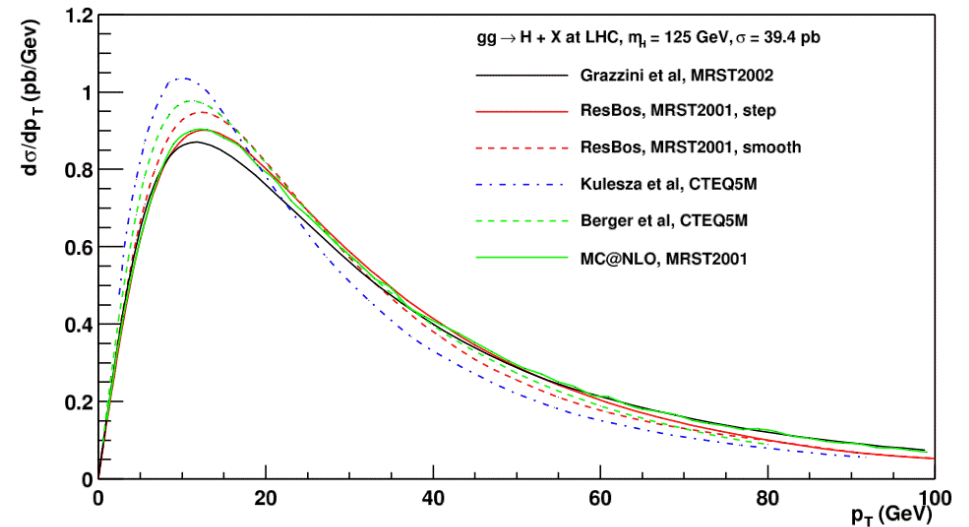


Figure 89. Predictions for the transverse momentum distributions for Z production at the Tevatron (solid squares) and LHC (open squares).

Higgs p_T distributions

- Effects of soft gluon initial state radiation reproduced by both parton shower Monte Carlos and by resummation programs
- Similar results, although Herwig does a bit better job than Pythia



PDF correlations

- Consider a cross section $X(a)$, a function of the Hessian eigenvectors
- i^{th} component of gradient of X is

$$\frac{\partial X}{\partial a_i} \equiv \partial_i X = \frac{1}{2}(X_i^{(+)} - X_i^{(-)})$$

- Now take 2 cross sections X and Y
 - or one or both can be pdf's
- Consider the projection of gradients of X and Y onto a circle of radius 1 in the plane of the gradients in the parton parameter space
- The circle maps onto an ellipse in the XY plane
- The angle ϕ between the gradients of X and Y is given by

$$\cos \varphi = \frac{\vec{\nabla} X \cdot \vec{\nabla} Y}{\Delta X \Delta Y} = \frac{1}{4\Delta X \Delta Y} \sum_{i=1}^N (X_i^{(+)} - X_i^{(-)}) (Y_i^{(+)} - Y_i^{(-)})$$

- The ellipse itself is given by

$$\left(\frac{\delta X}{\Delta X}\right)^2 + \left(\frac{\delta Y}{\Delta Y}\right)^2 - 2\left(\frac{\delta X}{\Delta X}\right)\left(\frac{\delta Y}{\Delta Y}\right)\cos \varphi = \sin^2 \varphi$$

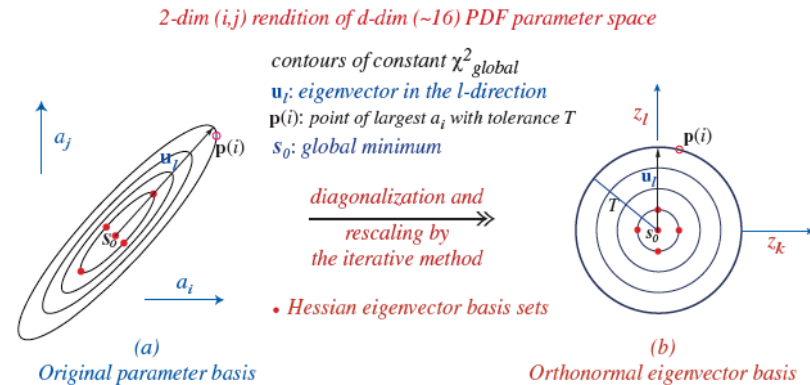


Figure 28. A schematic representation of the transformation from the pdf parameter basis to the orthonormal eigenvector basis.

- If two cross sections are very correlated, then $\cos \phi \sim 1$
- ...uncorrelated, then $\cos \phi \sim 0$
- ...anti-correlated, then $\cos \phi \sim -1$

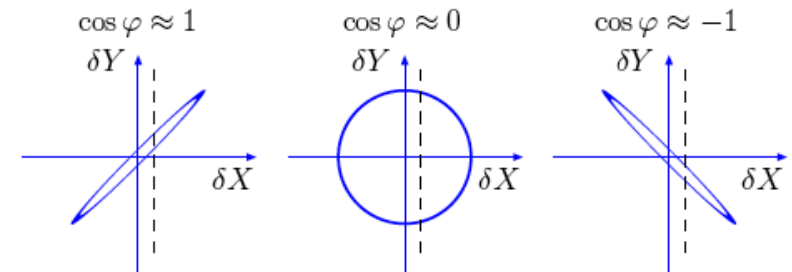


Figure 1: Dependence on the correlation ellipse formed in the $\Delta X - \Delta Y$ plane on the value of the correlation cosine $\cos \varphi$.

...from PDF4LHC report (CTEQ6.6)

Process	σ	PDF (asym)	PDF (sym)	$\alpha_s(m_Z)$ error	combined	correlation
$\sigma_{W^+} * BR(W^+ \rightarrow l^+ \nu)[nb]$	6.057	+0.123/-0.119	0.116	0.045	0.132	0.87
$\sigma_{W^-} * BR(W^- \rightarrow l^- \nu)[nb]$	4.106	+0.088/-0.091	0.088	0.029	0.092	0.92
$\sigma_{Z^0} * BR(Z^0 \rightarrow l^+ l^-)[nb]$	0.9469	+0.018/-0.018	0.018	0.006	0.0187	1.00
$\sigma_{t\bar{t}}[pb]$	156.2	+7.0/-6.7	6.63	4.59	8.06	-0.74
$\sigma_{gg \rightarrow Higgs}(120 GeV)[pb]$	11.59	+0.19/-0.23	0.21	0.20	0.29	0.01
$\sigma_{gg \rightarrow Higgs}(180 GeV)[pb]$	4.840	+0.077/-0.091	0.084	0.091	0.124	-0.47
$\sigma_{gg \rightarrow Higgs}(240 GeV)[pb]$	2.610	+0.054/-0.058	0.056	0.055	0.078	-0.73

Table 5: Benchmark cross section predictions and uncertainties for CTEQ6.6 for W^\pm , Z , $t\bar{t}$ and Higgs production (120, 180, 240 GeV) at 7 TeV. The central prediction is given in column 2. Errors are quoted at the 68% c.l.. Both the symmetric and asymmetric forms for the PDF errors are given. In the next-to-last column, the (symmetric) form of the PDF and $\alpha_s(m_Z)$ errors are added in quadrature. In the last column, the correlation cosine with respect to Z production is given.

The values of ΔX , ΔY , and $\cos \varphi$ are also sufficient to estimate the PDF uncertainty of any function $f(X, Y)$ of X and Y by relating the gradient of $f(X, Y)$ to $\partial_X f \equiv \partial f / \partial X$ and $\partial_Y f \equiv \partial f / \partial Y$ via the chain rule:

$$\Delta f = \left| \vec{\nabla} f \right| = \sqrt{(\Delta X \partial_X f)^2 + 2\Delta X \Delta Y \cos \varphi \partial_X f \partial_Y f + (\Delta Y \partial_Y f)^2}. \quad (9)$$

Used for LHC Higgs searches

Procedure for the LHC Higgs boson search combination in summer 2011

(LHC Higgs Combination Group Report)

A. Armbruster¹, K. A. Assamagan², S. Banerjee³, G. Gomez-Ceballos⁴, M. Chen⁵, G. Cowan⁶,
K. Cranmer⁷, S. Ferrag⁸, E. Gros⁹, J. Huston¹⁰, A. Korytov⁵, C. Mariotti¹¹, L. Moneta¹²,
W. J. Murray¹³, G. Petrucciani¹⁴, J. Qian², G. Schott¹⁵, V. Sharma¹⁴, G. E. Steele⁸,
R. Tanaka¹⁶, F. Tarrade¹⁷, O. Vitells⁹, and H. Wang⁴

¹*University of Michigan, Ann Arbor, MI, USA*

²*BNL, Upton, NY, USA*

³*University of Wisconsin, Madison, WI, USA*

⁴*Massachusetts Institute of Technology, Cambridge, MA, USA*

⁵*University of Florida, Gainesville, FL, USA*

⁶*Royal Holloway, University of London, Egham Hill, Egham, UK*

⁷*New York University, New York, NY, USA*

⁸*University of Glasgow, Glasgow, UK*

⁹*Weizmann Institute of Science, Rehovot, Israel*

¹⁰*Michigan State University, East Lansing, MI, USA*

¹¹*INFN, Torino, Italy*

¹²*CERN, Geneva, Switzerland*

¹³*Rutherford Appleton Laboratory, Didcot, UK*

¹⁴*University of California, San Diego, CA, USA*

¹⁵*IEKP, Karlsruhe Institute of Technology, Karlsruhe, Germany*

¹⁶*LAL, Orsay, France*

¹⁷*Carleton University, Ottawa, ON, Canada*

June 30, 2011

...in YR2 report

Table 10: The up-to-date PDF4LHC average for the correlations between all signal processes with other signal and background processes for Higgs production considered here. The processes have been classified in correlation classes, as discussed in the text.

$M_H = 120 \text{ GeV}$	ggH	VBF	WH	$t\bar{t}H$	$M_H = 160 \text{ GeV}$	ggH	VBF	WH	$t\bar{t}H$
ggH	1	-0.6	-0.2	-0.2	ggH	1	-0.6	-0.4	0.2
VBF	-0.6	1	0.6	-0.4	VBF	-0.6	1	0.6	-0.2
WH	-0.2	0.6	1	-0.2	WH	-0.4	0.6	1	0
$t\bar{t}H$	-0.2	-0.4	-0.2	1	$t\bar{t}H$	0.2	-0.2	0	1
W	-0.2	0.6	0.8	-0.6	W	-0.4	0.4	0.6	-0.4
WW	-0.4	0.8	1	-0.2	WW	-0.4	0.6	0.8	-0.2
WZ	-0.2	0.4	0.8	-0.4	WZ	-0.4	0.4	0.8	-0.2
$W\gamma$	0	0.6	0.8	-0.6	$W\gamma$	-0.4	0.6	0.6	-0.6
$Wb\bar{b}$	-0.2	0.6	1	-0.2	$Wb\bar{b}$	-0.2	0.6	0.8	-0.2
$t\bar{t}$	0.2	-0.4	-0.4	1	$t\bar{t}$	0.4	-0.4	-0.2	0.8
$t\bar{b}$	-0.4	0.6	1	-0.2	$t\bar{b}$	-0.4	0.6	1	0
$t(\rightarrow \bar{b})q$	0.4	0	0	0	$t(\rightarrow \bar{b})q$	0.6	0	0	0

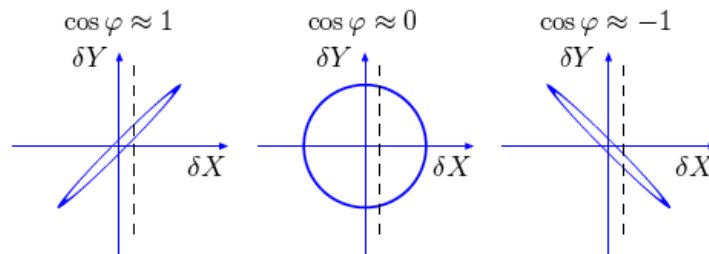


Figure 1: Dependence on the correlation ellipse formed in the $\Delta X - \Delta Y$ plane on the value of the correlation cosine $\cos \varphi$.

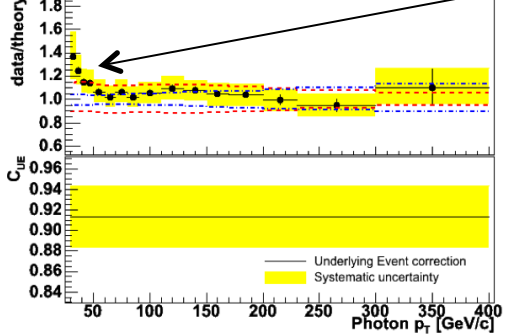
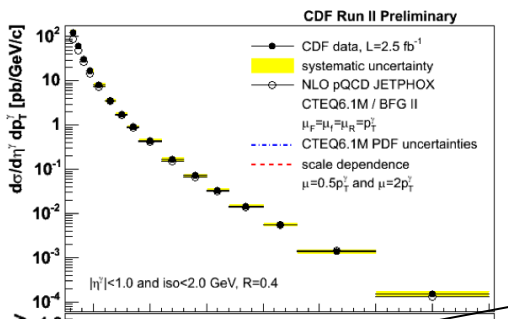
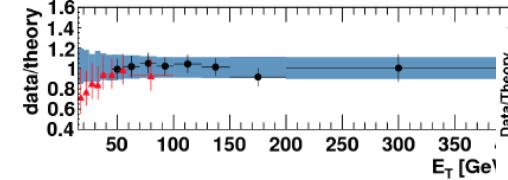
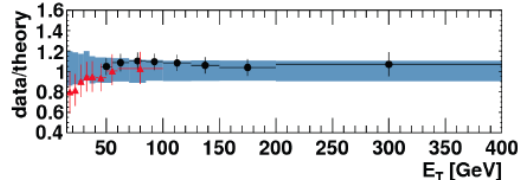
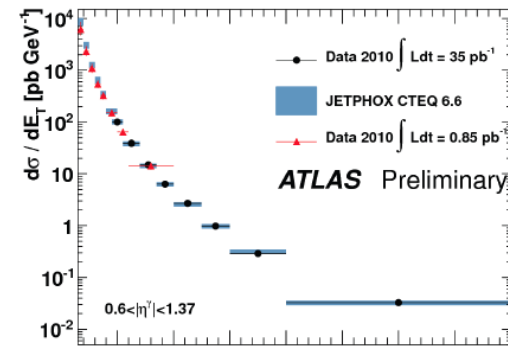
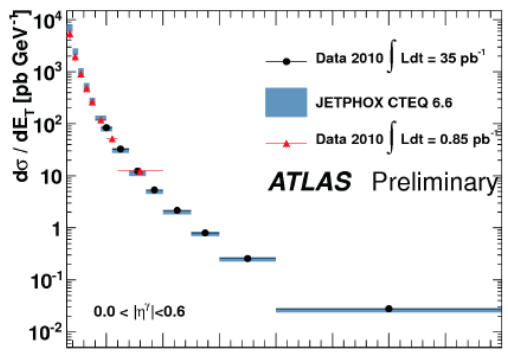
Followup for PDF4LHC

- Study of NNLO PDFs from all 6 PDF groups
 - ◆ drawing from what Graeme has done, but now including CT10/12 NNLO
 - ◆ detailed comparisons to LHC data which have provided detailed correlated systematic error information, keeping track of required systematic error shifts, normalizations, etc
 - ▲ ATLAS W/Z rapidity distributions
 - ▲ ATLAS inclusive jet cross section data
- Currently working on it with Pavel Nadolsky and Juan Rojo

LHC: inclusive photon production

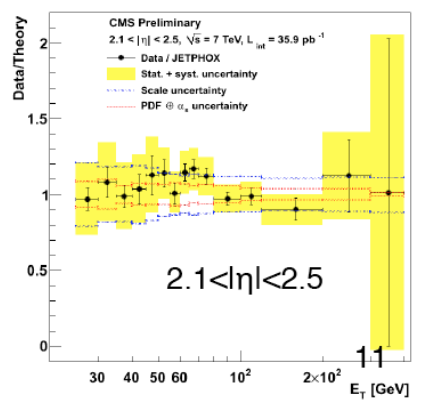
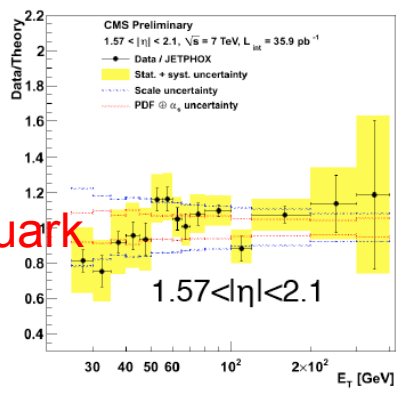
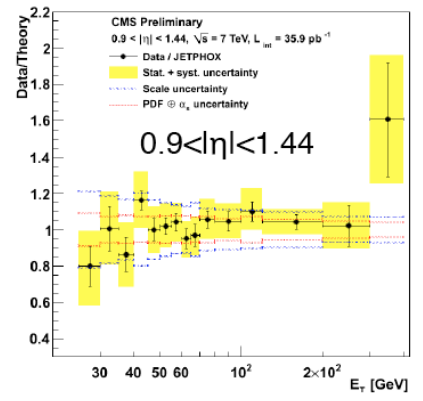
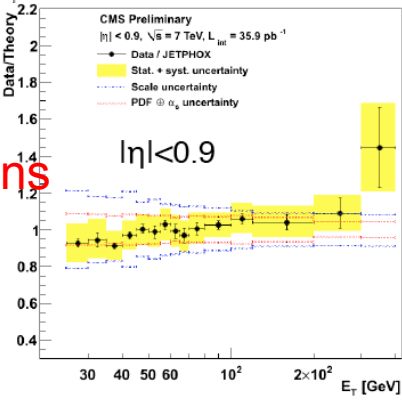
PRD83, 052005(2011)
ATLAS-CONF-2011-058

PRL106, 082001 (2011)
CMS-QCD 10-037



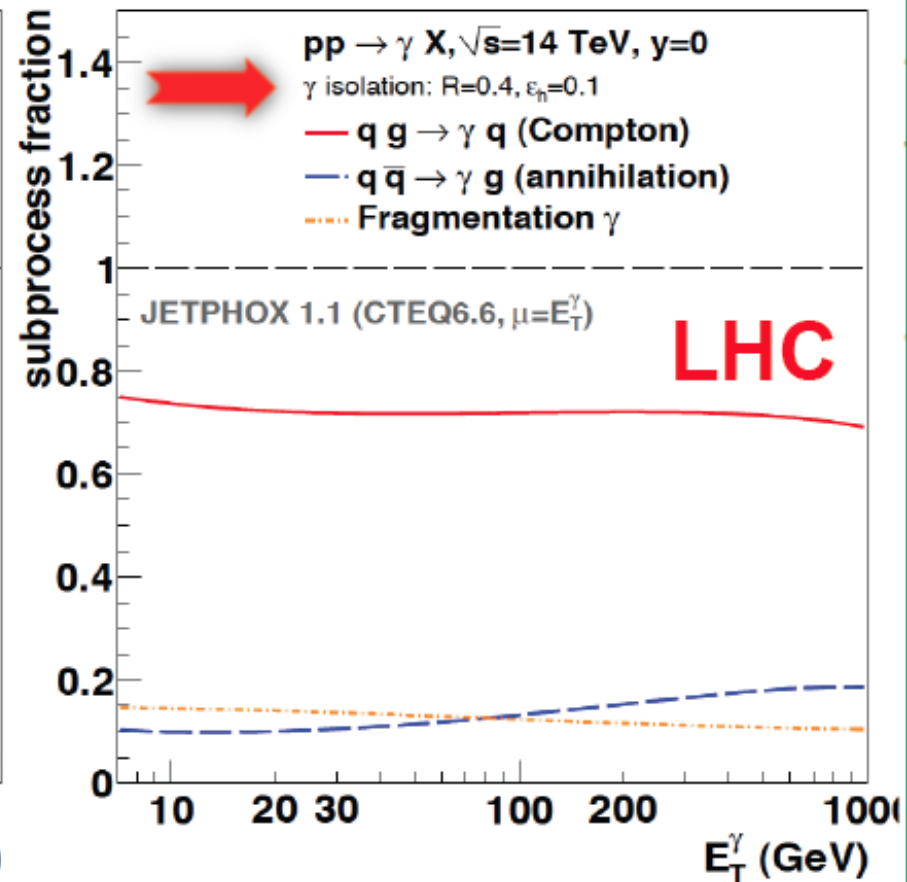
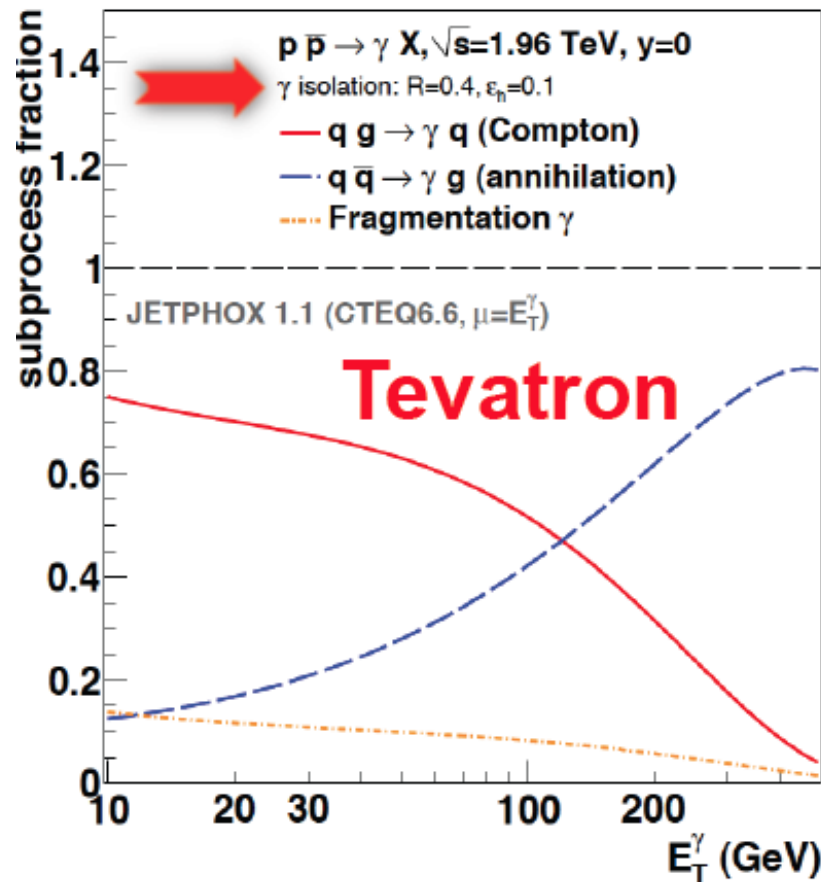
some (negative) deviations observed at low E_T , in contrast to positive deviations observed at Tevatron

still might be unresolved issues regarding fragmentation (quark \rightarrow quark + γ) and isolation, in theory vs experiment (my humble opinion)



Tevatron vs LHC

- High p_T direct photon production at the Tevatron is dominated by $q\bar{q}$ scattering
 - ◆ and so does not contribute much information about the gluon distribution at high x
- We have a much broader reach at the LHC, and a domination by the qg scattering process \rightarrow another handle on the gluon distribution in PDF fits



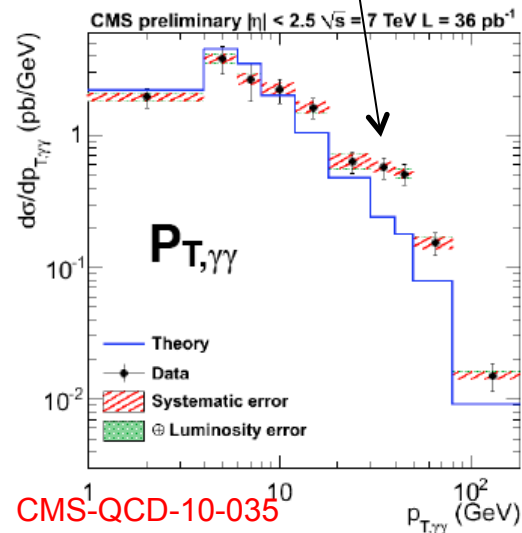
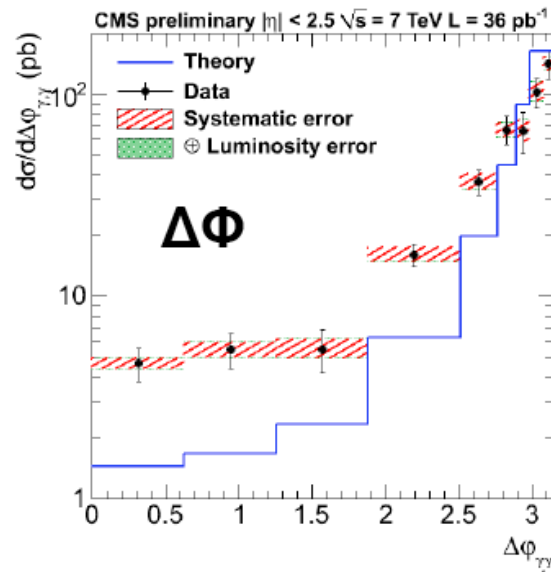
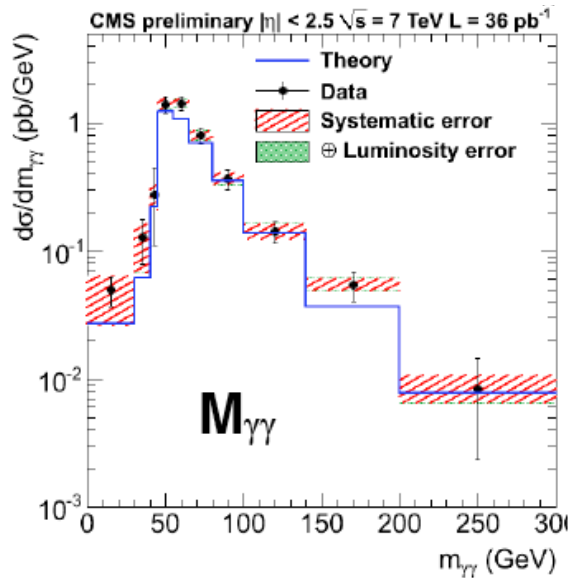
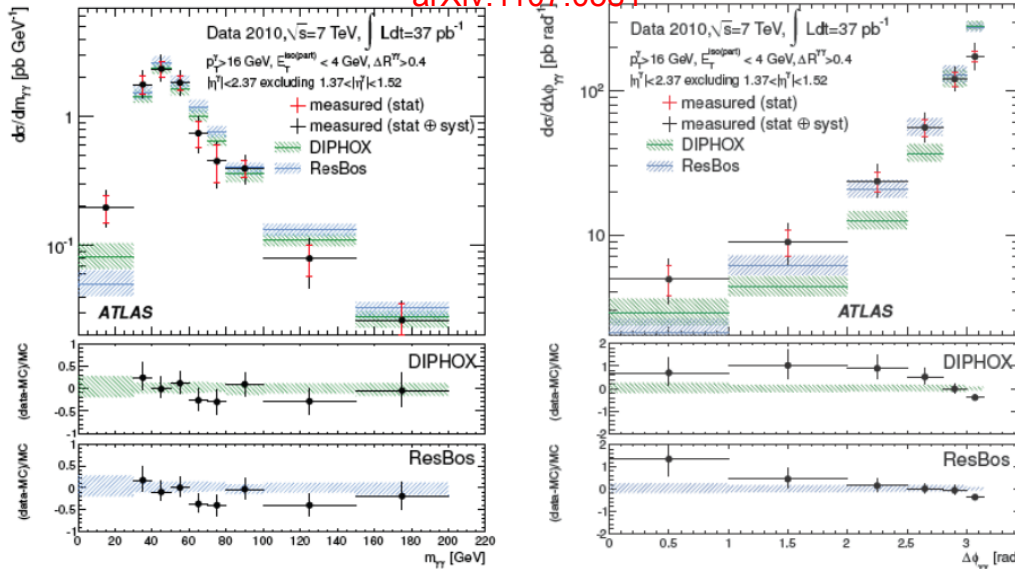
LHC: diphotons

arXiv:1107.0581

crucial channel for Higgs discovery/
measurement, potential new physics

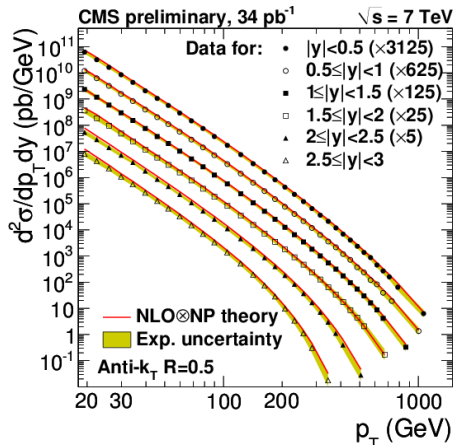
...again evidence for substantial
fragmentation contributions not
accounted for in perturbative
predictions

...luckily, fragmentation effects mostly
at low mass



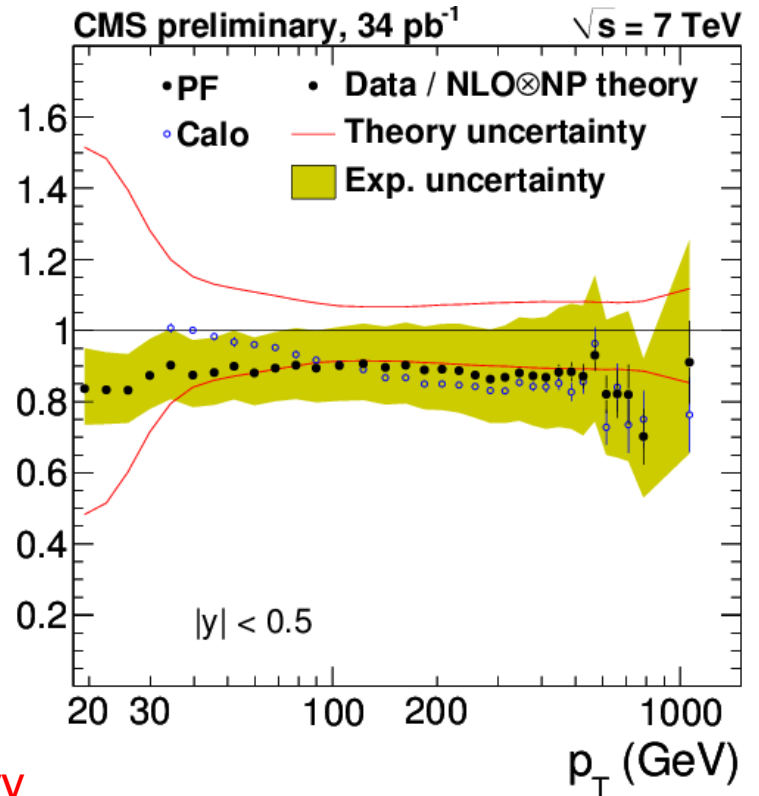
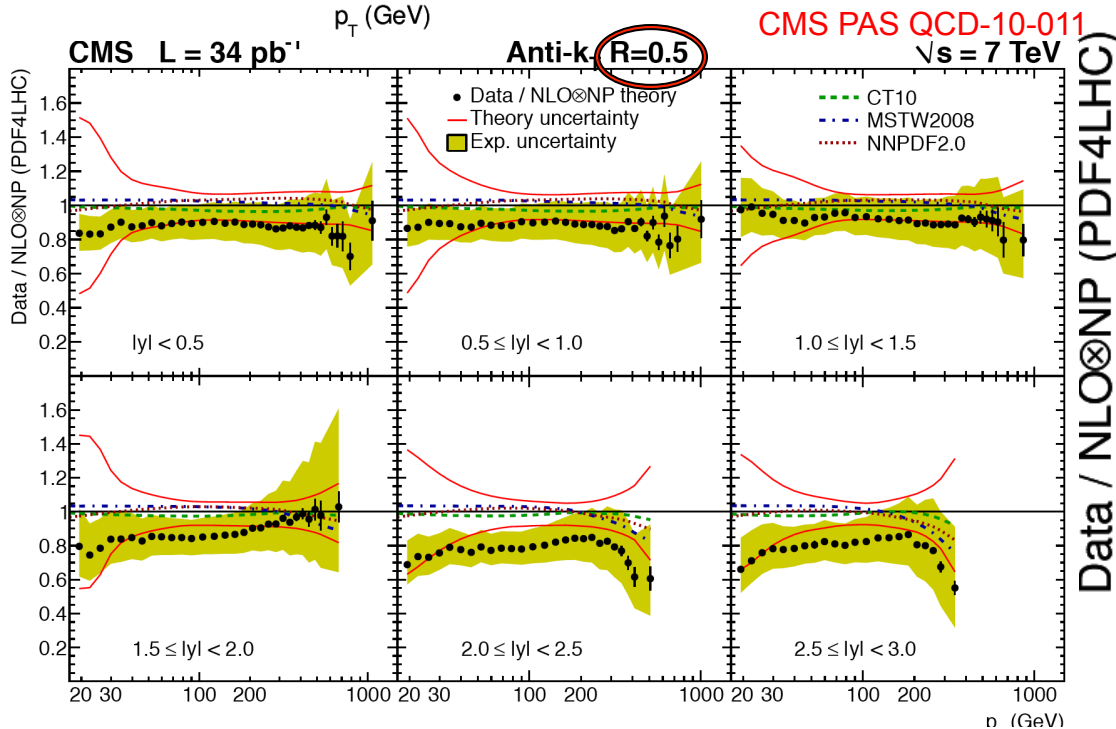
Guillet shoulder

CMS: inclusive jets



Here the comparison is to predictions using the midpoint of CT10, MSTW2008 and NNPDF2.0, with the error band given by the envelope (i.e. the PDF4LHC prescription). The theory error also includes the scale choice and NP uncertainties.

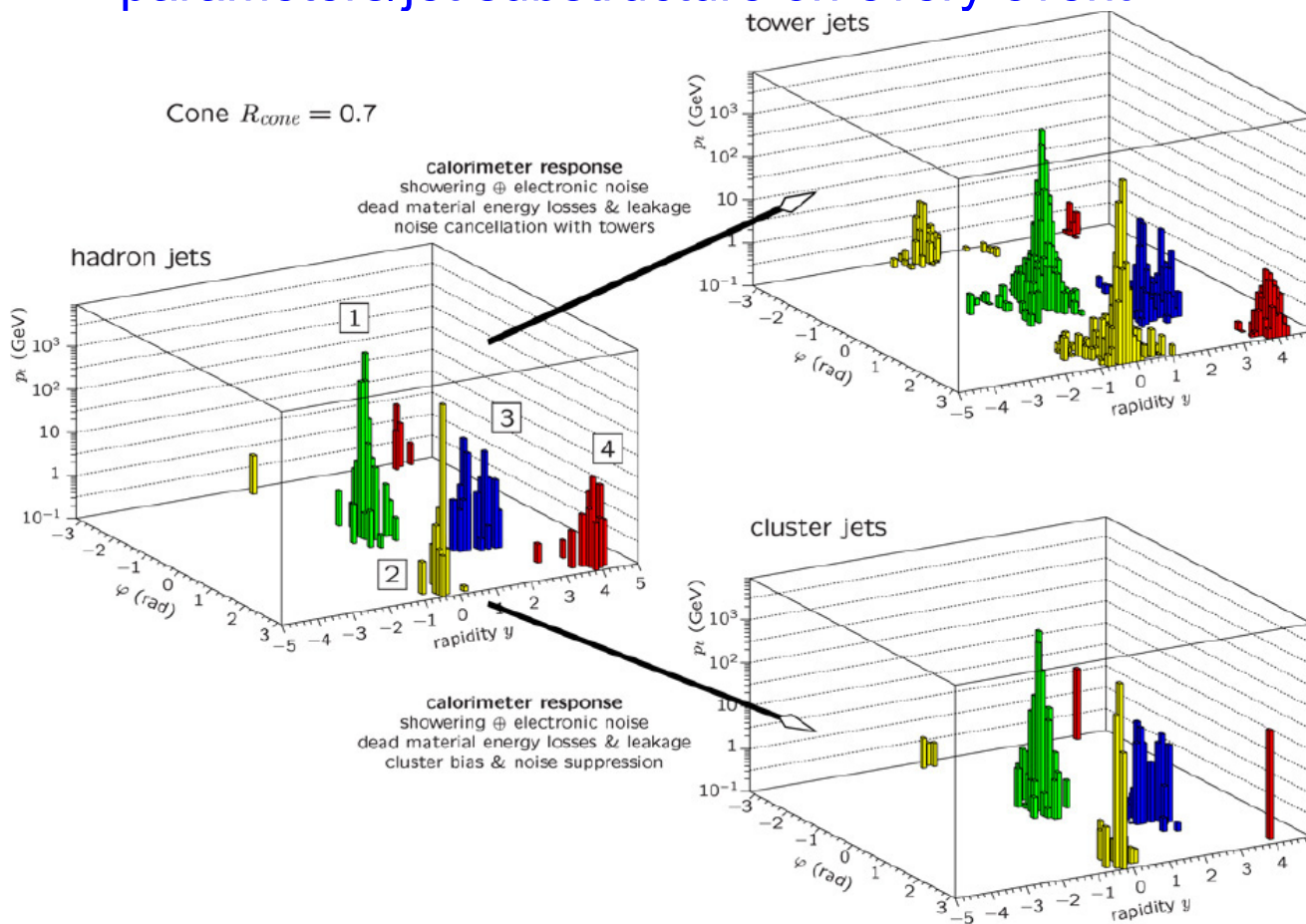
The physics results are more robust if they can be carried out with two (or more) measurement techniques, in this case a calorimetric measurement and one using the Particle Flow method.



...agreement but data a bit low compared to theory

ATLAS jet reconstruction

- Using calibrated topoclusters, ATLAS has a chance to use jets in a dynamic manner not possible in any previous hadron-hadron calorimeter, i.e. to examine the impact of multiple jet algorithms/parameters/jet substructure on every event



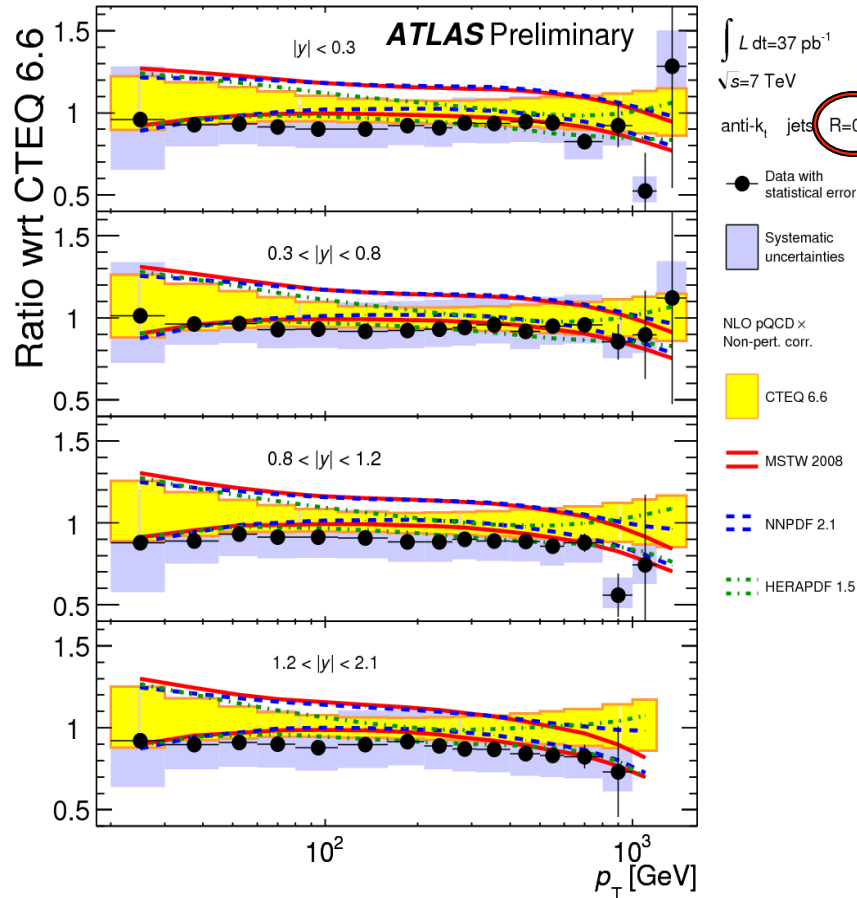
blobs of energy in the calorimeter correspond to 1/few particles (photons, electrons, hadrons); can be corrected back to hadron level

rather than jet itself being corrected

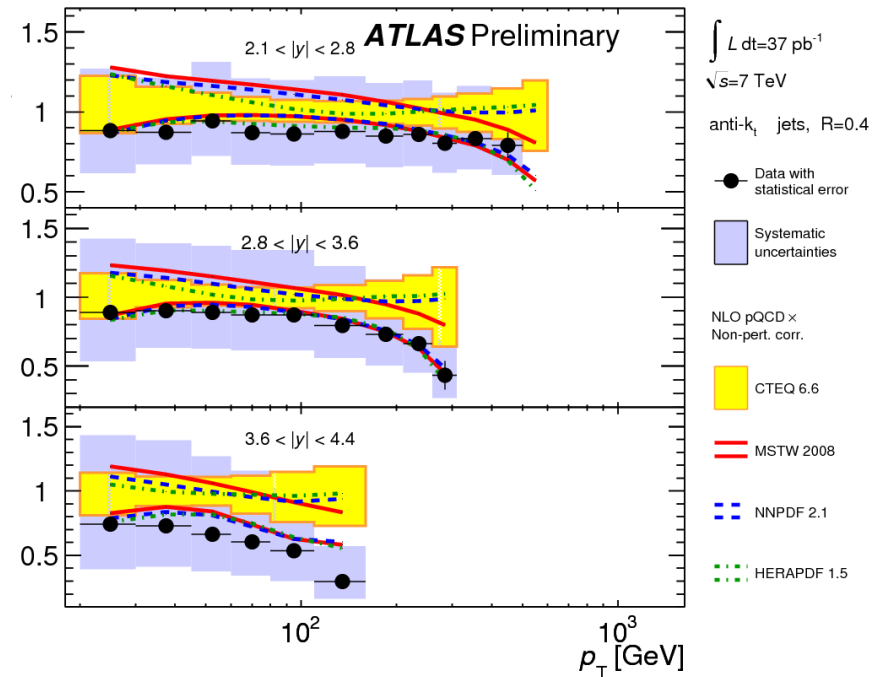
similar to running at hadron level in Monte Carlos

ATLAS inclusive jets

- Important to carry predictions out over wide rapidity range. New physics tends to be central. Old physics (PDFs) has an impact on all rapidity regions. This data (or higher statistics version can be fed back into global PDF fits and can/will have impact, especially on high x gluon.



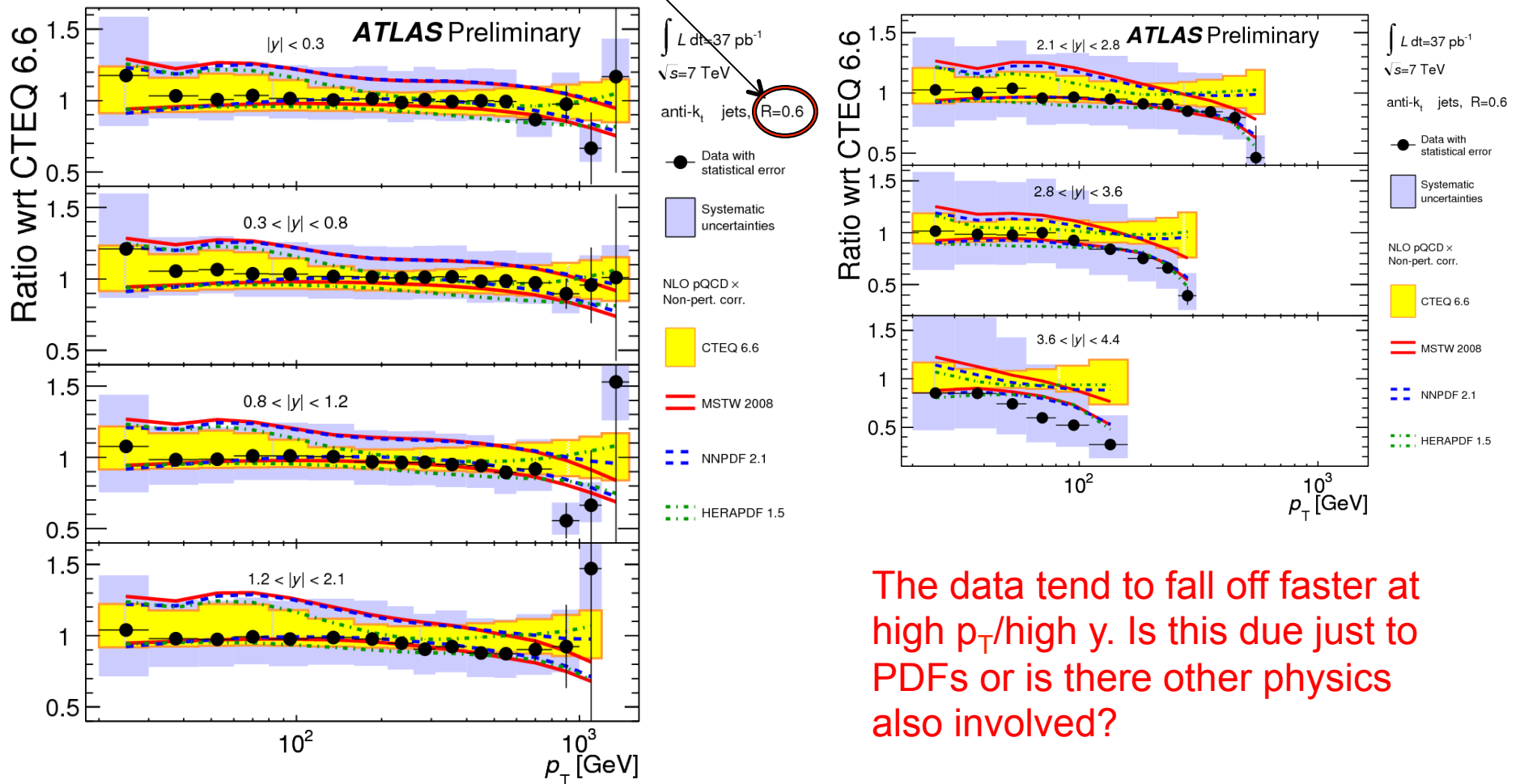
ATLAS-CONF-2011-047



but the use in global PDF fits is possible only once detailed correlated systematic error information is made available. For jets, systematic errors are much more important than statistical errors. This has been done for the ATLAS (but not CMS) 2010 data.

ATLAS: inclusive jets

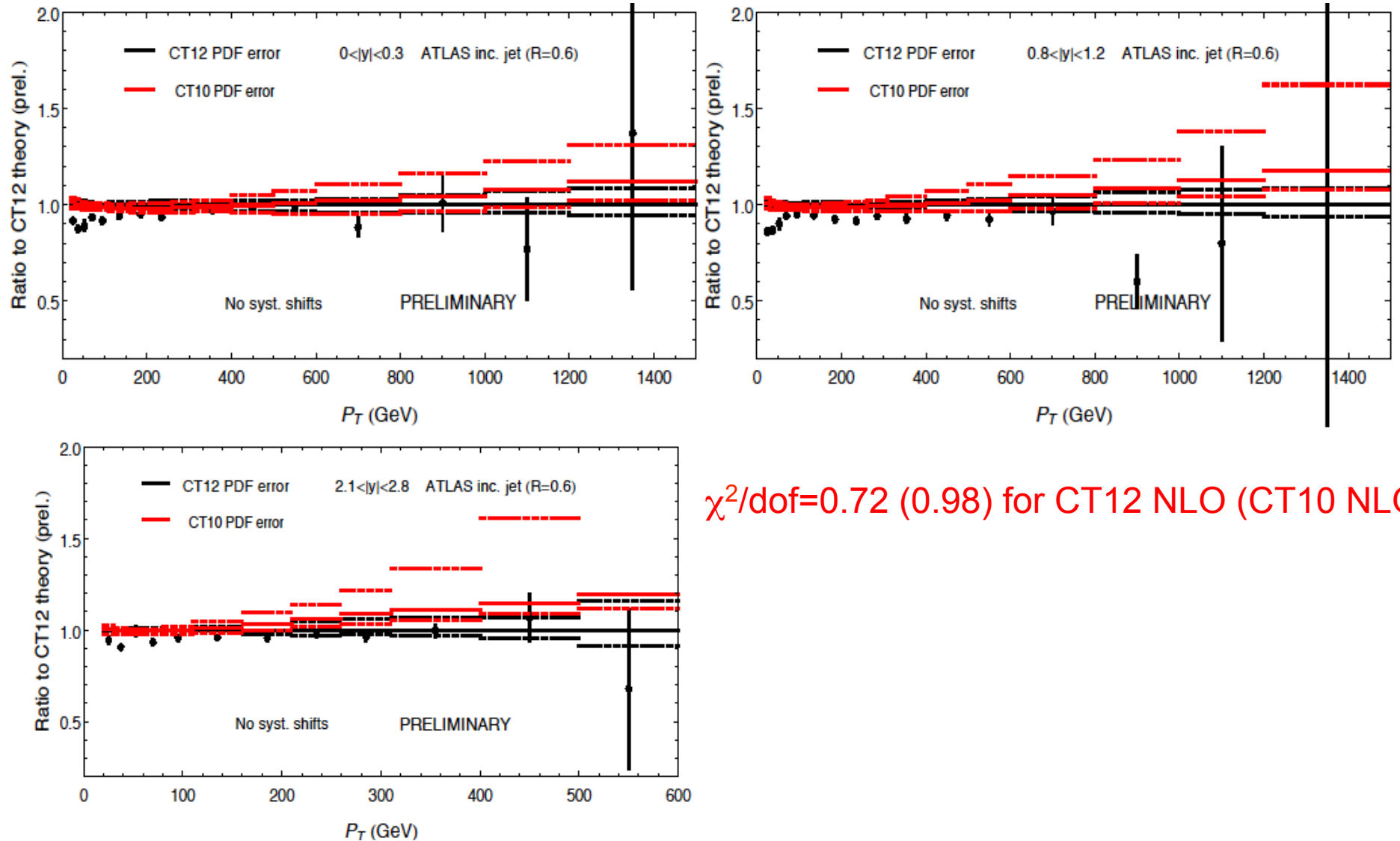
Important to use more than one jet size. Different dependence on underlying event, fragmentation and also on perturbative prediction.



The data tend to fall off faster at high p_T /high y . Is this due just to PDFs or is there other physics also involved?

CT12 NLO predictions for ATLAS jet production (preliminary)

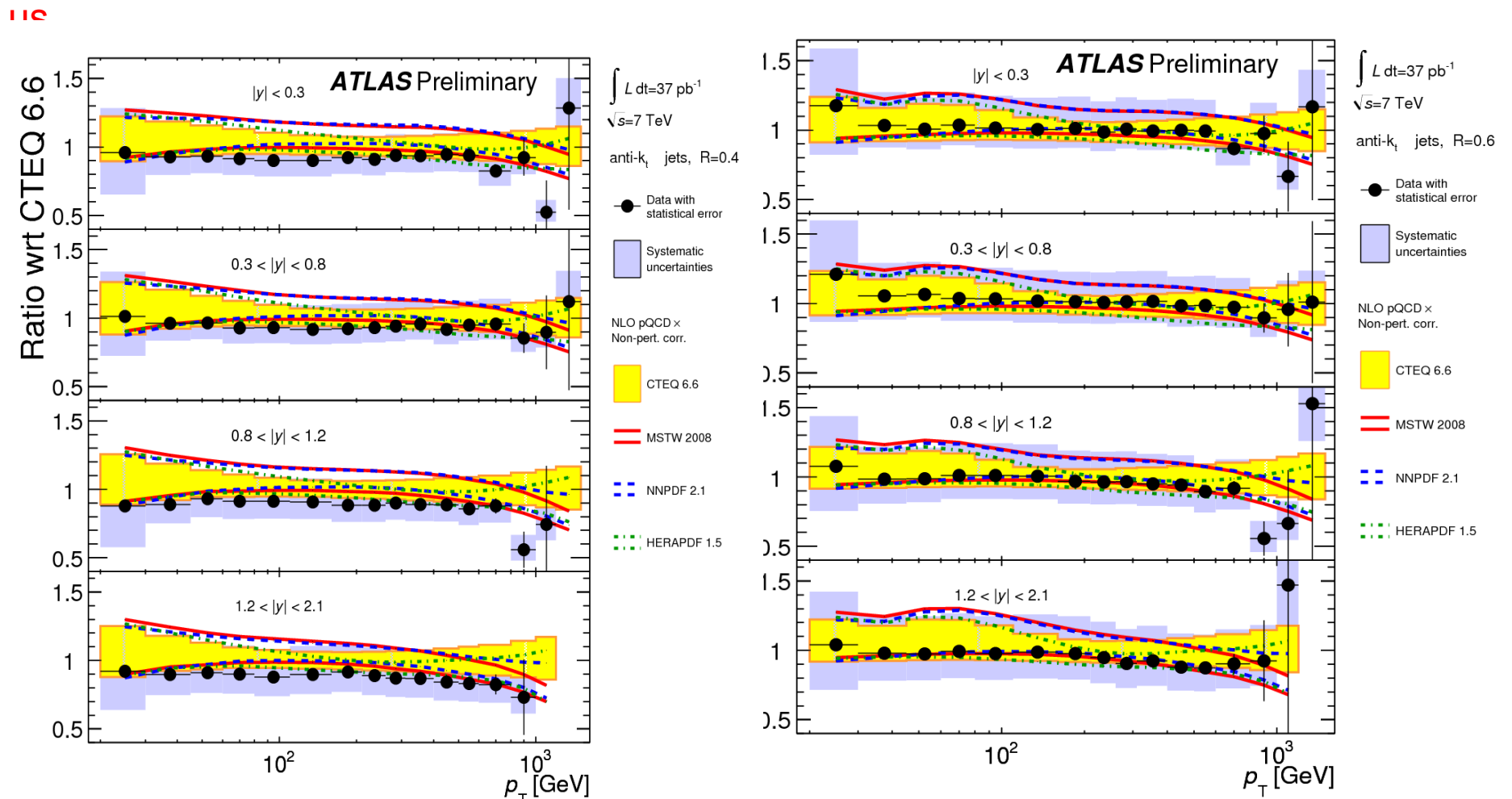
- CT12 NLO PDFs predict smaller jet cross sections at large p_T than CT10



$\chi^2/\text{dof}=0.72$ (0.98) for CT12 NLO (CT10 NLC)

ATLAS: inclusive jets

Relative agreement between the data and theory for the two jet sizes reasonable, but not perfect. Do we understand the R-dependence of jet cross sections? Note that correction for UE/hadronization implicitly assumes that NLO=parton shower as far as jet shape properties are concerned. Is that correct to the level we need it? NLO parton shower MC's should be able to tell



Cross-section ratio at different radii

Another potentially interesting ratio to look at is

$$\mathcal{R}(p_t; R_1, R_2) = \frac{d\sigma/dp_t(R = R_1)}{d\sigma/dp_t(R = R_2)} \quad \text{G. Soyez}$$

Better perturbative computation:

$$\begin{aligned} \sigma(p_t; R) &= \alpha_s^2 \sigma_{\text{tree}}^{2 \rightarrow 2} + \alpha_s^3 [\sigma_{\text{tree}}^{2 \rightarrow 3}(R) + \sigma_{1\text{-loop}}^{2 \rightarrow 2}] \\ &+ \alpha_s^4 [\sigma_{\text{tree}}^{2 \rightarrow 4}(R) + \sigma_{1\text{-loop}}^{2 \rightarrow 3}(R) + \sigma_{2\text{-loop}}^{2 \rightarrow 2}] + \mathcal{O}(\alpha_s^5) \end{aligned}$$

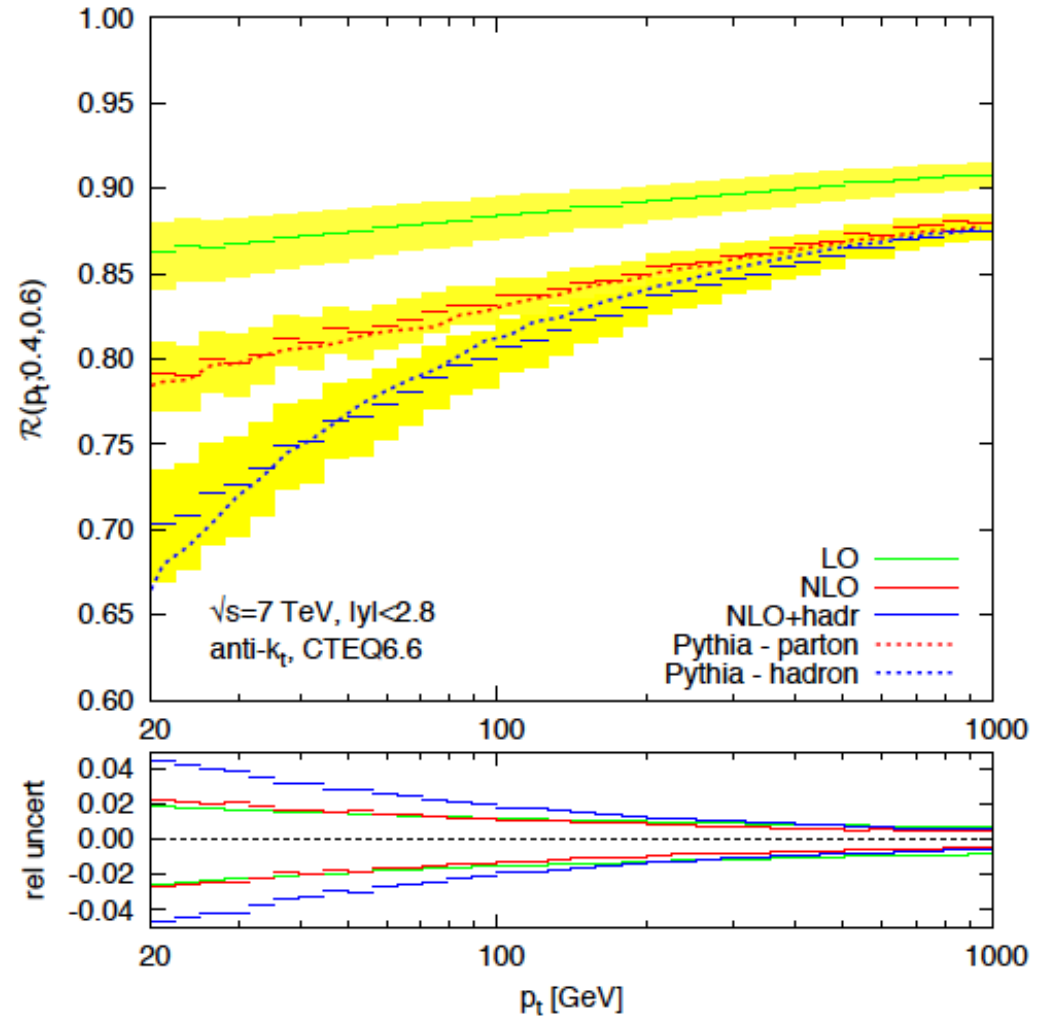
The unknown 2-loop contribution cancels in the ratio:

$$\begin{aligned} \mathcal{R} &= 1 + \alpha_s \frac{\Delta \sigma_{\text{tree}}^{2 \rightarrow 3}}{\sigma_{\text{tree}}^{2 \rightarrow 2}} \\ &+ \alpha_s^2 \frac{\Delta \sigma_{\text{tree}}^{2 \rightarrow 4} + \Delta \sigma_{1\text{-loop}}^{2 \rightarrow 3}}{\sigma_{\text{tree}}^{2 \rightarrow 2}} - \alpha_s^2 \frac{\sigma_{\text{NLO}}(R_2) \Delta \sigma_{\text{tree}}^{2 \rightarrow 3}}{[\sigma_{\text{tree}}^{2 \rightarrow 2}]^2} \end{aligned}$$

R=0.4/R=0.6

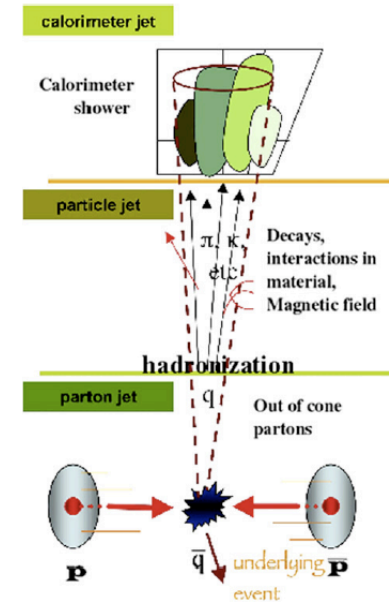
$$\mathcal{R} = 1 + \alpha_s \frac{\Delta\sigma_{\text{tree}}^{2\rightarrow 3}}{\sigma_{\text{tree}}^{2\rightarrow 2}} + \alpha_s^2 \frac{\Delta\sigma_{\text{tree}}^{2\rightarrow 4} + \Delta\sigma_{1\text{-loop}}^{2\rightarrow 3}}{\sigma_{\text{tree}}^{2\rightarrow 2}} - \alpha_s^2 \frac{\sigma_{\text{NLO}}(R_2) \Delta\sigma_{\text{tree}}^{2\rightarrow 3}}{[\sigma_{\text{tree}}^{2\rightarrow 2}]^2}$$

Prediction is that the ratio of 0.4 to 0.6 should be smaller than given by fixed NLO

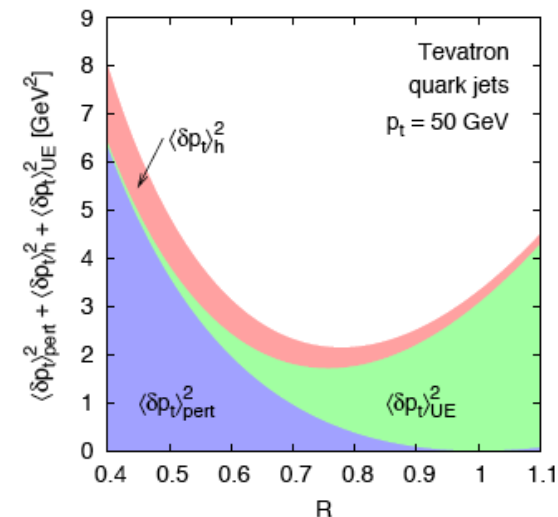


Choosing jet size

- Experimentally
 - ◆ in complex final states, such as $W + n$ jets, it is useful to have jet sizes smaller so as to be able to resolve the n jet structure
 - ◆ this can also reduce the impact of pileup/underlying event
- Theoretically
 - ◆ hadronization effects become larger as R decreases
 - ◆ for small R , the $\ln R$ perturbative terms can become noticeable
 - ◆ this restriction in the gluon phase space can affect the scale dependence, i.e. the scale uncertainty for an n -jet final state can depend on the jet size,



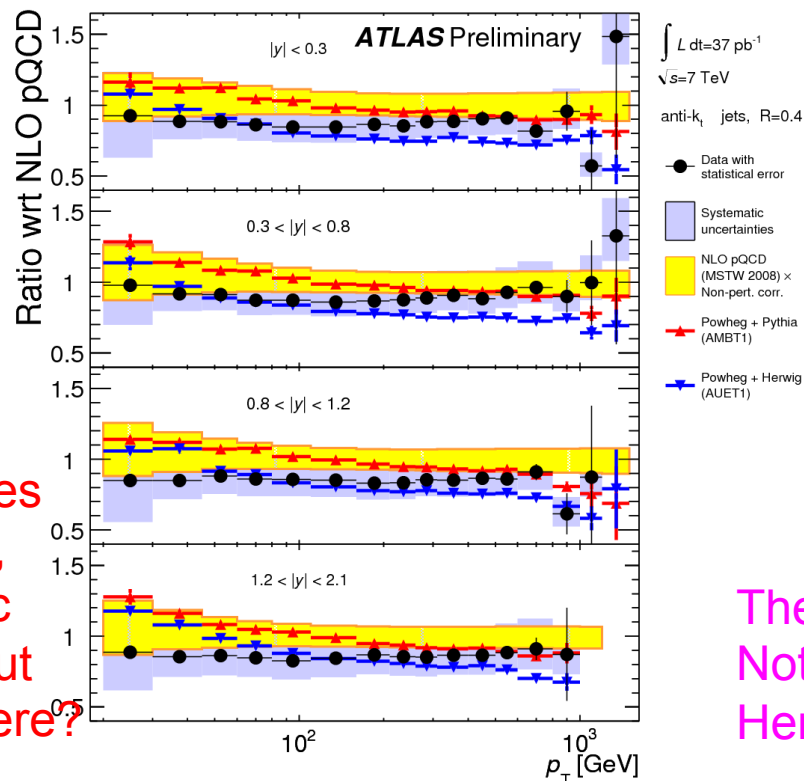
Dasgupta, Magnea, Salam arXiv0712.3014



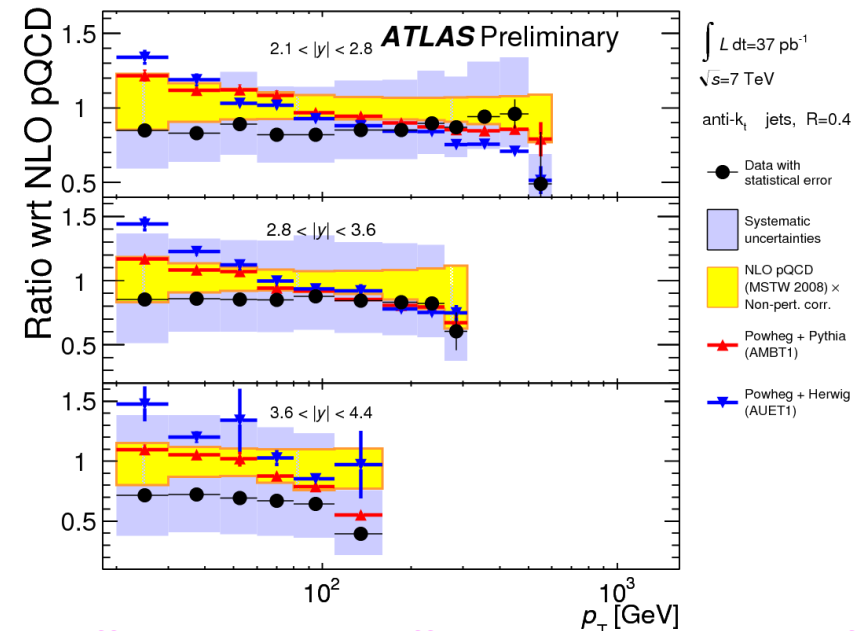
Another motivation for the use of multiple jet algorithms/parameters in LHC analyses.

Inclusive jets: Powheg

- Powheg is a method for the inclusion of NLO matrix element corrections into parton shower Monte Carlos
- Experimentalists were ecstatic when inclusive jet production was added
- Note that Powheg predictions have a different shape than fixed order perturbative predictions (NLOJET++). This is something that must be understood, and investigation is currently underway by Powheg authors.
- Also: dijets in aMC@NLO->S. Frixione



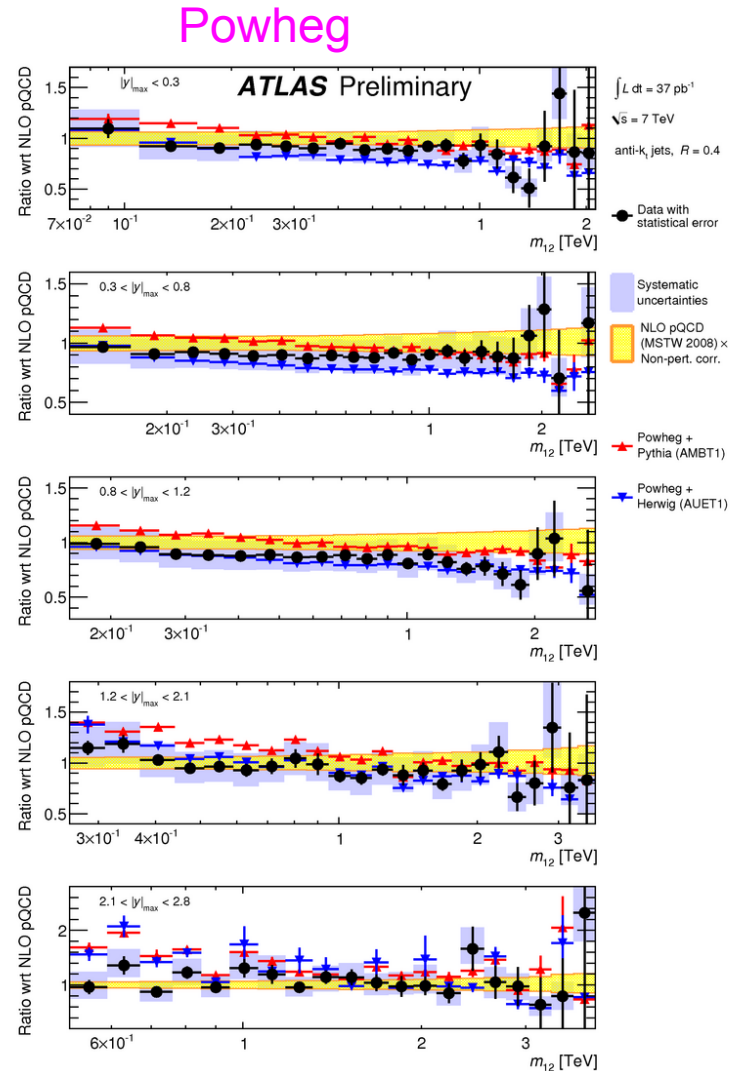
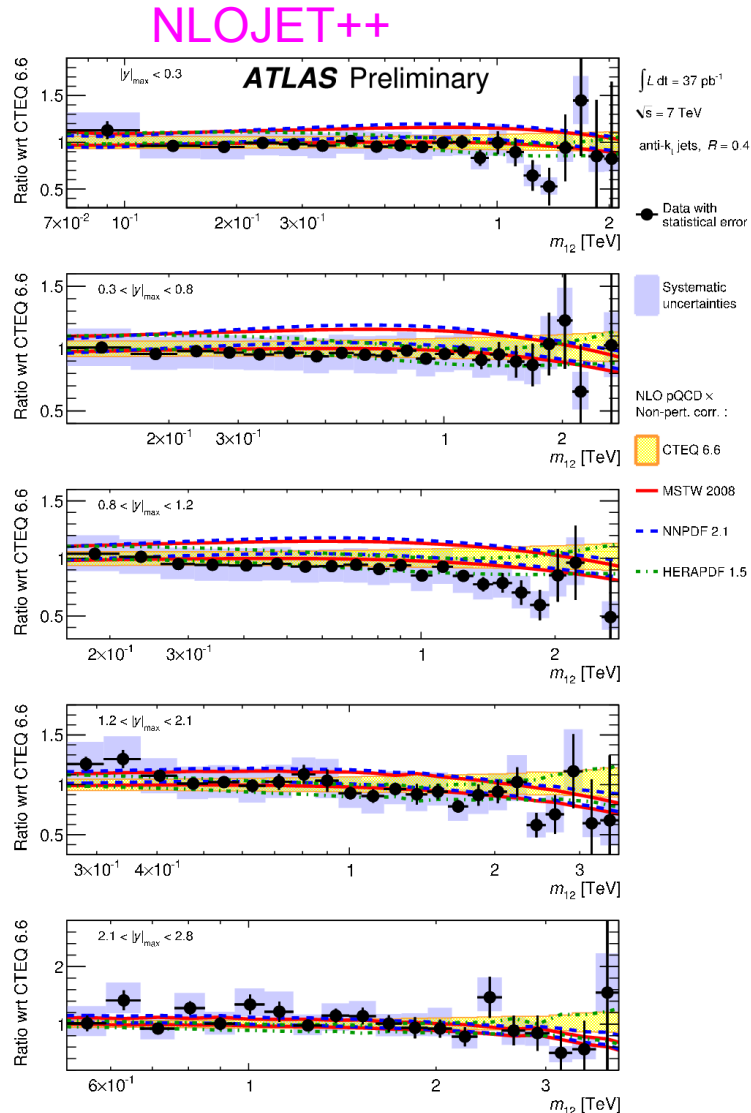
expect differences at low p_T , kinematic edges, but everywhere?



These differences will affect the global PDF fit
 Note also differences between Pythia and Herwig showering.

ATLAS: dijets

Plot the dijet cross section as a function of $|y_{\max}|$.



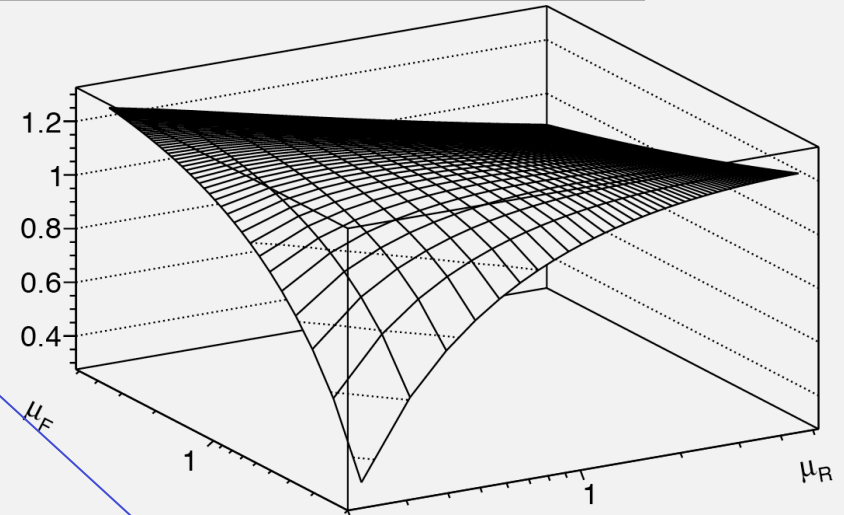
ATLAS-CONF-2011-047

Again, as for inclusive jet production, we see that there are some shape differences between fixed order and Powheg that need to be understood, especially in the forward region. If Powheg is right, our PDFs are wrong.

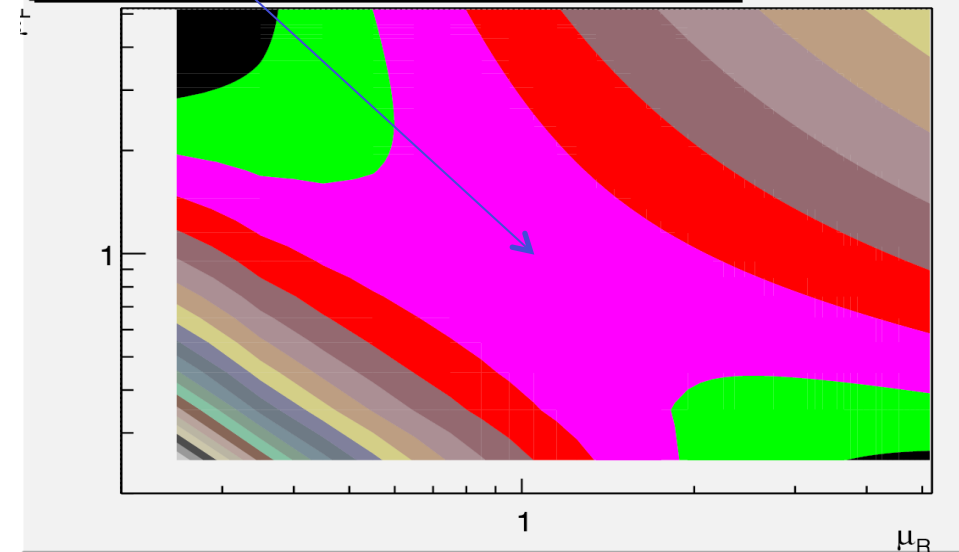
Now look at the dijet mass cross section

- In most cases, get a nice saddle region around p_T^{jet}

Scale dependence. $0.0 < |y| < 0.3$. $2780 < m_{jj} [\text{GeV}] < 3040$



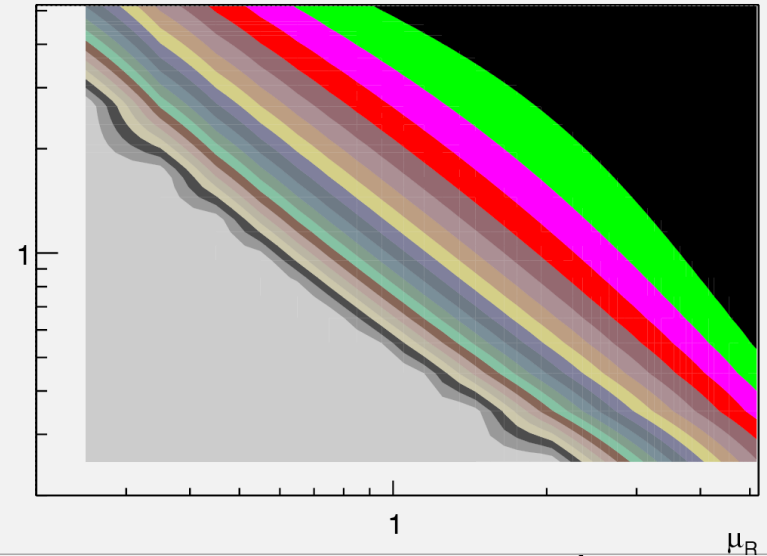
Scale dependence. $0.0 < |y| < 0.3$. $2780 < m_{jj} [\text{GeV}] < 3040$



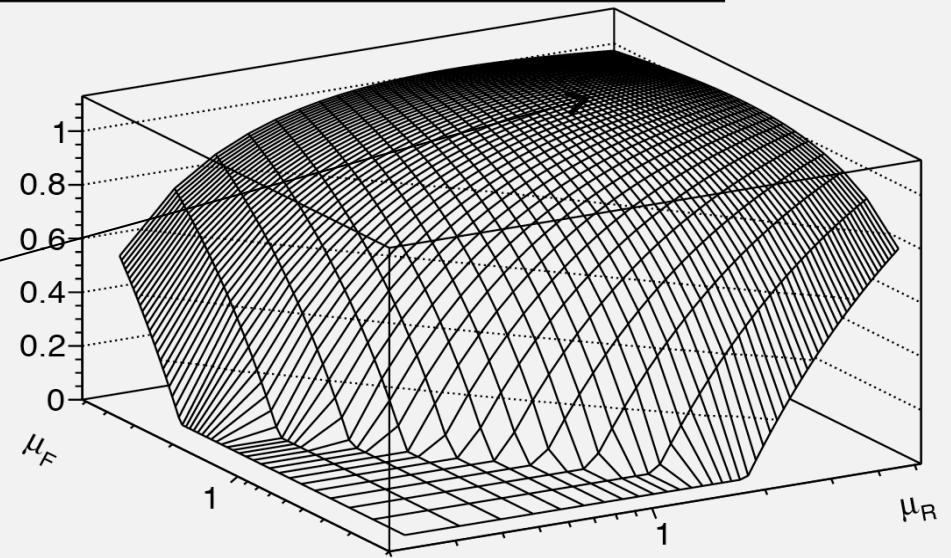
...but not for forward rapidities

- Is perturbation theory not valid here?
- It's ok as long as *reasonable scales* are chosen
- It's a continuation of the effect that we've been looking at
- To be on the plateau requires scales of the order of $3-4 \cdot p_T$
- Our 'motivated' scale, though, is p_T
 - ◆ in this case, I would argue that kinematics forces us to change
 - ◆ ok, here's the bizarre thing; this plateau cross section agrees with the data (great!) and with the Powheg cross section generated with a scale of p_T^{jet} (huh?)

Scale dependence. $2.1 < |y| < 2.8$. $3310 < m_{jj} [\text{GeV}] < 3610$



Scale dependence. $2.1 < |y| < 2.8$. $3310 < m_{jj} [\text{GeV}] < 3610$



...and now for something completely different

electroweak effects may be important at the LHC

$\alpha_s > \alpha_W$ but α_W runs more slowly than does α_s

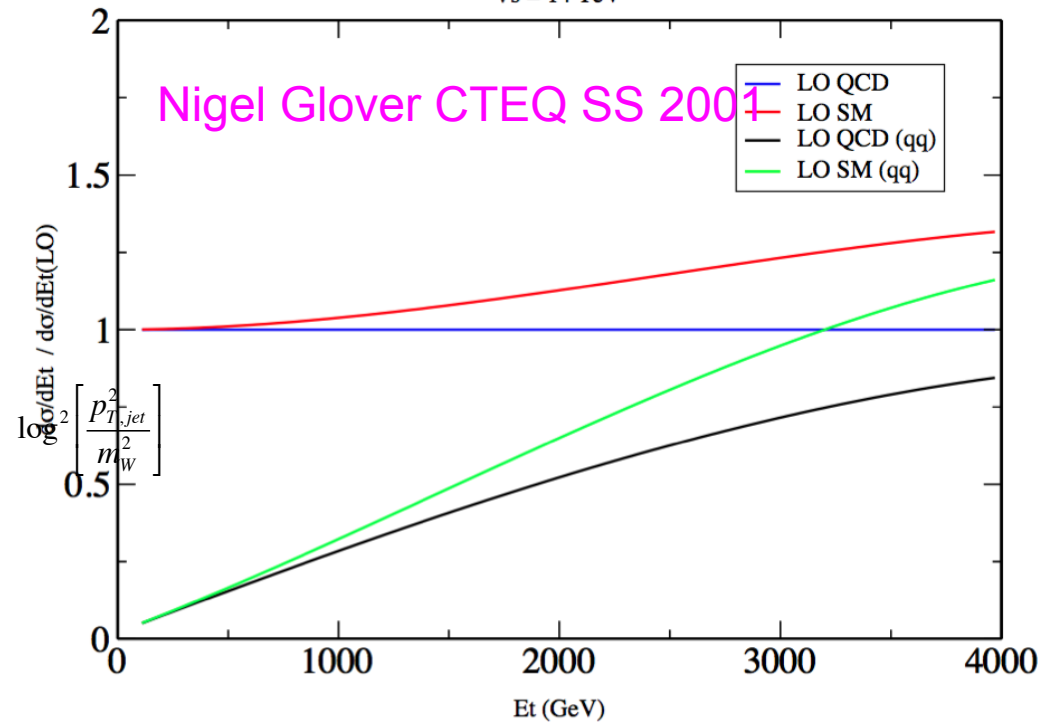
...in addition, and more importantly, there are EWK Sudakov logs that become important in the TeV range (that Nigel didn't take into account)

$$\log^2 \left[\frac{\mu^2}{m_W^2} \right] \quad \text{where } \mu \text{ is scale typical of the process}$$

due to a lack of cancellation between virtual and real W emission

Jet transverse energy distribution

$\sqrt{s} = 14 \text{ TeV}$



Will see same sort of rise over QCD as jet energy increases.

Due to new physics? or old physics?

In fact it is Standard Model $\mathcal{O}(\alpha_s \alpha_w)$ contributions to qq scattering processes - interference of t -channel Z exchange with u -channel gluon exchange.

Moretti, Nolten and Ross: hep/ph/0606201

- These Sudakov logs are important
 - ◆ negative contribution to cross section
 - ◆ real radiation (of W/Z's) gives a positive contribution
- Typically, real radiation terms contribute (positively) much less than NLO weak virtual terms (Sudakov FFs) contribute, so there's a very incomplete cancellation
- For 2 TeV/c jets, total effect on inclusive jet cross section is more like 20%
- This size of effect can't be ignored for precision comparisons and for inclusion of high p_T jet data in global PDF fits
- and in searches for new physics

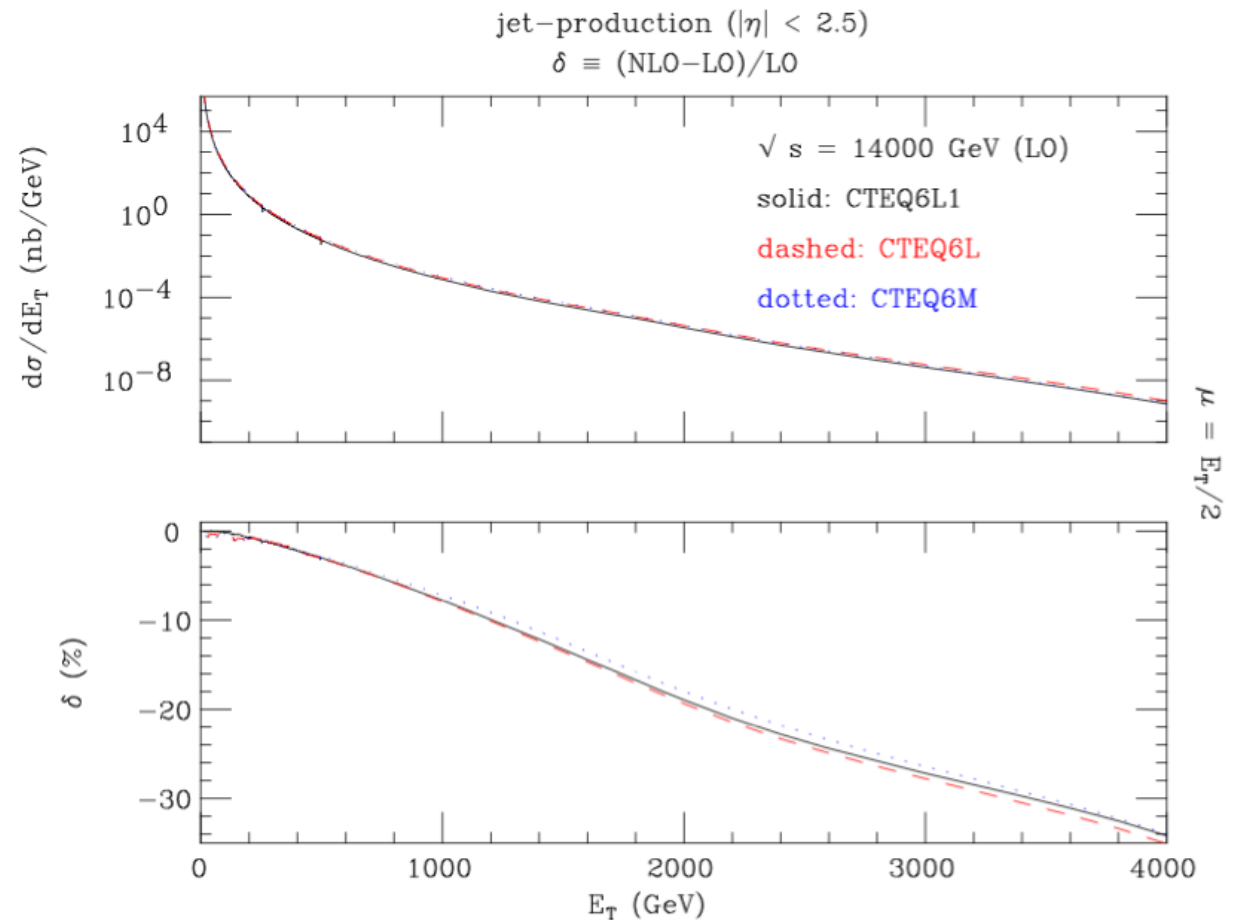
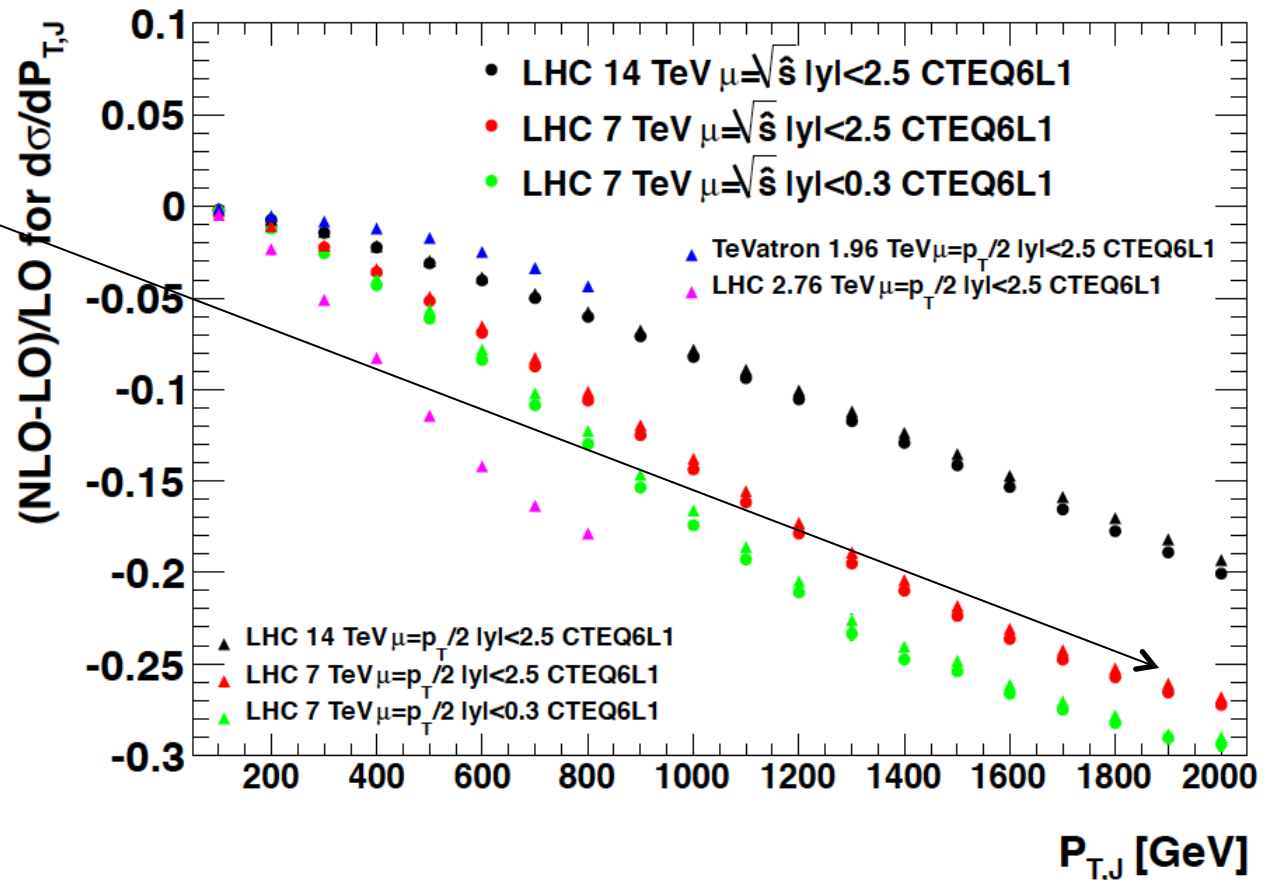


Figure 19: The effects of the $\mathcal{O}(\alpha_s^2 \alpha_W)$ corrections [bottom] relative to the full LO results (i.e., through $\mathcal{O}(\alpha_s^2 + \alpha_s \alpha_{EW} + \alpha_{EW}^2)$) [top] for the case of LHC for three choices of PDFs. They are plotted as function of the jet transverse energy E_T . The cut $|\eta| < 2.5$ has been enforced, alongside the standard jet cone requirement $\Delta R > 0.7$. The factorisation/renormalisation scale adopted was $\mu = \mu_F \equiv \mu_R = E_T/2$.

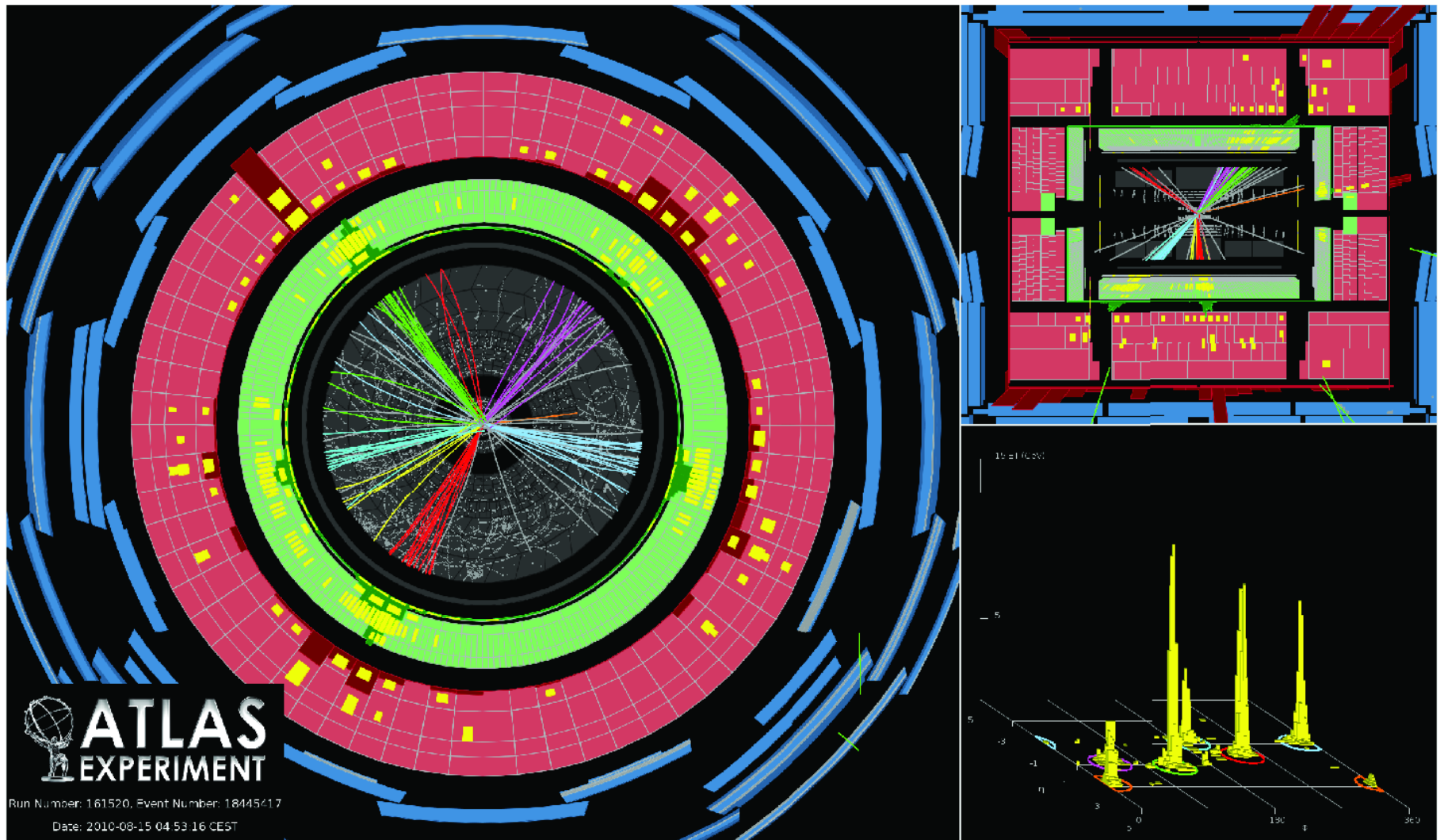
Electroweak corrections for hard processes at the LHC

- I'm working on a followup paper with Stefano Moretti, Doug Ross, Mario Campanelli and Juan Terron
- We are also organizing a workshop on electroweak corrections at the LHC to be held in Durham September 24-26

20-25% effect at high p_T

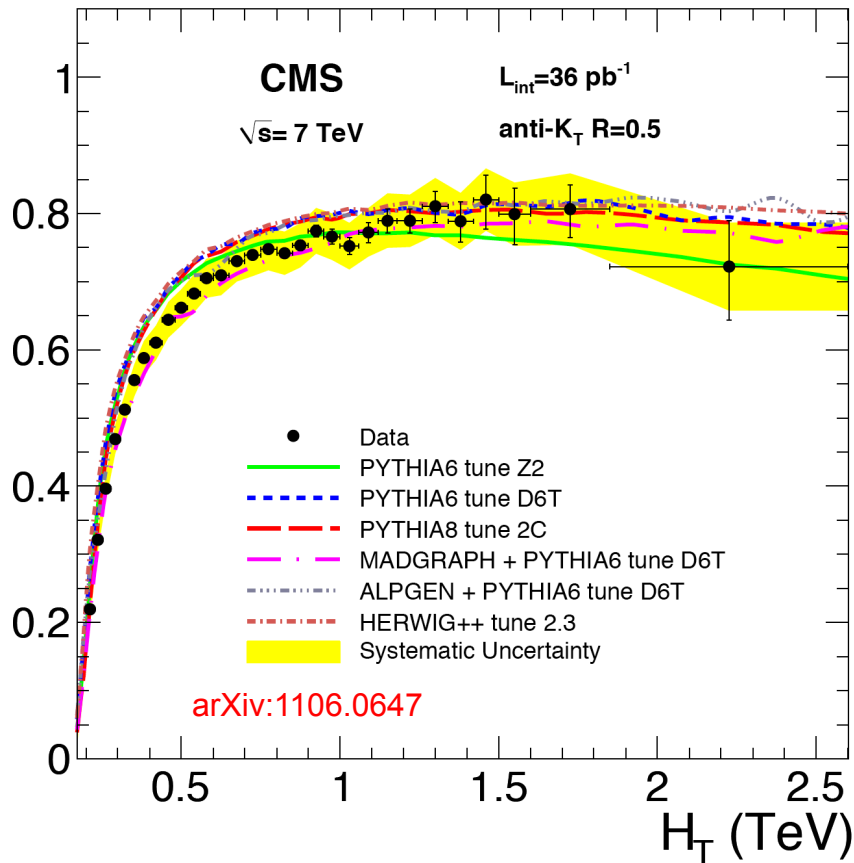


LHC: multijet production



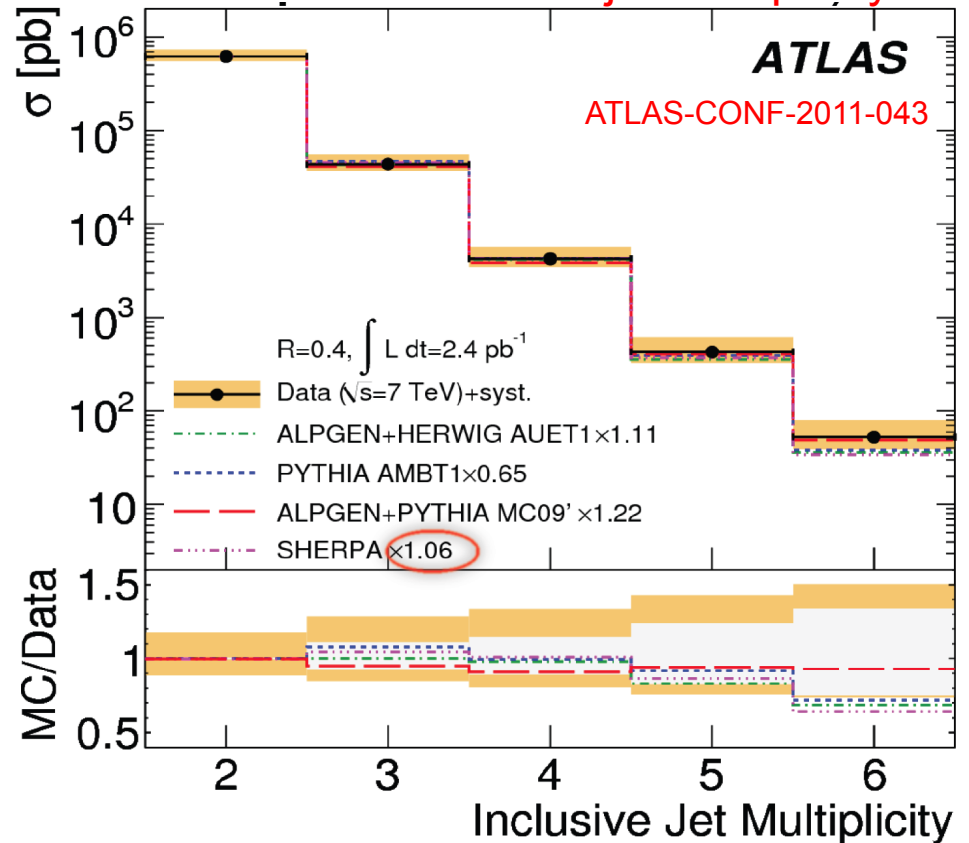
LHC: Multijet Production

CMS: 3 jet to 2 jet ratio vs H_T (sum of p_T 's)



Potential for a measurement of α_s .
 Note that you would expect α_s to decrease as the interaction gets harder; instead it increases up to some value. Why?

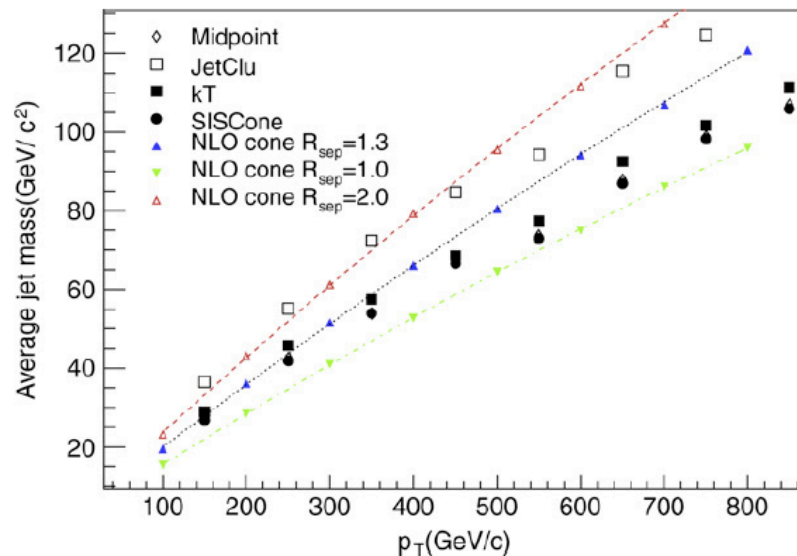
ATLAS: inclusive jet multiplicity



Good agreement with matrix element + parton shower predictions, if normalizations are allowed to float. Sherpa requires lowest normalization.

Jet masses

- Very useful if looking for resonance in boosted jet (*top jet*)
- Naturally produced by QCD radiation
- Depends on jet algorithm/size



In NLO pert theory

phase space from pdf' s

$$\sqrt{P_{J,\mu} P_J^\mu} = \sqrt{\langle M^2 \rangle_{NLO}} = f\left(\frac{p_J}{\sqrt{s}}\right) \sqrt{\alpha_s(p_J)} (p_J R)$$

dimension

jet size

Rule-of-thumb

$$\sqrt{\langle M^2 \rangle_{NLO}} \sim 0.2 p_J R$$

Fig. 53. The average jet mass is plotted versus the transverse momentum of the jet using several different jet algorithms with a distance scale ($D = R_{\text{cone}}$) of 0.7.

Distribution of jet masses

- Sudakov suppression for low jet masses
- fall-off as $1/m^2$ due to hard gluon emission
- algorithm suppression at high masses
 - ◆ jet algorithms tend to split high mass jets in two

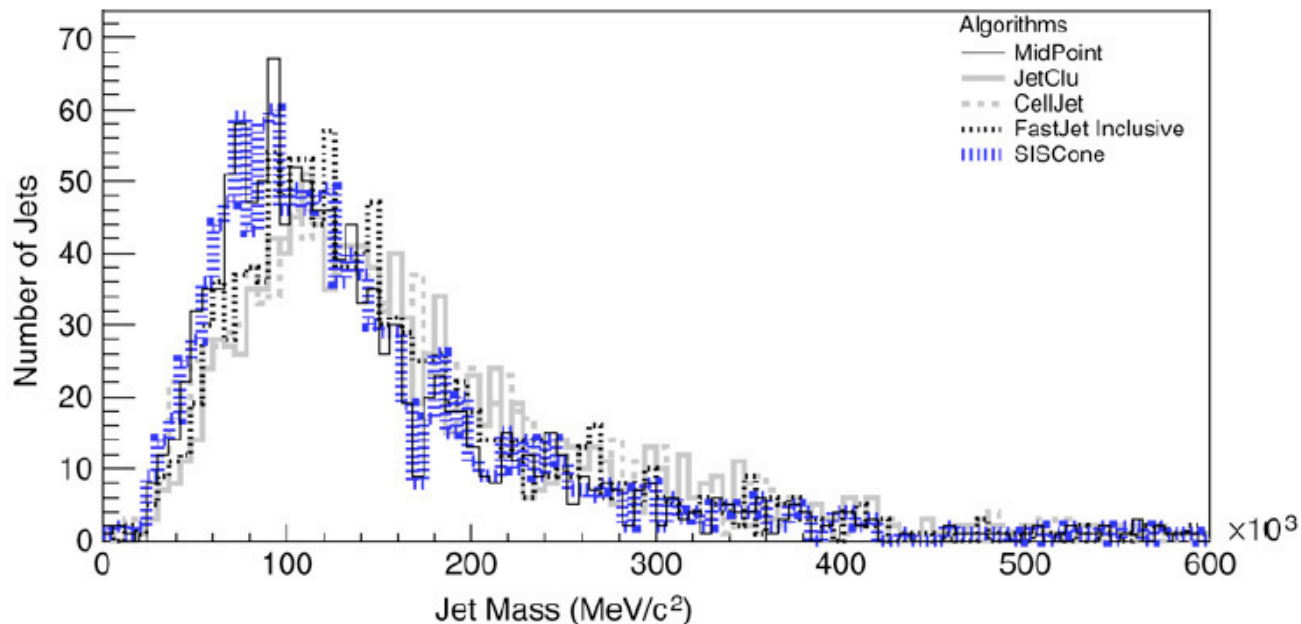
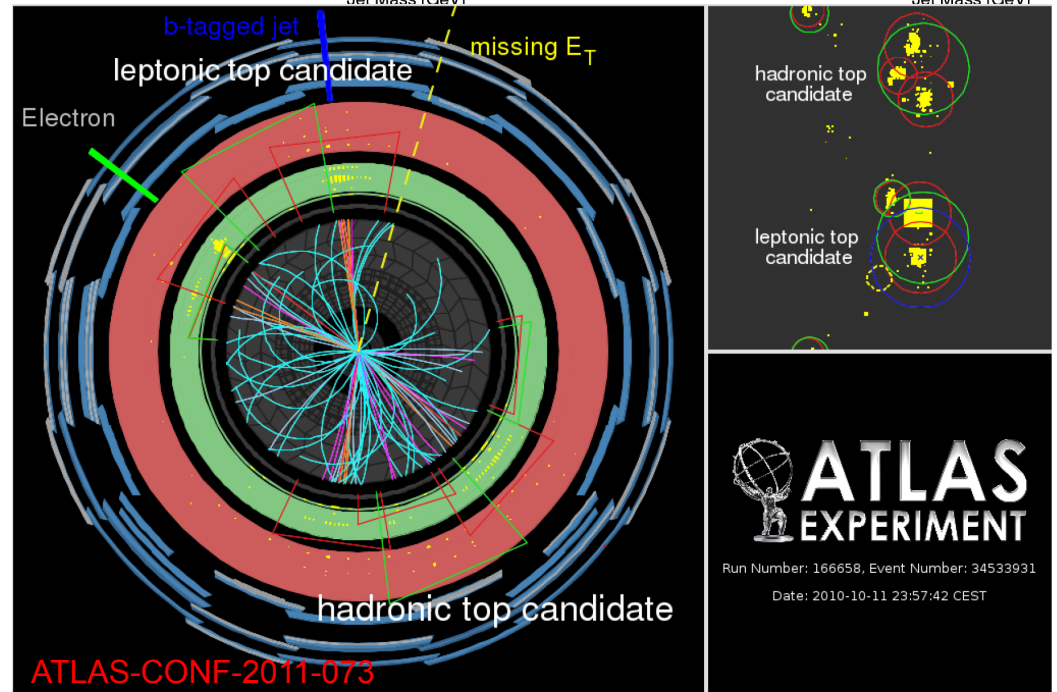
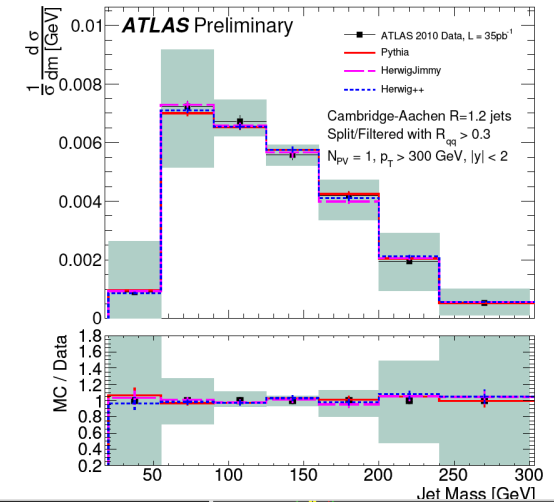
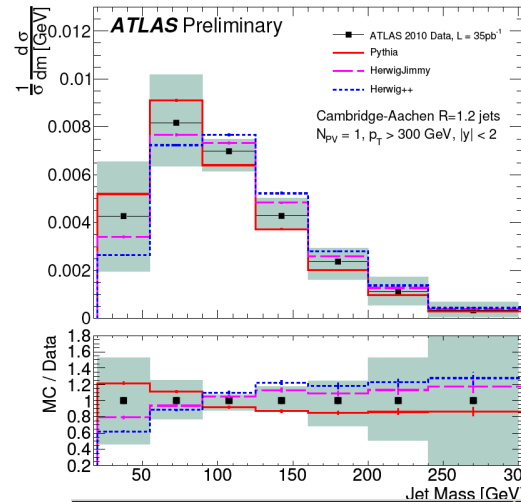


Fig. 51. The jet mass distributions for an inclusive jet sample generated for the LHC with a $p_{T,\min}$ value for the hard scattering of approximately 2 TeV/c, using several different jet algorithms with a distance scale ($D = R_{\text{cone}}$) of 0.7.

ATLAS: jet masses

- Quite an extensive technology has arisen in the last few years regarding trimming, filtering, pruning jets to reveal the underlying hard scatter/massive decay products, especially on boosted jets
- The top right plot shows the mass distribution for jets ($p_T > 300$ GeV, $|y| < 2$) reconstructed with the Cambridge-Aachen algorithm with $R=1.2$, before (left) and after (right) a splitting and filtering algorithm has been applied
- The bottom right plot shows a boosted top candidate ($p_T = 356$ GeV), clustered with the anti-kT algorithm with $R=1.0$

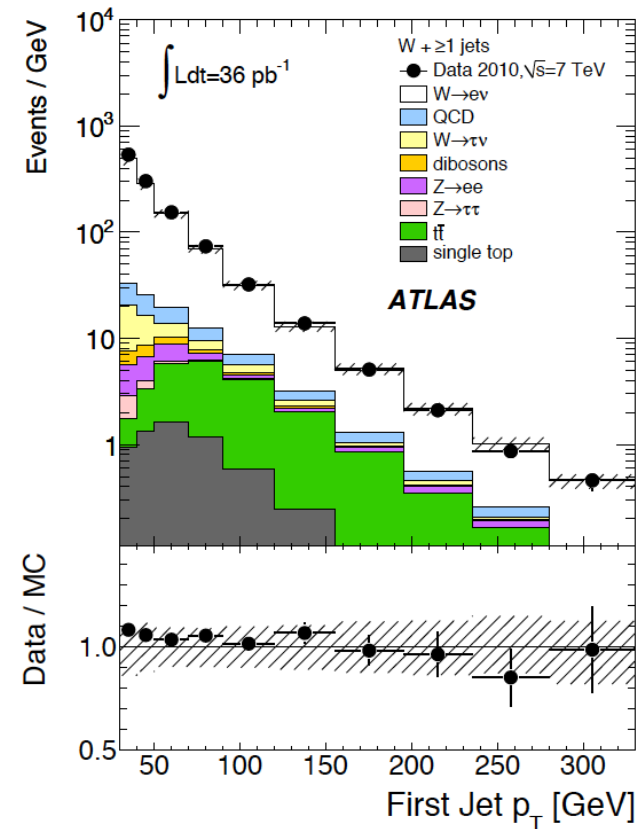
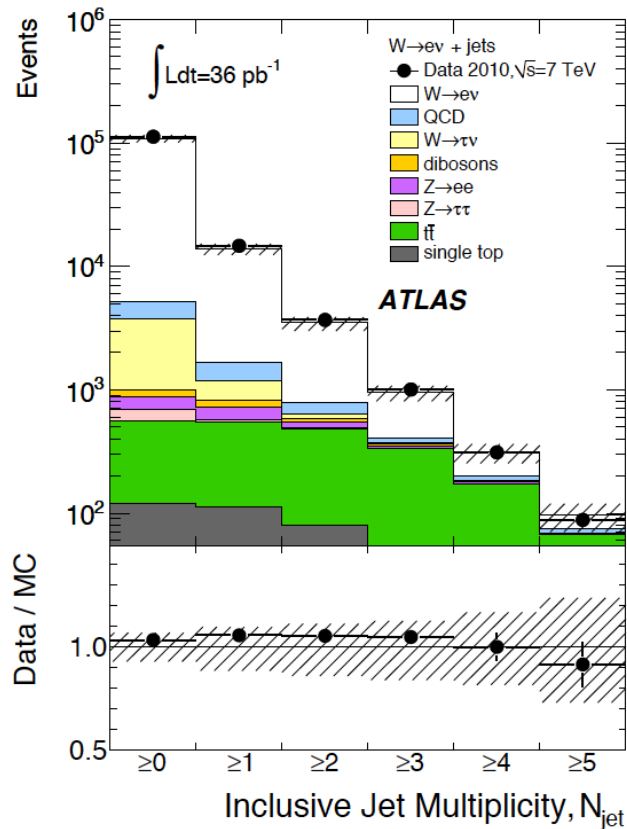


ATLAS: W+jets

- One of the key benchmark processes at both the Tevatron and the LHC
- 2010 data was enough to probe up to 5 jets with statistics
- Out to >300 GeV/c for lead jet transverse momentum

Note each higher jet emission suppressed by a factor of roughly α_s

no large logs



ATLAS: W+jets

- Measurements were conducted with the kinematic cuts listed to the right
- Theory is capable of forming predictions for same cuts, so no need for any corrections back to ‘full cross section’
- Resulting measurements were unfolded to hadron level; may seem obvious but CDF measurement was the first to do so
- Underlying event and fragmentation corrections determined to allow for partonic level theory to be compared to data at hadron level
- Two corrections are in opposite directions and of roughly equal size, so net correction tends to be small

- $p_T^{\text{lepton}} > 20 \text{ GeV}$,
- $|\eta^{\text{lepton}}| < 2.4$,
- $E_T^{\text{miss}} > 25 \text{ GeV}$,
- $m_{T,W} > 40 \text{ GeV}$,
- $p_T^{\text{jet}} > 30 \text{ GeV}$,
- $|y^{\text{jet}}| < 4.4$,
- $\Delta R^{\text{lepton-jet}} > 0.5$.

Table 3: Non-perturbative corrections: first jet p_T ($N_{jet} \geq 1$)

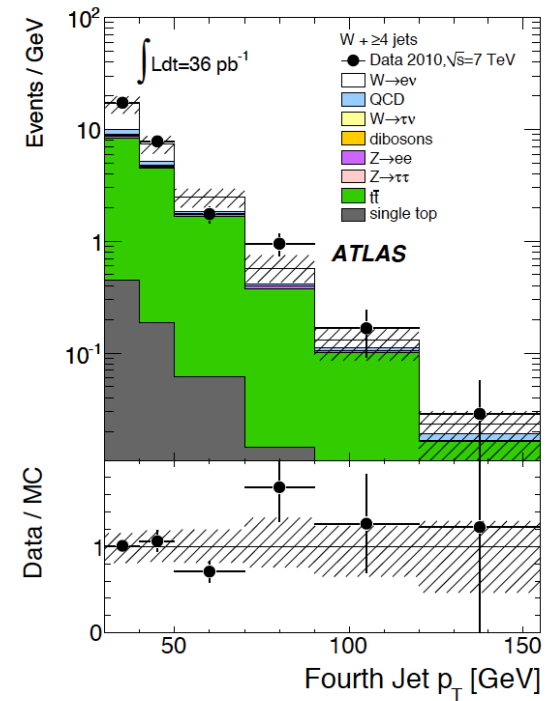
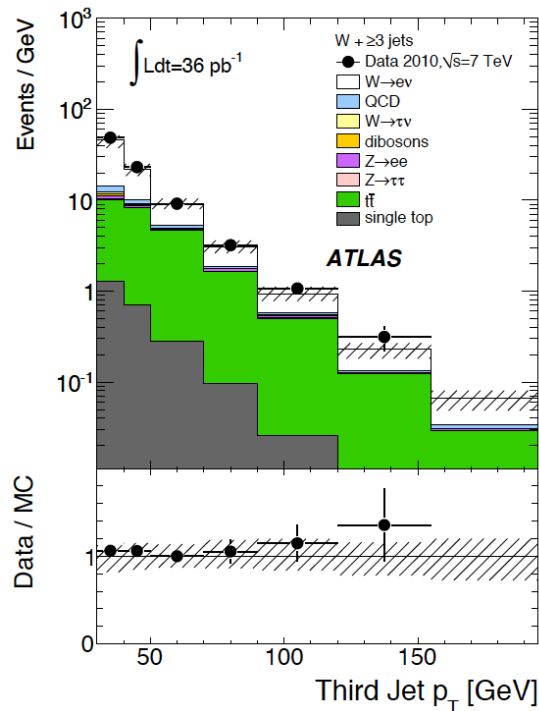
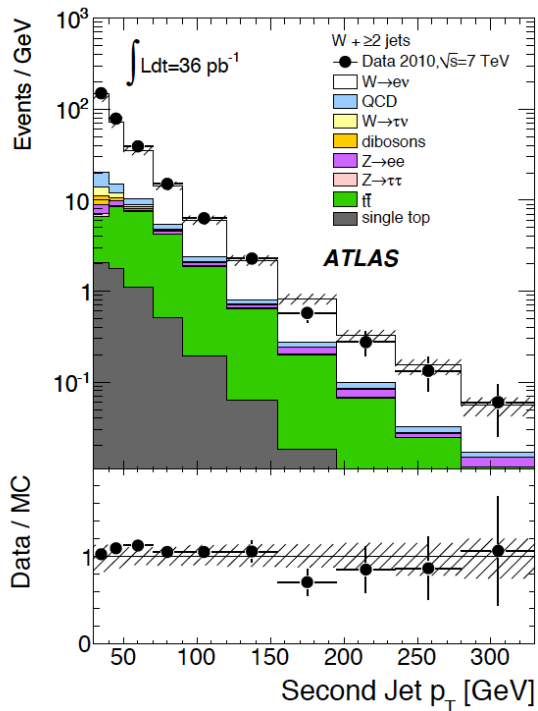
Bin	C_{UE}	C_{Had}
30-40	1.107 ± 0.001 (stat) ± 0.043 (sys)	0.926 ± 0.001 (stat) ± 0.009 (sy:
40-50	1.065 ± 0.001 (stat) ± 0.031 (sys)	0.939 ± 0.001 (stat) ± 0.006 (sy:
50-70	1.044 ± 0.001 (stat) ± 0.022 (sys)	0.948 ± 0.001 (stat) ± 0.006 (sy:
70-90	1.027 ± 0.001 (stat) ± 0.017 (sys)	0.957 ± 0.001 (stat) ± 0.002 (sy:
90-120	1.017 ± 0.000 (stat) ± 0.015 (sys)	0.965 ± 0.001 (stat) ± 0.004 (sy:
120-155	1.015 ± 0.001 (stat) ± 0.013 (sys)	0.969 ± 0.001 (stat) ± 0.005 (sy:
155-195	1.010 ± 0.002 (stat) ± 0.019 (sys)	0.971 ± 0.002 (stat) ± 0.001 (sy:
195-235	0.998 ± 0.003 (stat) ± 0.016 (sys)	0.978 ± 0.002 (stat) ± 0.001 (sy:
235-280	1.000 ± 0.004 (stat) ± 0.002 (sys)	0.980 ± 0.003 (stat) ± 0.001 (sy:
280-330	1.018 ± 0.003 (stat) ± 0.002 (sys)	0.979 ± 0.004 (stat) ± 0.000 (sy:

Table 6: Non-perturbative corrections: first jet p_T ($N_{jet} \geq 4$)

Bin	C_{UE}	C_{Had}
30-40	1.546 ± 0.162 (stat) ± 0.091 (sys)	0.734 ± 0.041 (stat) ± 0.073 (sys)
40-50	1.351 ± 0.066 (stat) ± 0.064 (sys)	0.775 ± 0.016 (stat) ± 0.032 (sys)
50-70	1.252 ± 0.023 (stat) ± 0.086 (sys)	0.807 ± 0.007 (stat) ± 0.010 (sys)
70-90	1.176 ± 0.020 (stat) ± 0.047 (sys)	0.825 ± 0.007 (stat) ± 0.008 (sys)
90-120	1.122 ± 0.010 (stat) ± 0.041 (sys)	0.852 ± 0.005 (stat) ± 0.000 (sys)
120-155	1.101 ± 0.013 (stat) ± 0.063 (sys)	0.869 ± 0.006 (stat) ± 0.006 (sys)
155-195	1.089 ± 0.014 (stat) ± 0.013 (sys)	0.886 ± 0.007 (stat) ± 0.005 (sys)
195-235	1.043 ± 0.012 (stat) ± 0.019 (sys)	0.885 ± 0.009 (stat) ± 0.012 (sys)
235-280	1.086 ± 0.025 (stat) ± 0.019 (sys)	0.891 ± 0.011 (stat) ± 0.015 (sys)
280-330	1.093 ± 0.024 (stat) ± 0.033 (sys)	0.900 ± 0.013 (stat) ± 0.017 (sys)

W+jets continued...

- All cross sections and corrections have been posted on the Durham website, so every theorist has direct access
- See later



Comparisons to theory

- All Blackhat+Sherpa predictions for the 2010 W+jets paper generated by ATLAS experimentalists (my student and myself) using ROOT ntuples generated by B+S

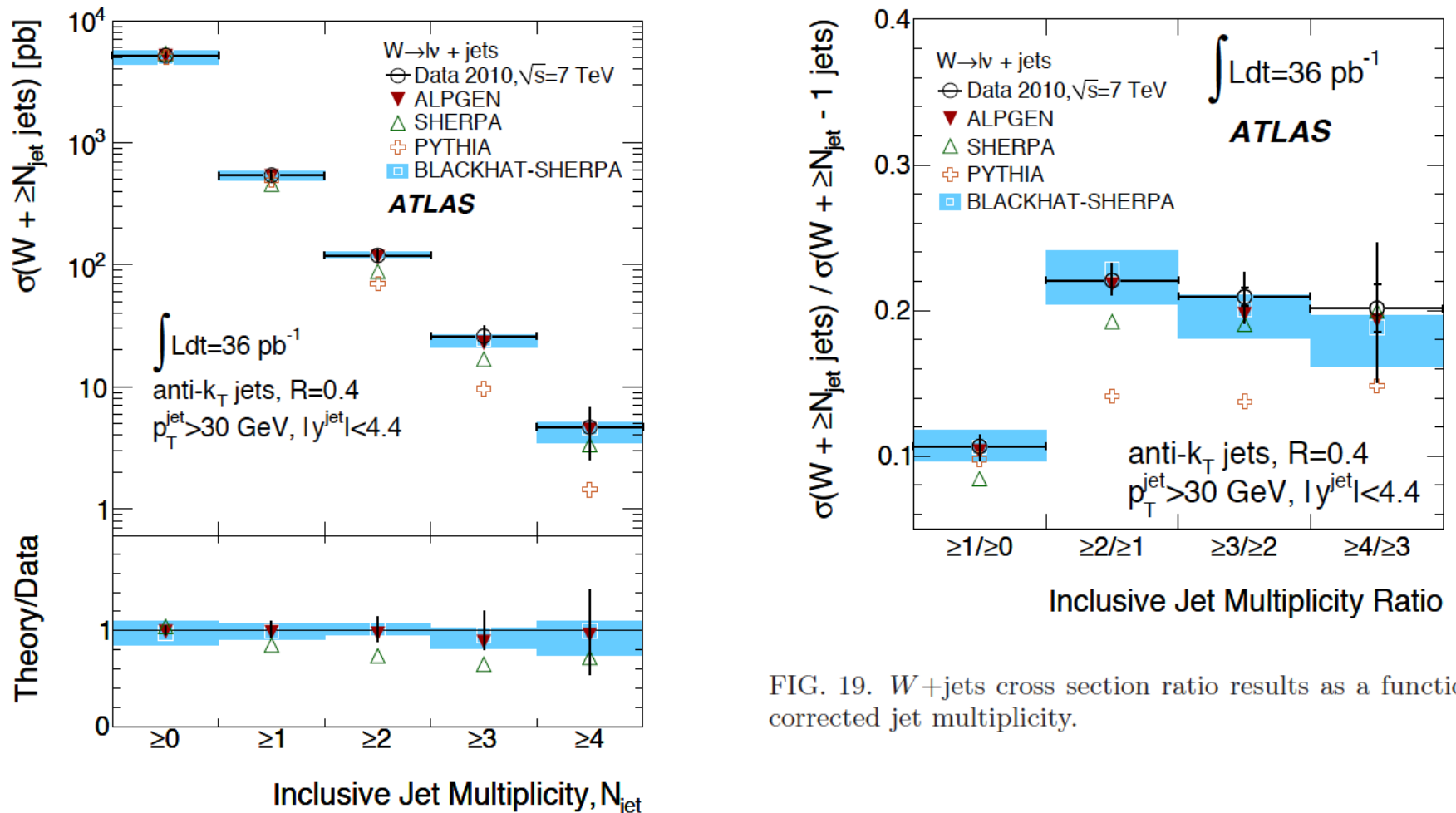


FIG. 19. W+jets cross section ratio results as a function of corrected jet multiplicity.

Remember: Jets in real life

- In NLO theory, can mimic the impact of the truncation of Region II by including a parameter called R_{sep}
 - ◆ only merge two partons if they are within $R_{\text{sep}} * R_{\text{cone}}$ of each other
 - ▲ $R_{\text{sep}} \sim 1.3$
 - ◆ ~4-5% effect on the theory cross section; effect is smaller with the use of p_T rather than E_T (see extra slides)
 - ◆ really upsets the theorists (but there are also disadvantages)
- Dark tower effect is also on order of few (<5)% effect on the (experimental) cross section

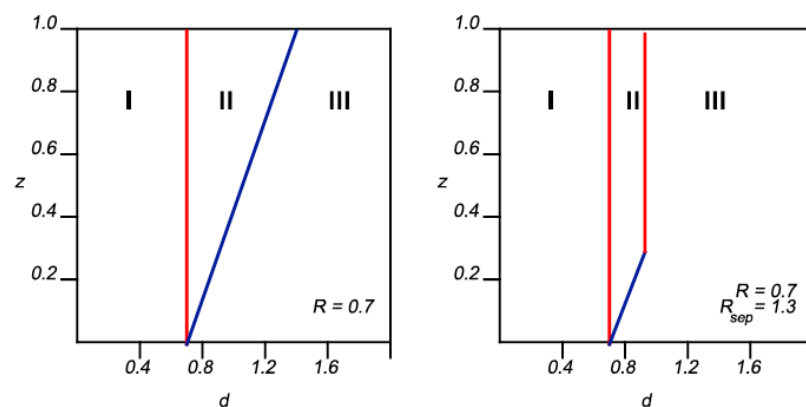
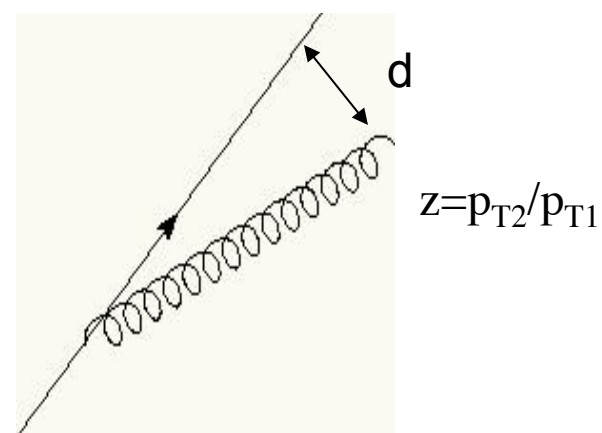


Figure 22. The parameter space (d, Z) for which two partons will be merged into a single jet.

Remember: Jets in real life

- In NLO theory, can mimic the impact of the truncation of Region II by including a parameter called R_{sep}
 - ◆ only merge two partons if they are within $R_{\text{sep}} * R_{\text{cone}}$ of each other
 - ▲ $R_{\text{sep}} \sim 1.3$
 - ◆ ~4-5% effect on the theory cross section; effect is smaller with the use of p_T rather than E_T (see extra slides)
 - ◆ really upsets the theorists (but there are also disadvantages)
- Dark tower effect is also on order of few (<5)% effect on the (experimental) cross section

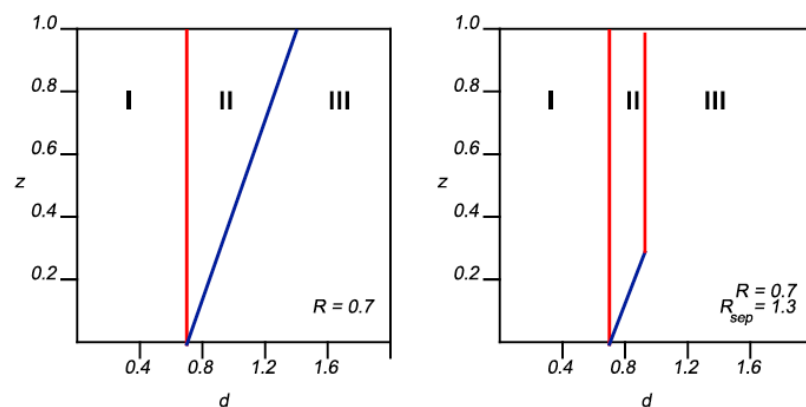
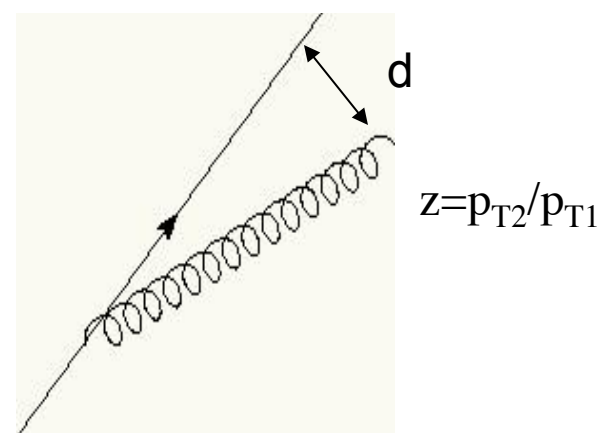
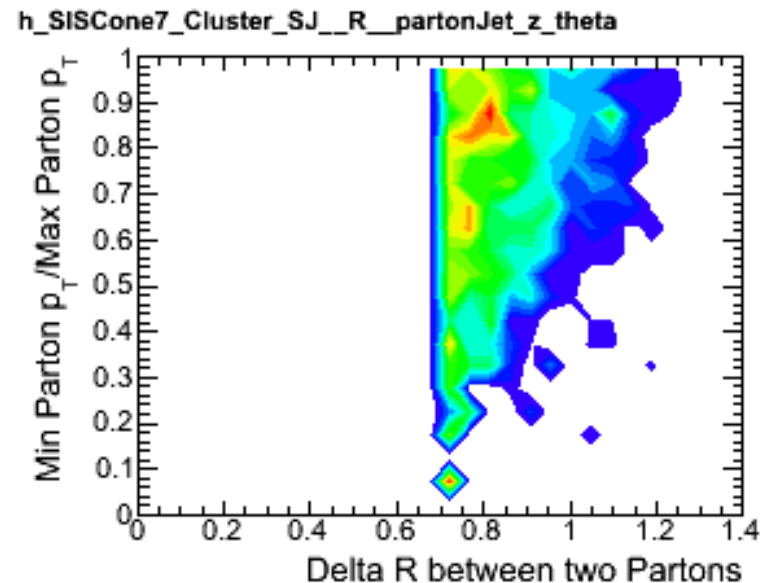
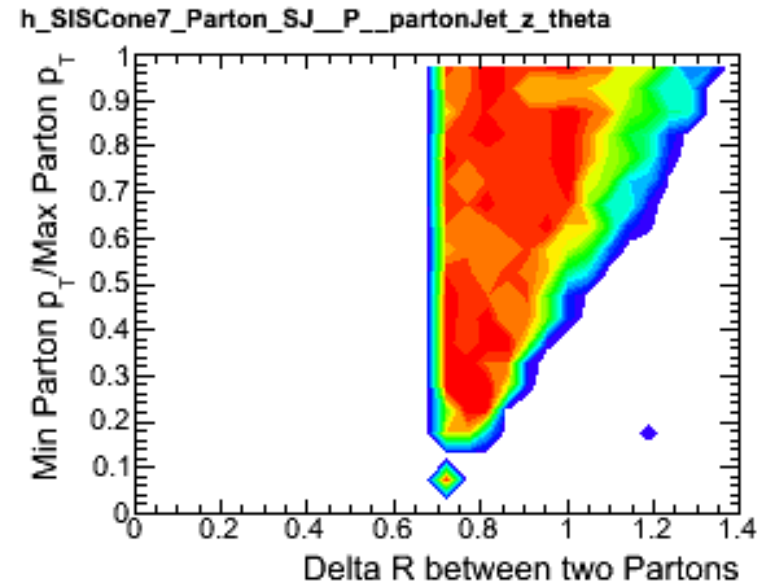


Figure 22. The parameter space (d, Z) for which two partons will be merged into a single jet.

Try this out in ATLAS Monte Carlo

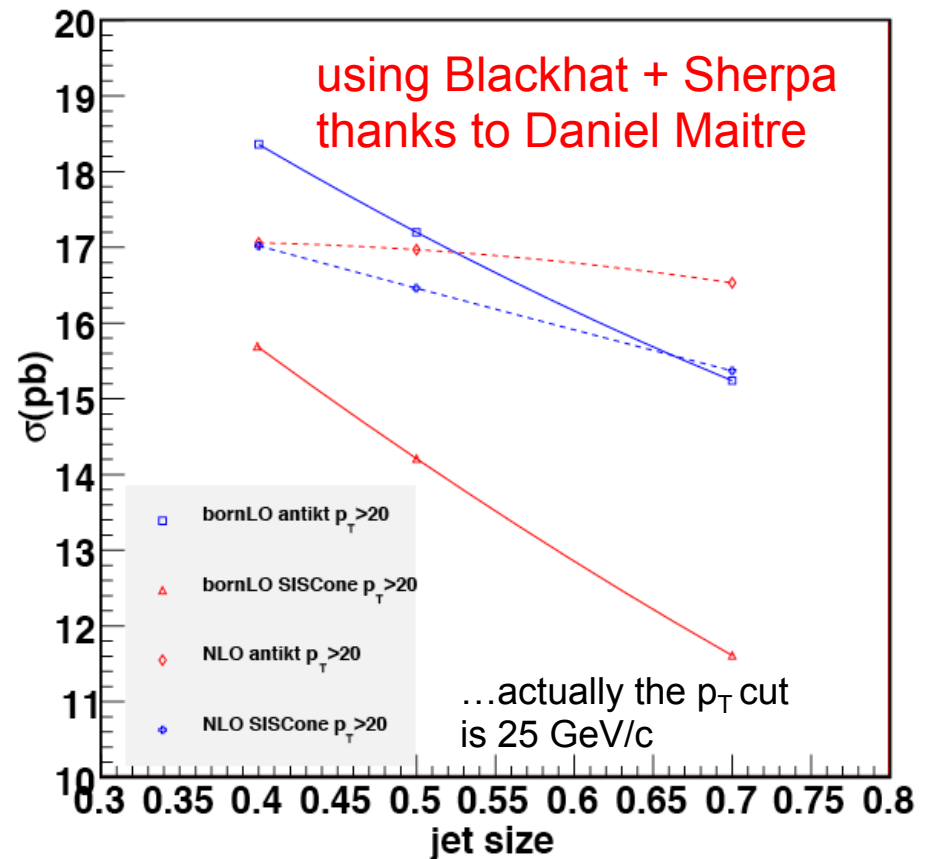
- Take $W + 2$ parton events (ALPGEN+PYTHIA), run SIScone 0.7 algorithm on parton level, hadron level (not shown) and topocluster level
- Plot the probability for the two sub-jets to merge as a function of the separation of the original two partons in ΔR
- Color code:
 - ◆ red: high probability for merging
 - ◆ blue: low probability for merging
- Parton level reconstruction agrees with naïve expectation
- Topocluster level reconstruction agrees with need for R_{sep}



Don't believe (fixed) LO predictions for jet cross sections

- Let's look at predictions for $W + 3$ jets for two different jet algorithms as a function of jet size at the LHC (7 TeV)
- At LO, both antiK_T and SISCone show a marked decrease in cross section as the jet size increases
 - ◆ because of the $\log(1/\Delta R)$ effect
- But at NLO, the two cross sections show little dependence on the jet size, and are similar to each other
- You'll see the same thing in ATLAS Monte Carlo

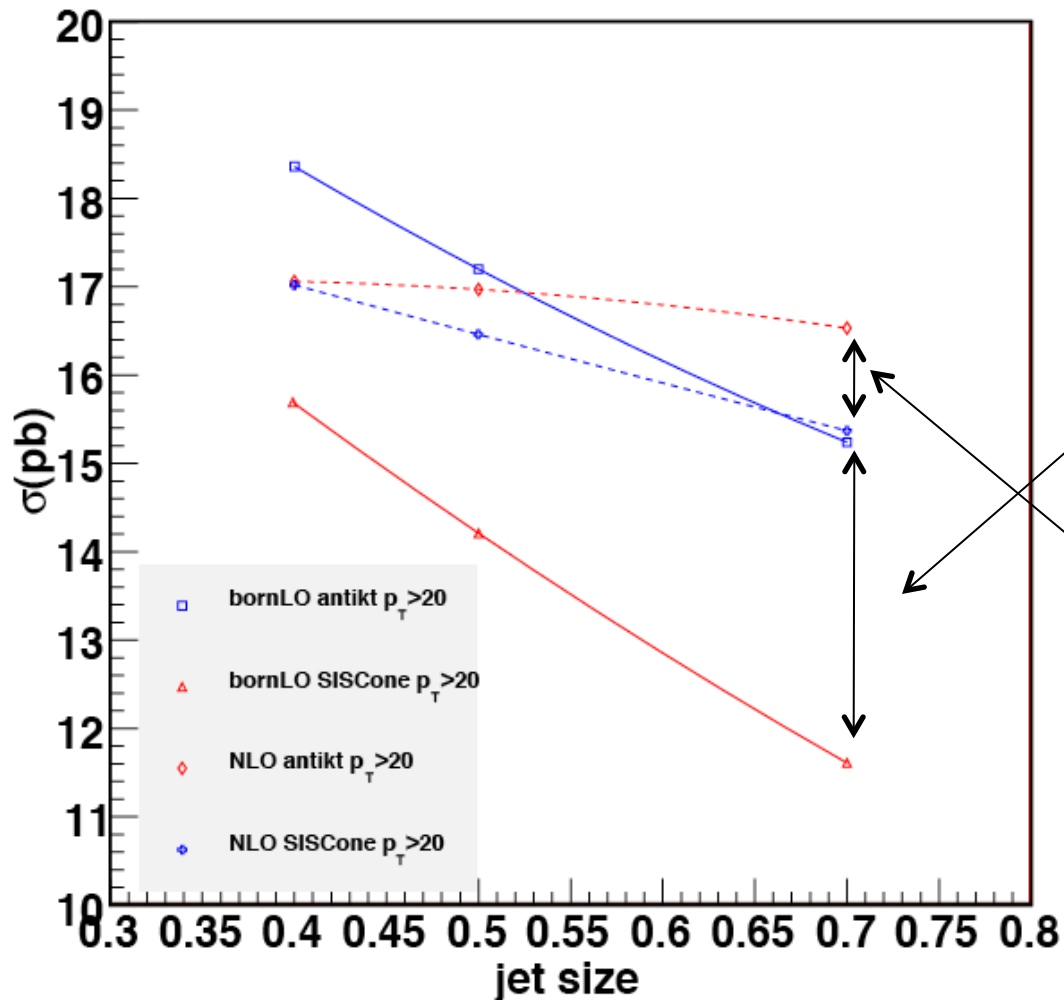
W + 3 jets cross section



note NLO~LO because a scale of H_T has been used

Don't believe (fixed) LO predictions for jet cross sections

W + 3 jets cross section



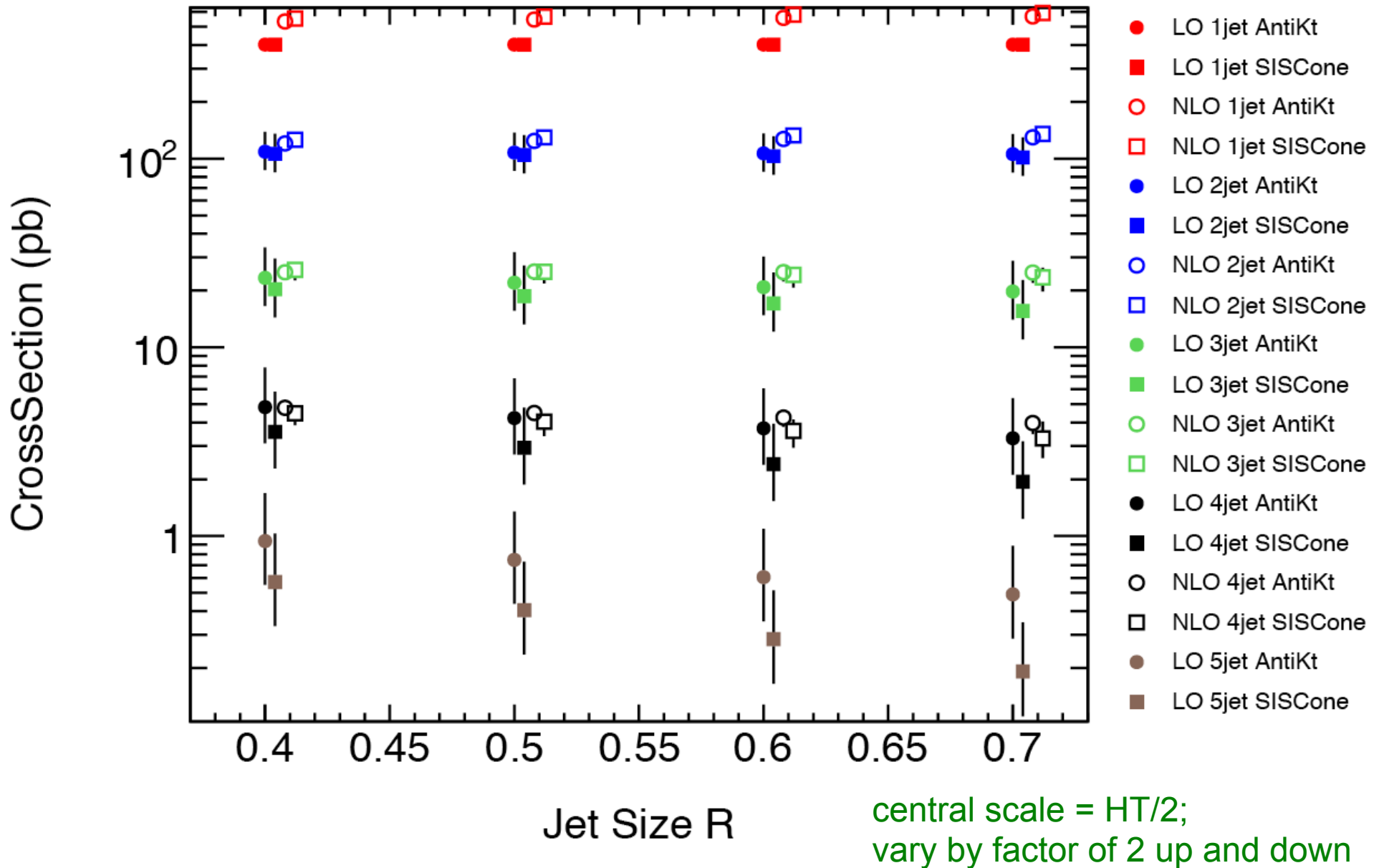
Compare to ATLAS ALPGEN+PYTHIA samples ($\Delta R=0.7$ matching so we can only compare to last jet size)

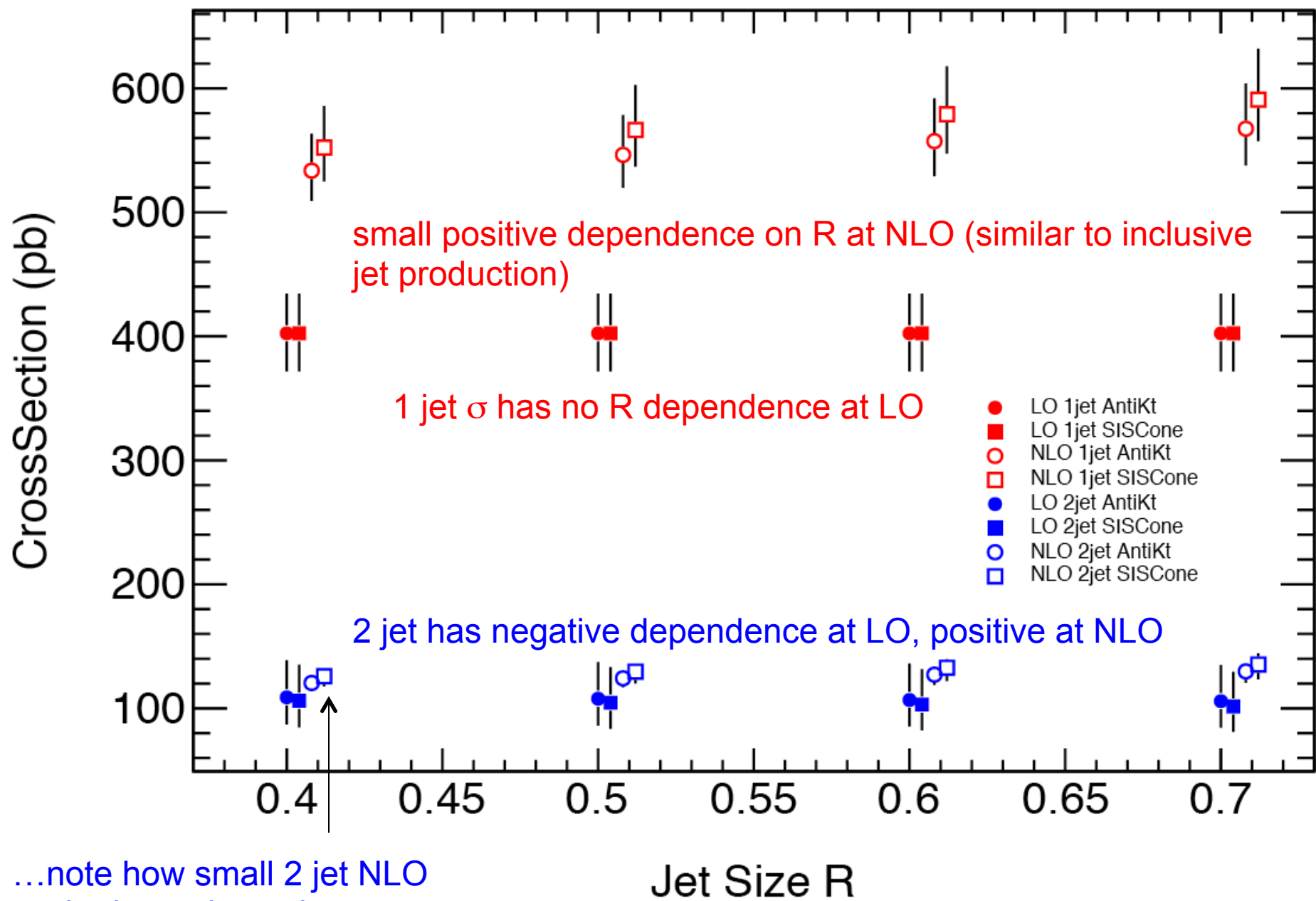
At parton level, antikt is ~25% higher than SIScone (same as we observe here at LO)

At topocluster level, antikt is ~2% higher than SIScone (not the 7% observed here)

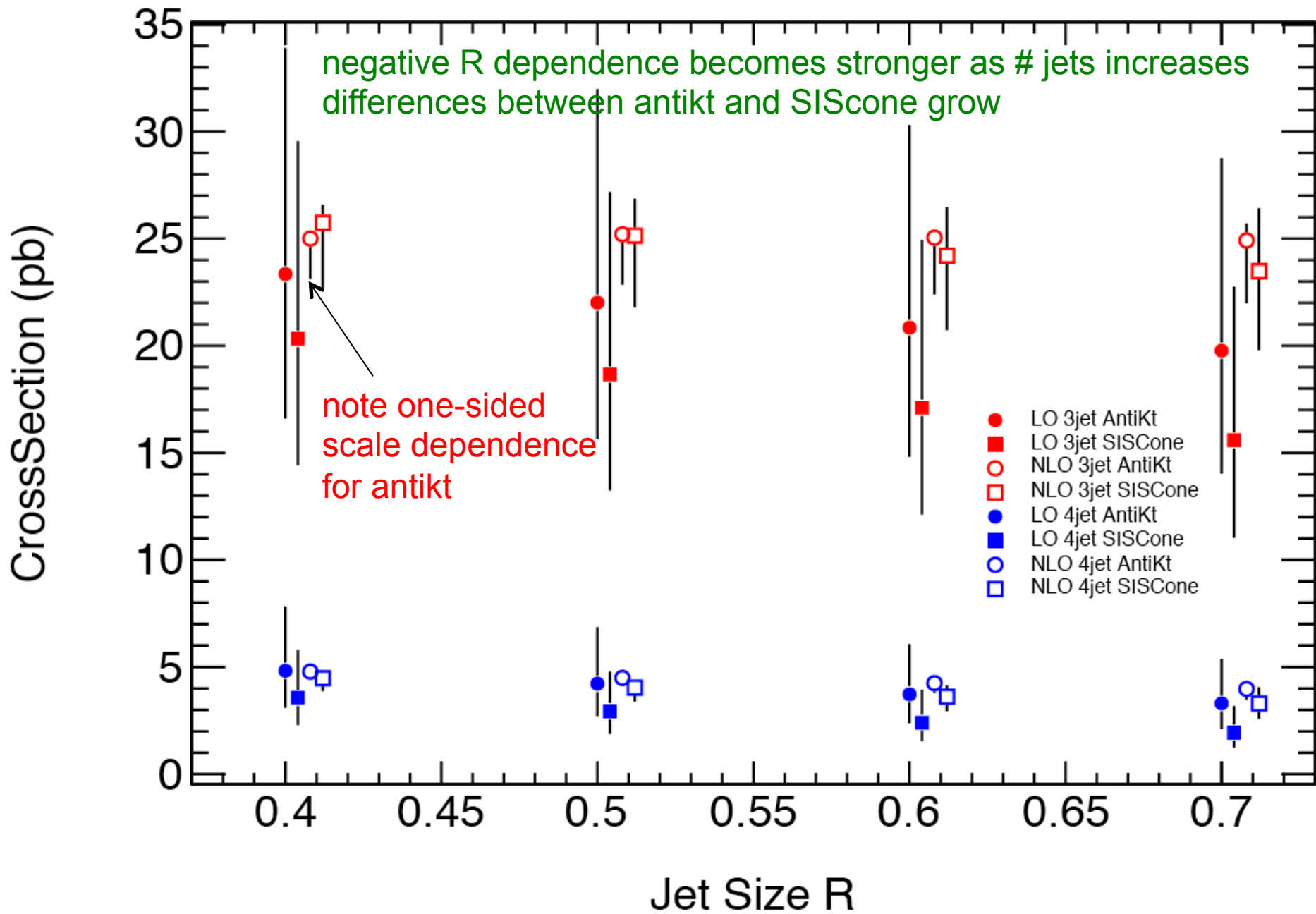
Why 2, not 7? Go back two slide: Some of the W + 3 parton events reconstructed as 2 jets at the parton level for SIScone are reconstructed as 3 jets at the hadron. The cross section for 3 jets increases.

Look at jet size, algorithm dependences; scale uncertainty



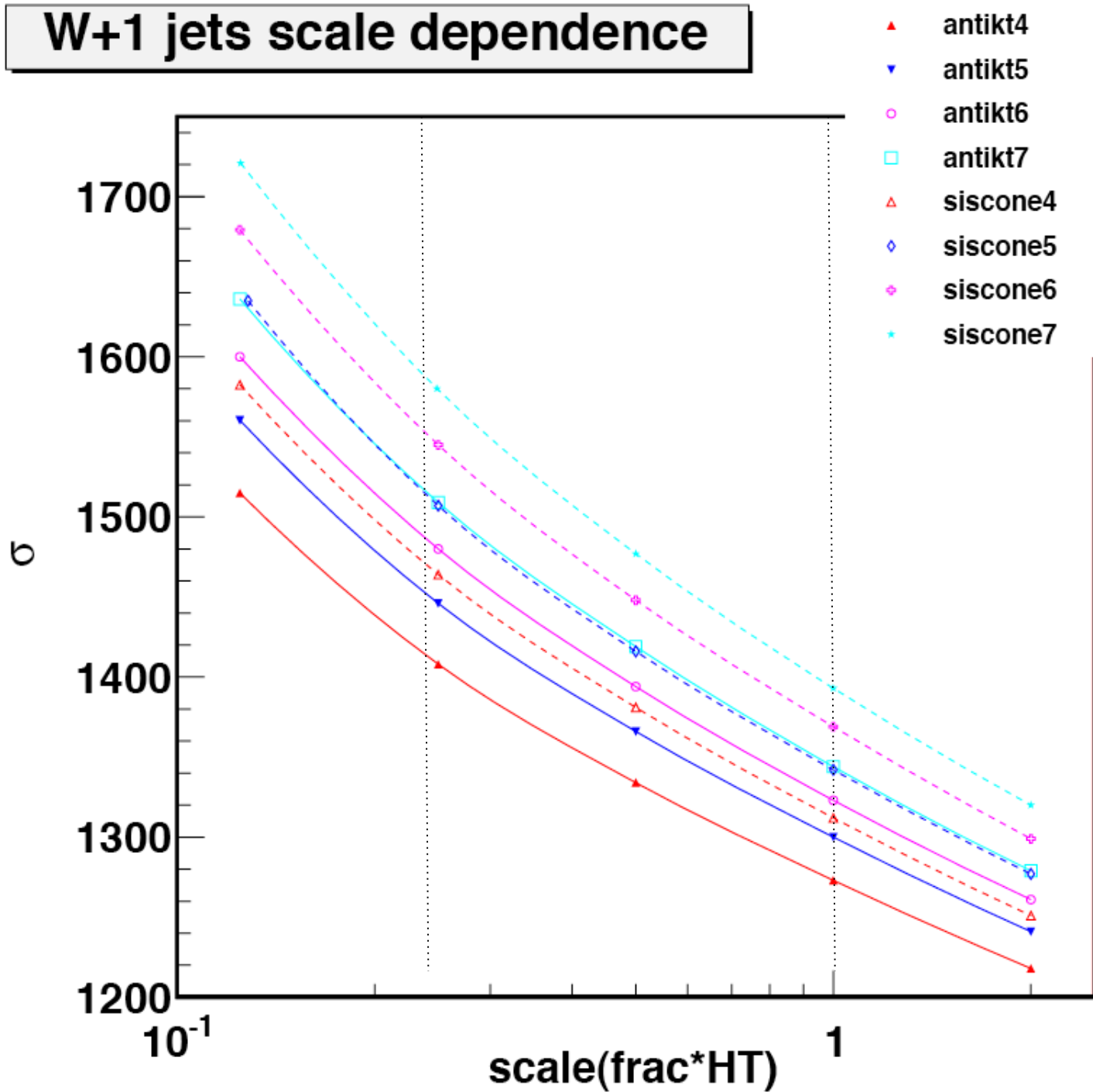


...note how small 2 jet NLO
 scale dependence is

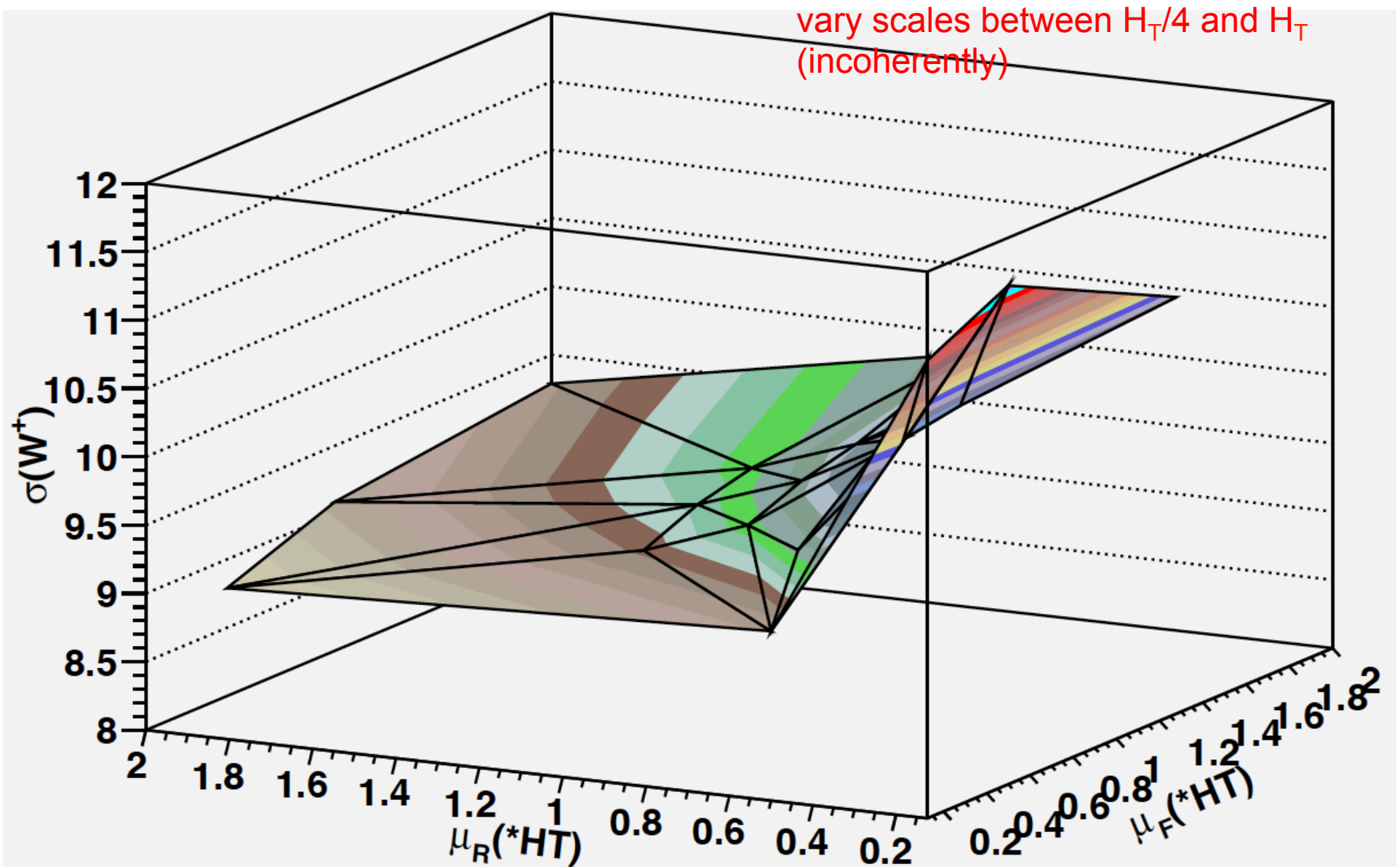


W+1 jets scale dependence

note monotonic scale dependence at NLO, similar to what is seen in a typical LO calculation

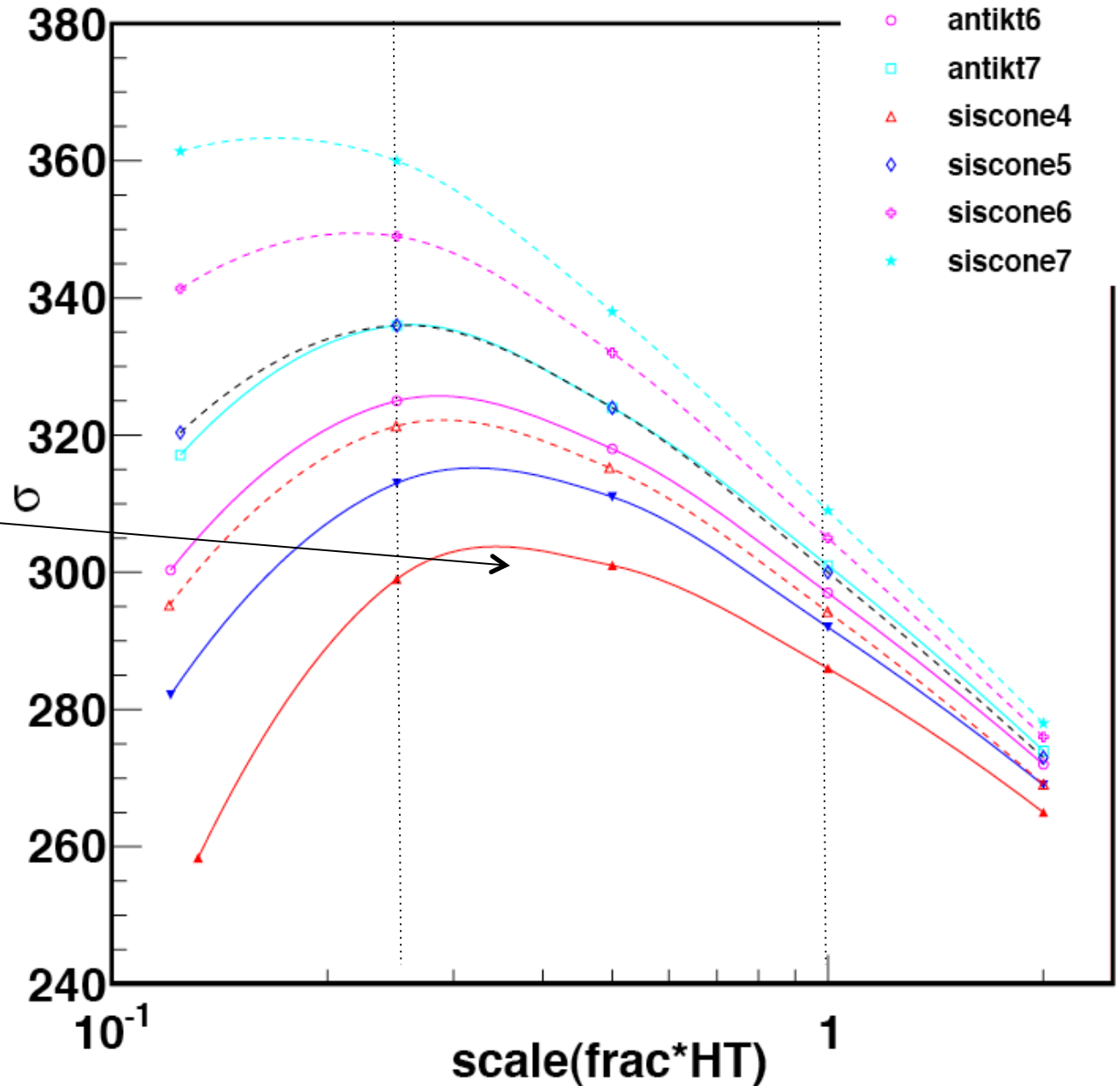


Look at 2D scale dependence



W+2 jets scale dependence

- ▲ antikt4
- ▼ antikt5
- antikt6
- antikt7
- △ siscone4
- ◇ siscone5
- ◇ siscone6
- ★ siscone7

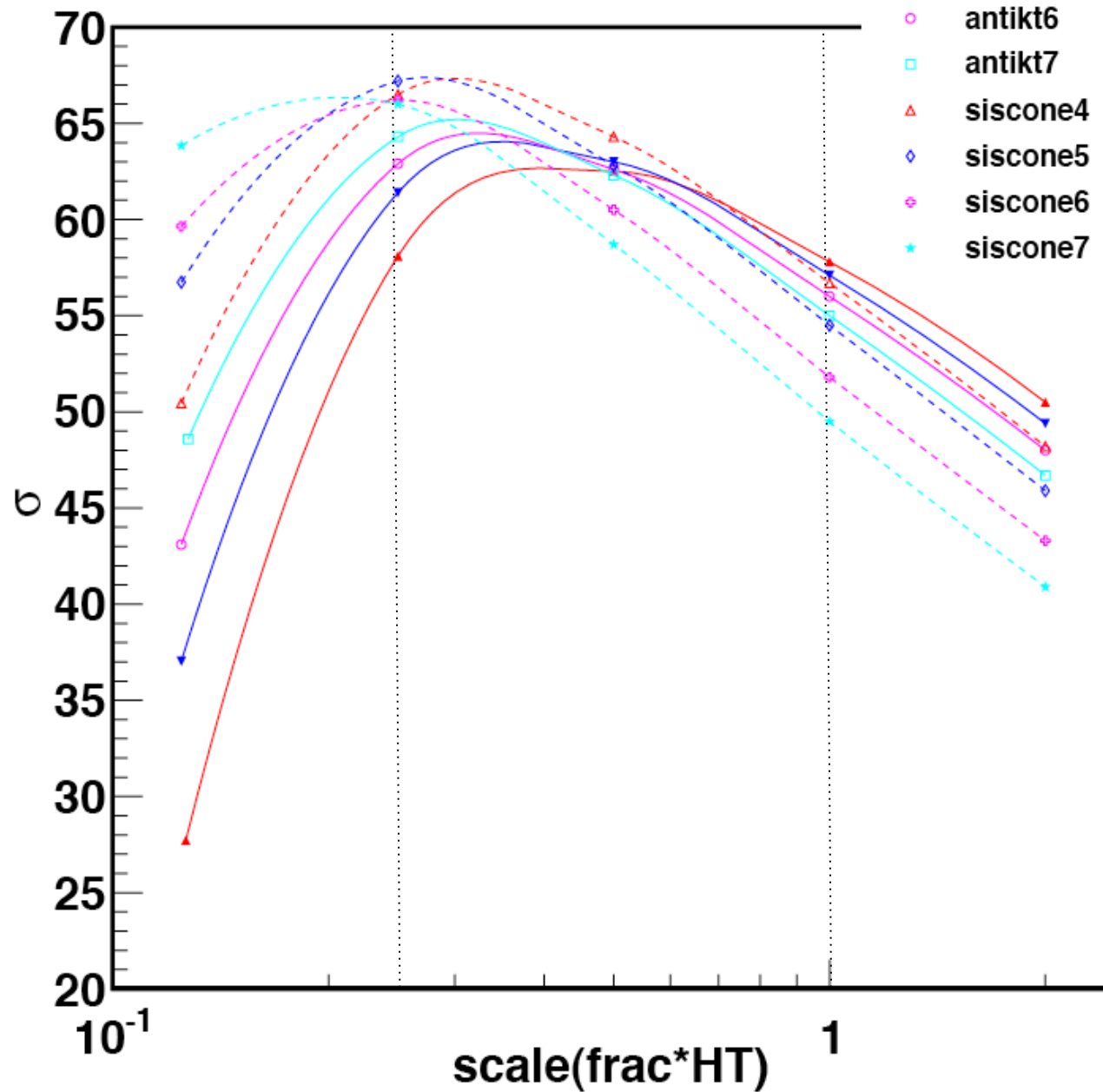


See parabolic shape for W+2 jets

Note that for antikt4, the scale $H_T/2$ is at the same point as $H_T/4$; scale dependence will appear smaller

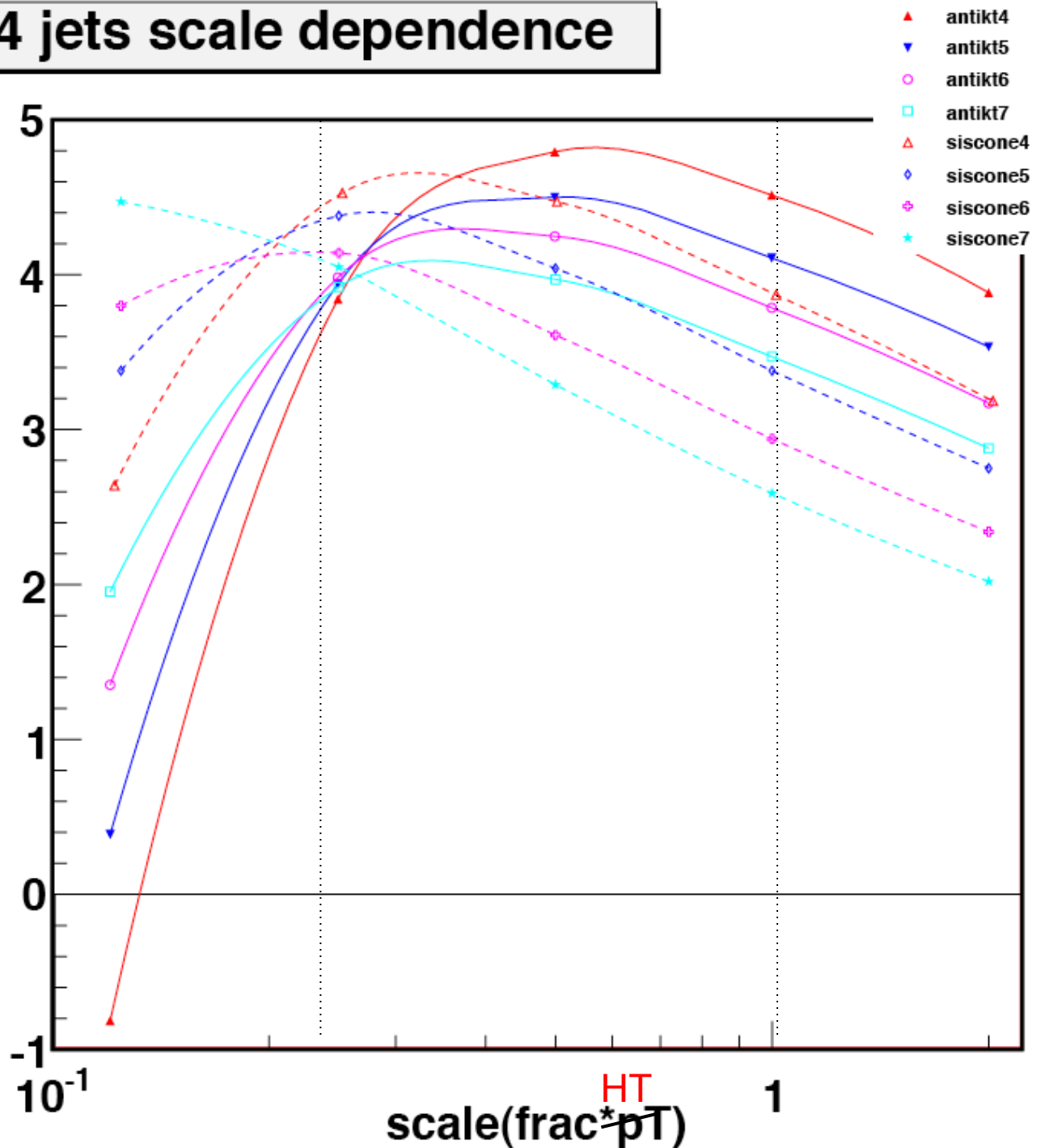
may be better to look for max/min over scale range (in 2D)

W+3 jets scale dependence



W+4 jets scale dependence

- A scale of HT/2 is \sim the peak for antikt4; so all deviations are negative
- Siscone peaks around HT/3
- Moves to smaller scales for larger R
- @HT/4, all antikt R give same result; that scale seems to be around HT/5 for siscone
- it is difficult to make conclusions about the uncertainty of any particular W + n jet cross section without understanding the scale dependence as the jet size/algorithm is varied



Scale choice: why is E_T^W a bad one at the LHC?

If configuration a dominated, then as jet E_T increased, E_T^W would increase along with it. But configuration b is kinematically favored for high jet E_T 's (smaller partonic center-of-mass energy); E_T^W remains small, and that scale does not describe the process very well

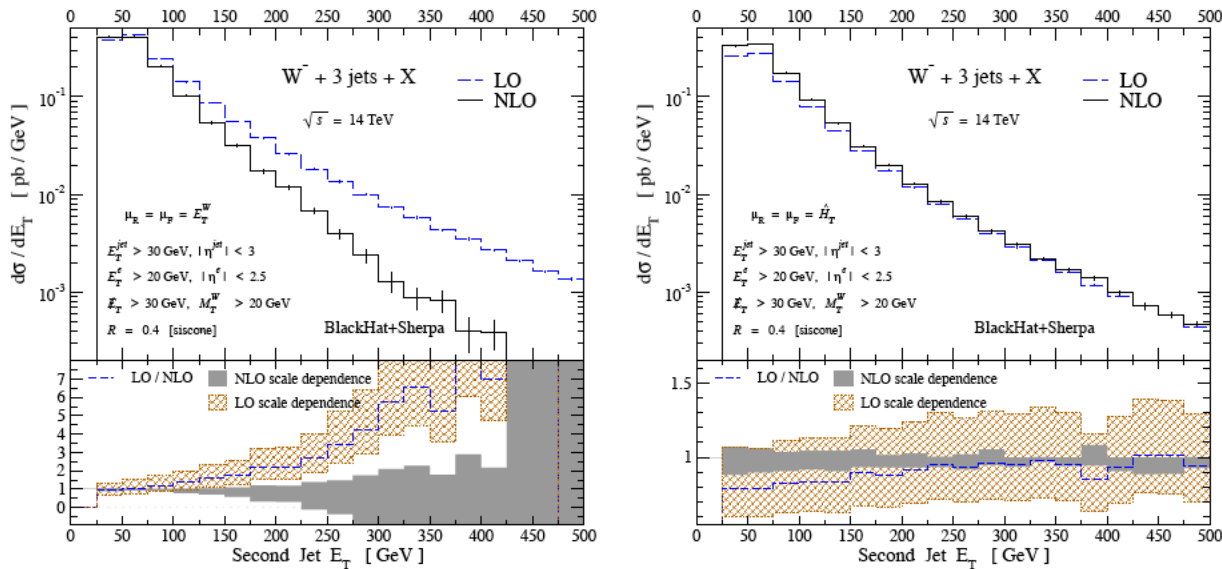
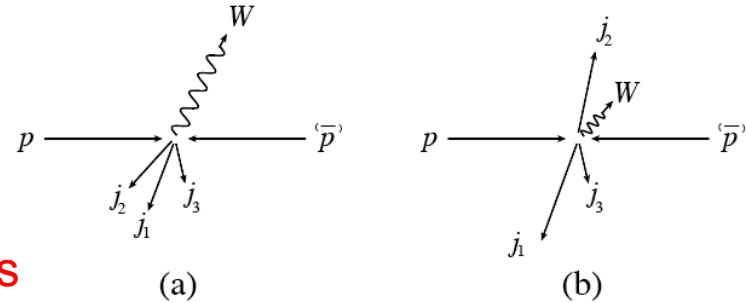
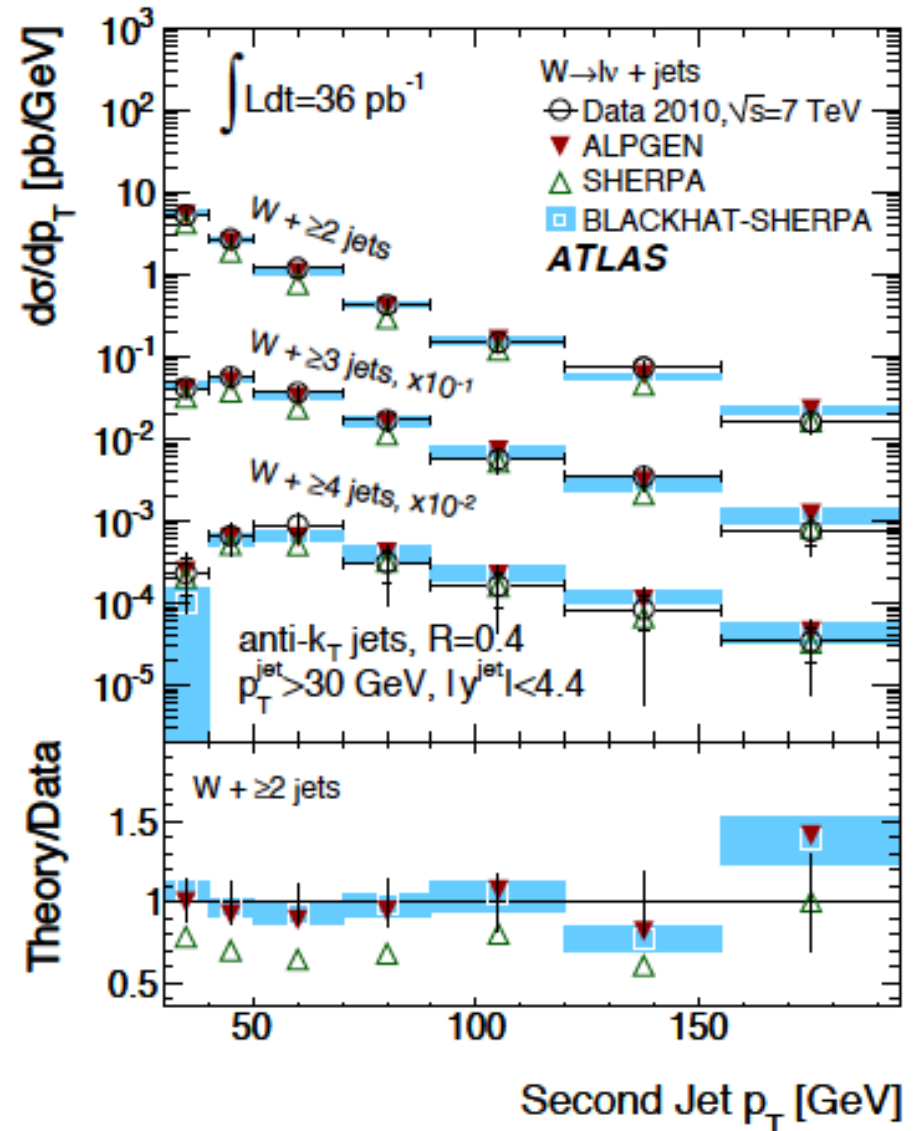
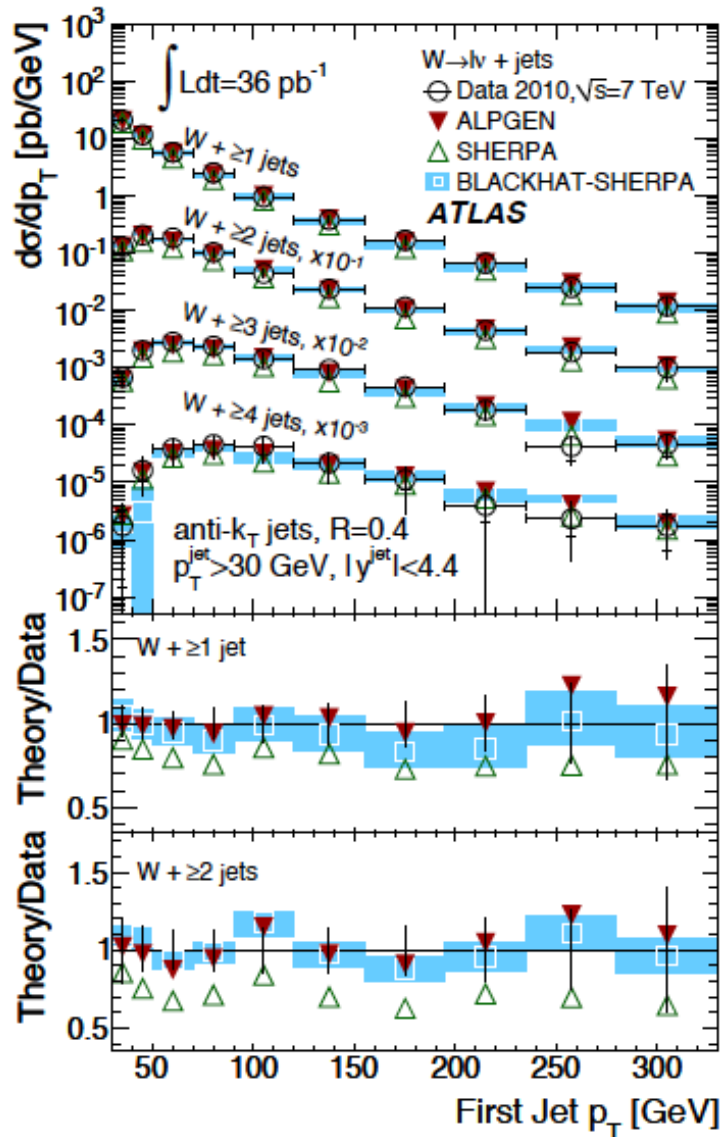


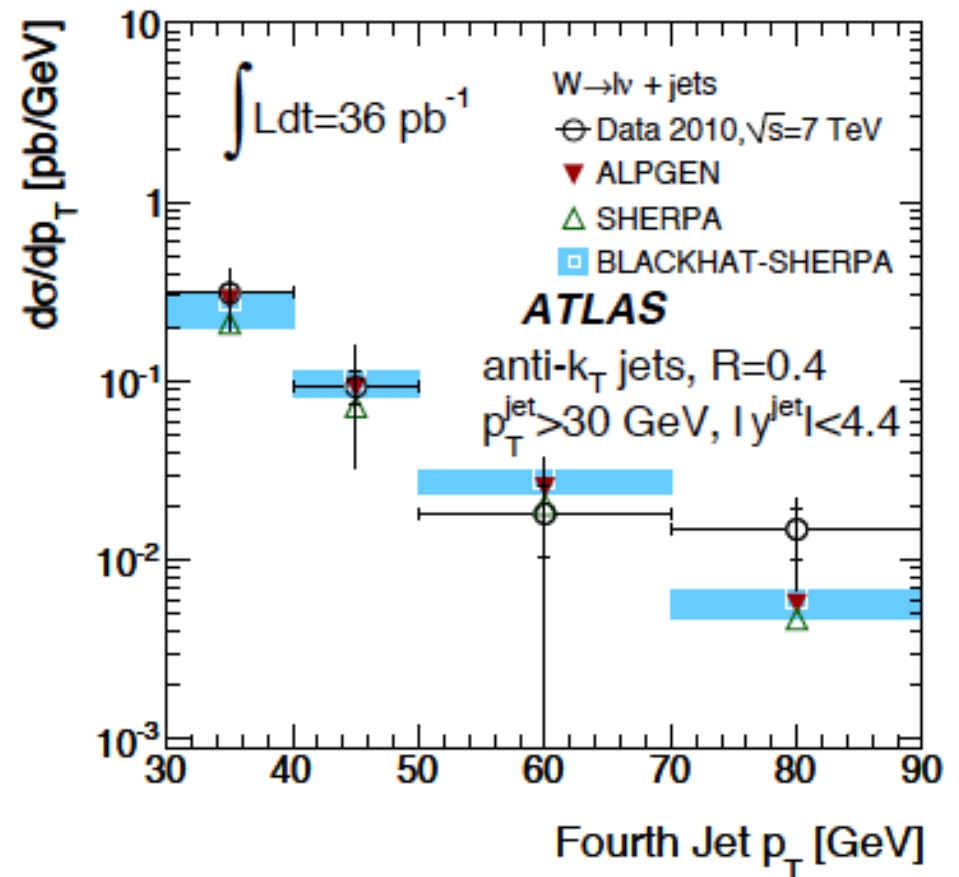
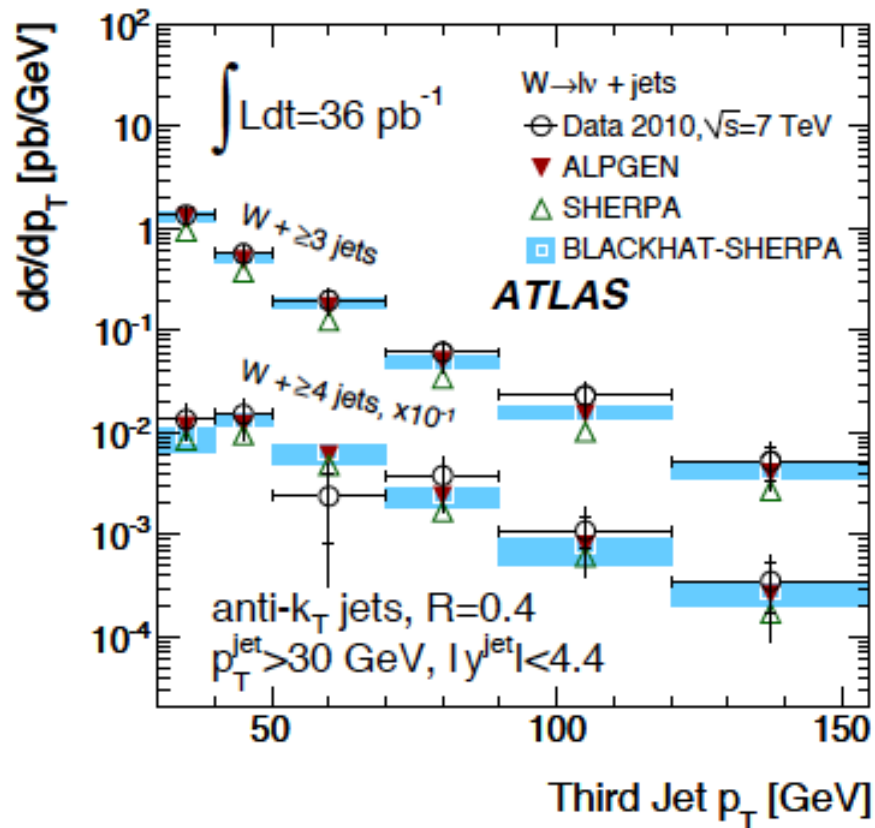
FIG. 9: The E_T distribution of the second jet at LO and NLO, for two dynamical scale choices, $\mu = E_T^W$ (left plot) and $\mu = \hat{H}_T$ (right plot). The histograms and bands have the same meaning as in previous figures. The NLO distribution for $\mu = E_T^W$ turns negative beyond $E_T = 475$ GeV.

Configuration b also tends to dominate in the tails of multi-jet distributions (such as H_T or M_{ij}); for high jet E_T , W behaves like a massless boson, and so there's a kinematic enhancement when it's soft

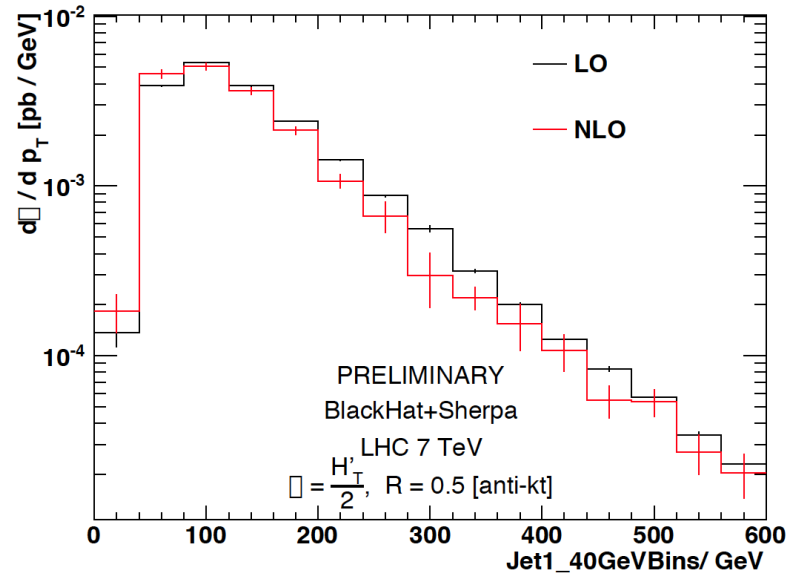
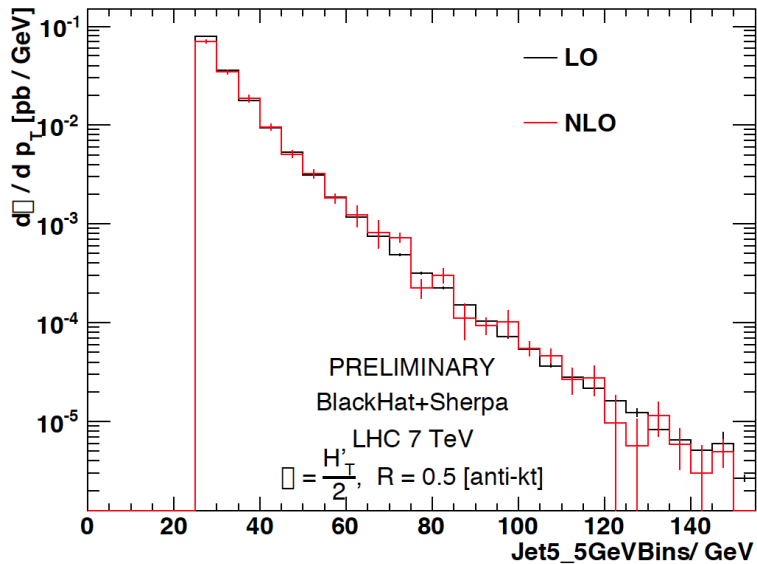
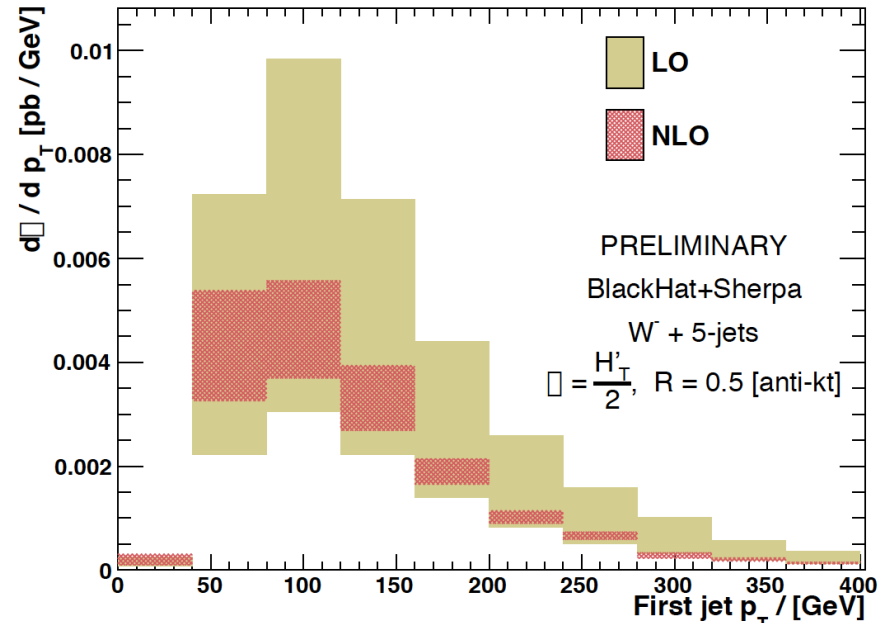
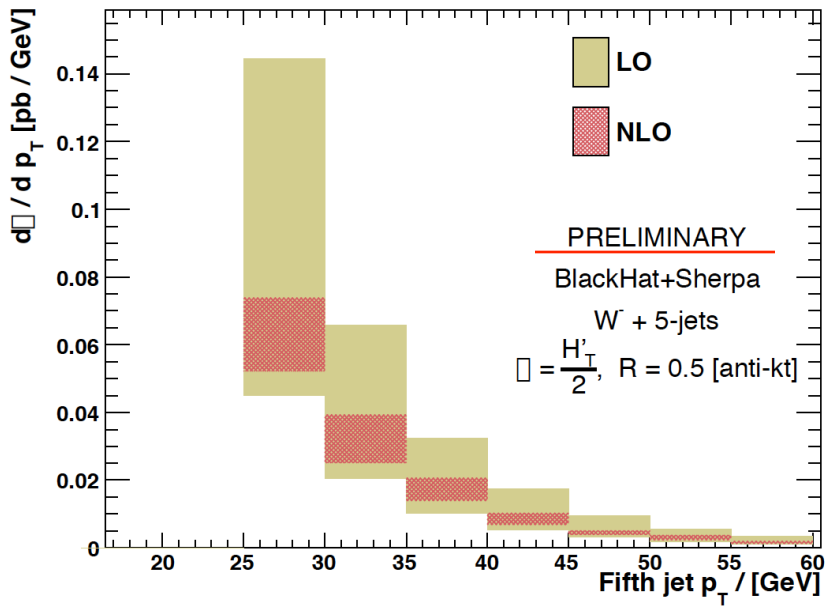
ATLAS: first and second jet p_T distributions



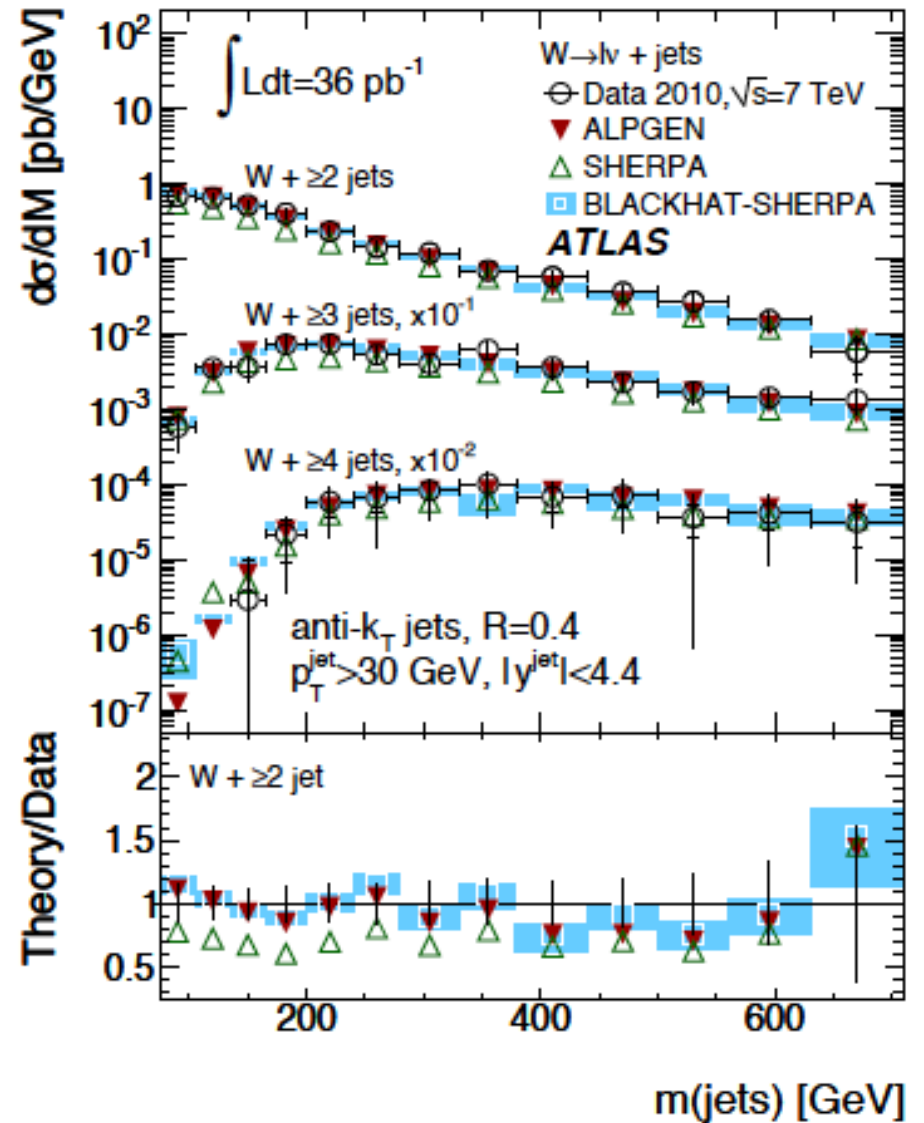
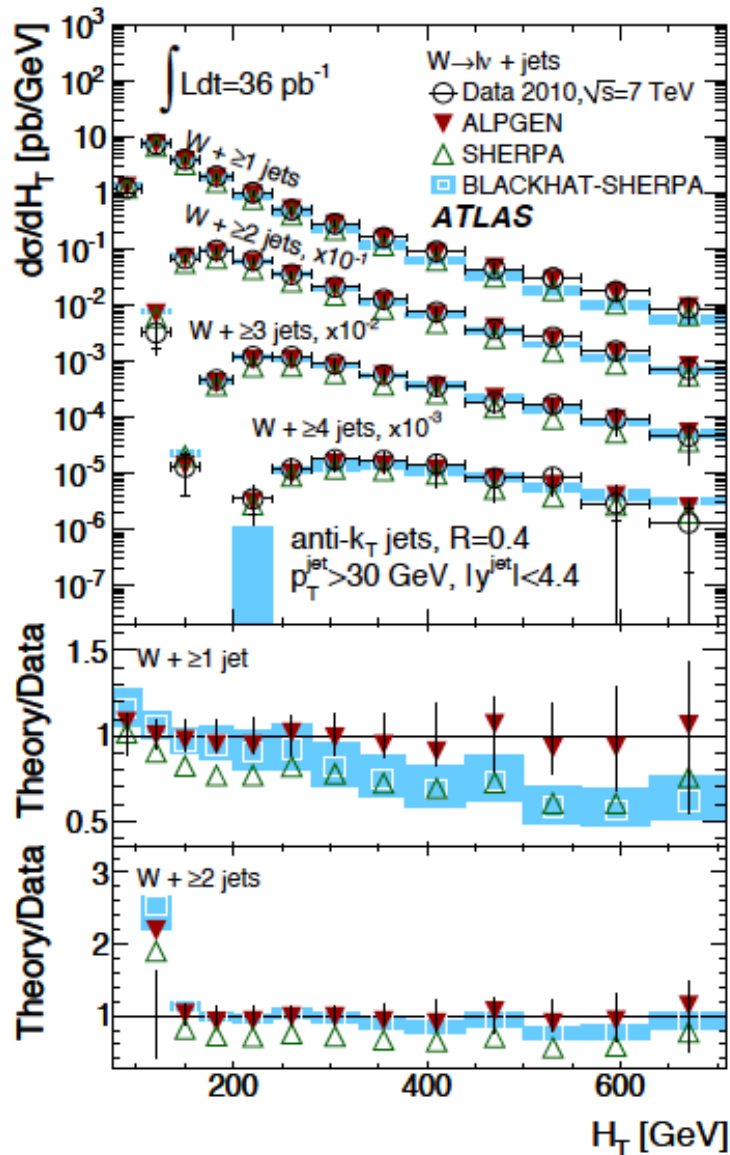
Third and fourth jet p_T distributions



Breaking news: W+5 jets at NLO

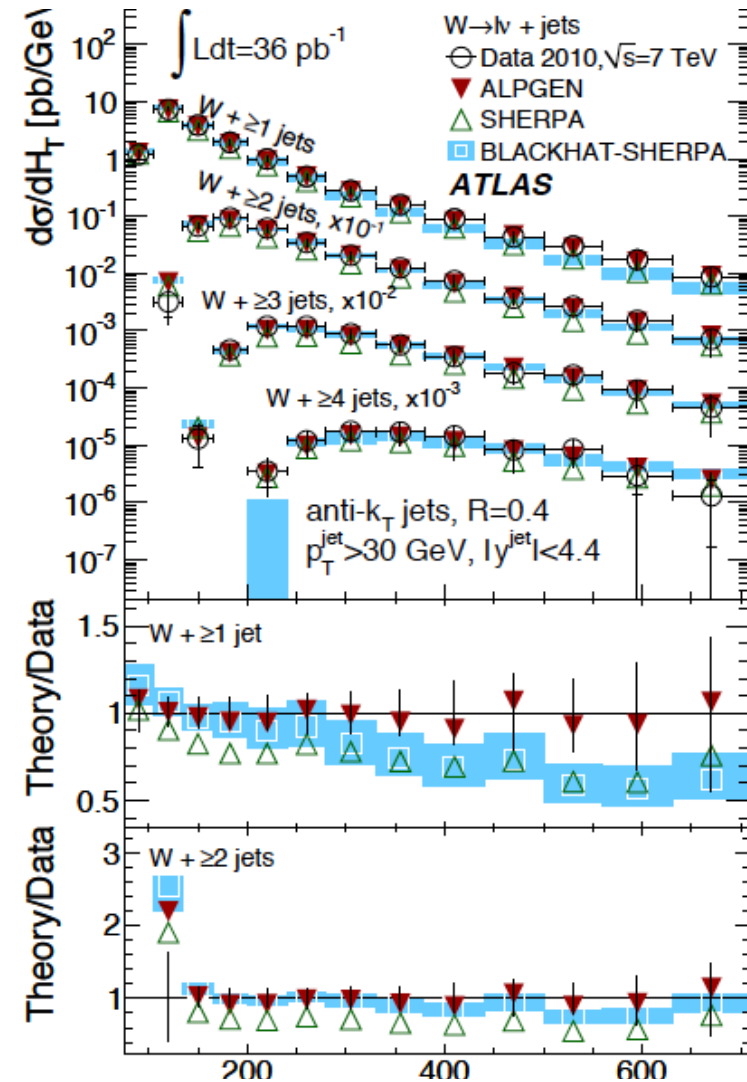


Look at very exclusive variables: H_T and m_{jets}



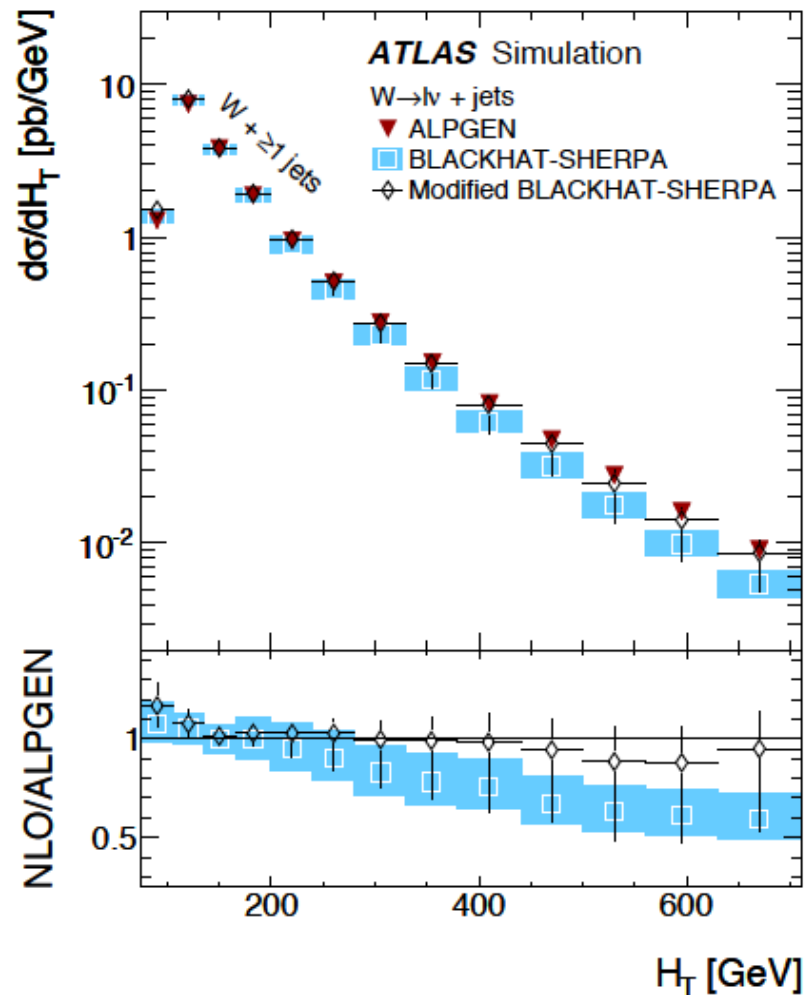
Going beyond NLO inclusive

- In the previous slide, we saw that the H_T distribution for $W+\geq 1$ jet was not well-described by the NLO $W+1$ jet prediction



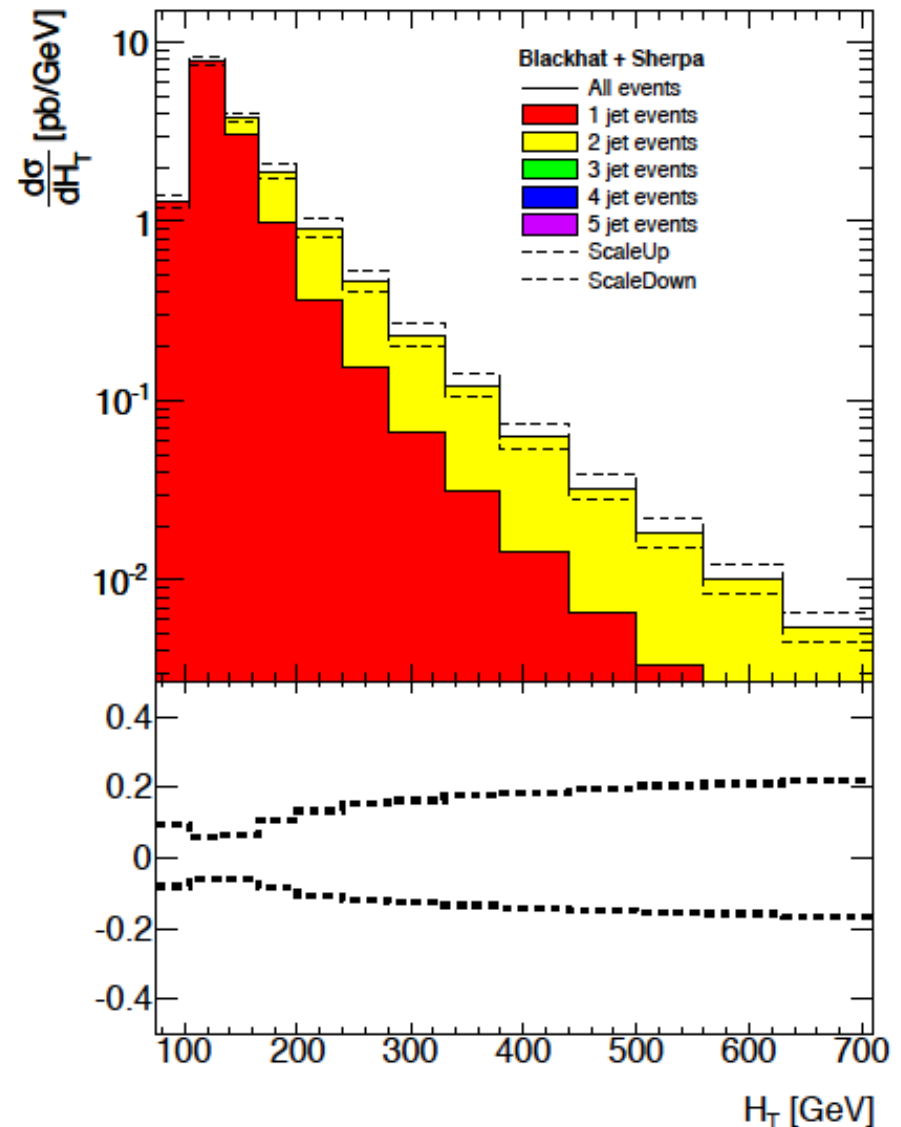
Going beyond NLO inclusive

- In the 2010 data, we saw that the H_T distribution for $W+\geq 1$ jet was not well-described by the NLO $W+1$ jet prediction
- However, it was better described when additional information was included from $W+2,3,4$ jets at NLO
- This is very tricky to do and Bryan will probably be offended
 - ◆ by definition the inclusive $W+1$ jet NLO calculation includes explicit $W+2$ jet information (at LO) and implicitly, through DGLAP evolution, information from 3,4,5, additional jets (in the collinear limit)
 - ◆ ...and the real correction for $W+1$ jet is the same as the born term for $W+2$ jets...so double-counting is a problem



...but first, consider scale dependence for inclusive $W+\geq 1$ jet

- Why does the scale dependence get worse as H_T increases?
- Large $H_T \rightarrow$ more perturbative, so you might naively expect it to get better
- As H_T increases, there is a large log (ratio of H_T to p_T cut (in this case 30 GeV)); this large log more than compensates for the extra factor of α_s need to add an extra jet, and most of cross section comes from $W+2$ jets, which is present only at LO in the calculation



Exclusive sums

- The NLO Blackhat+Sherpa calculations consist of separate ntuples for born, virtual, subtraction and real
- Suppose we define exclusive sums such that for W+n jets, we remove any events in the W+n jet sample where there is an n+1 jet with $p_T >$ some cutoff (30 GeV/c in the case of the 2010 data)
 - ◆ or we actually do the equivalent, where we keep all of the n+1 jets from the W+n jet real contribution, but remove the W+n+1 born events
- So we have explicit contributions for the exclusive sum W+1 jet cross section from 2 jets, 3 jets, 4 jets and 5 jets (LO)

$$\sigma^{\text{tot}} \equiv \sigma_m^{\text{inc}} = \sum_{n=m}^{M-1} \sigma_n^{\text{exc}} + \sigma_M^{\text{inc}}$$

- This is similar to the data where if we form the H_T cross section for ≥ 1 jet, we have contributions from all of those higher multiplicity final states
- So how does it work

Pretty well when adding W+2 jets

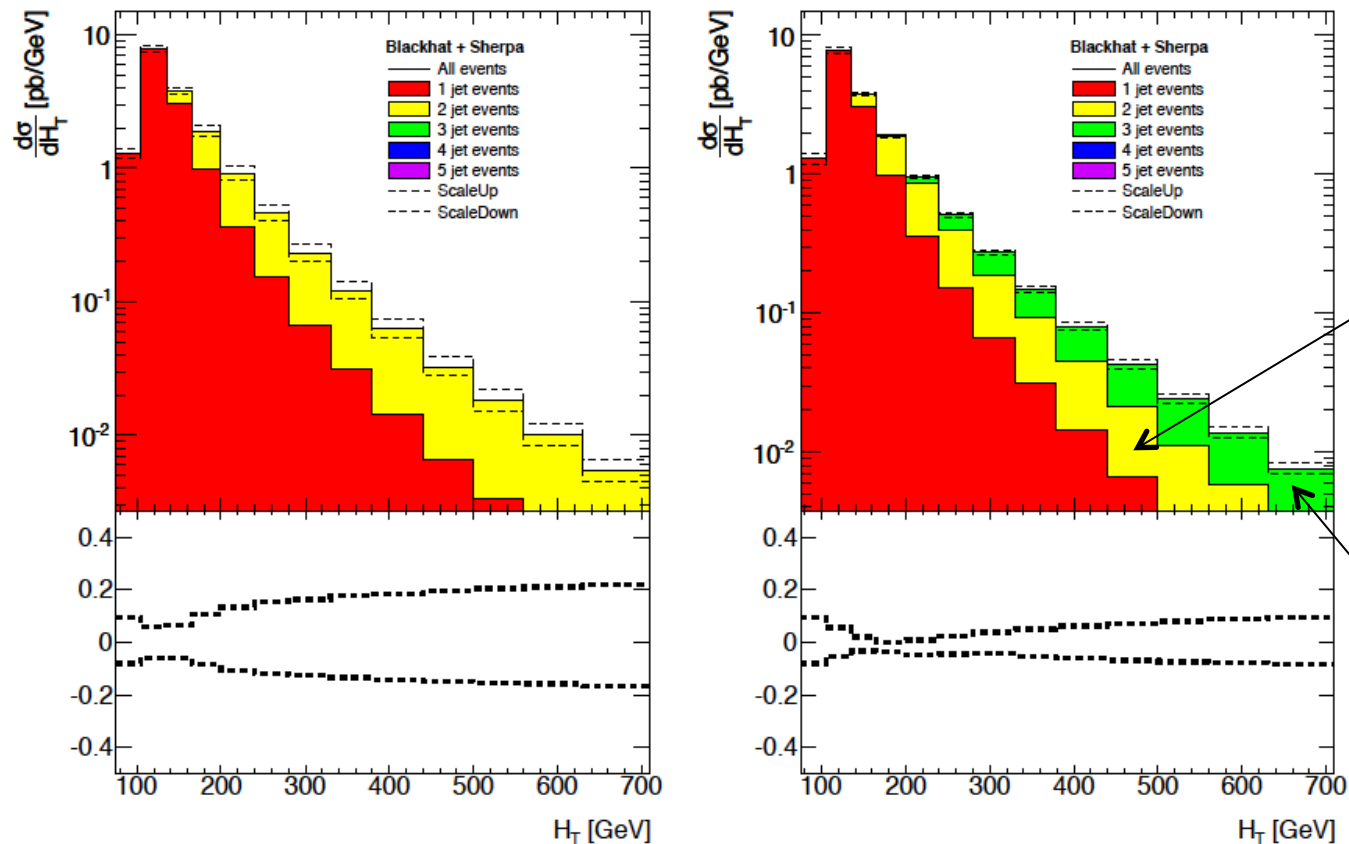
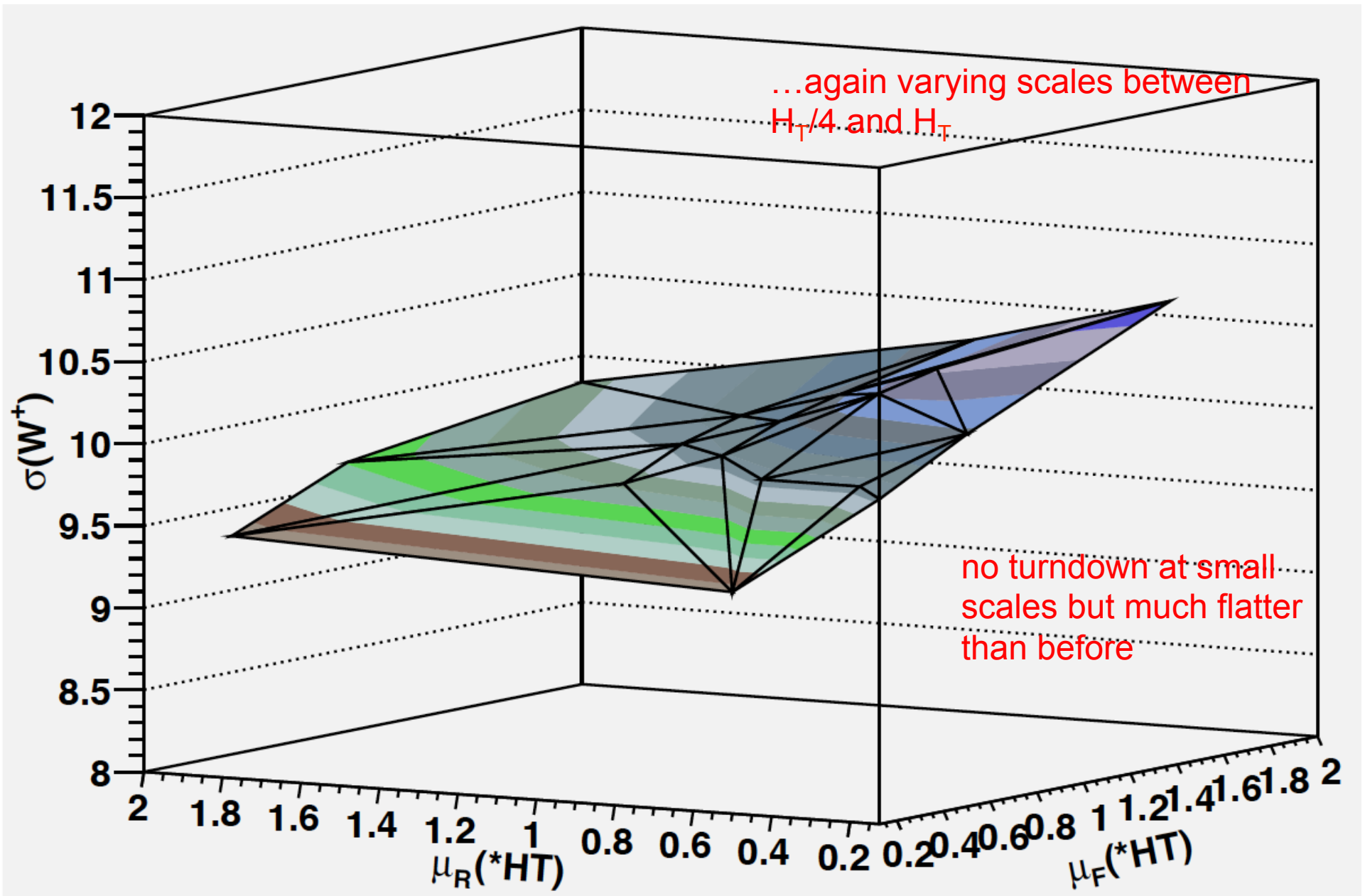
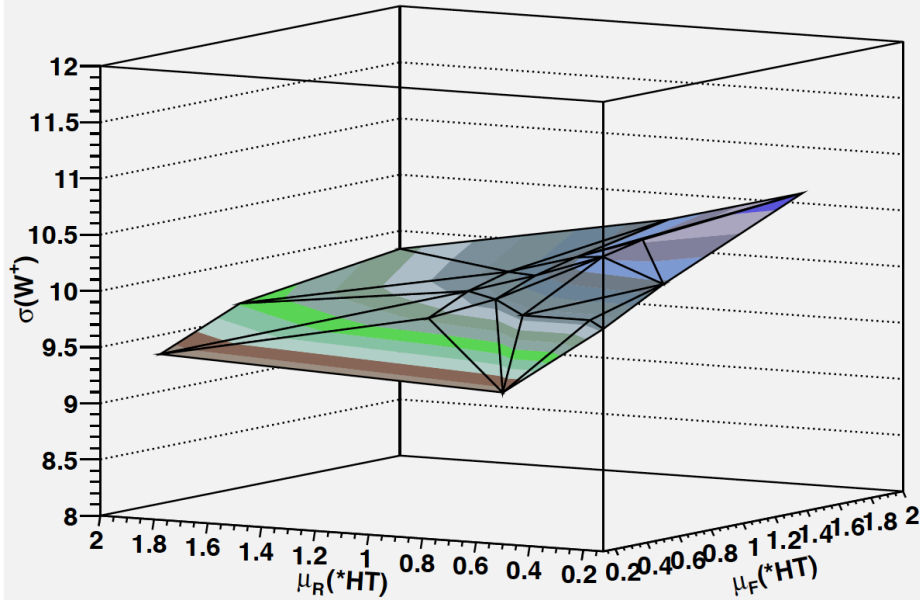


Fig. 1: The W + jets cross section, as a function of H_T , for the NLO inclusive $W + \geq 1$ jet prediction (left) and for the exclusive sums approach, adding in $W + 2$ jet production at NLO (right). The cross sections have been evaluated at a central scale of $H_T/2$ and the uncertainty is given by varying the renormalization and factorization scales independently up and down by a factor of 2, while ensuring that the ratio of the two scales is never larger than a factor of 2.

Look at 2D scale dependence for exclusive sum (W+1+2 jets at NLO)

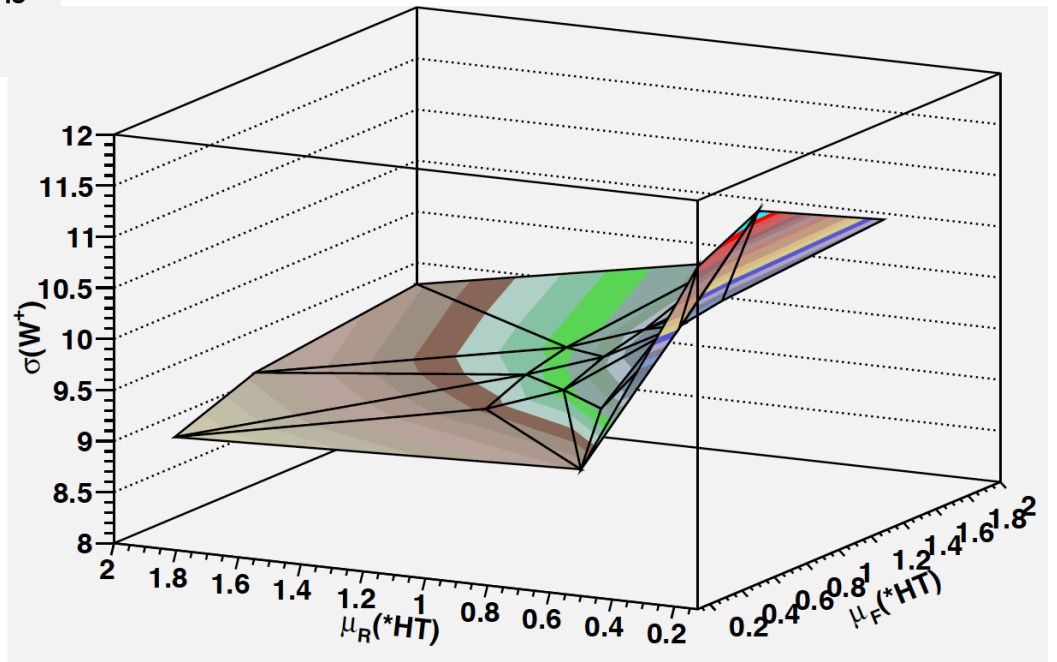


Comparison with inclusive case



exclusive NLO sum

inclusive NLO



Not quite as well for adding 3 and 4 jets

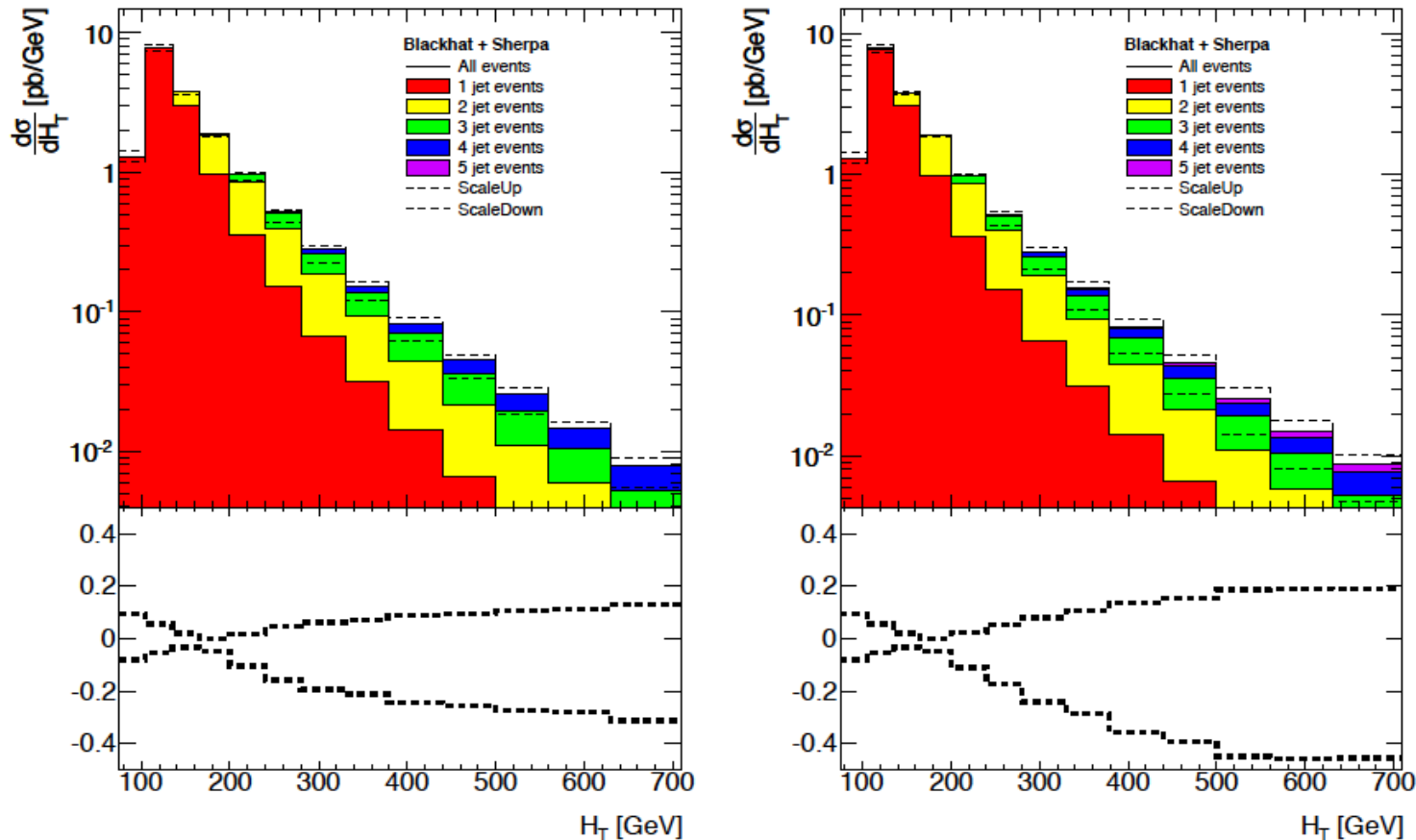


Fig. 2: The $W + \text{jets}$ cross section, as a function of H_T , for $W + \geq 1$ jet production using the exclusive sums approach, and adding up to 3 jets at NLO (left) and 4 jets at NLO (right). The cross sections have been evaluated at a central scale of $H_T/2$ and the uncertainty is given by varying the renormalization and factorization scales independently up and down by a factor of 2, while ensuring that the ratio of the two scales is never larger than a factor of 2.

So what went wrong...with the scale dependence

NLO predictions into fixed multiplicities sets³ and test the stability of the prediction. For the exclusive sums approach outlined here for $W+ \geq 1$ jets, contributions are added proportional to α_s^2 (W+1 jet at NLO), α_s^3 (W+2 jets at NLO), α_s^4 (W+3 jets at NLO) and α_s^5 (W+4 jets at NLO). So this procedure mixes powers of α_s and thus is missing essential Sudakov form factors that effectively bring each term to the same power of α_s . One could imagine accomplishing this by embedding the NLO matrix elements in a parton shower Monte Carlo framework, however the technology for merging different multiplicities of NLO calculations with a parton shower is still under development. Alternatively the LoopSim method can be used to provide approximations to the higher-loop terms missing in the exclusive sums approach. As we have seen here, prospects for using it together with Blackhat+Sherpa ntuples seem promising.

Performing the sum over n , which corresponds to summing an infinite tower of NLO exclusive jet calculations, leads to

...need something else to obtain necessary logarithmic accuracy ...we're currently working with LoopSim

$$\sigma(p_{t,W})^{\text{DLA}} = \sum_{n=1}^{\infty} \sigma_{n,\text{excl}}^{\text{NLO(DLA)}}(p_{t,W}) \quad (5a)$$

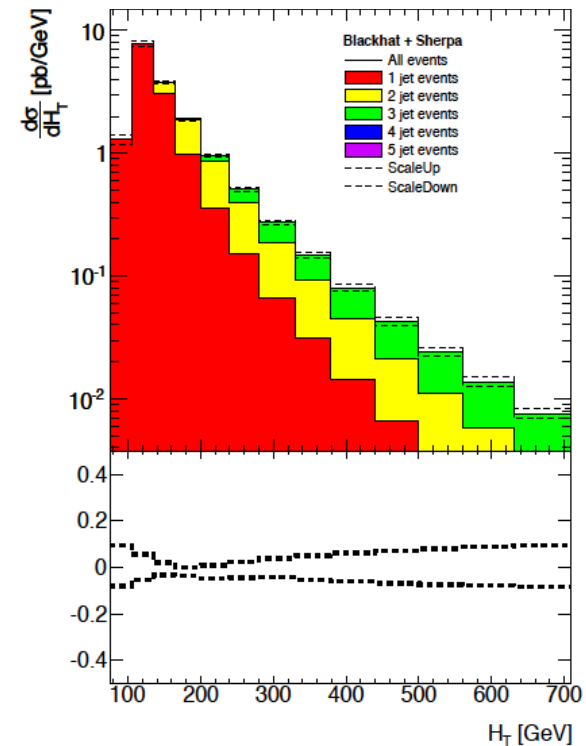
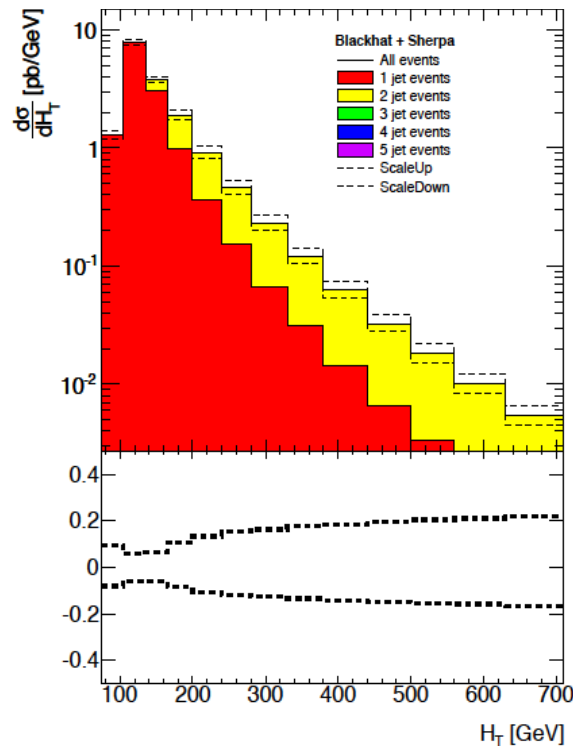
$$= \sigma_1^{\text{LO}}(p_{t,W}) \exp\left(\frac{2C\alpha_s}{\pi} L^2\right) \left(1 - \frac{2C\alpha_s}{\pi} L^2\right) \quad (5b)$$

$$= \sigma_1^{\text{LO}}(p_{t,W}) \left(1 - \frac{1}{2} \left(\frac{2C\alpha_s}{\pi} L^2\right)^2 + \mathcal{O}(\alpha_s^3 L^6)\right). \quad (5c)$$

As long as L^2 is not large, the difference between this and the correct answer of Eq. (3) is a straightforward NNLO correction, i.e. small. However in when $p_{t,W} \gg p_{t,\text{min}}$ the logarithms become large, the $\alpha_s^2 L^4$ term can be of order 1 and the exclusive sums method may then no longer be a good approximation. A similar analysis can be performed for an exclusive sum truncated at some finite order, as used below.

What went right with W+2?

- There are substantial $qq \rightarrow q'qW$ contributions that enter at LO for W+2 jet (so in the real terms for W+1 jet at NLO) that are stabilized by the addition of the W+2 jet full NLO terms
- So (I think) adding the W+1 and W+2 NLO using the exclusive sums approach gives a superior prediction compared to W+1 jet alone
- Higher multiplicities may need more work a la LoopSim to reduce the scale dependence
- But I think there must be a simpler way as well to take into account the proper Sudakovs



For more details, see the following contribution to Les Houches

W+jets production at the LHC: a comparison of perturbative tools

*J. Andersen*¹, *J. Huston*², *D. Maître*^{3,4}, *S. Sapeta*⁵, *G.P. Salam*^{3,5,6}, *J. Smillie*⁷, *J. Winter*³

¹CP³-Origins, Campusvej 55, DK-5230 Odense M, Denmark

² Physics and Astronomy Department, Michigan State University, East Lansing, MI, 48824 USA

³PH-TH Department, Case C01600, CERN, CH-1211 Geneva 23, Switzerland

⁴IPPP, University of Durham, Science Laboratories, South Rd, Durham DH1 3LE, UK

⁵LPTHE, UPMC and CNRS UMR 7589, 75252 Paris cedex 05, France

⁶Department of Physics, Princeton University, Princeton, NJ 08544, USA

⁷School of Physics and Astronomy, University of Edinburgh, Mayfield Road, Edinburgh EH9 3JZ, UK

Abstract

In this contribution, we discuss several theoretical predictions for W plus jets production at the LHC, compare the predictions to recent data from the ATLAS collaboration, and examine possible improvements to the theoretical framework.

...plus I'm working on some followup studies with LoopSim, maybe other ideas

...contribute your brilliant idea here

...also in Les Houches, a detailed systematic comparison of various predictions for W+jets

...differences were often larger than assumed by authors

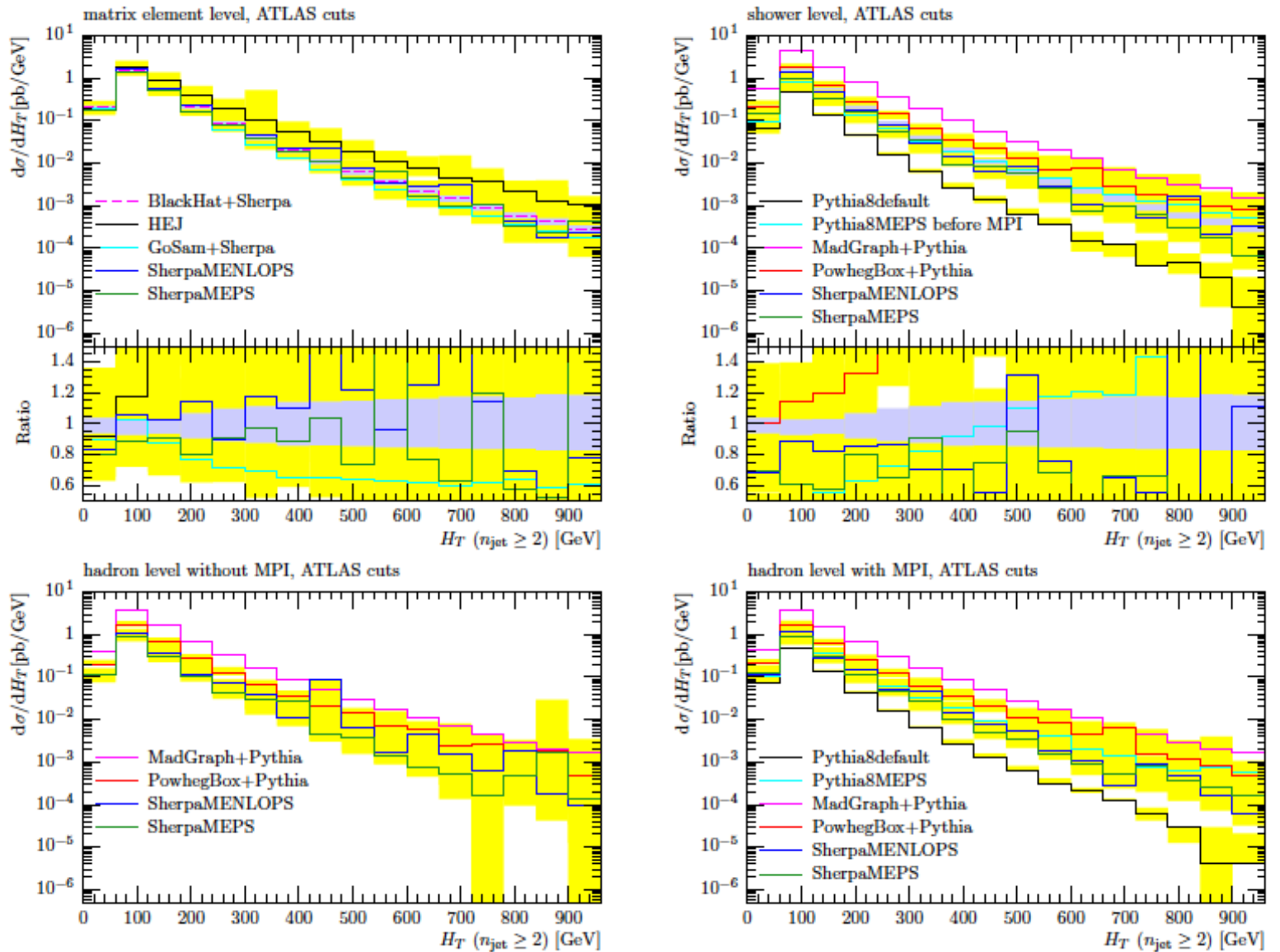
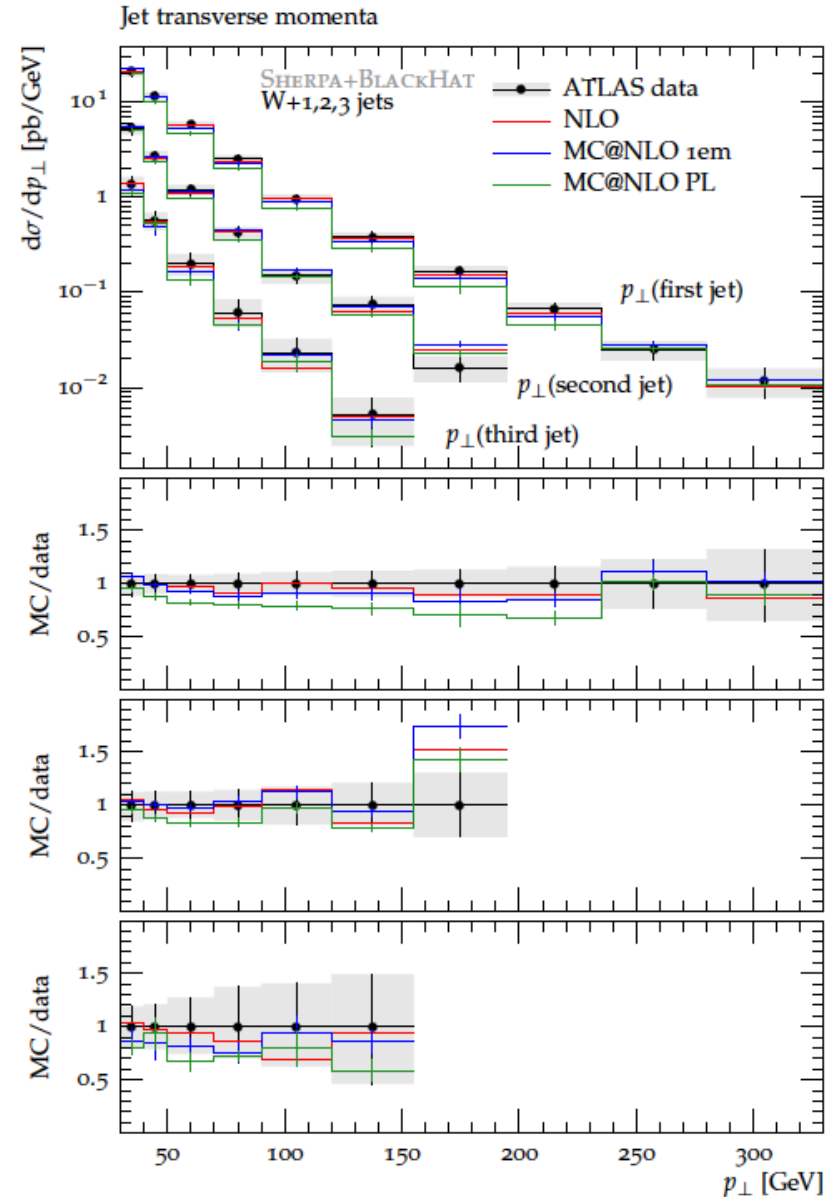


Fig. 32: $H_T = \sum_{i \in \{\text{jets}\}} E_{\perp i}$ of events with at least 2 jets on all levels of the simulation (for exact definitions and cuts see App. A1 and App. A2). Note that BLACKHAT uses the CTEQ6.6 pdf, PYTHIA8 and MADGRAPH+PYTHIA CTEQ6L1 and all the others use CT10. In both ratio plots the ratio is taken with respect to BLACKHAT+SHERPA (on matrix element level).

Sherpa+Blackhat

- Just to add to the confusion, here, the NLO virtual matrix elements of Blackhat have been used with Sherpa parton showering using the MC@NLO framework
- Comparing to the ATLAS data recorded at the Durham site
- W+1,2 and 3 jets at NLO
 - ◆ the last is a world record for the complexity of a final state in a NLO parton shower Monte Carlo (as far as I know)
 - ◆ aMC@NLO previously did W+2 jets at NLO
- What we would really like is CKKW@NLO
 - ◆ I know that Leif Lonnblad gave a talk on ongoing work at the CERN NLO PS workshop



...and finally



www.pa.msu.edu/~huston/qcd2012/QCD_LHC.html



...a continuation of the series that started in Trento (2010) and St. Andrews (2011)

[HOME](#) [PROGRAM](#) [REGISTRATION](#) [CONFERENCE FEE](#) [LOCATION](#) [TRAVEL](#) [LODGING](#)

QCD @ LHC 2012

20th-24th August 2012 at Michigan State University

This workshop aims at instigating discussions and future work between experimenters and theorists, working on strong interactions at the LHC.



Extras



Correlations: look at error PDFs

- As expected, W and Z cross sections are highly correlated
- Anti-correlation between tT and W cross sections
 - ◆ more glue for tT production (at higher x) means fewer anti-quarks (at lower x) for W production
 - ◆ mostly no correlation for H and W cross sections

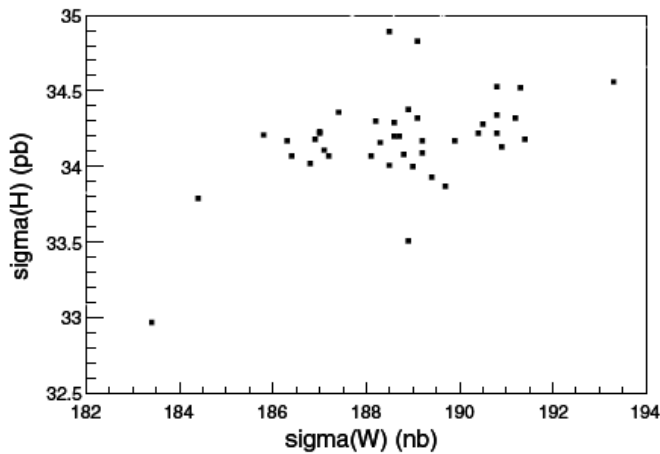


Figure 99. The cross section predictions for Higgs production versus the cross section predictions for W production at the LHC plotted using the 41 CTEQ6.1 pdfs.

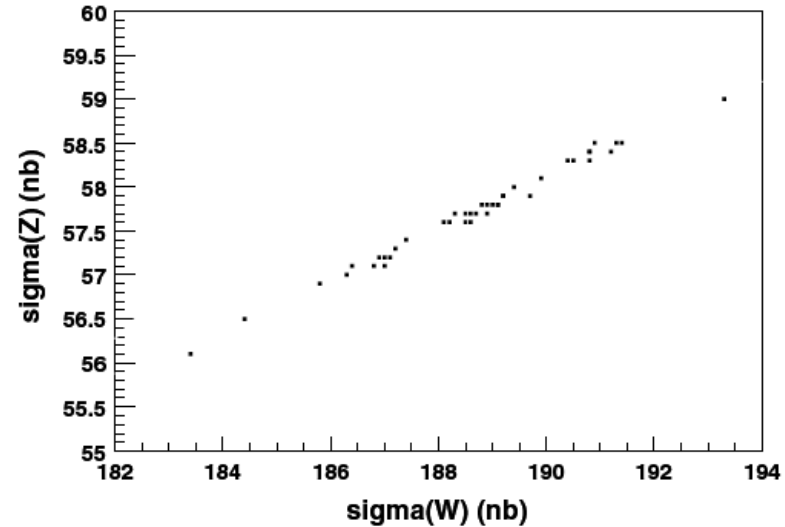


Figure 85. The cross section predictions for Z production versus the cross section predictions for W production at the LHC plotted using the 41 CTEQ6.1 pdfs.

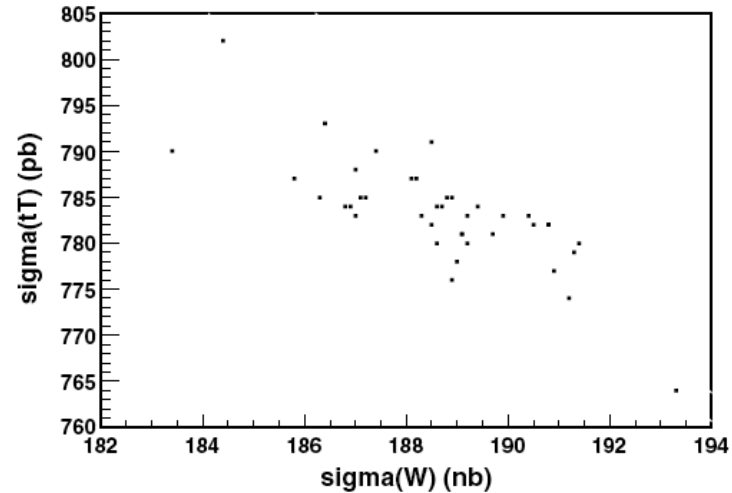


Figure 93. The cross section predictions for $t\bar{t}$ production versus the cross section predictions for W production at the LHC plotted using the 41 CTEQ6.1 pdfs.

Correlations: another look

Define a correlation cosine between two quan

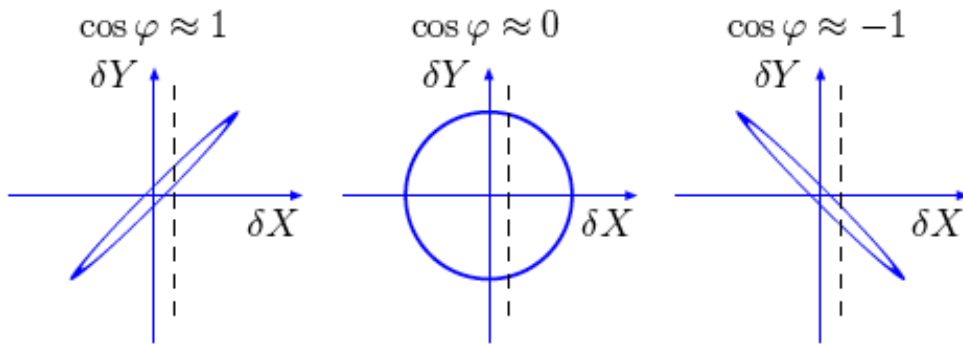
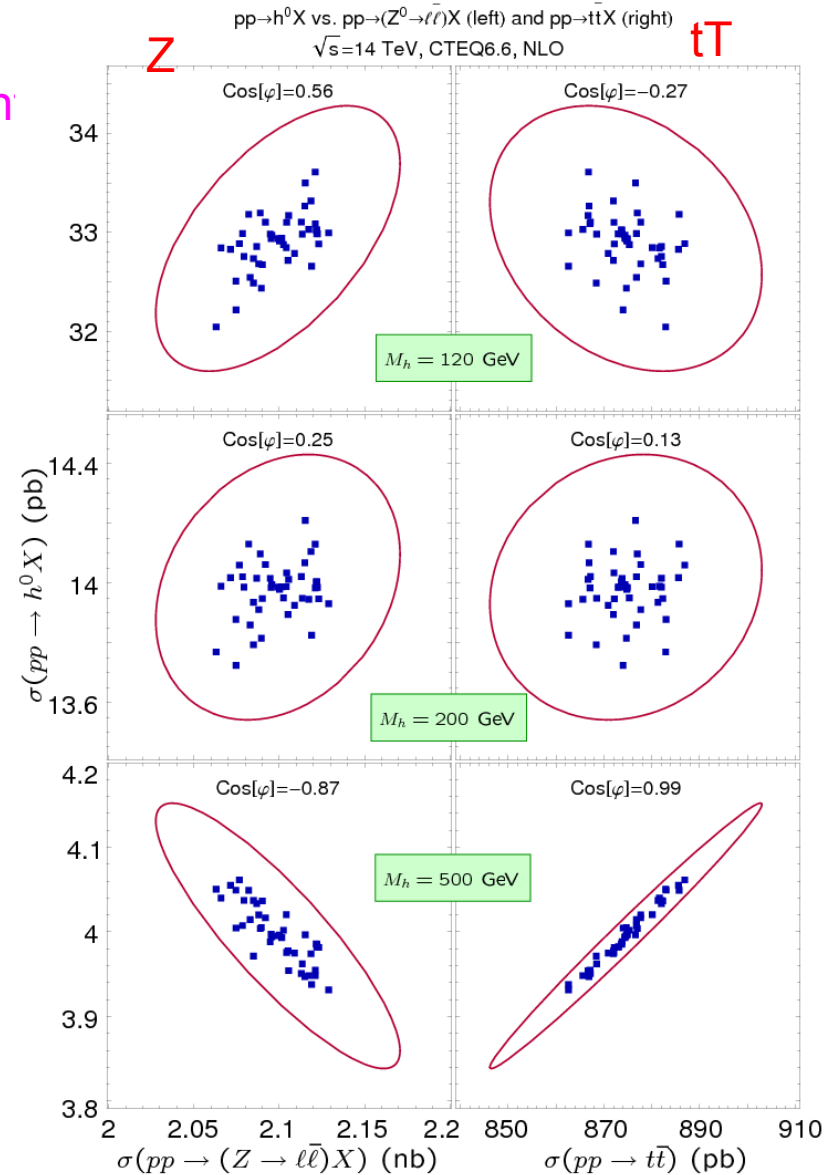


Figure 1: Dependence on the correlation ellipse formed in the $\Delta X - \Delta Y$ plane on the value of the correlation cosine $\cos \varphi$.

- If two cross sections are very correlated, then $\cos \phi \sim 1$
- ...uncorrelated, then $\cos \phi \sim 0$
- ...anti-correlated, then $\cos \phi \sim -1$



Correlations with Z, tT

Define a correlation cosine between two quantities

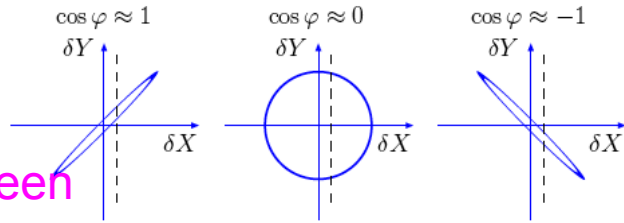
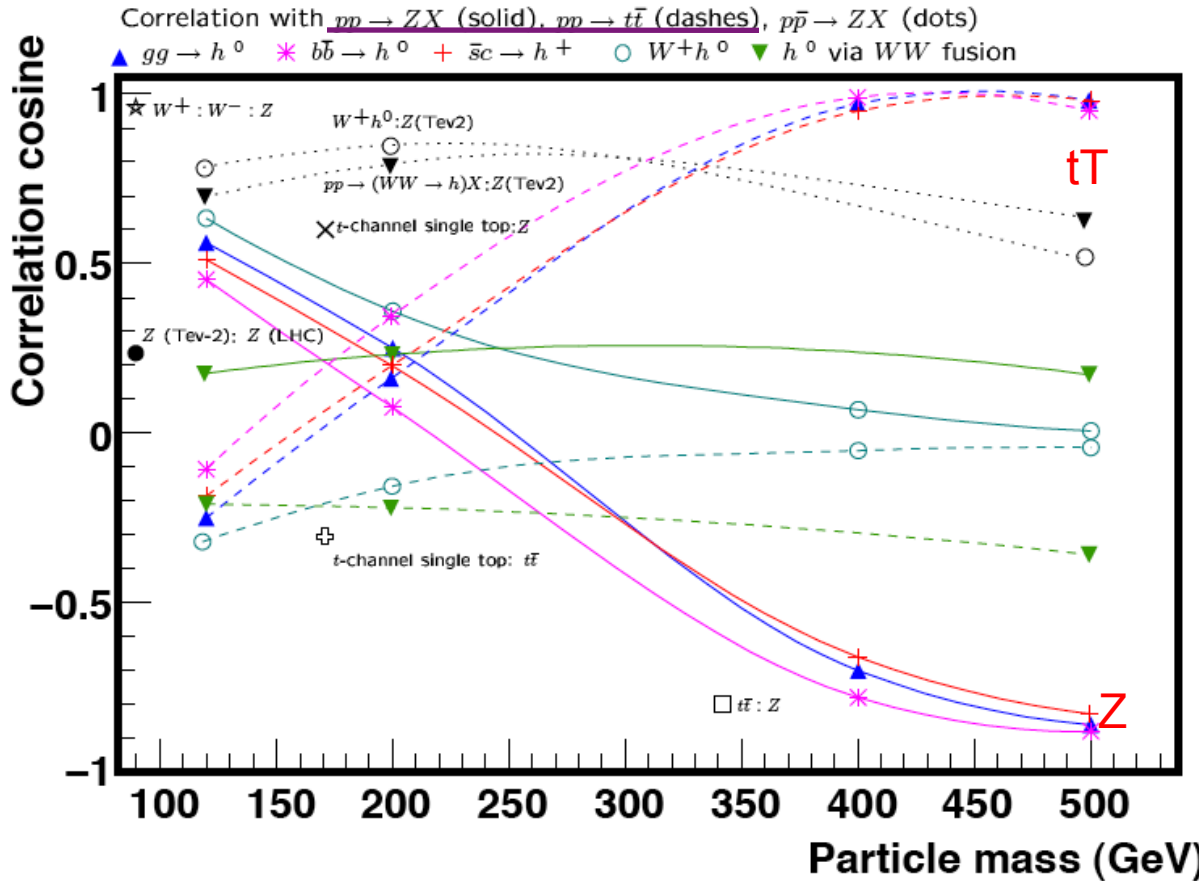


Figure 1: Dependence on the correlation ellipse formed in the $\Delta X - \Delta Y$ plane on the value of the correlation cosine $\cos \phi$.

- If two cross sections are very correlated, then $\cos \phi \sim 1$
- ...uncorrelated, then $\cos \phi \sim 0$
- ...anti-correlated, then $\cos \phi \sim -1$



• Note that correlation curves to Z and to tT are mirror images of each other

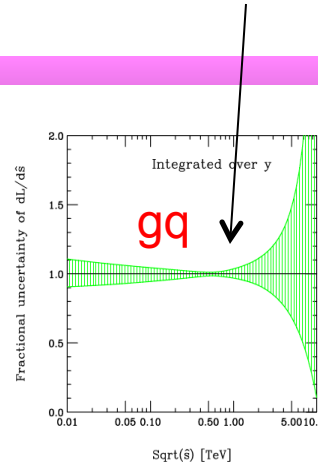
• By knowing the pdf correlations, can reduce the uncertainty for a given cross section in ratio to a benchmark cross section **iff** $\cos \phi > 0$; e.g. $\Delta(\sigma_W + / \sigma_Z) \sim 1\%$

• If $\cos \phi < 0$, pdf uncertainty for one cross section normalized to a benchmark cross section is larger

• So, for $gg \rightarrow H(500 \text{ GeV})$; pdf uncertainty is 4%; $\Delta(\sigma_H / \sigma_Z) \sim 8\%$

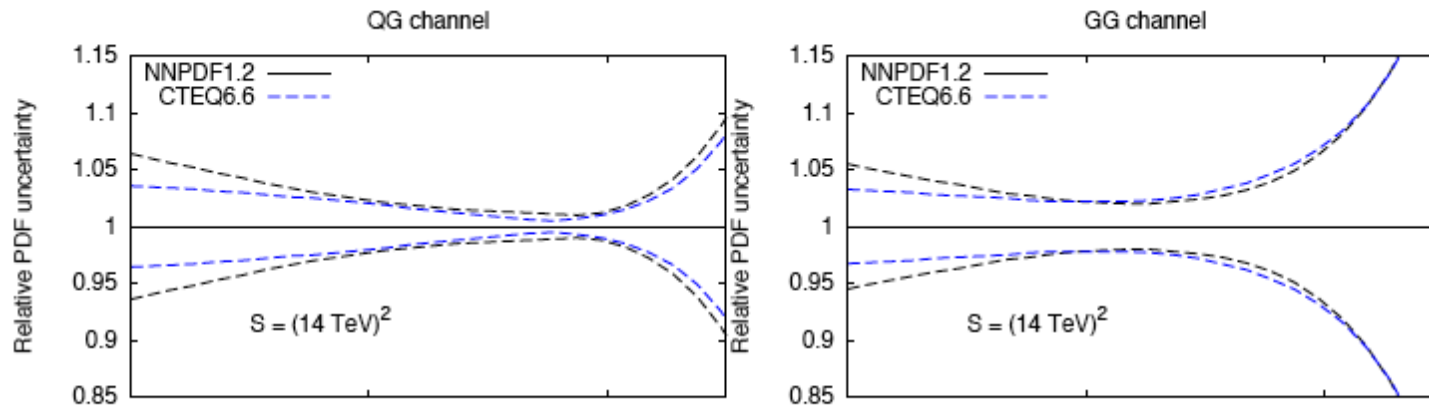
Remember the smallest uncertainty

...confirmed by NNPDF



Z produced at high p_T (~200 GeV/c) is produced primarily from gq scattering in this x range can we use Z production at high p_T as a normalization?

Fig. 6: Fractional uncertainty for Luminosity integrated over y for $g(d+u+s+c+b)+g(\bar{d}+\bar{u}+\bar{s}+\bar{c}+\bar{b})+(d+u+s+c+b)g+(d+\bar{u}+\bar{s}+\bar{c}+\bar{b})g$.



Errors (%) on $tt/Z(+j)$ ratios using CTEQ6ME

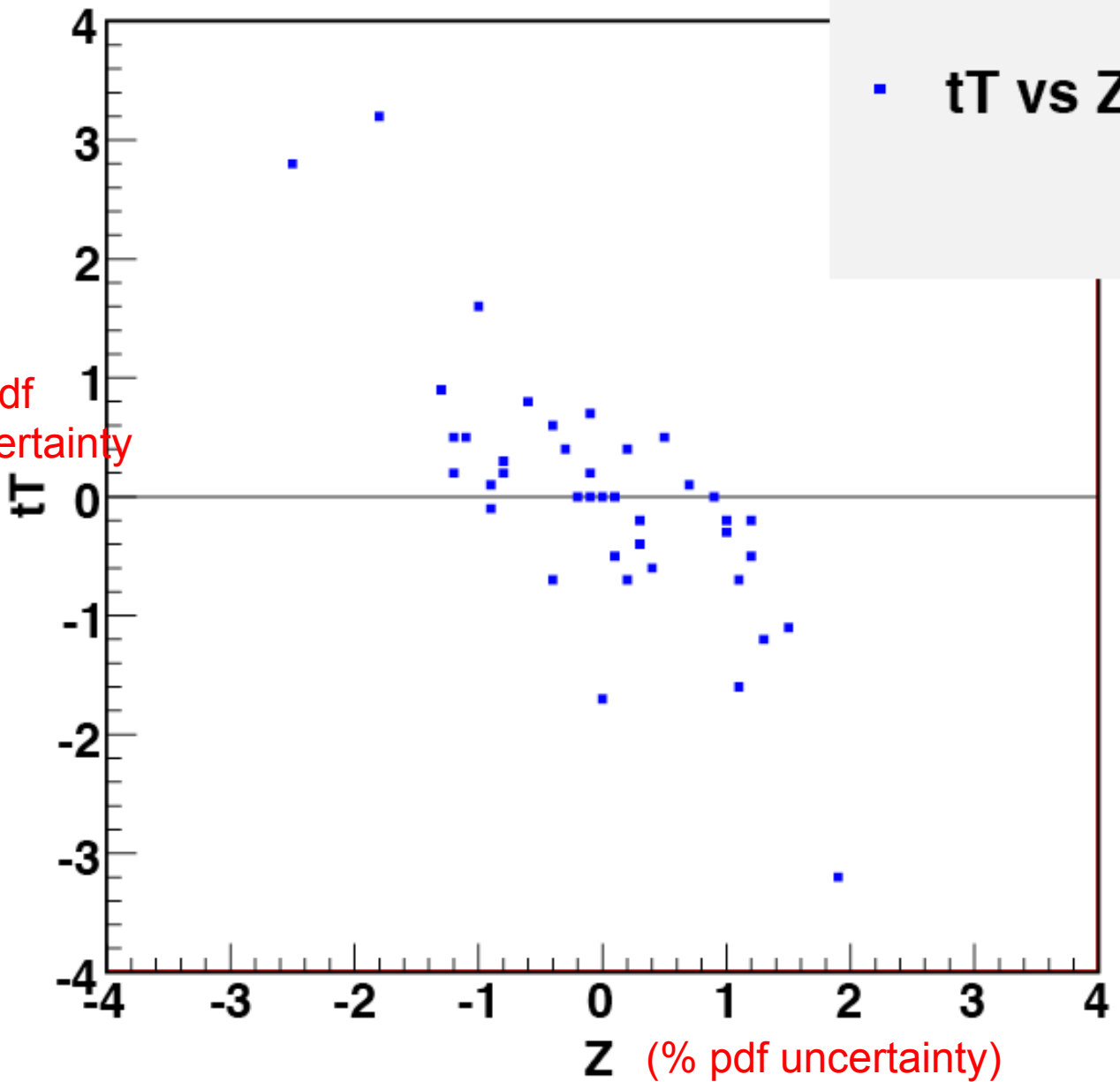
	$\delta \frac{\sigma(tt)}{\sigma(Z)}$	$\delta \frac{\sigma(tt)}{\sigma(Z+j)}$	$\delta \frac{\sigma(tt)}{\sigma(Z+j, P_{TZ} > 50)}$	$\delta \frac{\sigma(tt)}{\sigma(Z+j, P_{TZ} > 100)}$	$\delta \frac{\sigma(tt)}{\sigma(Z+j, P_{TZ} > 150)}$	$\delta \frac{\sigma(tt)}{\sigma(Z+j, P_{TZ} > 200)}$
Total	6.3	5.7	5.2	4.3	3.5	3.0

Idea appears to work !

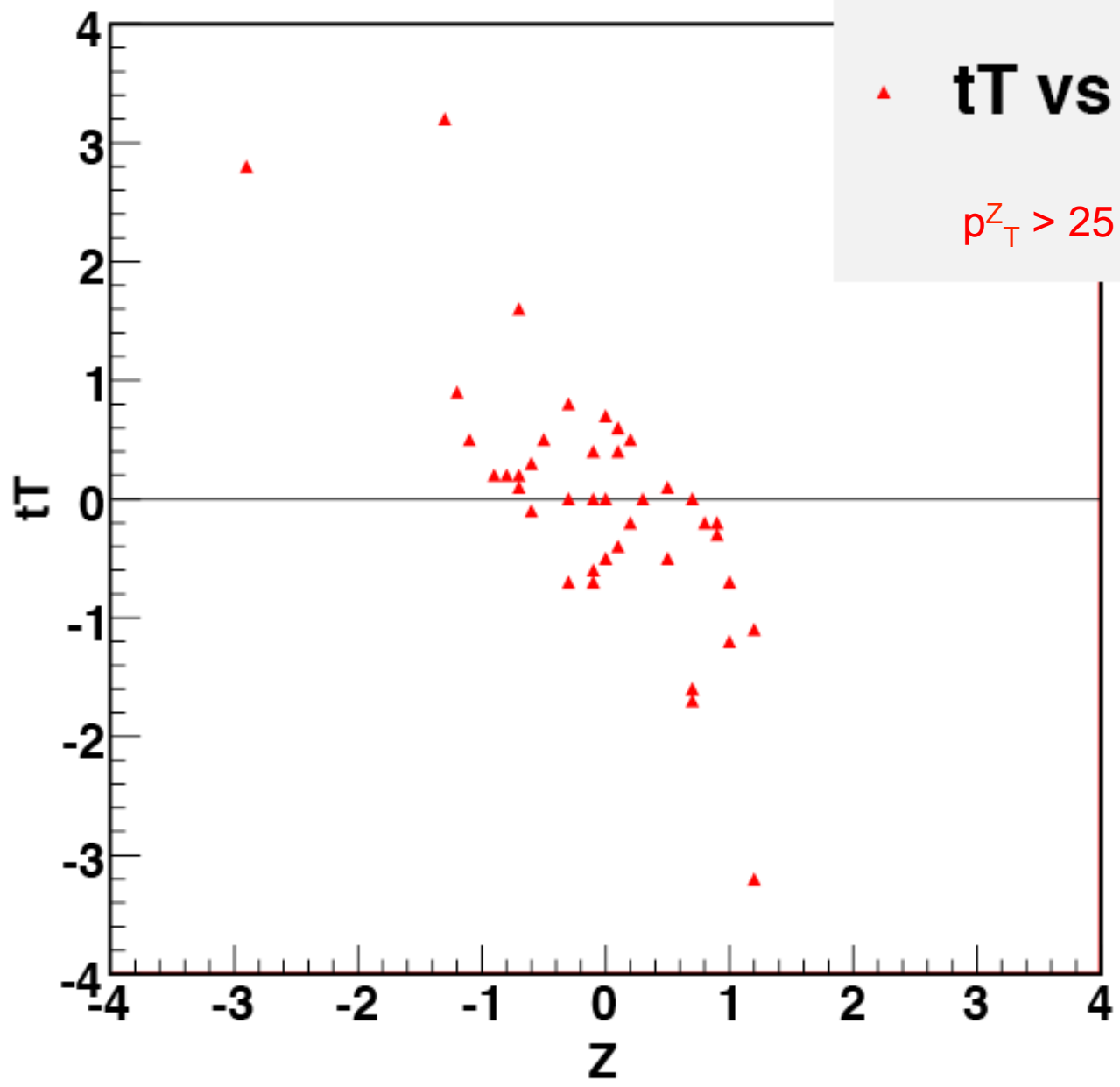
tT pdf error vs Z (+ jet)

■ tT vs Z

% pdf uncertainty



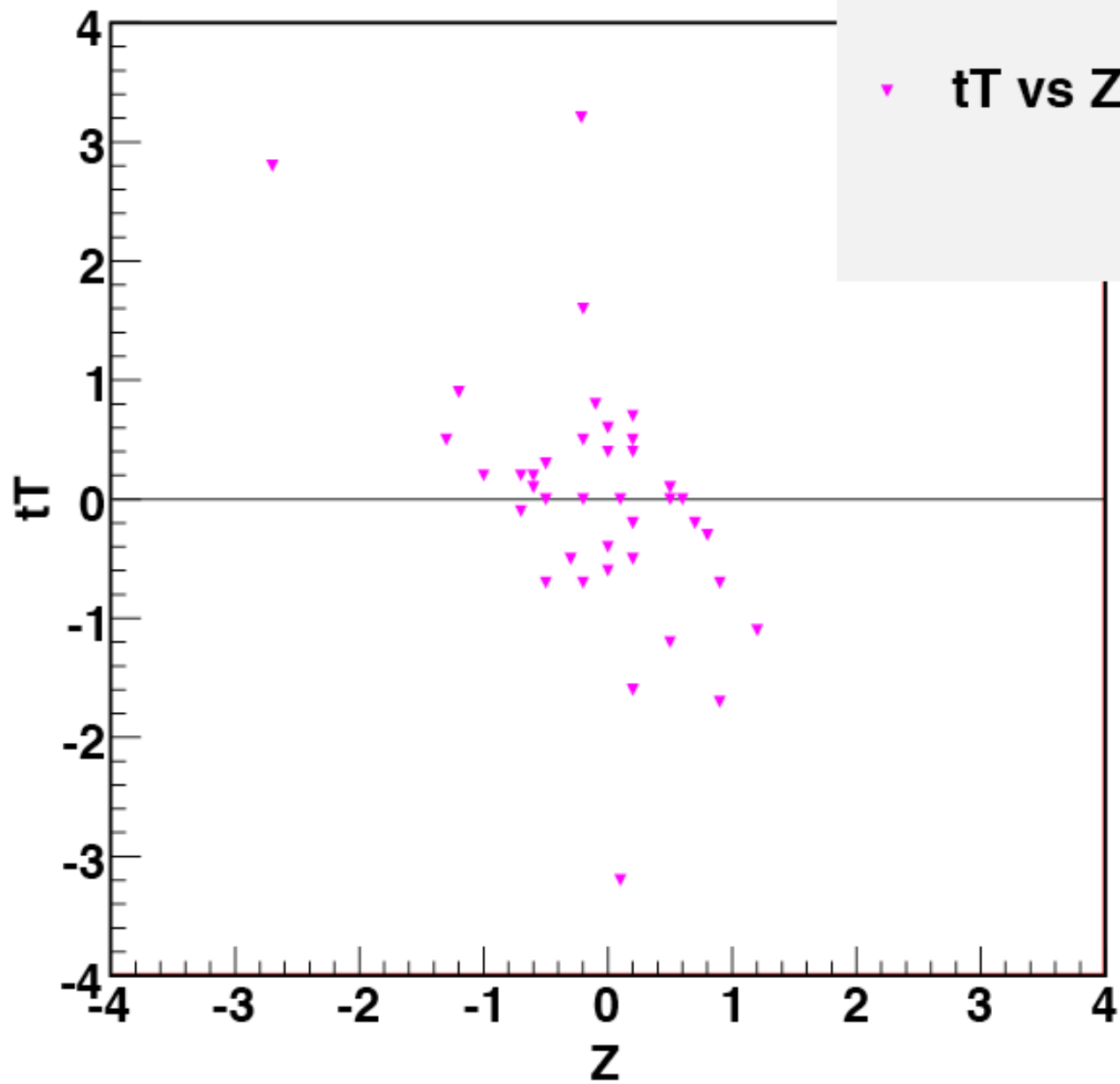
tT pdf error vs Z (+ jet)



tT vs Zj
 $p_T^Z > 25 \text{ GeV}/c$



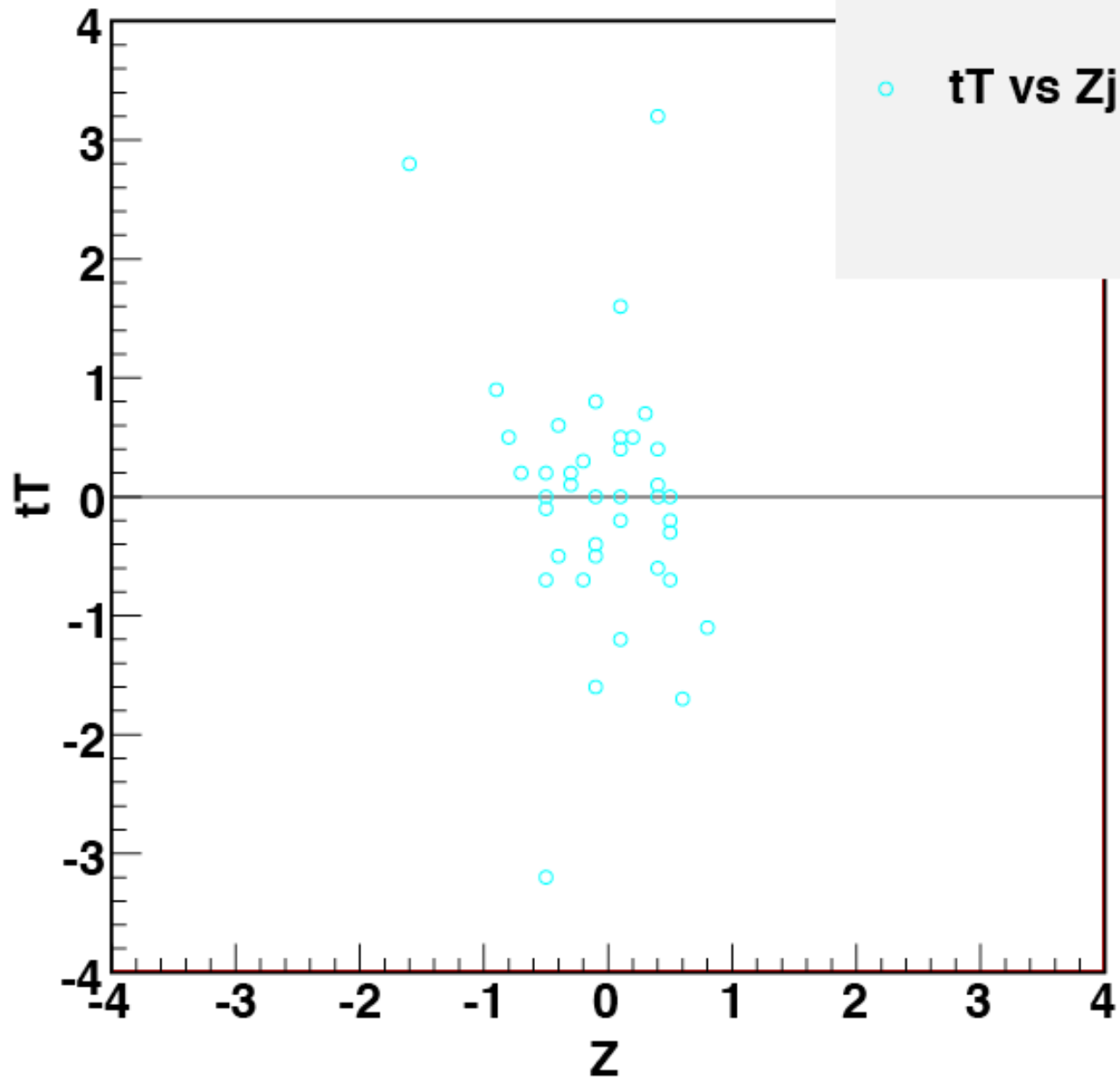
tT pdf error vs Z (+ jet)



▼ tT vs Zj50



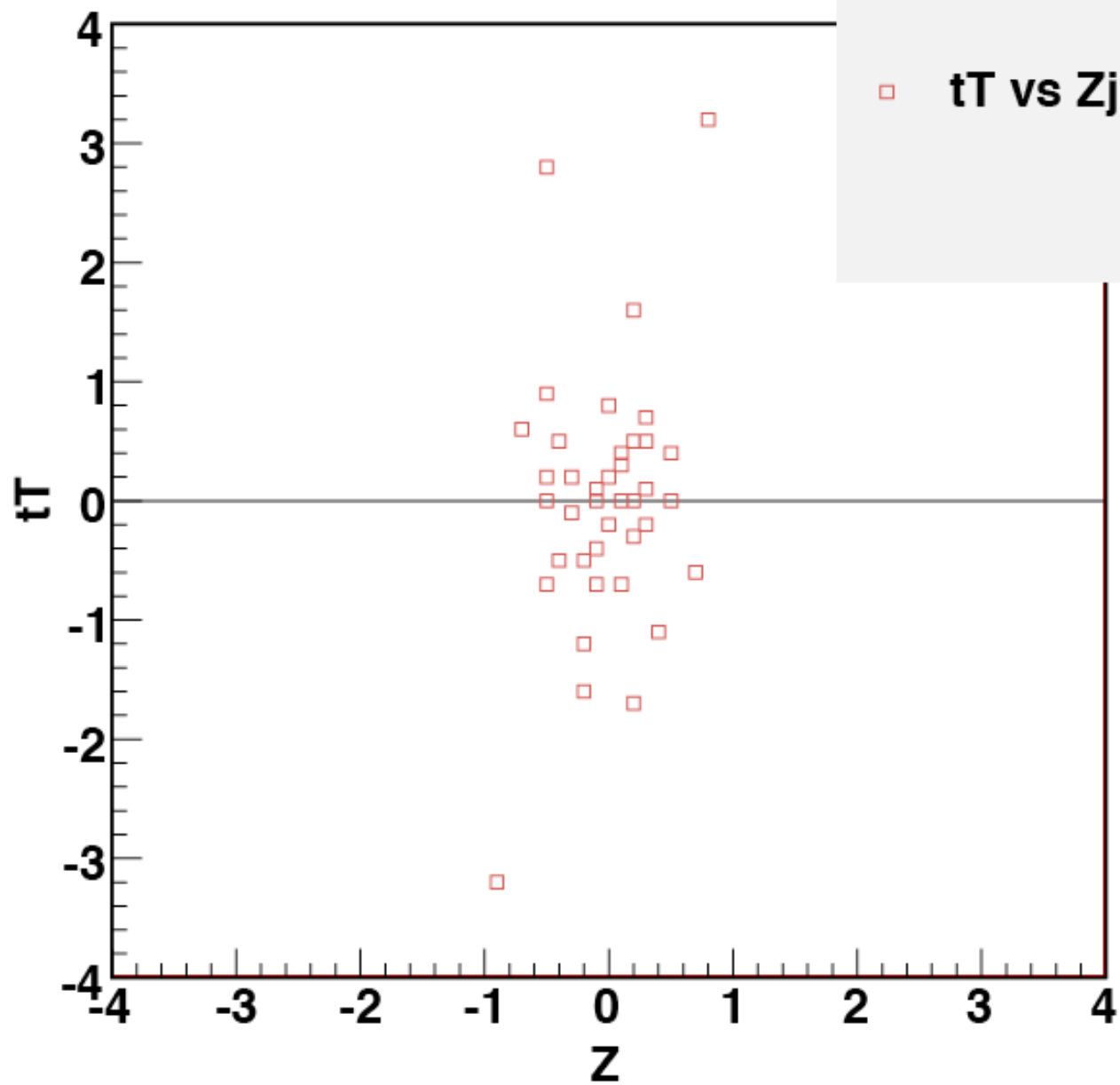
tT pdf error vs Z (+ jet)



○ tT vs Zj100

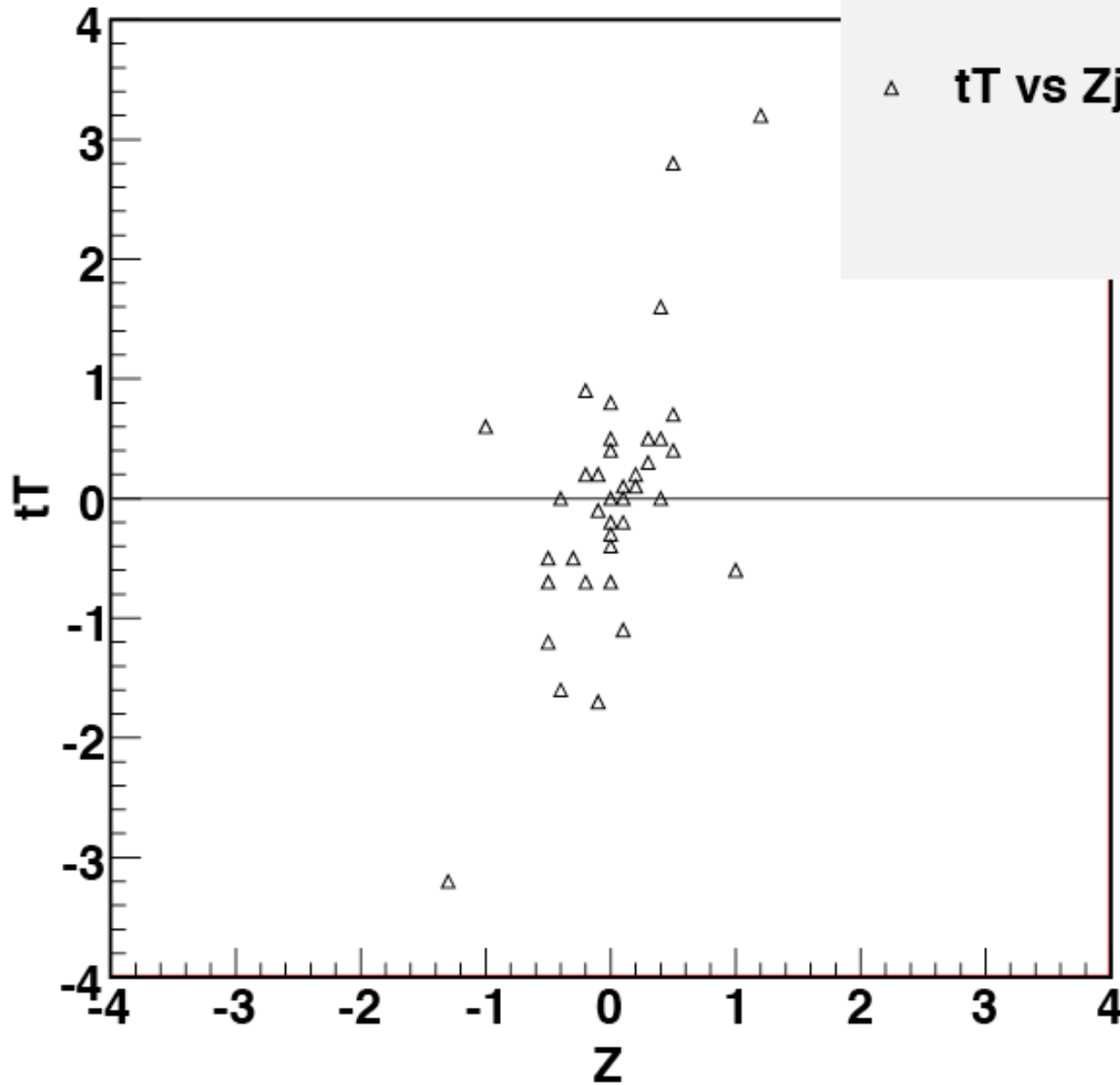


tT pdf error vs Z (+ jet)



tT vs Zj150

tT pdf error vs Z (+ jet)



△ tT vs Zj200

for $p_T^Z > 200$ GeV/c, not only does the Z uncertainty become small, but there's also a correlation developing with the tT cross section, because of the gluon being in a similar x range